

COPPER SOLUBILIZATION STRATEGIES FOR MOLD BIOMACHINING AND BIOLEACHING FROM PRINTED CIRCUIT BOARDS

ARRATE SANTAOLALLA RAMÍREZ

DEPARTAMENT OF CHEMICAL AND ENVIRONMENTAL ENGINEERING

2021

eman ta zabal zazu



Universidad
del País Vasco

Euskal Herriko
Unibertsitatea

University of the Basque Country (UPV/EHU)

Faculty of Engineering of Vitoria-Gasteiz

Department of Chemical and Environmental Engineering

**COPPER SOLUBILIZATION STRATEGIES FOR MOLD
BIOMACHINING AND BIOLEACHING FROM
PRINTED CIRCUIT BOARDS**

Arrate Santaolalla Ramírez

Vitoria-Gasteiz, 2021

Supervisors:

Dra. Astrid Barona Fernández

Dra. Naiara Rojo Azaceta

ACKNOWLEDGMENTS

Después de dedicar los últimos casi cuatro años a esta tesis y aunque parecía no llegar nunca este momento, aquí estoy, escribiendo los agradecimientos para *finiquitar* así este capítulo de mi vida. Por tanto, es el momento de agradecer a todas esas personas que han hecho de este viaje una experiencia de vida en vez de un simple proyecto de investigación y que han caminado junto a mi durante esta etapa.

Con el permiso de mi familia y amigos, me gustaría empezar agradeciendo de forma especial a quienes han hecho posible que yo ahora mismo este redactando estas palabras.

Quiero empezar mencionando de forma especial a mis directoras de tesis, Astrid y Naiara. Gracias por confiar en mí y darme la oportunidad de hacer esta tesis con vosotras. Gracias por vuestro apoyo, por vuestro esfuerzo y por vuestra dedicación a pesar de tener otras mil cosas que hacer. Este trabajo no habría sido posible sin vuestra ayuda.

A Gorka y Junkal, porque, aunque no han sido oficialmente parte de la dirección de mi tesis, siempre han estado para ayudarme y colaborarme en todo lo que he necesitado (y por esos dulces que siempre encontraba en mi taza al llegar). Me habéis dado mucho a cambio de muy poco.

A Esti, que me enseñó todo lo que debía saber sobre *nuestros bichos* y tuvo mucha paciencia para que aprendiera todo bien.

Me siento muy afortunada de haber podido formar parte del departamento de ingeniería química y del Medio Ambiente en general, y de la sección de Vitoria-Gasteiz en particular. Durante estos años he conocido gente espectacular que espero no dejen de formar parte de mi círculo. Gracias por hacerme sentir parte del departamento y por incluirme y contar conmigo siempre para todos los “rolletes” que iban surgiendo. A Zuriñe, Loli, Ainara, Jon, Irati, Nieves, y demás (lo siento si me dejo a alguien sois muchos), por esos cafés *solos* pero tan acompañados de interesantes conversaciones a media mañana. A los que no toman café, pero también forman parte de la sección.

I would like to thank also Pr. Piet Lens for giving me the opportunity to be part of his research group during my stay in Galway. I also want to thank Arindam for guiding me in my experiments during my stay. To whole research group for the very warm welcome to the group. A Borja, por su paciencia y por ayudarme en el laboratorio (y fuera de él).

Ahora, con el permiso de mis directoras y compañeros voy a dar las gracias a mi familia por haberme acompañado a lo largo de este camino. Todo lo que tengo que agradeceros es demasiado para dejarlo escrito, aunque voy a intentar resumirlo.

A mi padre, porque estés donde estés sé que estarás orgulloso de mí. Te echo de menos.

A mi madre, por haberme permitido llegar a ser quien soy hoy. Me has enseñado a trabajar duro para conseguir lo que quiero y a dar siempre lo mejor de mí. A ti te debo todo lo que soy y todo lo que he conseguido.

A mis hermanas *mayores*, Itziar y Leire. Por apoyarme a lo largo de este camino. Porque de vosotras he aprendido que nunca es suficiente y que siempre se puede un poquito más. Siempre habéis sido y seréis un ejemplo para mí.

A Iratxe, mi gemela, mi otra mitad, porque siempre estás para mí. Gracias por aguantarme siempre todas mis *chapas*, por acompañarme *a apagar el baño* a últimas horas del día, pero sobre todo por apoyarme siempre durante este camino. Porque aun estando ocupada, siempre me has permitido estar más ocupada que tú. Si es verdad que estamos conectadas sabrás lo agradecida que te estoy.

A Asier, porque aún sin saber muy bien de lo que le hablaba muchas veces, siempre me preguntaba por *mis bichos*. Por adaptarse siempre a mi disponibilidad (que a veces no ha sido tan amplia como nos hubiera gustado), pero sobre todo por apoyarme siempre y estar a mi lado. Porque en su compañía las cosas malas se convierten en buenas. Gracias por estar siempre ahí para mí.

A mis amigas, por perdonarme los *plantones* y estar ahí para los buenos ratos. A mis *Aitos*, por rezarle siempre a Santa Rita pidiéndole que todo me fuera bien. Al resto de mi familia. No puedo nombrar a todos porque somos muchos, pero ellos ya saben lo importantes que son para mí.

Siento que todas las palabras aquí escritas son insuficientes y espero algún día poder devolveros todo lo que me habéis dado.

Eskerrik asko!

TABLE OF CONTENTS

SUMMARY	vii
RESUMEN.....	xi
LABURPENA	xv
MOTIVATIONS AND THESIS OVERVIEW	1
OBJECTIVES	7
LITERATURE REVIEW.....	11
1. MICROORGANISM-ASSISTED METAL MOBILIZATION	13
2. MICROORGANISMS IN MICROORGANISM-ASSISTED METAL MOBILIZATION PROCESSES .	13
2.1. Chemolithoautotrophic bacteria.....	14
2.2. Heterotrophic bacteria.....	16
2.3. Fungi and yeasts.....	17
2.4. Microorganism consortium.....	18
3. <i>Acidithiobacillus ferrooxidans</i> GENUS	20
4. MECHANISMS OF MICROBIAL METAL MOBILIZATION	22
4.1. Direct mechanism	22
4.2. Indirect mechanism.....	23
4.3. Cooperative leaching/mechanism	24
4.4. Thiosulfate and polysulfide mechanism.....	24
4.5. Mechanisms according to the type of reaction	25
4.5.1. Redoxolysis.....	25
4.5.2. Acidolysis.....	26
4.5.3. Complexolysis.....	26
4.5.4. Bioaccumulation.....	26
5. FACTORS INFLUENCING MICROORGANISM-ASSISTED METAL MOBILIZATION	27
5.1. Temperature	27
5.2. pH.....	28
5.3. Shaking speed.....	28
5.4. Bacterial concentration and biomass immobilization.....	29
5.5. Iron concentration.....	30
5.6. Presence of process inhibitors	31
5.7. Precipitate formation.....	32
6. APPLICATIONS OF MICROORGANISM-ASSISTED MOBILIZATION OF METALS	33

6.1. Biomachining.....	35
6.1.1. Metal workpieces preparation.....	36
6.1.2. Specific metal removal rate (SMRR).....	36
6.1.3. Surface finish.....	37
6.2. Electronic waste bioleaching.....	38
6.2.1. PCB pre-treatment.....	42
6.2.2. Treatment mode: single and multi-stages bioleaching.....	44
6.2.3. Pulp density.....	45
7. REFERENCES.....	45
MATERIALS AND GENERAL METHODS.....	65
1. MATERIALS.....	67
1.1. Microorganisms.....	67
1.2. Copper workpieces.....	67
2. GENERAL METHODS.....	68
2.1. <i>Acidithiobacillus ferrooxidans</i> bacterial growth.....	68
2.2. Copper mobilization experiments.....	69
2.3. Determination of the bacterial concentration in the medium.....	69
2.4. Metal removal rate and specific metal removal rate.....	71
2.5. Determination of iron species in solution.....	71
2.6. Metal content analysis (ICP and AAS).....	73
2.7. Scanning electron microscopy (SEM).....	73
2.8. Other methods.....	74
3. REFERENCES.....	74
CHAPTER 1. OPERATION WITH SUSPENDED BIOMASS.....	77
1.1. OBJECTIVE.....	79
1.2. MATERIALS AND METHODS.....	79
1.2.1. Copper pieces.....	79
1.2.2. Microorganisms and culture media.....	80
1.2.3. Metal mobilization experiments.....	80
1.2.3.1. Effect of iron content on bacterial growth and metal mobilization.....	80
1.2.3.2. SMRR as a function of time during the metal mobilization process.....	81
1.2.4. Alternate process: metal mobilization + regeneration.....	82
1.2.5. Analytical methods.....	82
1.3. RESULTS.....	82
1.3.1. Metal mobilization experiments.....	82

1.3.1.1.	Influence of Fe ²⁺ concentration on bacterial growth	82
1.3.1.2.	Influence of Fe ³⁺ concentration on SMRR	86
1.3.1.3.	SMRR as a function of time during metal mobilization process	89
1.3.2.	Alternate process: metal mobilization + regeneration	91
1.4.	CONCLUSIONS	95
1.5.	REFERENCES	96
CHAPTER 2. OPERATION WITH IMMOBILIZED BIOMASS		99
2.1.	OBJECTIVE.....	101
2.2.	MATERIALS AND METHODS.....	102
2.2.1.	Microorganism and culture medium.....	102
2.2.2.	Synthesis of the support materials.....	102
2.2.2.1.	Bacterial cellulose.....	103
2.2.2.2.	Polyvinyl alcohol.....	104
2.2.2.3.	Modified cellulose triacetate membrane.....	105
2.2.2.4.	Cellulose triacetate spheres	106
2.2.2.5.	Chitosan.....	106
2.2.3.	Pre-treatment of the support material	107
2.2.4.	The design of a decision-making protocol	108
2.2.5.	Selection of the inoculum percentage	109
2.2.6.	Suitability of bacterial cellulose as support material for <i>A. ferrooxidans</i> immobilization.....	109
2.2.6.1.	Preparation of the Active Bacterial Cellulose (A-BC)	109
2.2.6.2.	Effect of operating parameters on Fe ²⁺ bio-oxidation	110
2.2.6.3.	Influence of dissolved copper concentration on bacterial immobilization and subsequent iron bio-oxidation stages	111
2.2.6.4.	Influence of active BC storage on bacterial activity	112
2.2.6.5.	Biocellulose cleaning and reuse	112
2.2.7.	Comparison of BC and PVA as support materials	113
2.2.8.	Analytical methods.....	113
2.3.	RESULTS.....	113
2.3.1.	Selection and characterization of suitable materials for <i>A. ferrooxidans</i> immobilization.....	113
2.3.2.	Selection of the inoculum percentage	117
2.3.3.	Suitability of bacterial cellulose as support material for <i>A. ferrooxidans</i> immobilization.....	118
2.3.3.1.	Preparation of the Active Bacterial Cellulose.....	118

2.3.3.2.	Effect of operating parameters on Fe ²⁺ bio-oxidation	121
2.3.3.3.	Influence of dissolved copper concentration on bacterial immobilization and subsequent iron bio-oxidation stages	125
2.3.3.4.	Material integrity	128
2.3.3.5.	Influence of BAMs storage on bacterial activity	129
2.3.3.6.	Reuse of BC as support material after washing	130
2.3.4.	Comparison of BC and PVA as support material	131
2.4.	CONCLUSIONS	135
2.5.	REFERENCES	136
CHAPTER 3. APPLICATION 1: BIOMACHINING OF COPPER PIECES FOR THE FABRICATION OF MICROFLUIDIC DEVICES		143
3.1.	OBJECTIVE.....	145
3.2.	MATERIALS AND METHODS.....	146
3.2.1.	Microorganisms and biomachining solution	146
3.2.2.	Workpiece preparation	146
3.2.2.1.	Workpiece dimensions and preparation.....	146
3.2.2.2.	Geometries to be biomachined.....	147
3.2.2.3.	Selection of the coating material for surface protection.....	147
3.2.3.	Mold-etching using cell suspension	148
3.2.3.1.	Influence of treatment time on mold-etching	148
3.2.3.2.	Extension of the lifespan of the BM solution	149
3.2.4.	Mold-etching using immobilized biomass.....	150
3.2.5.	Fabrication of the PDMS devices	151
3.2.6.	Analytical methods.....	152
3.3.	RESULTS.....	153
3.3.1.	Workpiece preparation: an alternative to the traditional techniques.....	154
3.3.2.	Mold-etching using cell suspension	155
3.3.2.1.	Specific metal removal rate and structure's height as a function of treatment time	156
3.3.2.2.	Prolonging the BM solution lifespan for a more sustainable process	162
3.3.3.	Biomachining with immobilized biomass.....	167
3.3.4.	Fabrication of PDMS devices.....	171
3.4.	CONCLUSIONS	173
3.5.	REFERENCES	174
CHAPTER 4. APPLICATION 2: BIOLEACHING OF METALS FROM PCBs.....		179

4.1. OBJECTIVE.....	181
4.2. MATERIAL AND METHODS	182
4.2.1. Microorganism and culture medium.....	182
4.2.2. PBC samples	182
4.2.3. Sample conditioning.....	183
4.2.3.1. Sample grinding.....	183
4.2.3.2. Removal of the epoxy layer.....	183
4.2.4. Bioleaching experiments	183
4.2.4.1. One-step bioleaching experiment.....	183
4.2.4.2. Two-step bioleaching experiment.....	184
4.2.5. Chemical leaching experiment	184
4.2.6. Preliminary design of a bioleaching reaction system.....	184
4.2.7. Analytical methods.....	185
4.3. RESULTS.....	186
4.3.1. Pretreatment of the PCBs	186
4.3.2. Metal composition of the PCBs	187
4.3.3. Bioleaching experiments	190
4.3.3.1. One-step bioleaching experiment.....	191
4.3.3.2. Two-step bioleaching experiment.....	193
4.3.4. Chemical leaching experiments	196
4.3.5. Preliminary design of a bioleaching reaction system.....	201
4.3.5.1. Bioleaching assembly	201
4.3.5.2. Reactors and components.....	202
4.4. CONCLUSIONS	206
4.5. REFERENCES	207
CHAPTER 5. RECOVERY OF COPPER FROM SPENT SOLUTIONS	213
5.1. OBJECTIVE.....	215
5.2. MATERIALS AND METHODS.....	216
5.2.1. Composition of the synthetic liquid residue (SLR)	216
5.2.2. Precipitation procedure	216
5.2.3. Electrodeposition procedure.....	217
5.2.4. Analytical methods.....	218
5.2.5. Economic Analysis	218
5.3. RESULTS AND DISCUSSION	219
5.3.1. Precipitation	220

5.3.2. Electrodeposition	223
5.3.3. Cost Analysis.....	226
5.4. CONCLUSIONS	227
5.5. REFERENCES	228
GENERAL CONCLUSIONS AND FUTURE OVERLOOK	231
APPENDIX 1.....	238
LIST OF PUBLISHED ARTICLES	239
LIST OF CONFERENCES.....	239
APPENDIX 2.....	241
LIST OF FIGURES	243
LIST OF TABLES	247

SUMMARY

The numerous applications of biotechnology play a key role in sustainable development. As far as mining is concerned, the microorganism-assisted solubilization process for metal extraction has traditionally been used for a long time. Nowadays, the fundamentals of this bioprocess are still being applied in new areas such as the manufacture of microstructures (biomachining) and the recovery of metals from electronic waste (bioleaching).

The global demand of micrometric scale components is continuously growing worldwide. Therefore, more affordable and sustainable micromachining methods in comparison to the conventional physical-chemical ones are being sought. In particular, biomachining is a promising alternative to engrave well-defined structures on copper workpieces. Based on its low energy consumption and low operating cost, it can be classified as a sustainable environmentally friendly process.

Similarly, the generation of waste from electrical and electronic equipment (WEEE) has increased exponentially in recent years and it has become a global concern. Metal recovery by improved bioleaching can contribute to the sustainable management of this waste and can offer an entrepreneurial opportunity in the metal exchange market.

Although these different applications are promising and pose clear advantages over other technologies, further research on improving the bioprocess efficiency is needed before the design and implementation at production scale can be attainable.

The main objective of this thesis is to improve the efficiency of the microorganism-assisted solubilization of copper by proposing strategies that can be applied in the two processes described before: the biomachining of copper pieces for engraving microstructures and the recovery of copper from disused mobile telephones. Both applications have been studied using the well-known bacterium *A. ferrooxidans*, as it is a very versatile and resistant microorganism with a low biosafety risk.

The first step in this study was to analyze the influence of the fundamental conditions on the microbial growth, copper solubilization and oxidant regeneration. Bearing in mind that the solubilization efficiency is directly related to the oxidant amount available in the medium, different concentrations of iron were tested. The 9K solution (containing Fe^{2+} or Fe^{3+}) was found to be the most suitable medium for both *A. ferrooxidans* growth and metal oxidation. Copper solubilization was noticeably increased by the presence of microorganisms in comparison to the abiotic system. Specifically, the Fe^{2+} biooxidation rate in 9K medium was 2.8-fold higher than in the other solutions and the bacterial activity was responsible for the 25 % increase in the dissolved copper, in comparison with the abiotic study.

The SMRR peaked during the first hour of treatment and thus, an alternate bioprocess was designed by performing first the step of copper solubilization from one metal piece followed by the iron regeneration step in absence of the metal piece. This strategy allowed the reduction of both the treatment time and the amount of depleted solution, which enhances the sustainability of the process by prolonging the solution lifespan.

The strategy of immobilizing the biomass for improving bacterial efficiency was searched by studying the suitability of several support materials. Among all the materials, the bacterial biocellulose (BC) was selected for further experiments based on its novelty and its outstanding properties such as its biodegradability, highly porous network structure and chemical stability. This hydrogel was concluded to immobilize the bacteria adequately, did not interfere the microbial growth, and the active BC could be stored at 4 °C and was effective in the presence of high concentrations of Cu^{2+} .

Regarding the applications, the feasibility of the biomachining for engraving copper molds for the manufacture of microfluidic structures was studied. This process required the efficient protection of the metal surface not to be exposed to the oxidant solution. The combination of one common lacquer (red light bulb lacquer) and a PSA adhesive was found to be an efficient solution. The equations for predicting the treatment time required to achieve a selected height in the copper piece were proposed in the 0-1 h and 1-7 h range. Although similar SMRR_{av} and height values were obtained when suspended or immobilized biomass were used in the biomachining experiments, shorter regeneration times were needed in the presence of the active biocellulose. The repeatability of the process when reusing the biomachining medium is particularly remarkable for this application. The solution's lifespan can be prolonged as it can be repeatedly utilized, contributing to the process sustainability. In addition, other benefit of using the biologically active material would lie in the easily handling (feeding and replacing) of the biomass in large-scale operation.

As far as microorganism-assisted solubilization of metals from PCBs is concerned, the heterogeneity of these materials was a challenge for obtaining representative samples. A decision was made on using the entire pieces without the epoxy cover, because grinding entailed an important cost and generated particulate matter in the environment. In addition, the use of the entire PCBs facilitated the management and separation of the pieces from the leachate, as well as providing a "cleaner" medium for microbial activity. The alternate (two step) bioleaching experiment with the entire PCBs rendered a total amount of 82 % of copper dissolved by the end of the assay (300 hours), which was attributed to the relevant contribution of the biomass in regenerating the oxidant.

The bioleaching and biomachining processes generated liquid residues with high metal concentrations. The two alternatives studied for recovering copper from a synthetic

solution, precipitation and electrodeposition, rendered high metal recovery at a reasonable cost and required the preliminary oxidation and precipitation of iron, which obviously implied the additional consumption of reagents and longer operation time. Although the precipitation method was more affordable (although time-consuming), the final product obtained by the electrorecovery was more attractive for the stock market.

Bearing in mind that the world demand of copper has been on the rise during the last three months and is expected to go further up, the metal recovery from the PCBs and the depleted solutions can be an entrepreneurial opportunity integrated in the circular economy.

In summary, the biomachining of metallic molds and the metal bioleaching from PCBs were concluded to be two attainable bioprocesses whose future implementation on a large scale will make an important contribution to sustainable production, efficient waste management and circular economy.

RESUMEN

Actualmente la biotecnología desempeña un papel fundamental en el desarrollo sostenible. En este ámbito, los fundamentos de los procesos de solubilización de metales empleando microorganismos, que tradicionalmente han sido empleados en la extracción de metales de minerales, están siendo aplicados a otras áreas, como la fabricación de microestructuras (biomecanizado) y la recuperación de metales presentes en residuos (biolixiviación).

El imparable aumento de la demanda mundial de componentes a escala micrométrica hace que la tecnología del micromecanizado esté en constante desarrollo con el fin de encontrar alternativas más económicas y sostenibles a los procesos físicos-químicos tradicionales. En este sentido, el biomecanizado se convierte en una prometedora alternativa que utiliza el potencial de los microorganismos para mejorar el proceso de grabado de microestructuras, resultando ser sostenible y respetuoso con el medio ambiente por su bajo consumo energético y su bajo coste operacional.

Por otro lado, el interés en avanzar en la recuperación de metales de residuos de aparatos eléctricos y electrónicos (RAEE) se debe a la posibilidad de devolver los metales a la cadena de valor y a la oportunidad de gestionar de manera sostenible estos residuos, cuya generación ha aumentado exponencialmente en los últimos años.

A pesar de que estas aplicaciones son prometedoras y presentan ventajas frente a otras tecnologías, todavía existe la necesidad de estudiar ciertos aspectos operacionales que permitan diseñar e implantar procesos mejorados a escala productiva.

El principal objetivo de esta tesis es investigar el proceso de solubilización de cobre en un medio bacteriano, con el fin de proponer estrategias que permitan mejorar el rendimiento de cara a dos aplicaciones concretas: el biomecanizado de moldes para la fabricación de dispositivos microfluídicos y la recuperación de metales a partir de placas de circuito impreso de teléfonos móviles en desuso.

La conocida bacteria extremófila *Acidithiobacillus ferrooxidans* fue seleccionada por su resistencia en medios ácidos y su nivel de bioseguridad. Antes de aplicar el proceso de movilización biológica de metales a los dos usos descritos, se estudiaron algunos aspectos relacionados tanto con el crecimiento microbiano, como con la solubilización del cobre y la operatividad del proceso propuesto.

Dado que el rendimiento de solubilización del cobre depende de la concentración de oxidante, inicialmente se estudió la influencia de esta variable en el medio biológico. La concentración de hierro (Fe^{2+} para el crecimiento microbiano o Fe^{3+} para la solubilización del metal) más eficaz resultó ser 9 g L^{-1} (medio 9K). La velocidad de biooxidación del Fe^{2+} en el medio 9K fue 2.8 veces superior que en otros medios y la actividad bacteriana

contribuyó a que la cantidad de cobre solubilizada fuera 25% más elevada que en un medio abiótico.

A continuación, teniendo en cuenta que la máxima tasa específica de eliminación (TEE) se alcanzó durante la primera hora de tratamiento, se diseñó un proceso que alternaba una etapa de solubilización del metal de 3 horas con la pieza metálica sumergida en la disolución y una etapa de bioregeneración del oxidante sin la pieza. Esta alternativa demostró ser efectiva para reducir el tiempo necesario para solubilizar una determinada cantidad de metal, así como para extender el tiempo de vida de la disolución de tratamiento.

Posteriormente, se llevó a cabo el estudio de la inmovilización de la biomasa sobre varios materiales de soporte, como una estrategia para favorecer la operatividad del sistema. Tras un ensayo con varias alternativas, se seleccionó la celulosa bacteriana por sus adecuadas propiedades mecánicas, estabilidad química, y estructura porosa. Asimismo, se optimizaron las condiciones de operación que permitieron una oxidación más rápida del Fe^{2+} . Este soporte presentó las ventajas de inmovilizar de manera satisfactoria la biomasa, de no interferir en el crecimiento bacteriano, de poder ser almacenada a 4 °C en estado activo y de tener capacidad para oxidar el Fe^{2+} en presencia de cantidades elevadas de Cu^{2+} . Asimismo, presentó mejor comportamiento que otro material también testado, el polivinil alcohol.

En relación a las aplicaciones, se estudió el biomecanizado como alternativa para la generación de moldes metálicos para la fabricación de estructuras microfluídicas. En este proceso es totalmente necesario proteger adecuadamente la superficie metálica que no se desea mecanizar (o grabar). Para ello se seleccionó una combinación de una laca roja y un adhesivo de PSA que no afectaron a la actividad microbiana. Un aspecto a destacar de esta aplicación es la repetitividad del proceso empleando tanto la disolución fresca como la disolución regenerada (varios ciclos). Esto permitió establecer las ecuaciones matemáticas que posibilitan predecir el tiempo necesario para obtener un molde con una altura definida (en dos tramos de tratamiento: 0-1 h y 1-7 h). Los tiempos de regeneración fueron más cortos cuando la biomasa estaba inmovilizada en biocelulosa, aunque los rendimientos de mecanizado fueron similares a los de la suspensión. La creciente acumulación de cobre disuelto en el medio tuvo un efecto negativo en la regeneración de la disolución de biomecanizado, aunque no fue importante para concentraciones inferiores a 3 g Cu^{2+} L⁻¹. El empleo de la biomasa inmovilizada en BC presentó además la ventaja de la facilidad operativa a la hora de reemplazar el medio bacteriano.

En la aplicación de biolixiviación de cobre a partir de placas de circuito impreso de móviles en desuso, la heterogeneidad de estos materiales en términos de tamaño, composición o estructura obligó a diseñar una etapa previa de adecuación. Se decidió

eliminar la cubierta epoxi y tratar las piezas enteras o parte de ellas, pero sin trituración previa. La biolixiviación se llevó a cabo en dos pasos (biooxidación y biolixiviación por separado). Esta estrategia contribuyó al aumento de la movilización de los metales de las placas, siendo la eficacia de la lixiviación en medio bacteriano significativamente más elevada en comparación con la lixiviación química. El empleo de placas sin triturar permitió trabajar con un medio “más limpio” y favorable para el crecimiento de la biomasa.

Las dos aplicaciones descritas generan disoluciones agotadas con alto contenido de metales que deben ser tratadas antes de su vertido. La recuperación de cobre de esas disoluciones devuelve este metal a la cadena de valor, mitiga el impacto ambiental, y contribuye a la viabilidad económica de ambas aplicaciones. En este estudio se ha trabajado con una disolución sintética agotada y se han aplicado dos sencillos tratamientos: precipitación química fraccionada y electrólisis. Ambas propuestas fueron eficaces en términos de recuperación del cobre de la disolución residual, aunque el proceso electrolítico da como resultado un producto más atractivo (Cu^0) desde el punto de vista de mercado.

En resumen, el mecanizado de moldes metálicos y la extracción de metales de placas de circuitos impresos en medio bacteriano son dos aplicaciones prometedoras cuya implantación futura a mayor escala supondrá una importante contribución a la producción sostenible, la gestión integrada de residuos y la economía circular.

LABURPENA

Gaur egun bioteknologiaren aplikazioek funtsezko garrantzia dute garapen jasangarria lortzeko. Arlo horretan, mikroorganismoak erabiltzen dituen solubilizazio prozesua aspalditik erabili izan da meatzaritzan, mineraletatik metalak erauzteko. Bioprozesu horren oinarriak beste alor batzuetan ere aplikatu dira azken urteotan, hala nola, mikroegituren fabrikazioan (biomekanizatuan) eta hondakinetan dauden metalen berreskurapenean (biolixibiazioan).

Mikroegituren fabrikazioari dagokionez, eskala mikrometrikoko osagaien eskaera asko igo da mundu mailan azken urteotan. Eskaera horrek, mikromekezazio teknologiaren garapen etengabea bultzatu du, ohiko prozesu fisiko-kimikoak baino alternatiba ekonomikoagoak eta jasangarriagoak aurkitzea premiazkoa delako. Aukeren artean, biomekezazioa deritzon teknika aipa daiteke bereziki, hau da, mikroorganismoek lagunduta, mikroegiturak grabatzeko teknika jasangarria. Energia-kontsumo baxua eta operazio-kostu moderatua dira beraren aldeko ezaugarrietako batzuk.

Bestaldetik, Tresna elektriko eta elektronikoen hondakinak (TEEH)gero eta kantitate handiagotan pilatzen dira munduan, eta horien kudeaketa arazoa oso larria da gaur egun. Hondakin horien kudeaketa eraginkorraren eta jasangarriaren helburu nagusia, metalak balorizatu eta balio-katera (lehengaien merkatura) bueltatzea da, metalen iturri naturalen agorpena saihesteko. Balorizazio hori, mikroorganismoek lagundutako biolixibiazioaren bidez burutu daiteke.

Aipatutako prozesu biek (biomekezazioak eta biolixibiazioak) abantaila nabarmenak dituzte betidanik erabili diren teknologiek alderatuta. Hala ere, zenbait aspektu operatibo sakon aztertu behar da hobetutako prozedurak diseinatu eta horiek ekoizpen eskalan (eskala handian) inplementatu ahal izateko.

Tesi honen helburu nagusia mikroorganismoek lagunduriko kobrearen solubilizazio prozesua ikertzea izan da, eta horretarako adierazitako aplikazio bien errendimendua hobetzeko estrategiak bilatu eta aztertu ziren. Aplikazio horiek ondokoak izan ziren: gailu mikrofluidikoak ekoizteko molde metalikoen biomekezazioa, eta sakeleko telefonoen zirkuitu inprimatuetan dauden metalen berreskurapena.

Acidithiobacillus ferrooxidans bakterioa extremofilo ezaguna aukeratu zen ikerketan, ingurune azidoetan hazteko duen gaitasun aipagarriagatik eta maneiatzeko duen biosegurtasun maila altuagatik. Metalen mobilizazio biologikoa adierazitako bi erabileratara aplikatu baino lehen, mikroorganismoen hazkuntzan, kobrearen solubilizazioan eta proposatutako prozesuaren eraginkortasunean eragina duten hainbat faktore aztertu ziren.

Lehenik, oxidatzailearen kontzentrazioaren eragina aztertu zen, kobrearen solubilizazioaren etekina horren menpekoa baita. Kobre kontzentrazio eraginkorra

(Fe^{2+} hazkuntza-fasean eta Fe^{3+} metalaren solubilizazioan) 9 g L^{-1} izan zen (9K hazkuntza-medioa). Burdin(II) espeziearen biooxidazio-abiadura 9K hazkuntza-medioan, beste kulturatan baino 2.8 aldiz handiagoa izan zen, eta bakterioen aktibitateari esker solubilizatutako kobre kantitatea ingurune abiotikoan baino % 25 altuagoa izan zen.

Operatibitateari dagokionez, metalaren solubilizazio-prozesua eta oxidatzailearen birsortze-prozesua txandaka (banatuta) aplikatzeko estrategia diseinatu zen, ezabatze-tasa espezifiko maximoa lehenengo orduan lortu zela kontuan hartuta. Estrategia hau oso egokia izan zen, metal kantitate jakina solubilizatzeko behar den denbora murrizteko eta disoluzioaren erabilgarritasuna luzatzeko.

Biomasaren immobilizazioaren eraginkortasuna aztertzeke, hainbat material hautatu ziren lehendabizi. Guztien artean, zelulosa bakterianoa aukeratu zen osteko esperimuetan erabiltzeko, ezaugarri mekaniko bikainak, egonkortasun kimiko altua, eta egitura porotsu egokia zituelako. Gainera, Fe^{2+} -aren oxidazio azkarragoa ahalbidetzen zuela eta ez zuela hazkuntza mikrobiarra kaltetzen ondorioztatu zen. Mikroorganismoak itsatsita zituen zelulosa bakterianoak (euskarri aktiboak) hainbat onura zituen suspentsio zelularrekin alderatuta, hala nola: biomasa efektiboki immobilizatzen zuen, 4°C an biltegian gordetzeko egokia izan zen, eta Cu^{2+} kontzentrazio handien presentzian Fe^{2+} -a oxidatzeko ahalmena mantendu zuen.

Lehenengo aplikazioari dagokionez, biomekanizazioa ikertu zen. Prozesu horretan, mekanizatu (grabatu) nahi ez den azalera egoki babestu behar da derrigorrez eta, ikerketa honetan, mikroorganismoen aktibitatean kalterik eragiten ez zuten laka eta PSA pegatina aukeratu ziren helburu horretarako. Nabarmentzekoa da prozesua errepikakorra izan zela, bai disoluzio oxidatzaile prestatu berria eta baita birsortutako disoluzioa erabili zirenean. Horri esker, eta datu esperimentaletan oinarrituta, altuera jakina duen moldea sortzeko behar den denbora aurreratzeko ekuazio matematiko bi proposatu ziren bi tratamendu-tarte bitan: 0-1 h eta 1-7 h tarteetan. Biomekanizazioaren etekina antzekoa izan zen biomasa zelulosa bakterianoan immobilizatu zenean eta bakteriak esekiduran (suspentsioan) erabili zirenean. Aitzitik, disoluzio oxidatzailearen birsortzea azkarragoa izan zen euskarri aktiboa erabili zenean. Disolbatutako kobre kontzentrazioaren igoera progresiboak eragin negatiboa izan zuen disoluzio oxidatzailearen birsortzean. Hala ere, $3 \text{ g Cu}^{2+} \text{ L}^{-1}$ baino kontzentrazio baxuagotan eragina ez zen larria izan. Zelulosa bakteriano aktiboa erabiltzearen beste abantaila bat medio biologikoa errazago eta azkarrago ordezkatzeko aukera ematen zuela zen.

Sakeleko telefonoen zirkuitu inprimatuek duten kobreaken berreskurapenari dagokionez, lehenbizi, laginen egokitze etapa diseinatu egin behar izan zen, zirkuitu hauek oso heterogenoak zirelako. Epoxi estalkia kentzea eta piezak osorik (edo horien parteak) tratatzea erabaki zen, birrinketarik gabe. Biolixibazioa bi pausuetan burutu zen:

biooxidazioa lehenengo eta ostean biolixibiazioa, zirkuitua mediotik aterata. Estrategia horrek metalen mobilizazioan eragin positiboa izan zuen eta, ondorioz, lixibiazioaren etekina handiagoa izan zen medio bakterianoan ingurune kimikoan baino. Zirkuituak birrindu gabe erabiltzeari esker, biomasaren hazkuntzarako egokiagoa izan zen medio “garbiagoa” erabili zen.

Deskribatutako bi aplikazioek, metal kontzentrazio altuko disoluzio agortuak sortu zituzten eta, ondorioz, hondakin likido hori kudeatzeko modu egokia aurkitu behar izan zen. Disolbaturik zegoen kobrea berreskuratzea irtenbide erakargarria izan zen, metal preziatu hori balio-katera (merkatura) bueltatzeko negozio-aukera zelako, bioprozesuen ingurumen-inpaktua murrizten zelako eta bi aplikazioen bideragarritasun ekonomikoan inpaktu positiboa izan zuelako. Ikerketa-lan honetan disoluzio agortu sintetikoa erabili zen eta bi tratamendu aplikatu zitzaizkion: hauspeatze zatikatua eta elektrolisia. Bi prozesuak eraginkorrak izan ziren eta kobreak berreskurapen-maila altua lortu zen, nahiz eta prozesu elektrolitikoaren bidez salmentarako produktu erakargarriagoa lortu.

Laburbilduz, ikerketa honetan aztertu diren bi bioprozesuak (metalezko moldeen biomekanizazioa eta zirkuitoen inprimatutik metalen bioerauzketa edo biolixibiazioa) eraginkorrak izateaz gain, ekoizpen jasangarriaren, hondakinen kudeaketa integratuaren eta ekonomia zirkularrean aldeko bultzada emateko etorkizun handiko tresnak dira.

MOTIVATIONS AND THESIS OVERVIEW

MOTIVATIONS

The thesis presented hereby has been conducted in the Department of Chemical and Environmental Engineering in the University of the Basque Country (UPV-EHU, Spain) within the research group Biofiltration. Most of the experimental work has been undertaken in the laboratories of the Faculty of Engineering of Vitoria-Gasteiz and the Faculty of Engineering of Bilbao.

With the objective of completing the research, national and international collaborations have been established. Thus, the section devoted to the mold biomachining for the manufacturing of the microfluidic structures has been carried out in collaboration with the research group of Analytical Microsystems & Materials for Lab-on-a-Chip Group (AMMa-LOAC) led by Dr. Fernando Benito López and Dr. Lourdes Basabe-Desmots from the Faculty of Pharmacy of Vitoria-Gasteiz (UPV/EHU). Another collaboration has been established with the Department of Microbiology of the School of Natural Sciences of the National University of Ireland (NUI) Galway, being Professor Dr. Piet Lens the supervisor of the experimental work. Additional analytical support has been received from the Analytical and High-Resolution Microscopy in Biomedicine and the SGIker service from the UPV/EHU.

This thesis has been funded by the State Agency for Research (AEI) of the Spanish Government and the European Regional Development Fund (FEDER-ERDF, European Union) within the Project CTM2016-77212-P “Desarrollo integral de un proceso de biomecanizado para la fabricación sostenible de piezas metálicas”. Financial support has also been received from the University of the Basque Country UPV/EHU within the research group funding [GIU18/118].

The motivation of this thesis is to efficiently improve the microorganism-assisted metal mobilization process for applications such as the environmentally friendly biomachining of copper pieces and the affordable and sustainable biorecovery of metals from electronic wastes (printed circuit boards). The bacterium *Acidithiobacillus ferrooxidans* (*A. ferrooxidans*) has been selected for exploring the limits of the process. Despite the fact that bioleaching has been studied as a metal mobilization technique for longer than 50 years, its fundamentals can still be used in new promising biotechnological applications, with the guarantee of its high biosecurity level. The selected metal to be biomachined or biorecovered (depending on the application) has been copper. Being an essential trace element for living organisms, copper is also a valuable material in circular economy, 100 % recyclable and one of the most demanded metals in industry. Indeed, a deficit in the copper market is expected to deepen over the next several years, as the supply of this widely used metal struggles to keep up with strong demand for the ever-increasing production of electrical and electronic products such as mobile phones (that,

by the way, still experience low recycling rates). This study aims to contribute to the development of a sustainable technological tool that could be included in the decision-making agenda of legislators, managers and entrepreneurs.

THESIS OVERVIEW

The thesis is divided into 5 sections and 4 chapters. The sections are: Motivations and Thesis Overview, Introduction, Objectives, General Materials and Methods and, Final Conclusions and Future Overlook. The four chapters are devoted to the results obtained for each objective and have the following structure: 1- chapter's objective; 2- particular materials and methods; 3- results and discussion, and 4- chapter's conclusions

A brief overview of each Section and Chapter is given below.

After the section "Motivations and Thesis Overview", the "Introduction" covers a detailed review of the published literature describing previous investigations on metal extraction from metal-containing materials by the action of microorganisms. The main current applications of metal mobilization are detailed in this chapter and the key factors that will affect microbial leaching operation are summarized.

The section "Objectives" deals with the general goals to be achieved. The particular attainable objectives have been included in the corresponding chapter.

The methodology, materials and equipment that are repetitively used throughout the experimental part of this study have been detailed in the section "General Materials and Methods".

Next, Chapter 1 is devoted to the study of the design of an attainable continuous bioprocess that allows the maintenance of the maximum metal removal rate while minimizing the amount of depleted solution.

The increase in cell density inside the bioreactor can lead to achieve greater bio-oxidation rates, rendering the desirable improvement of the metal mobilization efficiency. Therefore, Chapter 2 explores the potential of immobilizing biomass on different support materials for a more effective and sustainable microorganism-assisted metal solubilization process. Consequently, different support materials have been fabricated in the laboratory and the feasibility of each one for microbial immobilization has been studied. The best operating conditions for the successful bacterial immobilization have also been investigated in this section.

As far as applications are concerned, Chapter 3 deals with the biomachining of well-defined microfluidic structures on copper workpieces for the manufacturing of PDMS microfluidic devices. The possibility of engraving different structures with variable machining depths is examined as well as the efficiency of the process when successive treatment and medium regeneration stages are combined. This chapter also focuses on

the extension of the lifespan of the biomachining solution in order to improve the system sustainability and reduce the reagents consumption and waste management.

The electronic waste generation is a global growing concern that brings about the dumping of large amounts of valuable metals. The recovery of these metals could be tackled by biological methods, and thus, Chapter 4 is devoted to studying the applicability of the process for the metal leaching from PBCs contained in mobile phones. This chapter also covers the preliminary design of a lab-scale plant for performing the PCB bioleaching process.

Any metal mobilization system generates liquid residues with high metal concentrations. These solutions have to be adequately managed and, Chapter 5 aims to assess the technical and economic viability of two alternatives for treating one synthetic waste solution obtained in the copper pieces' biomachining. The first option involves recovering the metal by chemical precipitation while the second one investigates the electrochemical method.

Finally, the most relevant conclusions derived from the whole study, together with some suggestions for future work are presented in the section "Final Conclusions and Future Outlook".

OBJECTIVES

OBJECTIVES

The main objective of this thesis is to improve the efficiency of the microorganism-assisted solubilization of copper by proposing strategies that can be applied in the following processes: the biomachining of copper pieces for engraving microstructures and the recovery of that metal from disused mobile telephones. Both applications have been studied using the same bacterium (*A. ferrooxidans*) as it is a very versatile and resistant microorganism with a low biosafety risk.

The secondary objectives are:

- To contribute to the proposal of a semi-continuous metal mobilization process with suspended biomass that allows the maintenance of the maximum removal rate of copper while minimizing the amount of depleted solution. The continuous regeneration of the oxidant will allow the process to work on as long as the biomass is active.
- To explore the potential of using a support material for immobilizing the biomass. That material should be easily biosynthesized in the laboratory, affordable and sustainable.
- To assess the benefits of using immobilized biomass for improving the efficiency of the metal solubilization process, in comparison to suspended biomass.
- To design a process for engraving microstructures on copper pieces with the final objective of manufacturing molds for microfluidic devices. This new application of the biomachining has not been explored so far, and it is an innovative use of that bioprocess with manufacturing perspectives.
- To study the metal extraction efficiency when the printed circuit boards from obsolete mobile telephones are bioleached. The timely pretreatments of the heterogenous PCBs before metal extraction is a challenge to be faced.
- To assess the technical and economic viability of two alternatives for treating the waste solutions obtained in the copper biomachining: chemical precipitation and electrochemical method.

LITERATURE
REVIEW

1. MICROORGANISM-ASSISTED METAL MOBILIZATION

The hydrometallurgical extraction of metals from minerals and the subsequent precipitation and recovery is an ancient technology that was first used in China as early as 100-200 B.C. (Ehrlich, 2001). In the past, the mobilization of the metals in minerals was attributed to an abiotic process and it was only in the 1950s that the first acidophilic iron and sulfur oxidizing bacteria were isolated and identified from acid mining drains, and the on-going research clarified the basic mechanisms of the biosolubilization of the metals (Colmer et al., 1950; Mishra et al., 2005).

Copper extraction from its ores was introduced in Spain by the Arabs in the mines of Rio Tinto around the 18th century. Previously, during the 17th century, more than 2 million tons of copper were obtained by bioleaching in the deposits of the Falun mine (Sweden) (Ehrlich, 2001). It was not until the middle of the 20th century when this process began to be scientifically studied and the presence of the involved bacteria was discovered (Bosecker et al., 1997). Bacteria *A. ferrooxidans* (formerly *Thiobacillus ferrooxidans*) and *Acidithiobacillus thiooxidans* (*A. thiooxidans*) were reported to be responsible for the bioleaching process, being the most studied ones to date.

Nowadays, biohydrometallurgy (or bioleaching) is considered an environmental friendly technology that uses the activity of microorganisms for the recovery metals from minerals, concentrates and recycled or residual materials (Mishra et al., 2005; Rawlings and Johnson, 2007; Gumulya et al., 2018; Kaksonen et al., 2018; Habibi et al., 2020). The microbial role is the continuous bio-regeneration of the oxidizing agent (Fe^{3+}) responsible for the chemical dissolution of the metal. Theoretically, the oxidant is never depleted and the extraction continues as long as the microbial performance is maintained. Consequently, the oxidizing agent does not have to be continuously supplied by chemical addition, with the consequent economic and environmental benefits (Barona et al., 2018)

The most important application of bioleaching in the last century has been mineral extraction, but other biotechnological alternatives based on the same principle have also been studied in recent years. Two of these applications are the biomachining of metallic pieces (the machining of metal pieces by biological methods) and the recovery of metals from waste electrical and electronic equipment (WEEE). Both of them will be detailed in the last sections of this literature review.

2. MICROORGANISMS IN MICROORGANISM-ASSISTED METAL MOBILIZATION PROCESSES

The most distinctive characteristic of any microorganism-assisted metal mobilization process is the use of microorganisms. The main microbial groups involved in the process

are chemolithoautotrophic prokaryotes, heterotrophic bacteria and fungi. In addition, microbial consortiums have also been studied.

2.1. Chemolithoautotrophic bacteria

The group of autotrophic chemolithotrophic bacteria are the most studied microorganisms both in the biomachining of metallic pieces and in the bioleaching of PCBs. This type of organisms presents a high tolerance to heavy metals, being a crucial characteristic that makes them suitable for these applications (Orell et al., 2010). Chemolithotrophic bacteria obtain the energy required for growing from the oxidation of some inorganic compounds such as sulfides, elemental sulfur (S^0), ferrous ions, and, some of them, even from hydrogen ions (Hedrich and Johnson, 2013). In biohydrometallurgy, the most employed chemolithotrophic bacteria are acidophilic bacteria that grow preferably at pH values from 1.5 to 4 under aerobic conditions.

Among the acidophilic ones, the most studied bacterium is *A. ferrooxidans*, due to its ability to oxidize both soluble and non-soluble inorganic substrates (Uno et al., 1993; Wang et al., 2009; Liang et al., 2010; Hocheng et al., 2012b; Hocheng et al., 2012c; Díaz-Tena et al., 2014; Xenofontos et al., 2015; Nie et al., 2015a; Muhammad et al., 2015; Singh et al., 2018). However, the suitability of other microorganisms has also been evaluated both for their application in biomachining and in WEEE bioleaching. Figure 1 shows two common chemolithotrophic microorganisms used in bioleaching processes.

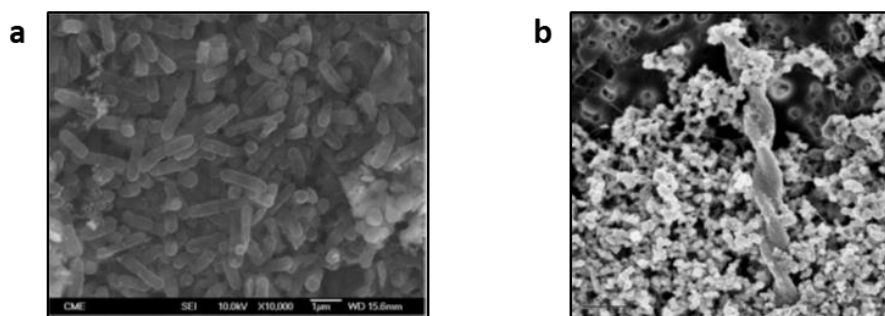


Figure 1. SEM micrograph: *A. thiooxidans* (published by Quatrini et al., 2017) (a) and *Leptospirillum ferrooxidans* (published by Vrdoljak and Spiller, 2005) (b).

Table 1 summarizes some chemolithotrophic microorganisms reported in bibliography.

Table 1. Some chemolithotrophic microorganisms used in microorganism-assisted metal mobilization processes reported in literature.

Name	Type	pH	T (°C)	Reference
<i>Acidithiobacillus ferrooxidans</i>	M.	1.5-4.0	28-35	Wang et al., 2009; Liang et al., 2010; Hocheng et al., 2012c; Díaz-Tena et al., 2014; Xenofontos et al., 2015; Muhammad et al., 2015; Nie et al., 2015a; Singh et al., 2018; Benzal et al., 2020
<i>Acidithiobacillus thiooxidans</i>	M.	2.0-3.5	28-30	Brandl et al., 2001; Chang et al., 2008; Wang et al., 2009; Liang et al., 2013; Isildar et al., 2016; Marra et al., 2018; Naseri et al., 2019; Lee et al., 2020
<i>Acidithiobacillus ferrivorans</i>	M.	1.9-3.4	27-32	Isildar et al., 2016; Peng et al., 2019
<i>Sulfobacillus thermosulfidooxidans</i>	M.T.	1.9-2.4	40-60	Deveci et al., 2004; Ilyas et al., 2007; Díaz-Tena et al., 2018
<i>Acidithiobacillus caldus</i>	M.T.	2.0-2.5	42-45	Zhou et al., 2007; Fu et al., 2008; Wang et al., 2012
<i>Sulfobacillus sibiricus</i>	M.T.	2.0	50	Zhang et al., 2015
<i>Leptospirillum ferriphilum</i>	M.T.	1.5-1.8	45-50	Fu et al., 2008; Gu et al., 2013; Zhao et al., 2015
<i>Acidianus manzaensis</i>	E.T.	1.0-5.0	60-90	He et al., 2009; Zhu et al., 2011; Liu et al., 2016
<i>Sulfolobus metallicus</i>	E.T.	1.3-1.7	65-80	Vilcáez et al., 2008; Plumb et al., 2008
<i>Acidianus brierleyi</i>	E.T.	2.0	65	Konishi et al., 1998; Bharadwaj and Ting, 2013; Samadzadeh et al., 2020
<i>Acidianus copahuensis</i>	E.T.	3.0	75	Castro and Donati, 2016
<i>Metallosphaera sedula</i>	E.T.	2.0-4.5	65-80	Mikkelsen et al., 2007; Yu et al., 2019
<i>Sulfolobus solfataricus</i>	E.T.	2.0-4.0	80	Roshani et al., 2017
<i>Acidithiobacillus albertensis</i>	M.	2.0-4.5	28-50	Xia et al., 2007
<i>Acidianus ambivalens</i>	E.T.	2.0-5.0	80	Roshani et al., 2017
<i>Metallosphaera hakonensis</i>	E.T.	3.0	70	Krok et al., 2013
<i>Sulfolobus acidocaldarius</i>	E.T.	1.0-6.0	55-85	Lindström et al., 1993
<i>Metallosphaera prunae</i>	E.T.	2.0-3.0	75	Stott et al., 2003
<i>Acidianus infernus</i>		1.0-5.5	65-96	Mikkelsen et al., 2006
<i>Thiobacillus prosperus</i>	M.	1.0-4.5	23-41	Huber and Stetter, 1989
<i>Ferroplasma cupricumulans</i>	M.T.	1.0-1.2	22-63	Hawkes et al., 2006

M.: Mesophilic; M.T.: Moderate thermophilic; E.T.: extreme thermophilic.

The thermophiles group can be classified into moderately thermophilic bacteria and extremely thermophilic bacteria according to their optimal growing temperature range. Moderately thermophilic bacteria have an optimal growth temperature between 40-60 °C and comprise strains such as *Sulfobacillus thermosulfidooxidans* (Devici et al., 2004; Ilyas et al., 2007), *Leptospirillum ferriphilum* (Gu et al., 2013, Zhao et al., 2015) or *Acidithiobacillus caldus* (Zhou et al., 2007; Wang et al., 2012). There is an increasing interest in studying thermophilic bacteria, especially for application in the chalcopyrite bioleaching, due to their unique metabolic characteristics and their tolerance to high temperatures, which can enhance the bioleaching kinetics (Deveci et al., 2004; Vilcáez et al., 2008; Zhao et al., 2019). Surprisingly, this group of bacteria apparently are more sensitive to high pulp densities and exhibit a lower tolerance to metal concentration (Panda et al., 2015). The extremely thermophilic bacteria that are able to grow at higher temperatures (between 60 and 90 °C) are scarce in literature. As an example, *Acidianus manzaensis* (He et al., 2009; Zhu et al., 2011) or *Sulfolobus metallicus* (Vilcáez et al., 2008; Plumb et al., 2008) strains can be mentioned.

2.2. Heterotrophic bacteria

Heterotrophic bacteria obtain the energy from the oxidation of organic compounds such as lipids, alcohols, sugars or hydrocarbons and, under appropriate conditions, they produce certain organic amino acids and other metabolites which are responsible for the metal dissolution in the processes (indirect mechanism) (Bosecker, 1997; Brandl et al., 2008; Shabani et al., 2013; Barnett et al., 2018). The ability of metal bioleaching from WEEE by heterotrophic microorganisms has also been reported in literature (Hassanien et al., 2014; Shin et al., 2015; Barnett et al., 2018). The genus *Bacillus* and *Pseudomonas* have been described as the most effective heterotrophic bacteria for metal solubilization (Bosecker et al., 1987; Groudev, 1987). Figure 2 shows two examples of these genus, particularly *Pseudomonas aeruginosa* and *Pseudomonas putida*.

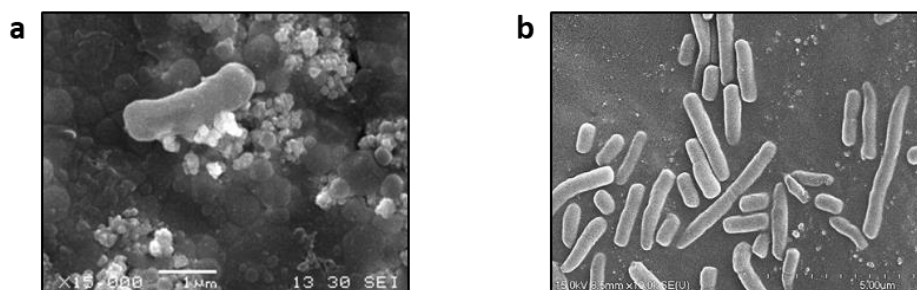


Figure 2. SEM micrograph: *Pseudomonas aeruginosa* (published by Kasuga et al., 2011) (a) and *Pseudomonas putida* (published by Merum et al., 2017) (b).

Heterotrophic cyanide (CN⁻) producing microorganisms such as *Chromobacterium violaceum*, *Bacillus megaterium*, *Pseudomonas fluorescens*, and *Pseudomonas plecoglossicida* have also been used in bioleaching experiments (Brandl et al., 2008; Chi et al., 2011; Natarajan and Ting, 2014; Arshadi and Mousavi, 2015a). In contrast to acidophilic bacteria, these cyanogenic microorganisms are able to mobilize metals under alkaline conditions (Brandl et al., 2008). They are mainly used for the bioleaching of precious metals so that the cyanide required for the complexolysis process is produced by strains like *Pseudomonas putida* and *Bacillus megaterium* (Arshadi and Mousavi, 2015a; Marra et al., 2018). Some heterotrophic microorganisms reported in bibliography are listed in Table 2.

Table 2. Some heterotrophic microorganisms reported in bibliography for microorganism-assisted metal mobilization processes.

Name	Type	Reference
<i>Bacillus cereus</i>	Heterotrophic	Štyriaková et al., 2003; Karwowska et al., 2014
<i>Bacillus licheniformis</i>	Heterotrophic	Mohanty and Misra 1993; Abraham et al., 2020
<i>Pseudomonas putida</i>	Heterotrophic	Isildar et al., 2016; Marra et al., 2018; Bolaños-Benítez et al., 2018
<i>Pseudomonas koreensis</i>	Heterotrophic	Saleh et al., 2019; Nasab et al., 2020
<i>Pseudomonas fluorescens</i>	Heterotrophic	Pham and Ting, 2009; Pradhan and Kumar, 2012; Isildar et al., 2016; Potysz et al., 2016
<i>Pseudomonas aeruginosa</i>	Heterotrophic	Pradhan and Kumar, 2012; Shabani et al., 2013; Yin et al., 2014
<i>Acidiphilium cryptum</i>	Heterotrophic	Beolchini et al., 2009; González et al., 2018
<i>Enterobacter aerogenes</i>	Heterotrophic	Fathollahzadeh 2018
<i>Bacillus mucilaginosus</i>	Heterotrophic	Zhang and Li, 2017
<i>Chromobacterium violaceum</i>	Cyanogenic	Pham and Ting, 2009; Chi et al., 2011; Pradhan and Kumar, 2012; Shin et al., 2013; Natarajan and Ting, 2014; Faramarzi et al., 2020
<i>Bacillus megaterium</i>	Cyanogenic	Arshadi and Mousavi, 2015a
<i>Pseudomonas Chlororaphis</i>	Cyanogenic	Ruan et al., 2014

2.3. Fungi and yeasts

Similarly to microbial leaching with heterotrophic bacteria, heterotrophic fungal bioleaching involves an indirect process in which microorganisms produce some organic

acids, amino acids or other kind of metabolites (Rezza et al., 2001; Ren et al., 2009). These metabolites dissolve metals from minerals by displacement of the metal ion from the ore matrix rendering soluble metal complexes and chelates (Burgstaller and Schinner 1993; Thangavelu et al., 2006; Sajjad et al., 2019). However, the fungal bioleaching process requires higher operating costs compared to the bacterial leaching since they need the continuous supply of organic compounds for their effective growth and consequent production of leaching agents (Wu and Ting, 2006; Ilyas et al., 2013a). Although several studies have been carried out in the field of fungi bioleaching, this process is far from being profitable because of the poor recovery performance (Tang and Valix, 2006; Pathak et al., 2021).

Nevertheless, fungal bioleaching presents a clear advantage over bacterial bioleaching since fungi are able to grow at higher pH values, generally in the range from 2 to 7. This feature makes them suitable for alkaline leaching since the process performance is higher at higher pH values (Burgstaller and Schinner, 1993; Jadhav et al., 2016).

Aspergillus and *Penicillium* are the most effective genus in biominery processes involving fungi. Particularly, *Penicillium simplicissimum* and *Aspergillus niger* strains have been extensively studied due to their ability to produce elevate concentrations of organic acids (Qu et al., 2013; Rasoulnia and Mousavi, 2016; Faraji et al., 2018; Chakankar et al., 2019).

Yeast is also another appealing alternative as it is able to adapt to extreme conditions of pH, temperature, toxicity... (Bahafid et al., 2017). *Rhodotorula rubra*, *Rhodotorula mucilaginosa*, *Blastoschizomyces capitatus*, *Brettanomyces* sp., *Yarrowia lipolytica* and *P. spartinae* are some of the yeasts studied in literature (Rezza et al., 2001; Gamache et al., 2001; Fang and Zhou, 2007; Gu and Wong, 2007; Zheng et al., 2009; Bankar et al., 2012).

2.4. Microorganism consortium

The simultaneous use of several types of microorganisms (pure strains or mixed cultures) can enhance the selective dissolution of metals. It is an effective alternative to pure strains since the selection of a consortium containing suitable microorganisms can accelerate the process (Ilyas et al., 2013b). For example, Shah et al. (2015) employed a consortium including *Leptospirillum ferriphilum* for the recovery of Cu, Zn, and Ni from the printed circuit boards of computers (PCBs). Vermeulen and Nicolay (2017) used a mixed culture of iron oxidizing bacteria composed of *A. ferrooxidans*, *Leptospirillum ferrooxidans* and *Leptospirillum ferriphilum* for the treatment of pure Cu. Likewise, Isildar et al. (2016) concluded that the mixed culture of *A. thiooxidans* and *A. ferrooxidans* enhanced the mobilization of Cu present in the dust of computer and mobile phones PCBs, compared to the performance with pure cultures. Similarly,

Pradhan and Kumar (2012) obtained a greater bioleaching efficiency of Cu, Au, Zn, Fe and Ag using mixed cultures of *Chromobacterium violaceum*, *Pseudomonas fluorescens* and *Pseudomonas aeruginosa* than the corresponding pure cyanogenic bacterial strains. Some of the microorganism consortiums employed in microorganism-assisted metal mobilization processes are listed in Table 3.

Table 3. Some of the microorganism consortiums employed in microorganism-assisted metal mobilization processes.

Microorganism consortium	Reference
Consortium of chemolithotrophic, mesophilic bacteria	
<i>Acidithiobacillus thiooxidans</i> and <i>Acidithiobacillus ferrooxidans</i>	Wang et al., 2009; Liang et al., 2010
<i>Acidithiobacillus ferrooxidans</i> , <i>Leptospirillum Ferrooxidans</i> and <i>Leptospirillum ferriphilum</i>	Vermeulen and Nikolay, 2017
<i>Thiobacillus ferrooxidans</i> , <i>Thiobacillus thiooxidans</i> and <i>Leptospirillum ferrooxidans</i>	Lewis et al., 2011
<i>Acidithiobacillus ferrooxidans</i> and <i>Leptospirillum ferrooxidans</i>	Díaz-Tena et al., 2016
Consortium of chemolithotrophic, thermophilic bacteria	
<i>Sulfobacillus thermosulfidooxidans</i> and <i>Thermoplasma acidophilum</i>	Ilyas et al., 2013b
<i>Sulfobacillus thermosulfidooxidans</i> and <i>Sulfobacillus acidophilus</i>	Ilyas et al., 2013b
Consortium of heterotrophic, cyanogenic bacteria	
<i>Chromobacterium violaceum</i> , <i>Pseudomonas fluorescens</i> and <i>Pseudomonas aeruginosa</i>	Pradhan and Kumar, 2012
Consortium of heterotrophic fungi	
<i>Purpureocillium lilacinum</i> and <i>Aspergillus niger</i>	Xia et al., 2018
<i>Penicillium simplicissimum</i>	Brandl et al., 2001

Regarding the microbial sources, an increasingly studied alternative to obtain the active biomass is the use of mixed cultures isolated directly from different natural sources. From a practical point of view, an additional advantage of this type of consortium is that the inoculum can be taken directly from the microbial source, and the need to isolate them and work in sterile conditions can be eliminated (Valix, 2017). Some of these sources are: mine leachates (Xiang et al., 2010; Zhu et al., 2017), active sludge from wastewater treatment stations (Wang et al., 2016; Wang et al., 2018), marine sponges

(Rozas et al., 2017), or metal contaminated soil (Xia et al., 2018). Table 3 shows some particular microorganism consortia used in these processes.

3. *Acidithiobacillus ferrooxidans* GENUS

As mentioned above, *A. ferrooxidans* is one of the most employed bacteria in metal mobilization process because is able to oxidize soluble and non-soluble inorganic substrates and due to its ability to survive at high metal concentrations (Wu et al., 2010; Cabrera et al., 2015).

A. ferrooxidans strain was originally isolated from acid mine drainage by Colmer and Hinkle in 1947 (Temple and Colmer, 1951). *A. ferrooxidans* is a Gram-negative chemolithoautotrophic aerobic bacterium which belongs to the genus *Acidithiobacillus* (Barron and Lueking, 1990; Valdés et al., 2008). It is characterized by rods and rounded ends and it is approximately 0.5–0.6 μm width by 1.0–2.0 μm length (Figure 3). A single polar flagellum is used for motion (Jensen and Web, 1995; Johnson, 2007; Liu et al., 2009).

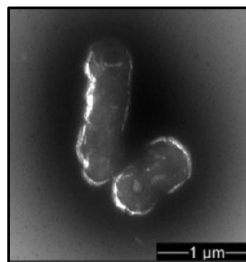


Figure 3. SEM micrograph of the mesophilic *A. ferrooxidans* bacteria (published by Diaz-Tena et al., 2014).

According to Nemati et al. (1998), *A. ferrooxidans* is characterized by five main properties:

- 1- It is a **chemolithotrophic** bacterium as it uses carbon dioxide as a carbon source and their energy source is the oxidation of ferrous iron or sulfur and the reduction of sulfur compounds in acidic environments (Temple and Colmer, 1951; Quatrini et al., 2006; Zhan et al., 2019).
- 2- It is an **autotrophic** microorganism since the main carbon source is carbon dioxide and it needs nitrogen and phosphorus as nutrients to grow, as well as trace minerals such as K, Mg, Na, Ca and Co.
- 3- *A. ferrooxidans* is an **aerobic** bacterium since oxygen is essential as an electron acceptor. Ambient air provides both oxygen and CO₂. Despite its classification as a strictly aerobic bacterium, it is also able to grow in the presence of elemental sulfur or metal sulfides under anaerobic conditions using ferric ions as electron acceptor (Pronk et al., 1992; Malki et al., 2006).

- 4- It is considered a **mesophilic** microorganism since it grows in the temperature range between 20 and 40 °C, being the optimum temperature 20-33 °C (Zhang et al., 2013).
- 5- It is an **acidophilic** bacterium since it can live at a pH between 1.5 and 4.0 with an optimum value of 2.0. It can unlikely survive at pH above 6.5 or below 1.0 (Valdés et al., 2008).

Based on their outstanding versatility, *A. ferrooxidans* bacteria are widely used in scientific studies because they are capable of oxidizing both iron and sulfur ores while other strains such as *L. ferrooxidans* or *A. thiooxidans* are exclusively iron-oxidizing and sulfur-oxidizing microorganisms respectively (Boon, 2001; Yang et al., 2009a). Additionally, it has been used in genome sequencing projects. Table 4 summaries some metal solubilization efficiencies reported in literature when employing *A. ferrooxidans* bacteria

Table 4. Metal solubilization efficiencies (%) reported in literature employing *A. ferrooxidans* bacteria.

Solubilized materials	Strain	Conditions	Particle size	Pulp density	Efficiency (%)	Reference
Low-grade uranium ore	--	pH 2.0, 30 °C, 150 rpm	20–40 meshes	15 g L ⁻¹	Cu: 96.8 Zn: 83.8 Al: 75.4	Pal et al., 2010
WPCBs	SW-02	pH 2.25, 30 °C, 170 rpm, 72 h	114 µm	8.5 g L ⁻¹	Cu: 100 Ni: 100	Yang et al., 2014
Spent household batteries	PTCC 1647	pH 1.0, 30 °C, 160 rpm, 20 d	95 µm	20 g L ⁻¹	Ni: 100 Cu: 100	Bajestani et al., 2014
Cellphone PCBs	PTCC1626	pH 1, 30 °C, 170 rpm, 17 d	--	5.0 %	Mn: 99.5 Zn: 78.4 As > 60 Cu: 31.5	Arshadi and Mousavi, 2015b
Mine tailings	--	pH 2.5, 30 °C, 200 rpm, 25 d	--	10.0 %	U: 49.0	Nguyen et al., 2015
PCB	Z1	pH 2.25, 30 °C, 160 rpm, 183 h	0.178–0.250 mm	12 g L ⁻¹	Cu: 92.6 Al: 85.2 Zn: 95.2	Yang et al., 2017
Uranium ore	--	pH 1.7, 30 °C, 120 rpm, 10 d	62 µm	10 g L ⁻¹	Ni: 87.0 Cd: 67.0 Co: 93.7	Wang et al., 2018
PCBs	ATCC 23270	pH 2.0, 30 °C 160 rpm, 7d	--	--	Cd: 71.9 Mn: 92.5 Zn: 89.1	Annamalai and Gurumurthy, 2019
PCBs	--	130 rpm, 30 °C, 25 d	<100 µm	1.5 %	Cu: 90 Ni: 88	Arshadi and Yaghmaei, 2020
WPCBs	ATCC 19859	170 rpm, 30 °C, pH 2.5, 18 d	0.075–1 mm	7.5 g L ⁻¹	Cu: 90 Ag: 42 Au: 31	Priya and Hait, 2020

4. MECHANISMS OF MICROBIAL METAL MOBILIZATION

Ideally, the metal oxidation can be an endless process as long as the microbial activity is maintained. The practical difficulties and limitations in maintaining that activity will be presented in next sections, but previously the main mechanisms of the bioprocess will be described below.

The mechanisms for microbial leaching were originally proposed for sulfide minerals and can be classified according to:

- 1- the type of contact between the bacteria and the solid: direct, indirect and cooperative mechanism (Tributsch, 2001; Mahmoud et al., 2017)
- 2- the type of intermediate compounds: Thiosulfate and Polysulfide mechanism
- 3- the type of reactions involved in the process: acidolysis, redoxolysis, complexolysis and, to a lesser extent, bioaccumulation.

4.1. Direct mechanism

In the direct mechanism, the solubilization of metal sulfides occurs directly through the oxidation by microorganisms. This mechanism is also called contact leaching mechanism since physical contact between mineral surfaces and the microorganisms is required and metals are solubilized by microorganism through the secretion of extracellular polymeric substance (EPS) by means of enzymatic reactions (Gehrke et al., 1998; Tributsch, 2001; Okoh et al., 2018). Contact bioleaching of minerals can occur even in the absence of oxidizing agents (e.g. ferric ions) (Rohwerder et al., 2003) (Figure 4a).

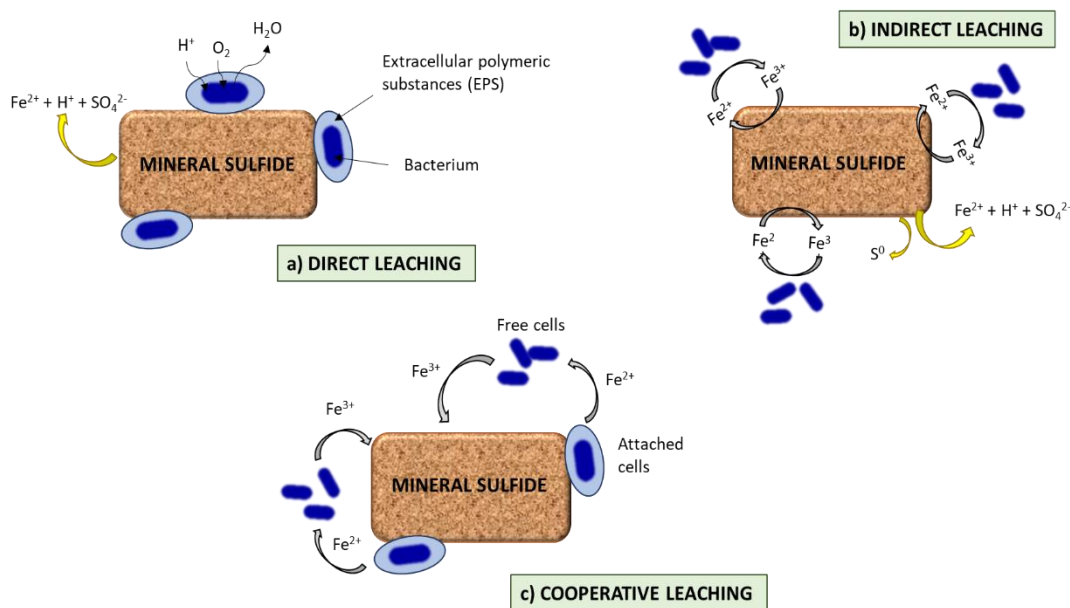
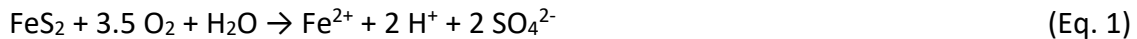


Figure 4. Schematic diagram of microbial leaching mechanisms: direct mechanism (contact leaching) (a), indirect mechanism (non-contact leaching) (b) and cooperative leaching (c).

Although the exact mechanism used by *A. ferrooxidans* to colonize surfaces has not been clarified yet, these bacteria can cover surfaces with a dense biofilm and a correlation between pilus expression and strong attachment has been found (Li et al., 2010). The EPSs produced by this microorganism are composed of neutral sugars, fatty acids and uronic acids. They mediate attachment to the surface and concentrate Fe^{2+} ions by complexation through uronic acids and other metabolites (Li et al., 2010)

The following direct or contact mechanism for iron leaching has been proposed (for *A. ferrooxidans* bacteria) (Sand et al., 2001):



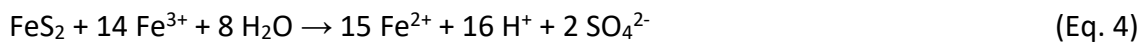
Or the general global equation shown below can be used to summarize the direct leaching mechanism from metal sulfides, where it can be noted that the final product is the metal sulphate (Bosecker et al., 1997):



4.2. Indirect mechanism

The indirect bioleaching process takes place without physical contact between the bacteria and the solid (Sand et al., 2001; Kumar and Yaashikaa, 2020). Therefore, it is also called non-contact mechanism (Tributsch, 2001). The metal is oxidized by the action of the ferric ion (oxidizing agent). Thus, the ferric iron is capable of oxidizing metals while being reduced to ferrous iron. The latter is microbially oxidized again into Fe^{3+} , leading to a cyclic oxidation process (Hamidian, 2011; Mishra and Rhee, 2014) (Figure 4b).

Indirect bioleaching mechanism for the oxidation from metal sulfides can be described as follows (for *A. ferrooxidans* bacteria) (Sand et al., 2001):

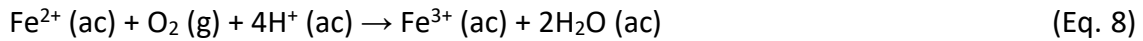


For the specific case of pure metal leaching the equations are as follows:

Chemical process for metal dissolution



Biochemical regeneration of the oxidant Fe^{3+}



4.3. Cooperative leaching/mechanism

It has been reported that cooperative leaching between attached and planktonic cells is possible (Rojas-Chapana et al., 1998). In this case, the bacteria attached to mineral surfaces supply Fe^{2+} and S to the planktonic cells as their energy source. Then the ferrous ion is oxidized by free cells, supplying the oxidant which is further used in indirect leaching (Tributsch, 2001; Li et al., 2013). Consequently, it is therefore a combination between the direct and indirect mechanism, or contact and non-contact mechanisms (Zhang et al., 2018) (Figure 4c).

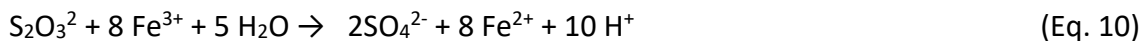
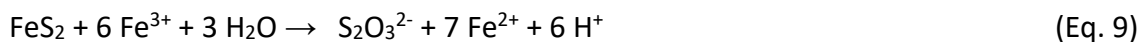
4.4. Thiosulfate and polysulfide mechanism

Thiosulfate mechanism is based on the oxidation of acid-insoluble sulfides FeS_2 , MoS_2 , and WS_2 (pyrite, molybdenite, and wolframite) by the Fe^{3+} ions with the thiosulfate as the main intermediate and sulfate as the end-product (Hamidian, 2011).

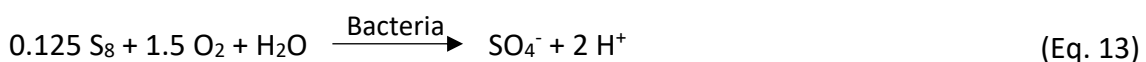
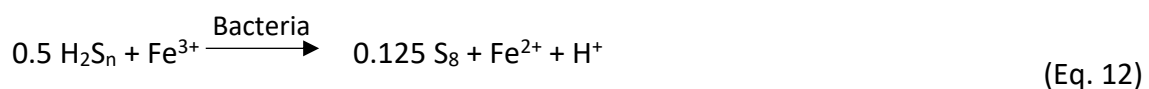
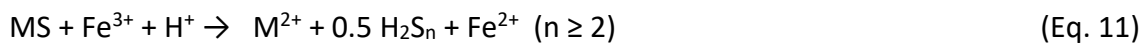
In the polysulfide mechanism, mineral solubilization such as sphalerite, galena, or chalcopyrite (ZnS , PbS , CuFeS_2 , respectively) occurs through a combined attack of ferric iron and protons. In this case, the main intermediates are polysulfides and elemental sulfur (Figure 5). The generated elemental sulfur can be oxidized to sulfate in the presence of sulfur-oxidizing microbes as shown in Equation 13.

The two mechanisms are summarized by the following equations (Sand et al., 2001):

Thiosulfate mechanism:



Polysulfide mechanism:



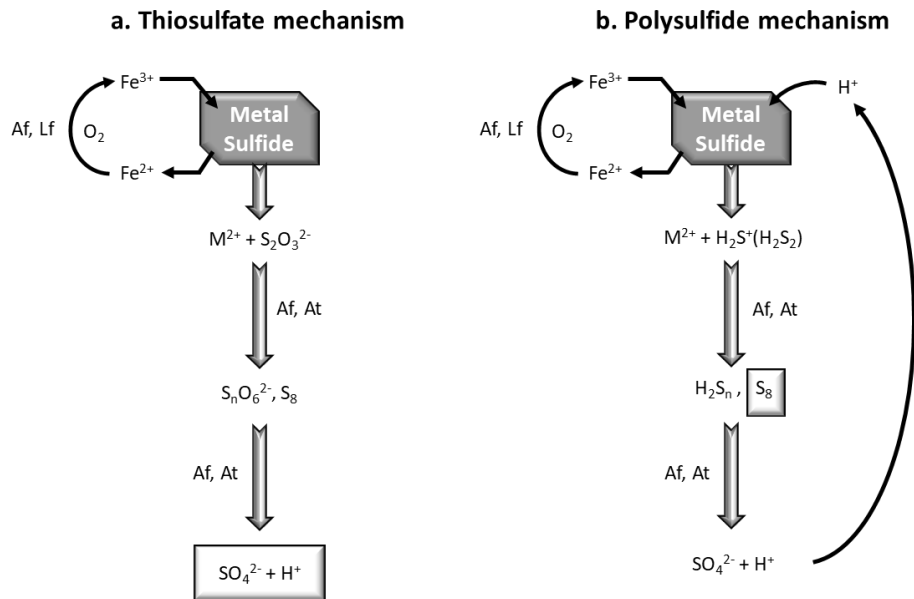


Figure 5. Schematic diagram of thiosulfate (a) and polysulfide (b) mechanisms in bioleaching (adapted from Rohwerder et al., 2003).

4.5. Mechanisms according to the type of reaction

Microbial metal mobilization can also be described according to the type of reaction involved. Thus, it can take place by acidolysis (formation of organic or inorganic acids), redoxolysis (oxidation-reduction process), complexolysis (formation of complexes and chelates) and, to a lesser extent, bioaccumulation (Bosshard et al., 1996; Wu and Ting, 2006; Okoh et al., 2018).

4.5.1. Redoxolysis

Redoxolysis mechanism is divided into direct and indirect mechanism (Watling, 2006). Thus, metals can be dissolved both directly by the direct contact with bacterial cells or with their extracellular compounds (direct mechanism or “contact” mechanism) or indirectly by the metabolic products generated by the biomass (indirect or non-contact mechanism) (Isildar et al., 2016; Cornu et al., 2017). Microorganisms playing a role in redoxolysis processes obtain energy from solid minerals and the iron oxidizing *A. ferrooxidans* or sulfur oxidizing *A. thiooxidans* bacteria can be particularly highlighted.

Ferric iron (Fe^{3+}) ion is one of the most common redoxolysis agents in leaching systems as it is a strong oxidant with a standard reduction potential of +0.770 V(SHE) (Diaz-Tena et al., 2016; Isildar et al., 2016). Redoxolysis process is based on the previously described non-contact mechanism where a cyclic oxidation process takes place. In addition, some microbial strains are capable of oxidizing S^0 under anaerobic conditions, reducing Fe^{3+} to Fe^{2+} (Rawlings, 2005).

In the redoxolysis mechanism, the redox potential is an essential parameter controlling the process since it is related to the $[\text{Fe}^{3+}]/[\text{Fe}^{2+}]$ concentration ratio. This value increases as long as the ferrous iron is being oxidized into ferric iron and it is related to the formation of sulfuric acid. Thus, the redox potential is a quick and convenient parameter to determine the biomachining/bioleaching progress (Rohwerder et al., 2003; Diaz-Tena et al., 2016).

4.5.2. Acidolysis

In this case, the metal solubilization is achieved by the action of organic (malic, oxalic, gluconic, acetic, citric) and inorganic (H_2SO_4) acids produced by microorganisms. The protons becoming from the acids synthesized by these microorganisms, are capable of weakening the bond of metal ions rendering the dissolution of the metal (Burgstaller et al., 1992; Brandl and Faramarzi, 2006). The oxygen atoms that cover the metal surface are quickly protonated. Then the protons and the oxygen combine with water and, therefore, the metal is detached from the surface (Amriri, 2012; Bahaloo-Horeh et al., 2018; Xia et al., 2018).

Although this mechanism can be performed by autotrophic sulfur oxidizer microorganisms (*A. thiooxidans*), acidolysis is the principal mechanism in metal mobilization processes involving heterotrophic fungal strains (Anjum, 2009, Vakilchap et al., 2016).

The following equation represents the mechanism of acidolysis,



(MeO, being the metal oxide)

4.5.3. Complexolysis

Unlike acidolysis, the organic acids produced by certain microorganisms (*Aspergillus niger*, *Penicillium spp.*, or *Rhizopus spp.*, among others) act as chelating agents which are capable of leaching metals through the formation of complexes (Mishra and Rhee, 2014; Horeh et al., 2016). Complexolysis process is slower than acidolysis, although both mechanisms can occur jointly (Okoh et al., 2018). Apart from organic acids, other metabolites, such as siderophores can form complex and solubilize metals such as the ferric iron (Shenker et al., 1999, Gadd, 2004; Osman et al., 2019).

4.5.4. Bioaccumulation

Bioaccumulation consists of the accumulation of organic or inorganic pollutants inside living microorganisms (Barron et al., 1995; Chatterjee et al., 2020). However, there is a

controversy about the “bioaccumulation” concept when the pollutant accumulation occurs in dead cells (biosorption) (Chojnacka, 2007; Velásquez and Dussan, 2009).

Several microorganisms such as bacteria, fungi, yeast, and some algae are able to accumulate heavy metals by bioaccumulation and by biosorption (Aksu and Karabayır, 2008; Park et al., 2010). For instance, *Aspergillus niger*, *Aspergillus foetidus*, *Aspergillus nomius*, *Trichoderma harzianum*, *Aspergillus lentulus* and *Yarrowia lipolytica* are reported to be metal bioaccumulators (Dursun et al., 2003; Ge et al., 2011; Mishra Malik, 2012; Zotti et al., 2014; Chatterjee et al., 2019).

The main drawback of this process is the toxicity of high concentrations of the metal in the medium which could cause the death of bioaccumulator strains (Chojnacka, 2007; Ge et al., 2011).

5. FACTORS INFLUENCING MICROORGANISM-ASSISTED METAL MOBILIZATION

As every biological system, this process is affected by several factors such as bacterial concentration, temperature, pH, shaking speed or the presence of inhibitors, among others (Díaz-Tena et al., 2016). In this type of processes, the iron concentration (oxidant) in the medium is also a relevant variable.

The studies carried out to date have concluded that the optimal operating conditions (optimal values for temperature, pH, Fe^{2+} concentration, and others) are dependent on the strain used in each specific case. Therefore, the influence of these factors is common to many biotechnological applications, although specific features have to be considered in each particular case.

The main factors that affect the microorganism-assisted metal mobilization process are described below.

5.1. Temperature

In order to maintain optimal bacterial growth conditions, it is necessary to establish a suitable temperature range during the bioleaching process. Each microorganism requires different optimal temperature conditions. Thus, mesophilic microorganisms (the most typical ones in bioleaching/biomachining processes) grow at temperatures between 25 and 40 °C (Rawlings, 1997; Leahy et al., 2007; Kumar and Yaashikaa, 2020), while thermophiles grow at temperatures above 40 °C (Plumb et al., 2008; Dopson and Johnson, 2012, Donati et al., 2016). For example, *A. ferrooxidans*, the most common microbe associated with bioleaching/biomachining processes, has its optimum growing temperatures at 30 °C, and it loses its activity at temperatures below 10 °C or above 40 °C (Modak et al., 1996, Mousavi et al., 2007, Karimi et al., 2010).

Temperature is also a determining parameter for increasing oxidation reaction rates, as deduced from the Arrhenius equation (Levenspiel, 2005; Franzmann et al., 2005; Leahy et al., 2007).

5.2. pH

In addition to being related to the microbial growth, the pH value is closely related to the metal dissolution efficiency and to the formation of precipitates in the culture medium. The pH in the 2.0 and 3.0 range is the optimal value for bacteria to oxidize ferrous iron (Kumar and Yaashikaa, 2020).

The metal solubilization process involves acid consuming reactions, which causes the pH increase thorough the process (Vilcaez et al., 2008) (Equation 8). If the pH exceeds the value of 2.2, the precipitation of metals and the formation of jarosite are clear inconvenients (Xenofontos et al., 2015). Therefore, working at pH values as low as possible (depending on the bacterial strain employed) can increase the efficiency of the metal mobilization since most of the metals are usually solubilized under low pH values (Ilyas et al., 2007; Xiang et al., 2010).

5.3. Shaking speed

An optimal shaking speed provides the appropriate conditions for the microbial growth, as well as an efficient contact between the material to be treated and the culture medium. In addition, shaking speed is a parameter that affects the bioprocesses such as biomachining and bioleaching of PCBs.

As far as the biomachining of metallic workpieces is concerned, some authors have concluded that the specific metal removal rate (SMRR) when using *A. ferrooxidans* strains keeps to a minimum if agitation is not provided, and that it considerably increases when increasing the shaking speed (Jadhav et al., 2013; Xenofontos et al., 2015; Díaz-Tena et al., 2016). However, this increase is not linear at high shaking speeds (Xenofontos et al., 2015). Jadhav et al. (2013) concluded that the optimal shaking speed is 150 rpm under the tested conditions (treatment of copper pieces at 30 °C using the supernatant from a culture of *A. ferrooxidans* (13823) strain with an initial iron concentration of approximately 3.6 g Fe²⁺ L⁻¹). These authors obtained the highest SMRR value (15.9 ± 1.3 mg Cu h⁻¹ cm⁻²) at 150 rpm, in comparison to the results obtained when shaking more vigorously.

In the case of bioleaching treatment of electronic waste, many experiments have been reportedly carried out at shaking speeds of 150 rpm (Brandl et al., 2001; Shah et al., 2015; Isildar et al., 2016; Marra et al., 2018; Wang et al., 2018), although, in a lesser

extent, lower speeds (120 rpm) (Xiang et al., 2010) and higher ones (up to 200 rpm) (Ilyas et al., 2007; Liang et al., 2010) have also been studied.

5.4. Bacterial concentration and biomass immobilization

The bacterial density plays an important role in the process efficiency, since it determines the time required by bacteria to re-oxidize all the Fe^{2+} to Fe^{3+} (Zhu et al., 2017). In general, a constant cell concentration is recommended during the process in order to avoid the reduction in the dissolution rate of metals (Díaz-Tena et al., 2016).

One of the alternatives proposed by some authors to increase the cell density through the process is the immobilization of the microorganisms on suitable support materials that allows growth on their surface. Some of the materials proposed by different authors for the immobilization of the *A. ferrooxidans* bacterium are shown in Table 5.

Table 5. Different support materials reported in bibliography for *A. ferrooxidans* immobilization.

Support material	Operating conditions ^a	Reference
Nickel alloy fibre	pH 1.8, 10 % inoc., 200 rpm, 30 °C, 600 mL	Gomez et al., 2000
Ceramic beads	pH 1.6, 10 % inoc., air, 30 °C, 500 mL	Junfeng et al., 2007
Hemp fibres	pH 1.6, 10 % inoc., 180 rpm, 30 °C, 50 mL	Akhlaghi, 2019
Monolithic particles	pH 1.6, 30 °C, air	Kahrizi et al., 2008
Chitosan beads	pH 1.8, air, 30 °C, 100 mL	Giaveno et al., 2008
Cotton gauze		
Activated carbon	pH 2.0, 10 % inoc., air, 30 °C, 500 mL	Zhu et al., 2017
Zeolite		
Cotton gauze	pH 2.0, 10 % inoc., air, 30 °C, 500 mL	Nie et al., 2015b
Foam material	pH 1.5-2.0, 10 % inoc., 240 rpm, 30 °C	Jaisankar and Modak, 2009
SulfSDVB-GAC		
SulfSDVB	pH 1.8, 10 % inoc., 200 rpm, 35 °C,	Koseoglu-Imer and
PUF	200 mL	Keskinler, 2013
Biocellulose	pH 1.8, 5 % inoc., 170 rpm, 31 °C, 100 mL	Santaolalla et al., 2021

^aProcesses that do not specify shaking speed is because are shaken by air injection, (indicated as air).

Most of the studies have been carried out with the *A. ferrooxidans* bacterium, due to its natural tendency to immobilization (Nemati et al., 1998; Giaveno et al., 2008; Jaisankar et al., 2009). These studies have focused on investigating the immobilization process and the capacity of the immobilized biomass to oxidize Fe^{2+} . On the contrary, little data is available about the activity of the immobilized biomass during the metal leaching stage or the influence of the increasing metal concentration throughout the process.

The encapsulation of the biomass in a matrix is another alternative for biomass immobilization. In addition to ensuring adequate cell density, this option has a protective effect against shaking turbulences (Vermeulen and Nikolay, 2017). Likewise, Giaveno et al. (2008) have concluded that a packed reactor with chitosan beads in which *A. ferrooxidans* had previously been grown could operate with a medium flow rate up to eight times higher than a reactor with free cells culture. Another advantage of biomass encapsulation is the greater tolerance to increasing copper concentrations, in comparison to the cell suspension mode (Vermeulen and Nikolay, 2017).

5.5. Iron concentration

Iron is the main actor in the bioleaching and biomachining process when the *A. ferrooxidans* bacterium is employed, since it contributes to the microbial growth and the metal dissolution process. As far as the growth stage of *A. ferrooxidans* bacteria is concerned, it is affected by the concentration of iron in the medium in different ways. First, the concentration of Fe^{2+} has an impact on the time required by the culture to oxidize all Fe^{2+} to Fe^{3+} , with longer times being necessary as the initial Fe^{2+} concentration increases (Jadhav et al., 2013). Second, the cell concentration also seems to be affected by the initial concentration of Fe^{2+} in the culture medium. In a study carried out by Hocheng et al. (2012c) using *A. ferrooxidans* (BCRC 13820) strain, these authors reported that the cell concentration practically doubled when the concentration of Fe^{2+} in the medium increased from 11 to 22 $\text{g Fe}^{2+} \text{ L}^{-1}$ while the increase was less noticeable when the concentration of Fe^{2+} was 3 and 4 times higher.

Kawabe et al. (2003) concluded that excessively high concentrations of Fe^{3+} can inhibit the oxidation of Fe^{2+} by *A. ferrooxidans* bacterium and that the degree of inhibition is a function of the strain used. Thus, the T23-3 strain is capable of oxidizing Fe^{2+} with concentrations of 26 $\text{g Fe}^{3+} \text{ L}^{-1}$ in the medium, while the activity of the ATCC19859 strain is completely inhibited at 16 $\text{g Fe}^{3+} \text{ L}^{-1}$.

In the biomachining process, the increasing concentrations of Fe^{3+} enforces the dissolution of the metal (copper in most studies) and allows a higher specific metal removal rate (SMRR) to be achieved. However, too high concentrations of this ion are not recommended for industrial application, since the final surface quality of the biomachined piece would be very poor, the sulfuric acid consumption would increase

and uncontrolled jarosite precipitation would take place (Díaz-Tena et al., 2016). Jadhav et al. (2013) have observed a linear tendency in the increment of SMRR with iron concentration (in the range 3.6-14.8 g L⁻¹, approximately), although the surface deterioration was considerably greater when the highest concentrations were tested (at 30 °C using the supernatant of *A. ferrooxidans* (13823) culture).

In the WEEE bioleaching process, Yang et al. (2009a) have concluded that the higher the concentration of Fe³⁺ in the medium, the faster the copper in the PCBs dissolved. Thus, the time required to solubilize all the copper present in the PCB was reduced from 96 to 36 h when the concentration was increased from 2.4 to 6.7 g Fe³⁺ L⁻¹ (*A. ferrooxidans* culture at 30 °C and 165 rpm). In a process in which the growth of microorganisms and the solubilization of metals took place simultaneously, Xiang et al. (2010) have found that the rate of metal leaching increased with the concentration of Fe²⁺ up to 9 g Fe²⁺ L⁻¹, but it decreased with the presence of 12 and 15 g Fe²⁺ L⁻¹, which was attributed to the jarosite precipitation and the consequent passivation of the surface to be treated. Xiang et al. (2010) and Khatri et al. (2018) have jointly concluded that an initial concentration of 9 g Fe²⁺ L⁻¹ is the adequate one that allows obtaining a higher solubilization of metals when using two consortiums of microorganisms with different origins.

5.6. Presence of process inhibitors

The presence of a variety of metals in the leaching medium can exert a toxicological effect on microbial growth. As an example, copper is essential for the metabolic activity of *A. ferrooxidans*, since it serves as an electron donor during the microbial growth process and it has been found in the structure of *Rusticyanin*, a protein that acts as an electron transporter (Lilova et al., 2007; Mykytczuk et al., 2011; Cornu et al., 2017). Conversely, high concentrations can induce the denaturation of proteins and nucleic acids, causing the biomass death (Valix, 2017). Therefore, the presence of certain concentrations of metals in solution, which are continuously produced during the process, can inhibit bacterial activity (Lilova et al., 2007). Nevertheless, some authors have suggested that the tolerance of microorganisms to different metals can be increased if they are adapted to the metal presence during their activation (Ilyas et al., 2007; Liang et al., 2013; Ravindra et al., 2015; Pourhossein and Mousavi, 2018).

In the particular case of the WEEEs bioleaching, toxic elements including a large number of metals (Ag, Al, As, Cd, Cr, Cu, Fe, Hg, Mn, Ni, Pb and Zn) can be dissolved, as well as other organic components and epoxy resins (Ongondo et al., 2011; Isildar et al., 2016).

In order to increase the tolerance of the microorganisms to the toxic presence, three main strategies have been studied: a) the pre-acclimation of the microorganisms to heavy metals' presence before carrying out the leaching stage (Ilyas et al., 2007; Liang et al., 2010), b) the use of consortia of microorganisms (Ilyas et al., 2007; Ilyas et al.,

2013b) and c) cellular adaptation by treating the wastes in several stages (Xiang et al., 2010).

The metal concentration values with toxicological effects reported in bibliography vary depending on the bacterial strain and the operating conditions. As an example, in the case of the culture of bacteria *A. ferrooxidans* isolated from Río Tinto (Huelva, Spain), Cabrera et al. (2005) concluded that this strain was able to tolerate the following metal concentrations: 0.4 g Cr³⁺ L⁻¹, 10 g Cu²⁺ L⁻¹, 10 g Cd²⁺ L⁻¹, 30 g Zn²⁺ L⁻¹ and 30 g Ni²⁺ L⁻¹. These limit values varied when a consortium of heterotrophic *Acidiphilium* bacteria was added to the culture, obtaining in this case limit values of 0.4 g Cr³⁺ L⁻¹, 4 g Cu²⁺ L⁻¹, 10 g Cd²⁺ L⁻¹, 40 g Zn²⁺ L⁻¹ and 15 g Ni²⁺ L⁻¹. Das et al. (1998) used an *A. ferrooxidans* strain isolated from the Malanjhand copper mine (India) and it was found to survive in the presence of 20 g Cu²⁺ L⁻¹ in a single culture stage.

Tolerance was significantly increased in a study by Vermeulen and Nikolay (2017), in which the encapsulation of *A. ferrooxidans* (DSM 11477) in polyvinyl alcohol allowed to obtain an oxidation rate of Fe²⁺ to Fe³⁺ in the presence of 40 g Cu²⁺ L⁻¹ 2-3 times higher than that obtained by the free cells.

5.7. Precipitate formation

When Fe³⁺ accumulates in the leaching medium and the pH of the solution increases, Fe³⁺ may precipitate as jarosite, which can lead to a loss of 77 % of the iron available in the solution (Xiang et al., 2010; Wang et al., 2018). Likewise, precipitates can cover the surface to be treated, thus preventing the dissolution of the metals (Pradhan et al., 2008; Xiang et al., 2010). Therefore, the formation of precipitates has an influence both on the process efficiency and cost.

In the case of a bioleaching/biomachining solution containing Fe³⁺, the main precipitates are iron hydroxides and jarosite (MFe₃(SO₄)₂(OH)₆, where M = K⁺, Na⁺, NH₄⁺, Ag⁺ or H₃O⁺). The formation of these precipitates is related to pH, temperature, cation availability or SO₄²⁻ concentration (Wang et al., 2018).

In addition, the joint presence of a high variety of metals (such as in PCB bioleaching solutions) can result in a formation of more complex precipitates. Ilyas et al. (2013b) analyzed the precipitate obtained in a PCB bioleaching process using a bacterial consortium including *Sulfobacillus thermosulfidooxidans* and *Thermoplasma acidophilum* thermophilic bacteria. The precipitate was determined to be composed of PbSO₄, Ag₂SO₄, SnO₂, AgFe₃(SO₄)₂(OH)₆ and H₂SnO₃, in the presence of Al 0.5±0.04 %, Pb 17±0.9 %, Sn 8.5±0.034 %, Zn 0.08±0.004 %, Fe 0.8±0.05 %, Cu 0.5±0.05 %, and Ag 0.003±0.002 %.

In another PCB treatment study carried out by Adhasure et al. (2013), the precipitate obtained at an initial pH 2.4 was concluded to be composed of Sn (59.96 %), Cu (23.97 %), Pb (9.30 %) and Fe (5.92 %).

Besides the formation of precipitates during PCB bioleaching, another drawback lies in the difficulty of separating the precipitates from the PCB dust. Likewise, when employing PCB powder, the non-metallic fractions are mixed with the precipitate formed at the end of the bioleaching process making difficult the final separation of the non-metallic fraction from the precipitate (Adhasure et al., 2014).

6. APPLICATIONS OF MICROORGANISM-ASSISTED MOBILIZATION OF METALS

Biological metal recovery process is based on the same mechanism (principles) as hydrometallurgical process and both of them are feasible to solubilize metals from waste printed circuit boards (PCBs) (Birloaga et al., 2013; Isildar et al., 2016; Hossain et al., 2018; Priya and Hait, 2020).

Hydrometallurgical recovery of metals generally consists of three steps: chemical leaching, solution concentration and purification, and metal recovery (Harikrushnan et al., 2016). Hydrometallurgical lixivants usually involves alkaline or acids solutions which solubilize solid matrix liberating metals in solution phase (Priya and Hait, 2017). The most employed inorganic and oxidant acid leaching agents include HCl, H₂SO₄, HNO₃/H₂SO₄, H₂O₂, aqua regia, among others (Sheng and Etsell, 2007; Huang et al., 2009; Yang et al., 2011; Van Yken et al., 2020).

On the other hand, as mentioned above, bio-hydrometallurgical processes exploit leaching ability of the microorganisms to convert metals into their soluble form for their recovery in an eco-friendlier, energy conservative way. As in most biological processes, microbial activities can be affected by biotic and abiotic factors, which can consequently, affect the metal extraction process during microbial leaching process (Choi et al., 2004).

Leaching rates achieved with hydrometallurgical processes are relatively higher than those obtained with biologically-assisted ones. However, biological leaching technologies are more environmentally friendly and cost-effective processes than the chemical alternatives. Therefore, some authors have recently proposed a hybrid technology which combined chemical with biological leaching processes, thus taking advantage of the benefits of both alternatives, with the chemical option being more efficient and the microorganism-assisted metal mobilization option being more environmentally friendly (Pant et al., 2012, Ilyas and Lee, 2015; Priya and Hait, 2018).

Bioleaching is a simple process that poses several advantages over hydrometallurgical processes. First, biohydrometallurgy, in comparison to hydrometallurgy, offers the advantage of moderate capital investment with low operating cost (Watling, 2006).

The energy consumption is lower than in conventional leaching technologies and its easy management due to low temperature working conditions required makes it a sustainable technology for metal recovery (Santhiya and Ting, 2005). Moreover, it involves basic equipment compared to the usual equipment in other leaching technologies (Watling, 2006). The mayor advantage, however, is that the necessary reagents are biologically produced by microorganisms, reducing the need of the continuous addition of reagents (Beolchini et al., 2012). Moreover, it is considered a flexible process for treatment of a wide range of metals (Kumar and Yaashikaa, 2020).

However, biohydrometallurgical processes are more time-consuming in comparison to the other metallurgical processes (Cui and Forssberg, 2003; Yang et al., 2009a). Despite the advantages, factors such as the slower dissolution kinetics are still hindering its large-scale application (Pathak et al., 2017). In Table 6 are summarized the main advantages and drawbacks of microorganism-assisted metal mobilization process.

Table 6. Advantages and drawbacks of microorganism-assisted metal mobilization process compared to other metal extraction processes.

	Advantages	Drawbacks
Other metal extraction processes (chemical, thermal...)	<ul style="list-style-type: none"> • Lower required process time 	<ul style="list-style-type: none"> • High energy consumption • Higher reagent consumption • More complex equipment and maintenance • Higher operational cost • Polluting emissions
Microorganism-assisted metal mobilization	<ul style="list-style-type: none"> • Environmentally friendly • Economically competitive • Lower working temperatures • Lower energy consumption • Simpler equipment and maintenance • No polluting emissions 	<ul style="list-style-type: none"> • Time-consuming • Rigorous conditions for proper bacterial growth • Slow kinetics

Although hydrometallurgy has been extensively employed in metal solubilization experiments, this process has been widely used in applications such as the biomachining of metallic pieces and the bioleaching of PCBs due to its potential advantages over the hydrometallurgical processes.

6.1. Biomachining

The constant increase in the world demand for micro-components, together with the social pressure on sustainable production and consumption, bring about that more and more companies understand the strategic relevance of sustainable manufacturing (Badurdeen and Jawahir, 2017). This is the driving force for the micromachining technology to be in constant development with one clear objective: to seek more economical and sustainable alternatives than the traditional physical and chemical processes. In the microfabrication sector, the physicochemical methods, such as milling, turning, drilling, laser or electrical discharge machining, and chemical machining have traditionally been applied (Díaz-Tena et al., 2018). Nevertheless, the machining of metal pieces by biological methods (biomachining or selective bioleaching) is a sustainable alternative that engraves complex geometries in small metal pieces within a wide range of applications (medicine, microelectronics, etc.) (Whulanza et al., 2016). Figure 6 shows several geometries biomachined on copper pieces published by Díaz-Tena et al. (2016).

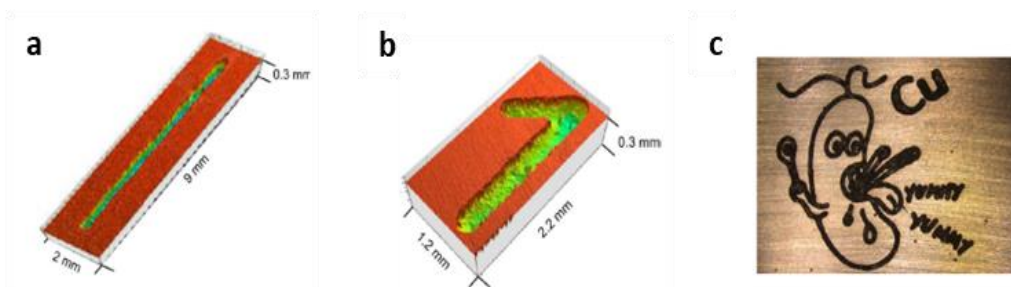


Figure 6. Some of the geometries biomachined in OFE workpieces published by Díaz-Tena et al. (2016).

In comparison to other available physical-chemical processes characterized by high energy consumption and waste generation, the advantages of biomachining are low energy consumption, the elimination of thermal and structural damage on the pieces and the possible regeneration/reusing of the exhausted solution among others. These features make it a competitive alternative, despite the fact that metal removal rates may be lower than those obtained using chemical machining processes for the same operation time (Johnson, 2007; Xenofontos et al., 2015).

Another advantage of biological machining is its versatility when obtaining pieces of different geometry and functionality, since the process offers the opportunity to remove material from specific areas on the metal surface. Thus, geometries as simple as lines or circles, or complex geometries can be engraved successfully (Istiyanto et al., 2011; Hocheng et al., 2012a; Muhammad et al., 2015; Singh et al., 2018).

Despite the fact that bibliographic references and previous works support the potential and advantages of biomachining as a micro-machining technique (Díaz-Tena et al., 2014; Xenofontos et al., 2015), many aspects of the process, including the variety of microorganisms to be used, the selection of metals that can be machined or the operating conditions, among others, require further study.

The factors that influence this application of the biomachining process are described below.

6.1.1. Metal workpieces preparation

The first step in the biomachining (selective biomachining or etching) of a metal piece is the decision about the geometry design to be engraved. The geometry must be transferred to the metal piece so that only the parts to be etched in the workpiece are exposed to the oxidant medium.

The most employed alternative for the preparation of the metallic piece is the photolithography technique, which is widely employed in electronics for the manufacture of semiconductor devices or integrated circuits. This technique consists of covering the piece with a photoresist resin (substance that changes its chemical characteristics with exposure to light) and, subsequently, “printing” the pattern of the geometry from a photomask. The photomask lets the light remove the resin only from the exposed areas (geometry) so that only resin free parts can be biomachined (Hocheng et al., 2012a; Istiyanto et al., 2012).

6.1.2. Specific metal removal rate (SMRR)

The parameter used to evaluate the efficiency of the machining process at industrial operation is the specific metal removal rate (SMRR), which represents the amount of metal removed per unit of time and surface ($\text{mg h}^{-1} \text{cm}^{-2}$). This parameter is related to the productivity/efficiency of the manufacturing method and determine both the time required to machine a metallic piece and the overall operating costs and profitability of the process.

The SMRR achieved during the process can be controlled by accurately selecting the operating conditions, the material to be biomachined, the concentration of Fe^{3+} in the medium or the microorganism strain, among others (Díaz-Tena et al., 2016). In fact, Xenofontos et al. (2015) concluded that the difference in the biomachining rate of copper pieces among different *A. ferrooxidans* strains can be considerable.

As an example, Table 7 shows some of the SMRR values reported in the bibliography for biomachined pieces using the *A. ferrooxidans* bacteria in the process.

Table 7. SMRR ($\text{mg h}^{-1} \text{cm}^{-2}$) values reported in literature for different strains of the *A. ferrooxidans* bacterium.

SMRR	Metal	Strain ^a	Reference
20.0	Cu	DSM 14882	Díaz-Tena et al., 2016
2.0	Cu	BCRC 13820	Hocheng et al., 2012b
5.5	Cu	BCRC 13820 Supernatant	Hocheng et al., 2012c
1.9	Fe	ATCC 21834	Muhammad et al., 2015
0.55	Al	BCRC 13820	Hocheng et al., 2012b
0.7	Al	BCRC 13820 Supernatant	Hocheng et al., 2012c
4.2	Ni	BCRC 13820 Supernatant	Hocheng et al., 2012c
1.6	Ni	BCRC 13820	Hocheng et al., 2012b
3.2	Zn	BCRC 13820 Supernatant	Hocheng et al., 2012c
1.0	Sn	BCRC 13820 Supernatant	Hocheng et al., 2012c
0.208	Aluminum Alloy 4004	Not defined	Verma et al., 2019
10	Cu	Isolated from acidic pit water	Ma et al., 2020

^aExperiments carried out with the supernatant were obtained after filtering the culture medium

As far as the evolution of both parameters throughout treatment time is concerned, several authors have concluded that the SMRR decreases throughout time, reaching the maximum value in the first hour of treatment and then decreasing gradually (Jadhav et al., 2013; Xenofontos et al., 2015; Díaz-Tena et al., 2016). On the contrary, Yang et al. (2009b) concluded that the rate of the etched depth of the microstructures increases linearly during 8 h of treatment, reporting average values in that period (8 h) of 9.20, 10.82 and 13.62 $\mu\text{m h}^{-1}$ for brass, bronze and copper, respectively.

6.1.3. Surface finish

Regarding the surface finish quality and roughness, the microbial action is known to cause an unfavorable effect on the final quality of the piece, leading to irregular surfaces (Xenofontos et al., 2015). However, recent studies have revealed that there is a direct relationship between some operating parameters and the surface roughness, which makes it possible to improve the final result.

Jadhav et al. (2013) studied the roughness of copper pieces treated for 1 h using the supernatant from a culture of *A. ferrooxidans* with an initial concentration of $\text{Fe}^{3+} \approx 3.6 \text{ g L}^{-1}$. The roughness values varied between $0.38 \pm 0.009 \mu\text{m}$ (at 0 rpm) and 1.46 ± 0.04

μm (at 200 rpm), being $1.07\pm 0.08 \mu\text{m}$ at the optimal speed of 150 rpm. The Fe^{3+} concentration also determined the roughness of the piece, which was $1.07\pm 0.12 \mu\text{m}$ and $5.18\pm 0.62 \mu\text{m}$ with an initial Fe^{3+} concentration of 3.6 g L^{-1} ($10 \text{ g FeSO}_4 \text{ L}^{-1}$) and 14.8 g L^{-1} ($40 \text{ g FeSO}_4 \text{ L}^{-1}$), respectively.

6.2. Electronic waste bioleaching

Another potential application of the bioleaching process is the metal recovery from urban residues such as electrical and electronic residues. The generation of WEEE has increased exponentially in recent years, due to the rapid innovation in the electronics sector, the increased demand for this type of equipment in developing countries and the reduction in the average lifetime of these devices (Lixandru et al., 2017; Isildar et al., 2019). In fact, the production of electrical and electronic devices has become one of the main growing sectors in the manufacturing industry (Ortuño et al., 2013; Hadi et al., 2015).

The WEEE includes any type of discarded electrical or electronic equipment that has become obsolete, has failed to work or has manufacturing defects (Silvas et al., 2015; Benzal et al., 2020). About 44.7 million metric tons of this waste type were generated worldwide in 2016 (6.1 kg per inhabitant) and it is estimated that this value will grow to 52.2 tons in 2021 (Baldé et al., 2017). As shown in Figure 7, WEEE are usually made up of a wide range of materials, such as metals, glass, cables or plastics among other materials (Widmer et al., 2005).

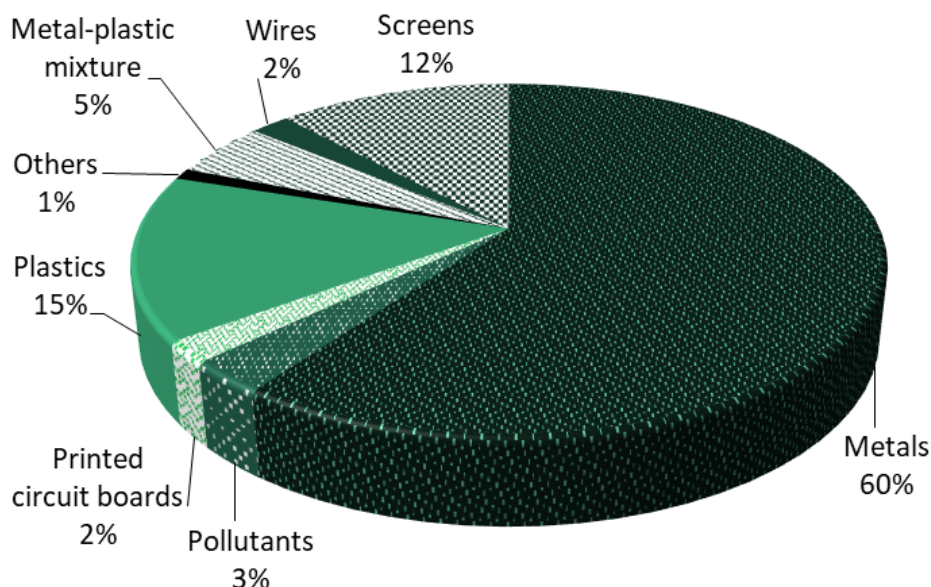


Figure 7. Main material fractions in WEEE composition (adapted from Widmer et al., 2005).

Thus, the proper management of discarded electrical and electronic equipment (EEE) has become one of the main environmental concerns in developed countries due to serious effects their components generate both for human health and for the environment (Ortuño et al., 2013; Jadhao et al., 2016; Horlgersson et al., 2017). Regarding the environmental impact of WEEE, the European Union (EU) attempted to limit the use of hazardous substances in the manufacturing of these equipment through the enactment of the RoHS Directive 2002/95/EC (Kumar et al., 2017).

As far as the Directive 2012/19/EU of the European Parliament on WEEE is concerned, these residues are classified in the following categories: 1. Temperature exchange equipment; 2. Screens, monitors, and equipment containing screens having a surface greater than 100 cm²; 3. Lamps; 4. Large equipment (any external dimension more than 50 cm); 5. Small equipment (no external dimension more than 50 cm); 6. Small IT and telecommunication equipment (no external dimension more than 50 cm). Among these categories, the total amount of WEEE generated in 2019 was basically made up of small equipment (17.4 Mt), large equipment (13.1 Mt), temperature exchange equipment (10.8 Mt) and screens (6.7 Mt). Lamps and small telecommunication equipment, with 0.9 Mt and 4.7 Mt respectively, represented smaller fractions (Figure 8) (Nithya et al., 2020). It has been predicted that the generation of wastes from temperature exchange devices and small and large devices will register the highest growth rates among all the categories. Conversely, screen waste is expected to decrease in the coming years due to the replacement of heavy cathode-ray tube (CRT) screens by flat alternatives (Baldé et al., 2017).

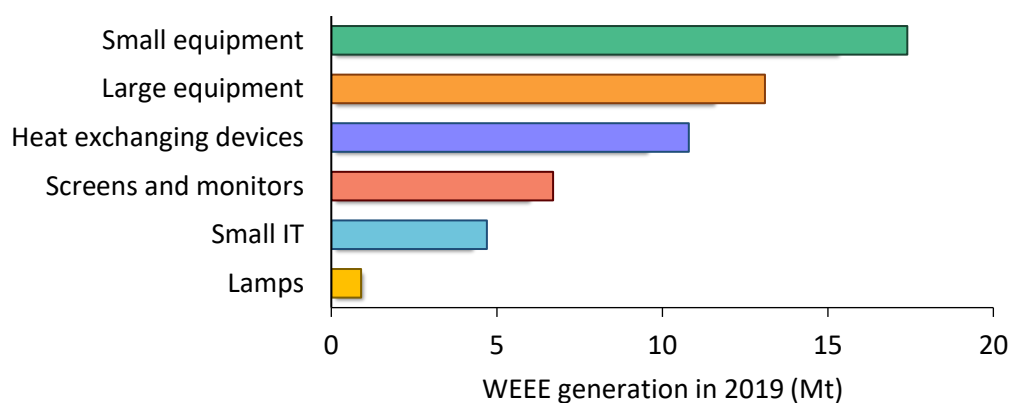


Figure 8. Total WEEE generation in 2019 per category (adapted from Nithya et al., 2020).

Despite regulations in force, the effective management of most WEEE is still scarce. In Europe, approximately only 35 % of that waste is recycled, while the rest is dumped, transferred to developing countries, or “simply lost” (Isildar et al., 2019). However, WEEE is an important secondary source of high-value metals, so its sustainable recovery

is mandatory to avoid the depletion of natural sources, mitigate the pollution that causes its disuse and achieve its efficient recycling within the application of the circular economy principles. Due to its high content of valuable materials, several studies on WEEE recycling have been carried out as an attempt to recover those valuable materials (Mizero et al., 2018; Priya and Hait, 2020; Roy et al., 2021).

In addition to legal regulations, the “waste principle” was included in the Waste Framework Directive, Directive 2008/98/EC of the European Parliament and Council, in 2008. Thus, the commonly known waste hierarchy pyramid (Figure 9) is composed of five measures: prevention, preparing for reuse, recycling, recovery (including energy recovery), and disposal. This waste hierarchy pyramid gives the highest priority to the prevention and reduction of waste generation, and, if generated, it gives priority to direct reuse and recycling methods (Directive 2008/98 / CE).

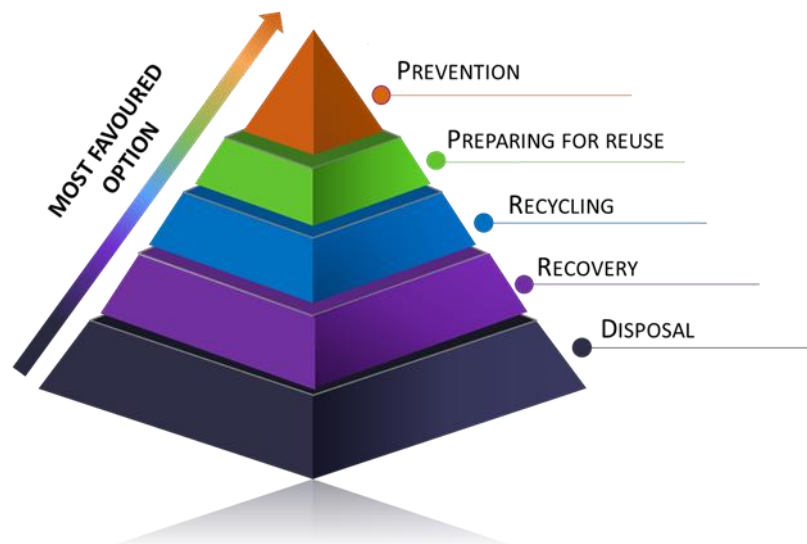


Figure 9. Waste hierarchy according to directive 2008/98/CE.

Among the different WEEE types, mobile phones (included in category 6) significantly contribute to the waste amount to be managed (Hira et al., 2017). In 2016, about 435 Kt of disused mobile phones were generated worldwide (Baldé et al., 2017). The average weight composition of a standard mobile phone is approximately 50 % plastics, 15 % glass and ceramic, 15 % metals, and the rest other materials (Moltó et al., 2011; Tesfaye et al., 2017). It is used as a support for electronic components and as a basis for connecting those using conductive pathways (Hadi et al., 2015). The main environmental impact of this type of waste is attributed to the printed circuit boards (PCBs), which have a high metal content. Figure 10 shows the average weight composition of a standard mobile phone PCB (Yamane et al., 2011; Palmieri et al., 2014).

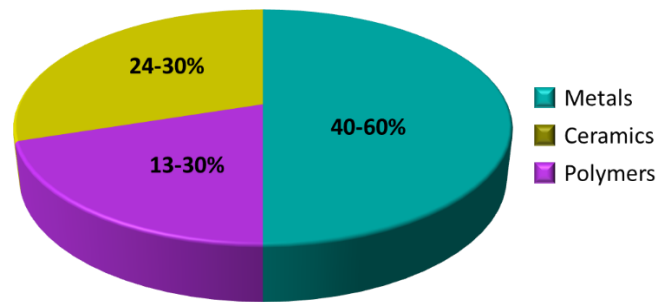


Figure 10. Average weight composition of a standard mobile phone PCB.

A mobile phone can contain up to 40 different elements, such as commonly used metals (copper and tin), precious metals (gold and silver), and others such as platinum and palladium (Kaya, 2016). Between 65 and 80 % of the materials in a mobile phone are recyclable (Moltó et al., 2011) but, recycling PCBs can be particularly difficult due to the wide variety of components.

The extraction of the metals contained in the PCBs (so called urban mining) is an undoubted economic opportunity and a priority measure to protect the environment and public health. It is estimated that the value of the raw materials contained in discarded mobile phones in 2016 was € 9,400 million (Baldé et al., 2017).

The traditional techniques used for the recycling of PCBs are grouped into two main types: hydrometallurgical processes (based on the extraction of metals using aqueous and organic liquid solutions) and pyrometallurgical processes (based on heating). These treatments are responsible for several environmental problems such as the formation of brominated and chlorinated di-benzo furans, the generation of dioxins or the toxicity of the employed reagents (Ning et al., 2017; Khatri et al., 2018; Liu et al., 2020). Conversely, the bioleaching process is an environmentally friendly recycling alternative, as it has advantages over current technologies: it has a low treatment cost, and its environmental impact is moderate. However, some technical issues require further research for improving process performance and subsequent high scale implementation (Isildar et al., 2019; Arya and Kumar, 2020).

As far as the techno-economic assessment of hydrometallurgy and biohydrometallurgy is concerned, Isildar (2018) and Baniasadi et al. (2019) calculated the treatment cost per kg PCB and the contribution of each method to the climate change. They concluded that the most affordable and environmentally friendly process is the biological alternative (Table 8, reproduced from Sodha et al., 2020).

Table 8. Economical and environmental assessment comparison of hydrometallurgy and biohydrometallurgy methods for PCB treatment (Sodha et al., 2020).

Technique	Cost (€ kg ⁻¹ PCB)			Climate change contribution
	Investment	Operational	Total cost	kg CO ₂ kg ⁻¹ PCB
Biohydrometallurgy	0.457	0.159	0.616	8.26
Hydrometallurgy	0.446	0.224	0.670	14.6

The main drawbacks that must be overcome for the industrial implementation of this technology are: the complex nature of some PCB materials (Brandl et al., 2001; Xiang et al., 2010), the possible toxicity of the non-metallic fraction of PCBs (Ilyas et al., 2007; Shah et al., 2015; Isildar et al., 2019), the inhibition of bacteria by the presence of high metal concentrations in the solution (Ilyas et al., 2013b; Arshadi and Mousavi, 2015a), and the lack of a standardized process for the recovery of the metals present in the depleted solutions.

The previous dismantling or removal of components from PCBs is an additional problem that can be overcome by a novel application of bioleaching: biodismantling. Monneron-Enaud et al. (2020) presented the biodismantling (dismantling using bioleaching) as a novel feasible application for removing the PCB components. It can be implemented as a new unit operation in the recycling process.

The specific key aspects for the successful bioleaching of mobile phone PCB such as the pre-treatment of the PCBs (entire pieces or crushed PCB), the treatment of the material in multi-stages or the amount of material to be treated per volume of medium cultivation (pulp density) are described below.

6.2.1. PCB pre-treatment

The materials used in the manufacturing of mobile phone PCBs are divided in two main fractions: non-metallic and metallic components. The non-metallic components are fiberglass (inorganic), epoxy resin (organic) and brominated flame retardants. The other fraction, made up of metallic elements, contains a single layer or multilayer of Cu, lead solder, tin solder, and other metals such as nickel, iron, lead, cobalt, aluminium, gold, indium, or antimony (Arshadi and Mousavi, 2015b). The recycling of the non-metallic fraction has not received much attention in literature because it is not profitable to date (Ilyas et al., 2007; Adhasure et al., 2014). Two types of PCB pre-treatments have been proposed: removal of the non-metallic fraction and size reduction.

The non-metallic fraction (epoxy resin) covering the boards is toxic to microorganisms (Isildar et al., 2019) and it hinders the interaction between the metallic surface and the bioleaching solution. For this reason, some authors separate the metallic and non-metallic fraction before immersing the waste into the bioleaching medium (Jujun et al., 2015; Wu et al., 2018).

The removal of the non-metallic materials by washing the PCB dust samples with a saturated solution of NaCl has proved to improve the process (Ilyas et al., 2007; Shah et al., 2015). Senophiyah-Mary et al. (2018) have studied the efficiency of other different pre-treatment methods for epoxy coating removal from PCBs. These authors have tested different solutions containing NaOH and solvents like ethanol, acetone, tween-80, carbinol, benzyl alcohol, and acids like sulfuric acid, nitric acid and hydrochloric acid. No epoxy removal has obtained with solvents while complete epoxy cover removal was achieved with sodium hydroxide solutions and with sulfuric and nitric acids. However, they selected the NaOH as the best pre-treatment method since the acid attack dissolved many components simultaneously. Moyo et al. (2020), have also reported the best results when employing NaOH for epoxy cover removal, and Adhapure et al. (2014) concluded that immersing the PCBs in 10 M NaOH overnight was the optimal pre-treatment for eliminating the epoxy covering. Once the epoxy resin is removed, the entire PCB (without crushing) can also be treated. This last alternative of entire pieces is very interesting for the industrial scale application, since it simplifies the pre-treatment (no crushing is required) and, facilitates the extraction of the depleted piece from the solution.

Regarding size reduction, particle size obviously determines the contact surface area between the medium and the material to be treated so that, when the particle size decreases, the mass transfer increases accordingly. On the contrary, when particle size is high, the collisions between the microorganisms and the PCB particles can damage the bacterial cells (Arshadi and Mousavi, 2015a). Most of the PCB bioleaching studies have been carried out using pulverized samples (Liang et al., 2010; Arshadi and Mousavi, 2015a; Arshadi et al., 2016; Isildar et al., 2016; Wang et al., 2018; Khatri et al., 2018). The usual equipment for crushing the boards is a metal crusher, hammer or ball mill. Initially, the PCB grinding step can be carried out in a hammer mill to grind the coarser particles and subsequently a ball mill to grind the fine ones (Kasper et al., 2011).

The main difficulties of these pre-treatments are the loss of material (which can be up to 40 %), the high energy consumption and the formation of a fine mixture of metallic or non-metallic particles that can be dangerous to health and difficult to separate (Kumar et al., 2017). Once the material is crushed, sieves are used to classify the particles according to particle size.

Most authors employ particles smaller than 200 μm , although there are studies that use larger particle sizes (Table 9).

Table 9. Pulp densities (g L^{-1}) and particle sizes (μm) reported in literature.

Microorganism	Particle size	Pulp density	Metals ^a	Reference
<i>A. ferrooxidans</i>	37-150	1-20 (optimal: 8.5)	Cu, Ni	Arshadi and Mousavi., 2015b
<i>Bacillus megaterium</i>	37-150	1-20 (optimal: 8.1)	Cu, Au	Arshadi et al., 2016
<i>S. thermosulfidooxidans</i>	50-150	10	Cu, Ni, Al, Zn	Ilyas et al., 2007
<i>A. ferrooxidans</i> and <i>A. thiooxidans</i>	100- 200	4-12	Cu, Zn, Ni	Liang et al., 2010
<i>A. ferrivorans</i> and <i>A. thiooxidans</i>	≤ 500	5-50 (optimal: 10)	Cu, Ag	Isildar et al., 2016
<i>P. putida</i> and <i>P. fluorescens</i>	≤ 500	5-50 (optimal: 10)	Cu, Ag	Isildar et al., 2016
Enriched mixed culture (origin: active sludge)	≤ 180	50	Cu	Wang et al., 2018
Microorganism consortium dominated by <i>L. ferriphilum</i>	≤ 200 - 250	10-100 (optimal: 10)	Cu, Fe, Zn, Ni, Pb, Cd, Au, Ag, Co	Khatri et al., 2018
<i>A. thiooxidans</i>	<75	10-50 (optimal: 30)	Li, Co, Mn	Naseri et al., 2019
<i>A. ferrooxidans</i> and <i>A. acidophilum</i>	75- 1000	7.5-15 (optimal: 7.5)	Cu, Zn, Ni, Pb, Ag, Au, Sc, Ce, La, Nd	Priya and Hait, 2020
<i>A. ferrooxidans</i>	< 100	5-100	Co, Li	Roy et al., 2021

^aanalyzed dissolved metals

6.2.2. Treatment mode: single and multi-stages bioleaching

The bioleaching experiments with PCBs can be carried out in one (Arshadi et al., 2016; Khatri et al., 2018) or two stages (Brandl et al., 2001; Shah et al., 2015; Isildar et al., 2016; Khatri et al., 2018; Marra et al., 2018). In the first case, the extraction process takes place in the presence of the microorganisms (biotic medium), while in the two-stage process the metal extraction is carried out by immersing the PCB in the filtered supernatant (abiotic medium) that is obtained in a previous stage where the microbial oxidation of Fe^{2+} to Fe^{3+} occurs. The two-stage operation allows a better control of the

process, since the parameters corresponding to the biotic stage and the abiotic stage can be optimized separately.

6.2.3. Pulp density

The pulp density is the ratio between the amount of material to be treated (usually powder or dust) and the volume of leaching medium (Xin et al., 2012). This is another relevant parameter because high values of pulp density can be detrimental for the extraction if the samples are not previously pretreated. In this case, the amount of dissolved organic material in the medium can be too high, which can definitively inhibit microbial activity (Ilyas et al., 2007; Vestola et al., 2010; Zhou et al., 2013; Valix, 2017). Obviously the higher the pulp density, the higher metal extraction, which would quickly increase toxicity of the medium. Likewise, a low material:medium ratio requires large reactors and higher investment costs (Valix, 2017), as well as a greater energy requirement for heating and mixing. Some of the pulp density values tested by different authors are shown in Table 9.

The optimal concentration reported by most authors is equal to or lower than 10 g PCB L⁻¹. However, Liang et al. (2010) proposed a procedure based on the addition of the PCB powder in three steps (4 g L⁻¹ after 48 h of culture, 6 g L⁻¹ after 96 h and 8 g L⁻¹ after 144 h). A total concentration of 18 g L⁻¹ was treated and the leaching results were 93, 89, 91 and 86 % for Cu, Ni, Zn and Pb, respectively. Similarly, Khatri et al. (2018) reported that it is possible to obtain a 95 % solubilization of Cu and more than 50 % of Ni by using a PCB pulp density of 100 g L⁻¹ (10 %), although the values obtained were lower than those registered with lower pulp densities.

7. REFERENCES

- Abraham, J., Chatterjee, A., Sharma, J., 2020. Isolation and Characterization of a New *Bacillus licheniformis* Strain for Bioleaching Heavy Metals. *Journal of Applied Biotechnology Reports*. 7, 139-144.
- Adhapure, N.N., Waghmare, S.S., Hamde, V.S., Deshmuck, A.M., 2013. Metal solubilization from powdered printed circuit boards by microbial consortium from bauxite and pyrite ores. *Applied Biochemistry and Microbiology*. 49, 256-262.
- Adhapure, N.N., Dhakephalkar, P.K., Dhakephalkar, A.P., Tembhurkar, V.R., Rajgure, A.V., Deshmuck, A. M., 2014. Use of large pieces of printed circuit boards for bioleaching to avoid precipitate contamination problem' and to simplify overall metal recovery. *MethodsX*. 1, 181-186.
- Akhlaghi, N., 2019. Hemp fibres as novel green support material for immobilization of *Acidithiobacillus ferrooxidans*. *International Journal of Engineering*. 32, 1225-1230.

- Aksu, Z., Karabayır, G., 2008. Comparison of biosorption properties of different kinds of fungi for the removal of Gryfalan Black RL metal-complex dye. *Bioresource Technology*. 99, 7730-7741.
- Amiri, F., Mousavi, S.M., Yaghmaei, S., Barati M., 2012. Bioleaching kinetics of a spent refinery catalyst using *Aspergillus niger* at optimal conditions. *Biochemical Engineering Journal*. 67, 208-217.
- Anjum, F., Bhatti, H.N., Ghauri, M.A., Bhatti, I.A., Asgher, M., Asi, M.R., 2009. Bioleaching of copper, cobalt and zinc from black shale by *Penicillium notatum*. *African Journal of Biotechnology*. 8, 5038-5045.
- Annamalai, M., Gurusurthy, K., 2019. Enhanced bioleaching of copper from circuit boards of computer waste by *Acidithiobacillus ferrooxidans*. *Environmental Chemistry Letters*. 17, 1873-1879.
- Arshadi, M., Mousavi, S., 2015a. Enhancement of simultaneous gold and copper extraction from computer printed circuit boards using *Bacillus megaterium*. *Bioresource Technology*. 175, 315-324.
- Arshadi, M., Mousavi, S.M., 2015b. Multi-objective optimization of heavy metals bioleaching from discarded mobile phone PCBs: Simultaneous Cu and Ni recovery using *Acidithiobacillus ferrooxidans*. *Separation and Purification Technology*. 147, 210-219.
- Arshadi, M., Mousavi, S.M., Rasoulnia, P., 2016. Enhancement of simultaneous gold and copper recovery from discarded mobile phone PCBs using *Bacillus megaterium*: RSM based optimization of effective factors and evaluation of their interactions. *Waste Management*. 57, 158-167.
- Arshadi, M., Yaghmaei, S., 2020. Advances in bioleaching of copper and nickel from electronic waste using *Acidithiobacillus ferrooxidans*: evaluating daily pH adjustment. *Chemical Papers*. 74, 2211-2227.
- Arya, S., Kumar, S., 2020. Bioleaching: urban mining option to curb the menace of e-waste challenge. *Bioengineered*. 11, 640-660.
- Badurdeen, F., Jawahir, I.S., 2017. Strategies for value creation through sustainable manufacturing. *Procedia Manufacturing*. 8, 20-27.
- Bahafid, W., Joutey, N.T., Asri, M., Sayel, H., Tirry, N., El Ghachtouli, N., Sayel, N.T.H., 2017. Yeast Biomass: An Alternative for Bioremediation of Heavy Metals. *Yeast-Industrial Applications*, 2017.
- Bahaloo-Horeh, N., Mousavi, S. M., Baniasadi, M., 2018. Use of adapted metal tolerant *Aspergillus niger* to enhance bioleaching efficiency of valuable metals from spent lithium-ion mobile phone batteries. *Journal of Cleaner Production*. 197, 1546-1557.
- Bajestani, M.I., Mousavi, S.M., Shojaosadati, S.A., 2014. Bioleaching of heavy metals from spent household batteries using *Acidithiobacillus ferrooxidans*: statistical evaluation and optimization. *Separation and Purification Technology*. 132, 309-316.
- Balde, C. P., Forti, V., Gray, V., Kuehr, R., Stegmann, P., 2017. The Global e-Waste Monitor 2017: Quantities, Flows and Resources (United Nations University, International Telecommunication Union and International Solid Waste Association).

- Baniasadi, M., Vakilchah, F., Bahaloo-Horeh, N., Mousavi, S.M., Farnaud, S., 2019. Advances in bioleaching as a sustainable method for metal recovery from e-waste: A review. *Journal of Industrial and Engineering Chemistry*. 76, 75-90.
- Bankar, A., Winey, M., Prakash, D., Kumar, A.R., Gosavi, S., Kapadnis, B., Zinjarde, S., 2012. Bioleaching of fly ash by the tropical marine yeast, *Yarrowia lipolytica* NCIM 3589. *Applied Biochemistry and Biotechnology*. 168, 2205-2217.
- Barnett, M., Palumbo-Roe, B., Gregory, S., 2018. Comparison of heterotrophic bioleaching and ammonium sulfate ion exchange leaching of rare earth elements from a madagascan ion-adsorption clay. *Minerals*. 8, 236.
- Barona, A., Etxebarria, M.B., Rojo, N., Santaolalla, A., Otegi, J.R., Díaz-Tena, E., Gallastegui, G., 2018. A perspective on a white biotechnology under development: biomachining. *Current Topics in Biotechnology*. 9, 45-54.
- Barron, J.L.C., Lueking, D.R., 1990. Growth and maintenance of *Thiobacillus ferrooxidans* cells. *Applied and Environmental Microbiology*. 56, 2801-2806.
- Barron, M.G., Galbraith, H., Beltman, D., 1995. Comparative reproduction and developmental toxicology of birds. *Comparative Biochemistry and Physiology*. 112c, 1-14.
- Benzal, E., Cano, A., Solé, M., Lao-Luque, C., Gamisans, X., Dorado, A.D., 2020. Copper recovery from PCBs by *Acidithiobacillus ferrooxidans*: Toxicity of bioleached metals on biological activity. *Waste Biomass Valorization*. 11, 5483-5492
- Beolchini, F., Fonti, V., Ferella, F., Centofanti, M., Veglio, F., 2009. Bioleaching of nickel, vanadium and molybdenum from spent refinery catalysts. *Advanced Materials Research Institute*. 71-73, 657-660.
- Beolchini, F., Fonti, V., Dell'Anno, A., Rocchetti, L., Veglio, F., 2012. Assessment of biotechnological strategies for the valorization of metal bearing wastes. *Waste Management*. 32, 949-956.
- Bharadwaj, A., Ting, Y.P., 2013. Bioleaching of spent hydro treating catalyst by acidophilic thermophilic *Acidithiobacillus brierleyi*: leaching mechanism and effect of decoking. *Bioresource Technology*. 130, 673-680.
- Bigham, J.M., Jones, F.S., Özkaya, B., Sahinkaya, E., Puhakka, J.A., Tuovinen, O.H., 2010. Characterization of jarosites produced by chemical synthesis over a temperature gradient from 2 to 40 °C. *International Journal of Mineral Processing*. 94, 121-128.
- Birloaga, I., De Michelis, I., Ferella, F., Buzatu, M., Vegliò, F., 2013. Study on the influence of various factors in the hydrometallurgical processing of waste printed circuit boards for copper and gold recovery. *Waste Management*. 33, 935-941.
- Bolaños-Benítez, V., Hullebusch, E.D.V., Lens, P.N.L., Quantin, C., Vossenberg, J.V.D., Subramanian, S., Sivry, Y., 2018. (Bio)leaching Behavior of Chromite Tailings. *Minerals-Basel*. 8, 261.
- Boon, M., 2001. The mechanism of 'direct' and 'indirect' bacterial oxidation of supplied minerals. *Hydrometallurgy*. 62, 67-70.
- Bosecker, K., 1987. Microbial recycling of mineral waste products. *Acta Biotechnologica*. 7, 487-497.
- Bosecker, K., 1997. Bioleaching: metal solubilisation by microorganisms. *FEMS Microbiology Reviews*. 20, 591-604.

- Bosshard, P.P., Bachofen, R., Brandl, H., 1996. Metal leaching of fly ash from municipal waste incineration by *Aspergillus niger*. *Environmental Science and Technology*. 30, 3066-3070.
- Bosshard, R., Wegmann, M., 2001. Computer-munching microbes: metal leaching from electronic scrap by bacteria and fungi. *Hydrometallurgy*. 59, 319-326.
- Brandl H., Faramarzi M. A., 2006. Microbe-metal-interactions for the biotechnological treatment of metal-containing solid waste. *China Particuology*. 4, 93-97.
- Brandl, H., Lehmann, S., Faramarzi, M. A., Martinelli, D., 2008. Biomobilization of silver, gold and platinum from solid waste materials by HCN-forming microorganisms. *Hydrometallurgy*. 94, 14-17.
- Burgstaller W., Stxaser H., Shinner F., 1992. Solubilization of zinc oxide from filter dust with *Penicillium simplicissimum*: bioreactor, leaching and stoichiometry. *Environmental Science and Technology*. 26, 340-346.
- Burgstaller W., Schinner F., 1993. Leaching of metals with fungi. *Journal of Biotechnology*. 27, 91-116.
- Cabrera, G., Gómez, J.M., Cantero, D., 2005. Influence of heavy metals on growth and ferrous sulphate oxidation by *Acidithiobacillus ferrooxidans* in pure and mixed culture. *Process Biochemistry*. 40, 2683-2687.
- Castro, C., Donati, E., 2016. Effects of different energy sources on cell adhesion and bioleaching of a chalcopyrite concentrate by extremophilic archaeon *Acidianus copahuensis*. *Hydrometallurgy*. 162, 49-56.
- Chakankar, M., Su, C.H., Hocheng, H., 2019. Leaching of metals from end-of-life solar cells. *Environmental Science and Pollution Research*. 26, 29524-29531.
- Chang, J.H., Hocheng, H., Chang, H.Y., Shih, A., 2008. Metal removal rate of Thiobacillus thiooxidans without pre-secreted metabolite. *Journal of Materials Processing Technology*. 201, 560-564.
- Chatterjee, A., Das, R., Abraham, J., 2019. Bioleaching of heavy metals from spent batteries using *Aspergillus nomius* JAMK1. *International journal of Environmental Science and Technology*, 17, 49-66.
- Chi, T.D., Lee, J.C., Pandey, B.D., Yoo, K., Jeong, J., 2011. Bioleaching of gold and copper from waste mobile phone PCBs by using a cyanogenic bacterium. *Minerals Engineering*. 24, 1219-1222.
- Choi, M.S., Cho, K.S., Kim, D.S., Kim, D.J., 2004. Microbial recovery of copper from printed circuit boards of waste computer by *Acidithiobacillus ferrooxidans*. *Journal of Environmental Science and Health*. 39(11- 12), 2973-2982.
- Chojnacka, K., 2007. Bioaccumulation of Cr (III) ions by Blue-Green alga *Spirulina* sp. Part I. A comparison with biosorption. *American Journal of Agricultural and Biological Sciences*. 2, 218-223.
- Colmer, A.R., Temple, K.L., Hinkle, M.E., 1950. An iron-oxidizing bacterium from the acid drainage of some bituminous coal mines. *Journal of Bacteriology*. 59(3), 317-328.
- Cornu, J.Y., Huguenot, D., Jezequel, K., Lollier, M., Lebeau, T., 2017. Bioremediation of copper-contaminated soils by bacteria. *World Journal of Microbiology and Biotechnology*. 33, 26.

- Cui, J., Forssberg, E., 2003. Mechanical recycling of waste electric and electronic equipment: A review. *Journal of Hazardous Materials*. 99, 243-263.
- Daoud, J., Karamanev, D., 2006. Formation of jarosite during Fe²⁺ oxidation by *Acidithiobacillus ferrooxidans*. *Minerals Engineering*. 19, 960-967.
- Das, A., Modak, J.M.; Natarajan, K A., 1998. Surface chemical studies of *Thiobacillus ferrooxidans* with reference to copper tolerance. *Antonie van Leeuwenhoek*. 73, 215-222.
- Deveci, H., Akcil, A. and Alp, I., 2004. Bioleaching of complex zinc sulphides using mesophilic and thermophilic bacteria: comparative importance of pH and iron. *Hydrometallurgy*. 73, 293-303.
- Díaz-Tena, E., Gallastegui, G., Hipperdinger, M., Donati, E. R., Ramírez, M., Rodríguez, A., López de Lacalle, L. N., Elías, A., 2016. New advances in copper biomachining by iron-oxidizing bacteria. *Corrosion Science*. 112, 385-392.
- Díaz-Tena, E., Gallastegui, G., Hipperdinger, M., Donati, E. R., Rojo, N., Santaolalla, A., Ramírez, M., Barona, A., Elías, A., 2018. Simultaneous culture and biomachining of copper in MAC medium: a comparison between *Acidithiobacillus ferrooxidans* and *Sulfobacillus thermosulfidooxidans*. *ACS Sustainable Chemistry and Engineering*. 6, 17026-17034.
- Díaz-Tena, E., Rodríguez-Ezquerro, A., López de Lacalle, Marcaide, L. N., Gurtubay L., Elías, A., 2014. A sustainable process for material removal on pure copper by use of extremophile bacteria. *Journal of cleaner production*. 84, 752-760.
- Directive 2012/19/EU. The restriction of the use of certain hazardous substances in electrical and electronic equipment. European Parliament, Council of the European Union. <https://eur-lex.europa.eu/legal-content/EN/TXT/PDF/?uri=CELEX:32012L0019&from=EN>. (Last accessed May 2021).
- Directive 2008/98/EC. Waste and repealing certain Directives. European Parliament and the Council of the European Union. <https://eur-lex.europa.eu/legal-content/EN/TXT/PDF/?uri=CELEX:32008L0098&from=EN>. (Last accessed May 2021).
- Directive 2002/95/EC. The restriction of the use of certain hazardous substances in electrical and electronic equipment. European Parliament and the Council of the European Union. <https://eur-lex.europa.eu/legal-content/EN/TXT/PDF/?uri=CELEX:32002L0095&from=ES>. (Last accessed May 2021).
- Donati, E.R., Castro, C., Urbietta, M.S., 2016. Thermophilic microorganisms in biominning. *World Journal of Microbiology and Biotechnology*. 32, 179.
- Dopson, M., Johnson, D.B., 2012. Biodiversity, metabolism and applications of acidophilic sulfur-metabolizing microorganisms. *Environmental Microbiology*. 14, 2620-2631.
- Dursun, A.Y., Uslu, G., Cuci, Y., Aksu, Z., 2003. Bioaccumulation of copper(II), lead(II) and chromium(VI) by growing *Aspergillus niger*. *Process Biochemistry*. 38 1647-1651.
- Ehrlich, H.L., 2001. Past, present and future of biohydrometallurgy. *Hydrometallurgy*. 59, 127-134.
- Fang, D., Zhou, L. X., 2007. Enhanced Cr bioleaching efficiency from tannery sludge with coinoculation of *Acidithiobacillus thiooxidans* TS6 and *Brettanomyces* B65 in an air-lift reactor. *Chemosphere*. 69, 303-310.

- Faraji, F., Golmohammadzadeh, R., Rashchi, F., Alimardani, N., 2018. Fungal bioleaching of WPCBs using *Aspergillus niger*: observation, optimization and kinetics. *Journal of Environmental Management*. 217, 775-787.
- Faramarzi, M.A., Mogharabi-Manzari, M., Brandl, H., 2020. Bioleaching of metals from wastes and low-grade sources by HCN-forming microorganisms. *Hydrometallurgy*. 191, 105228.
- Fathollahzadeh, H., Becker, T., Eksteen, J.J., Kaksonen, A.H., Watkin, E.L., 2018. Microbial contact enhances bioleaching of rare earth elements. *Bioresource Technology*. 3, 102-108.
- Franzmann, P.D., Haddad, C.M., Hawkes, R.B., Robertson, W.J., Plumb, J.J., 2005. Effects of temperature on the rates of iron and sulfur oxidation by selected Bacteria and Archaea: application of the Ratkowsky equation. *Minerals Engineering*, 18, 1304-1314.
- Fu, B., Zhou, H., Zhang, R., Qiu, G., 2008. Bioleaching of chalcopyrite by pure and mixed cultures of *Acidithiobacillus spp.* and *Leptospirillum ferriphilum*. *International Biodeterioration and Biodegradation*. 62, 109-115.
- Gadd, G.M., 2004. Mycotransformation of organic and inorganic substrates. *Mycologist*. 18, 60-70.
- Gamache, M., Blais, J. F., Tyagi, R. D., Meunier, N., 2001. Microflore hétérotrophe impliquée dans le procédé simultané de biolixiviation des métaux et de digestion des boues de purification'. *Canadian Journal of Civil Engineering*. 28, 158-174.
- Ge, W., Zamri, D., Mineyama, H., Valix, M., 2011. Bioaccumulation of heavy metals on adapted *Aspergillus foetidus*. *Adsorption*. 17, 901-10.
- Gehrke, T., Telegdi, J., Thierry, D., Sand, W., 1998. Importance of extracellular polymeric substances from *Thiobacillus ferrooxidans* for bioleaching. *Applied and Environmental Microbiology*. 64, 2743-2747.
- Giaveno, A., Lavallo, L., Guibal, L., Donati, E., 2008. Biological ferrous sulfate oxidation by *A. ferrooxidans* immobilized on chitosan beads. *Journal of Microbiological Methods*. 72, 227-234.
- Gomez, J.M., Cantero, D., Webb, C., 2000. Immobilization of *Thiobacillus ferrooxidans* cells on nickel alloy fibre for ferrous sulphate oxidation. *Applied Microbiology and Biotechnology*. 54, 335-340.
- González, E., Rodríguez, J.M., Muñoz, J.Á., Blázquez, M.L., Ballester, A., González, F., 2018. The contribution of *Acidiphilium cryptum* to the dissolution of low-grade manganese ores. *Hydrometallurgy*. 175, 312-318.
- Groudev, S.N., 1987. Use of heterotrophic microorganisms in mineral biotechnology. *Acta Biotechnologica*. 7, 299-306.
- Gu, X.Y., Wong, J.W.C., 2007. Degradation of inhibitory substances by heterotrophic microorganisms during bioleaching of heavy metals from anaerobically digested sewage sludge. *Chemosphere*. 69, 311-318.
- Gu, G., Hu, K., Zhang, X., Xiong, X., Yang, H., 2013. The stepwise dissolution of chalcopyrite bioleached by *Leptospirillum ferriphilum*. *Electrochimica Acta*. 103, 50-57.
- Gumulya, Y., Boxall, N.J., Khaleque, H.N., Santala, V., Carlson, R.P., Kaksonen, A.H., 2018. In a quest for engineering acidophiles for biomining applications: challenges and opportunities. *Genes (Basel)*. 9, 116.

- Habibi, A., Kourdestani, S.S., Hadadi, M., 2020. Biohydrometallurgy as an environmentally friendly approach in metals recovery from electrical waste: A review. *Waste Management and Research*. 38, 232-244.
- Hadi, P., Xu, M., Lin, C.S.K., Hui, C.W., McKay, G., 2015. Waste printed circuit board recycling techniques and product utilization. *Journal of Hazardous Materials*. 11, 234-243.
- Hamidian, H., 2011. Microbial Leaching of Uranium Ore. En: Tsvetkov, P. V. (ed.) *Nuclear Power - Development, operation and sustainability*. 291-304, InTech.
- Harikrushnan, B., Shreyass, G., Hemant, G., Pandimadevi, M., 2016. Recovery of metals from printed circuit boards (PCBs) using a combination of hydrometallurgical and biometallurgical processes. *International Journal of Environmental Research*. 10, 511-518.
- Hassanien, W.A.G., Desouky, O.A.N., Hussien, S.S.E., 2014. Bioleaching of some Rare Earth Elements from Egyptian Monazite using *Aspergillus ficuum* and *Pseudomonas aeruginosa*. *Walailak Journal of Science and Technology*. 11, 809-823.
- Hawkes, R.B., Franzmann, P.D., O'hara, G., Plumb, J.J., 2006. *Ferroplasma cupricumulans* sp. nov., a novel moderately thermophilic, acidophilic archaeon isolated from an industrial-scale chalcocite bioleach heap. *Extremophiles*. 10, 525-530.
- He, H., Xia, J.L., Yang, Y., Jiang, H.C., Xiao, C.Q., Zheng, L., Ma, C.Y., Zhao, Y.D., Qiu, G.Z., 2009. Sulfur speciation on the surface of chalcopyrite leached by *Acidianus manzaensis*. *Hydrometallurgy*. 99, 45-50.
- Hedrich, S., Johnson, D.B., 2013. *Acidithiobacillus ferridurans* sp. nov., an acidophilic iron-, sulfur- and hydrogen-metabolizing chemolithotrophic gammaproteobacterium. *International Journal of Systematic and Evolutionary Microbiology*. 63, 4018-4025.
- Hira, M., Yadav, S., Morthekai, P., Linda, A., Kumar, S., Sharma, A., 2017. Mobile Phones—An asset or a liability: A study based on characterization and assessment of metals in waste mobile phone components using leaching tests. *Journal of Hazardous Materials*. 342, 29-40.
- Hocheng, H., Jadhav, U.U., Chang, J.H., 2012a. Biomachining rates of various metals by *Acidithiobacillus thiooxidans*. *International Journal of Surface Science and Engineering*. 6, 101-111.
- Chang, J. H., Hsu, H. S., Han, H. J., Chang, Y. L., Jadhav, U. U., 2012b. Metal removal by *acidithiobacillus ferrooxidans* through cells and extra-cellular culture supernatant in biomachining. *CIRP Journal of Manufacturing Science and Technology*. 5, 137-141.
- Hocheng, H., Chang, J., Jadhav, U.U., 2012c. Micromachining of various metals by using *Acidithiobacillus ferrooxidans* 13820 culture supernatant experiments. *Journal of Cleaner Production*. 20, 180-185.
- Holgersson, M.B., Landgren, F., Rylander, L., Giwercman Y.L., 2017. Mortality is linked to low serum testosterone levels in younger and middle-aged men. *European Urology*. 71, 991-992.
- Horeh, N. B., Mousavi, S. M., Shojaosadati, S. A., 2016. Bioleaching of valuable metals from spent lithium-ion mobile phone batteries using *Aspergillus niger*. *Journal of Power Sources*. 320, 257-266.
- Hossain, M.S., Yahaya, A.N.A., Yacob, L.S., Rahim M.Z.A., Yusof, N.N.M., Bachmann, R.T., 2018. Selective recovery of copper from waste mobile phone printed circuit boards using sulphuric acid leaching. *Materials Today: Proceedings*. 5, 21698-21702.

- Huang, K., Guo, J., Xu, Z., 2009. Recycling of waste printed circuit boards: A review of current technologies and treatment status in China. *Journal of Hazardous Materials*. 164, 399-408.
- Huber, H., Stetter, K.O., 1989. *Thiobacillus prosperus* sp. nov., represents a new group of halotolerant metal-mobilizing bacteria isolated from a marine geothermal field. *Archives of Microbiology*. 151, 479-485.
- Ilyas, S., Anwar, M.A., Niazi, S.B., Ghauri, M.A., 2007. Bioleaching of metals from electronic scrap by moderately thermophilic acidophilic bacteria. *Hydrometallurgy*. 88, 180-188.
- Ilyas, S., Chi, R., Lee, J., 2013a. Fungal Bioleaching of Metals From Mine Tailing. *Mineral Processing and Extractive Metallurgy Review*. 34, 185-194.
- Ilyas, S., Lee, J., Chi, R., 2013b. Bioleaching of metals from electronic scrap and its potential for commercial exploitation. *Hydrometallurgy*. 131, 138-143.
- Ilyas, S., Lee, J.C., 2015. Hybrid leaching: an emerging trend in bioprocessing of secondary resources. In: *Microbiology for minerals, metals, materials and the environment*, CRC Press, 359-382.
- Isildar, A., van de Vossenberg, J., Rene, E. R., van Hullebusch, E. D., Lens, P. N. L., 2016. Two-step bioleaching of copper and gold from discarded printed circuit boards (PCB). *Waste Management*. 57, 149-157.
- Isildar A., 2018. *Metal Recovery from Electronic Waste: Biological Versus Chemical Leaching for Recovery of Copper and Gold*, CRC Press, Leiden, the Netherlands.
- Isildar, A., van Hullebusch, E.D., Lenz, M., Du Laing, G., Marra, A., Cesaro, A., Panda, A., Akcil, A., Kucuker, M.A., Kuchta, K., 2019. Biotechnological strategies for the recovery of valuable and critical raw materials from waste electrical and electronic equipment (WEEE) – A review. *Journal of Hazardous Materials*. 362, 467-481.
- Istiyanto, J., Kim, M.Y., Ko, T.J., 2011. Profile characteristics of biomachined copper. *Microelectronic Engineering*. 88, 2614-2617.
- Istiyanto, J., Saragih, A.S., Ko, T.J., 2012. Metal based micro-feature fabrication using biomachining process. *Microelectronic Engineering*. 98, 561-565.
- Jadhao, P., Chauhan, G., Pant, K.K., Nigam, K.D.P., 2016. Greener approach for the extraction of copper metal from electronic waste. *Waste Management*. 57, 102-112.
- Jadhav, U., Hocheng, H., Weng, W.H., 2013. Innovative use of biologically produced ferric sulfate for machining of copper metal and study of specific metal removal rate and surface roughness during the process. *Journal of Materials Processing Technology*. 213, 1509-1515.
- Jadhav, U., Su, C., Hocheng, H., 2016. Leaching of metals from printed circuit board powder by an *Aspergillus niger* culture supernatant and hydrogen peroxide. *RSC Advances*. 6, 43442-43452.
- Jaisankar, S., Modak, J.M., 2009. Ferrous iron oxidation by foam immobilized *Acidithiobacillus ferrooxidans*: experiments and modeling. *Biotechnology Progress*. 25, 1328-1342.
- Jensen, A.B., Webb, C., 1995. Ferrous sulphate oxidation using *Thiobacillus ferrooxidans*: a review. *Process Biochemistry*. 30, 225-236.
- Johnson, D.B., 2007. Physiology and ecology of acidophilic microorganisms. In: Gerday C, Glansdorff N (eds) *Physiology and biochemistry of extremophiles*. ASM, Washington, DC, 257-270.

- Jujun, R., Zheng, J., Jian, H., Jianwen, Z., 2015. A novel designed bioreactor for recovering precious metals from waste printed circuit boards. *Scientific Reports*. 5, 13481.
- Junfeng, Y., Guoliang, L., Wei, C., 2007. Ferrous sulphate oxidation using *Acidithiobacillus ferrooxidans* cells immobilized in ceramic beads. *Chemical and Biochemical Engineering Quarterly*. 21, 175-179.
- Kahrizi, E., Alemzadeh, I., Vossoughi, M., 2008. Bio-oxidation of ferrous ions by *Acidithiobacillus ferrooxidans* in a monolithic bioreactor. *Journal of Chemical Technology and Biotechnology*. 84, 504-510.
- Kaksonen, A.H., Boxall, N.J., Gumulya, Y., Khaleque, H.N., Morris, C., Bohu, T., Cheng, K.Y., Usher, K.M., Lakaniemi, A.M., 2018. Recent progress in biohydrometallurgy and microbial characterisation. *Hydrometallurg*. 180, 7-25.
- Karimi, G. R., Rowson, N. A., Hewitt, C. J., 2010. Bioleaching of copper via iron oxidation from chalcopyrite at elevated temperatures. *Food and Bioproducts Processing*. 88, 21-25.
- Karwowska, E., Andrzejewska-Morzuch, D., Lebkowska, M., Tabernacka, A., Wojtkowska, M., Telepko, A., Konarzewska, A., 2014. Bioleaching of metals from printed circuit boards supported with surfactant producing bacteria. *Journal of Hazardous Materials*. 264, 203-210.
- Kasper, A., Berselli, G.B.T., Freitas, B. D., Tenório, J. A.S., Bernardes, A. M., Veit, H., 2011. Printed wiring boards for mobile phones: Characterization and recycling of copper. *Waste Management*. 31, 2536-2545.
- Kasuga, E., Kawakami, Y., Matsumoto, T., Hidaka, E., Oana, K., Ogiwara, N., Yamaki, D., Sakurada, T., Honda, T., 2011. Bactericidal activities of woven cotton and nonwoven polypropylene fabrics coated with hydroxyapatite-binding silver/titanium dioxide ceramic composite "Earth-plus". *International Journal of Nanomedicine*. 6, 1937-1943.
- Kawabe, Y., Inoue, C., Suto, K., Chida, T., 2003. Inhibitory effect of high concentrations of ferric ions on the activity of *Acidithiobacillus ferrooxidans*. *Journal of Bioscience and Bioengineering*. 96, 375-379.
- Kaya, M., 2016. Recovery of metals and nonmetals from electronic waste by physical and chemical recycling processes. *Waste Management*. 57, 64-90.
- Khatri, B. R., Sodha, A. B., Shah, M. B., Tipre, D. R., Dave, S. R., 2018. Chemical and microbial leaching of base metals from obsolete cell-phone printed circuit boards. *Sustainable Environment Research*. 28, 333-339.
- Konishi, Y., Nishimura, H., Asai, S., 1998. Bioleaching of sphalerite by the acidophilic thermophile *Acidianus brierleyi*. *Hydrometallurgy*. 47, 339-352.
- Koseoglu-Imer, D.Y., Keskinler, B., 2013. Immobilization of *Acidithiobacillus ferrooxidans* on sulfonated microporous poly (styrene-divinylbenzene) copolymer with granulated activated carbon and its use in bio-oxidation of ferrous iron. *Materials Science and Engineering C*. 33, 53-58.
- Krok, B., Schippers, A., Sand, W., 2013. Copper recovery by bioleaching of chalcopyrite: A microcalorimetric approach for the fast determination of bioleaching activity. *Advanced Materials Research*. 825, 322-325.

- Kumar, A., Holuszko, M., Espinosa, D. C. R., 2017. E-waste: an overview on generation, collection, legislation and recycling practices. *Resources, Conservation and Recycling*. 122, 32–42.
- Kumar, P.S., Yaashikaa, P.R., 2020. Recent trends and challenges in bioleaching technologies. In *Biovalorisation of Waste to Renewable Chemicals and Biofuels*; Rathinam, N.K., Sani, R.K., Eds.; Elsevier: Amsterdam, The Netherlands, 373-388.
- Leahy, M.J., Davidson, M.R., Schwarz, M.P., 2007. A model for heap bioleaching of chalcocite with heat balance: mesophiles and moderate thermophiles. *Hydrometallurgy*. 85, 24-41.
- Lee, Y., Sethurajan, M., Vossenbergh, J.V.D., Meers, E., Hullebusch, E.D., 2020. Recovery of phosphorus from municipal wastewater treatment sludge through bioleaching using *Acidithiobacillus thiooxidans*. *Journal of Environmental Management*. 270, 110818.
- Levenspiel, O., 2005. *Ingeniería de las Reacciones Químicas*. Editorial Reverte. España. 55-78.
- Lewis, G., Gaydardzhiev, S., Bastin, D., Bareel, P.F., 2011. Bio hydrometallurgical recovery of metals from fine shredder residues. *Minerals Engineering*. 24, 1166-1171.
- Li, Y.-Q., Wan, D.-S., Huang, S.-S., Leng, F.-F., Yan, L., Ni, Y.-Q., Li, H.-Y., 2010. Type IV pili of *Acidithiobacillus ferrooxidans* are necessary for sliding, twitching motility, and adherence. *Current Microbiology*. 60, 17-24.
- Li, Y., Kawashima, N., Li, J., Chandra, A.P., Gerson, A.R., 2013. A review of the structure, and fundamental mechanisms and kinetics of the leaching of chalcopyrite. *Advances in Colloid and Interface Science*. 197-198, 1-32.
- Liang, G.B., Mo, Y.W., Zhou, Q.F., 2010. Novel strategies of bioleaching metals from printed circuit boards (PCBs) in mixed cultivation of two acidophiles. *Enzyme and Microbial Technology*. 47, 322-326.
- Liang, G.B., Tang, J., Liu, W., Zhou, Q., 2013. Optimizing mixed culture of two acidophiles to improve copper recovery from printed circuit boards (PCBs). *Journal of Hazardous Materials*. 250, 238-245.
- Lilova, K., Karamanev, D.; Flemming, R.L., Karamaneva, T., 2007. Biological oxidation of metallic copper by *Acidithiobacillus ferrooxidans*. *Biotechnology and Bioengineering*. 97, 308-316.
- Lindström, E.B., Wold, S., Ketteneh-Wold, N., Sääf, S., 1993. Optimization of pyrite bioleaching using *Sulfolobus acidocaldarius*. *Applied Microbiology and Biotechnology*. 38, 702-707.
- Liu, J., Tao, X., Cai, P., 2009. Study of formation of jarosite mediated by *thiobacillus ferrooxidans* in 9K medium. *Procedia Earth and Planetary Science*. 1, 706-712.
- Liu, H., Xia, J., Nie, Z., Ma, C., Zheng, L., Hong, C., Zhao, Y., Wen, W., 2016. Bioleaching of chalcopyrite by *Acidianus manzaensis* under different constant pH. *Minerals Engineering*. 98, 80-89.
- Liu, R., Mao, Z., Liu, W., Wang, Y., Cheng, H., Zhou, H., Zhao, K., 2020. Selective removal of cobalt and copper from Fe (III)-enriched high-pressure acid leach residue using the hybrid bioleaching technique. *Journal of Hazardous Materials*. 384, 121462.

- Lixandru, A., Venkatesan, P., Jönsson, C., Poenaru, I., Hall, B., Yang, Y., Gutfleisch, O., 2017. Identification and recovery of rare-earth permanent magnets from waste electrical and electronic equipment. *Waste Management*. 68, 482-489.
- Ma F., Huang H., Cui C., Mater J., 2020. Biomachining properties of various metals by microorganisms. *Process Technology*. 278, 116512.
- Mahmoud, A., Cézac, P., Hoadley, A.F.A., Contamine, F., D'Hugues, P., 2017. A review of sulfide minerals microbially assisted leaching in stirred tank reactors. *International Biodeterioration and Biodegradation*. 19, 118-146.
- Malki, M., González-Toril, E., Sanz, J.L., Gómez, F., Rodríguez, N., Amils, R., 2006. Importance of the iron cycle in biohydrometallurgy. *Hydrometallurgy*. 83, 223-228.
- Marra, A., Cesaro, A., Rene, E.R., Belgiorno, V., Lens, P.N.L., 2018. Bioleaching of metals from WEEE shredding dust. *Journal of Environmental Management*. 210, 180-190.
- Merum, P., Chu, Y., Shi, F., Cao, Y., 2017. Biological effects in *Pseudomonas* species by the non-thermal atmospheric pressure plasma conditions. *Advances in Engineering Research*. 143, 828-833.
- Mikkelsen, D., Kappler, U., McEwan, A.G., Sly, L.I., 2006. Archaeal diversity in two thermophilic chalcopyrite bioleaching reactors. *Environmental Microbiology*. 8, 2050-2056.
- Mikkelsen, D., Kappler, U., Webb, R.I., Rasch, R., McEwan, A.G., Sly, L.I., 2007. Visualisation of pyrite leaching by selected thermophilic archaea: Nature of microorganism-ore interactions during bioleaching. *Hydrometallurgy*. 88, 143-153.
- Mishra, D., Kim, D.J., Ahn, J.G., Rhee, Y.H., 2005. Bioleaching: a microbial process of metal recovery; A review. *Metals and Materials International*. 11, 249-256.
- Mishra, A., Malik, A., 2012. Simultaneous bioaccumulation of multiple metals from electroplating effluent using *Aspergillus lentulus*. *Water Research*. 46, 4991-4998.
- Mishra, D., Rhee, Y.H., 2014. Microbial leaching of metals from solid industrial wastes. *Journal of Microbiology*. 52, 1-7.
- Mizero, B., Musongo, T., Rene, E.R., Battes, F., Lens, P.N., 2018. Optimization of process parameters for the chemical leaching of base metals from telecom and desktop printed circuit boards. *Process Safety and Environmental Protection*. 120, 14-23.
- Modak, J.M., Natarajan, K.A., Mukhopadhyay, S., 1996. Development of temperature-tolerant strains of *Thiobacillus ferrooxidans* to improve bioleaching kinetics. *Hydrometallurgy*. 42, 51-61.
- Mohanty, B.K., Mishra A.K., 1993. Scanning electron micrograph study of *Bacillus licheniformis* during bioleaching of silica from magnesite ore. *Journal of Applied Bacteriology*. 74, 284-289.
- Moltó, J., Egea, S., Conesa, J.A., Font, R., 2011 Thermal decomposition of electronic wastes: Mobile phone case and other parts. *Waste Management*. 31, 2546-2552.
- Monneron-Enaud, B., Wiche, O., Schlömann, M., 2020. Biodismantling, a Novel Application of Bioleaching in Recycling of Electronic Wastes. *Recycling*. 5, 22.
- Mousavi, S. M., Yaghmaei, S., Jafari, A., 2007. Influence of process variables on biooxidation of ferrous sulfate by an indigenous *Acidithiobacillus ferrooxidans*. Part II: Bioreactor experiments. *Fuel*. 86, 993-999.

- Moyo, T., Chirume, B.H., Petersen, J., 2020. Assessing alternative pre-treatment methods to promote metal recovery in the leaching of printed circuit boards. *Resources, Conservation and Recycling*. 152, 104545.
- Muhammad, I., Sana Ullah, S. M., Sup Han, D., Jo Ko, T., 2015. Selection of optimum process parameters of biomachining for maximum metal removal rate. *International Journal of Precision Engineering and Manufacturing-Green Technology*. 2, 307-313.
- Mykytczuk, N. C. S., Trevors, J. T., Ferroni, G. D., Leduc, L. G., 2011. Cytoplasmic membrane response to copper and nickel in *Acidithiobacillus ferrooxidans*. *Microbiological Research*. 166, 186-206.
- Nasab, M.H., Noaparast, M., Abdollahi, H., Amoozegar, M.A., 2020. Indirect bioleaching of Co and Ni from iron rich laterite ore, using metabolic carboxylic acids generated by *P. putida*, *P. koreensis*, *P. bilaji* and *A. niger*. *Hydrometallurgy* 193, 105309.
- Naseri, T., Bahaloo-Horeh, N., Mousavi, S.M., 2019. Environmentally friendly recovery of valuable metals from spent coin cells through two-step bioleaching using *Acidithiobacillus thiooxidans*. *Journal of Environmental Management*. 235, 357-367.
- Natarajan, G., Ting, Y-P., 2014. Pretreatment of e-waste and mutation of alkali-tolerant cyanogenic bacteria promote gold biorecovery. *Bioresource Technology*. 152, 80-85.
- Nemati, M., Harrison, S.T.L., Hansford, G.S., Webb, C., 1998. Biological oxidation of ferrous sulphate by *Thiobacillus ferrooxidans*: a review on the kinetic aspects. *Biochemical Engineering Journal*. 1, 171-190.
- Nguyen, V. K., M. H. Lee, H. J. Park, and J. U. Lee., 2015. Bioleaching of arsenic and heavy metals from mine tailings by pure and mixed cultures of *Acidithiobacillus spp.* *Journal of Industrial and Engineering Chemistry*. 21, 451-458.
- Nie, H.C.Y., Zhu, N., Wu, P., Zhang, T., Zhang, Y., Xing, Y., 2015a. Isolation of *Acidithiobacillus ferrooxidans* strain Z1 and its mechanism of bioleaching copper from waste printed circuit boards. *Journal of Chemical Technology and Biotechnology*. 90, 714-721.
- Nie, H., Zhu, N., Cao, Y., Xu, Z., Wu, P., 2015b. Immobilization of *Acidithiobacillus ferrooxidans* on cotton gauze for the bioleaching of waste printed circuit boards. *Applied Biochemistry and Biotechnology*. 177, 675-688.
- Ning, C., Lin, C.S.K., Hui, D.C.W., McKay, G., 2017. Waste Printed Circuit Board (PCB) Recycling Techniques. *Topics in Current Chemistry*. 375, 43.
- Nithya, R., Sivasankari, C., Thirunavukkarasu, A., 2020. Electronic waste generation, regulation and metal recovery: a review. *Environmental Chemistry Letters*.
- Okoh, M.P., Olobayetan, I.W., Machunga-Mambula, S.S., 2018. Bioleaching, a technology for metal extraction and remediation: mitigating health consequences for metal exposure. *International Journal of Sustainable Development*. 7, 2103-2118.
- Ongondo, F.O., Williams, I.D., Cherrett, T.J., 2011. How are WEEE doing? A global review of the management of electrical and electronic wastes. *Waste Management*. 31, 714-730.
- Orell, A., Navarro, C.A., Arancibia, R., Mobarec, J.C., Jerez, C.A., 2010. Life in blue: Copper resistance mechanisms of bacteria and Archaea used in industrial biomining of minerals. *Biotechnology Advances*., 28, 839-848.

- Ortuño, N., Moltó, J., Egea, S., Font, R., Conesa, J.A., 2013. Thermogravimetric study of the decomposition of printed circuit boards from mobile phones. *Journal of Analytical and Applied Pyrolysis*. 103, 189-200.
- Osman, Y., Gebreil, A., Mowafy, A.M., Anan, T.I., Hamed, S.M., 2019. Characterization of *Aspergillus niger* siderophore that mediates bioleaching of rare earth elements from phosphorites. *World Journal of Microbiology and Biotechnology*. 35, 93.
- Pal, S., Pradhan, D., Das, T., Sukla, L.B., Roy Chaudhury, G., 2010. Bioleaching of low-grade uranium ore using *Acidithiobacillus ferrooxidans*. *Indian Journal of Microbiology*. 50, 70-75.
- Palmieri, R., Bonifazi, G., Serranti, S., 2014. Recycling-oriented characterization of plastic frames and printed circuit boards from mobile phones by electronic and chemical imaging. *Waste Management*. 34, 2120-2130.
- Panda, S., Akcil, A., Pradhan, N., Deveci, H., 2015. Current scenario of chalcopyrite bioleaching: a review on the recent advances to its heap-leach technology. *Bioresource Technology*. 196, 694-706.
- Pant, D., Joshi, D., Upreti, M.K., Kotnala, R.K., 2012. Chemical and biological extraction of metals present in E waste: a hybrid technology. *Waste Management*. 32, 979-990.
- Park, C.-Y., Cheong, K.-H., Kim, B.-J., 2010. The bioleaching of sphalerite by moderately thermophilic bacteria. *Economic and Environmental Geology*. 43, 573-587.
- Pathak, A., Morrison, L., Healy, M.G., 2017. Catalytic potential of selected metal ions for bioleaching, and potential techno-economic and environmental issues: A critical review. *Bioresource Technology*. 229, 211-221.
- Pathak, A., Kothari, R., Vinoba, M., Habibi, N., Tyagi, V.V., 2021. Fungal bioleaching of metals from refinery spent catalysts: A critical review of current research, challenges, and future directions. *Journal of Environmental Management*. 280, 111789.
- Peng, T.J., Ma, L.Y., Feng, X., Tao, J.M., Nan, M.H., Liu, Y.D., Li, J.K., Shen, L., Wu, X.L., Yu, R.L., Liu, X.D., Qiu, G.Z., Zeng, W.M., 2017. Genomic and transcriptomic analyses reveal adaptation mechanisms of an *Acidithiobacillus ferrivorans* strain YL15 to alpine acid mine drainage. *PLoS ONE*. 12, 0178008.
- Pham, V., Ting, Y. P., 2009. Gold bioleaching of electronic waste by cyanogenic bacteria and its enhancement with bio-oxidation. *Advanced Materials Research*. 71, 661-664.
- Plumb, J.J., Muddle, R., Franzmann, P.D., 2008. Effect of pH on rates of iron and sulfur oxidation by bioleaching organisms. *Minerals Engineering*. 21, 76-82.
- Potysz, A., Lens, P.N.L., van de Vossenberg, J., Rene, E.R., Grybos, M., Guibaud, G., Kierczak, J., van Hullebusch, E.D., 2016. Comparison of Cu, Zn and Fe bioleaching from Cu-metallurgical slags in the presence of *Pseudomonas fluorescens* and *Acidithiobacillus thiooxidans*. *Applied Geochemistry*. 68, 39-52.
- Pourhossein, F., Mousavi, S.M., 2018. Enhancement of copper, nickel, and gallium recovery from led waste by adaptation of *Acidithiobacillus ferrooxidans*. *Waste Management*. 79, 98-108.
- Pradhan, N., Nathsarma, K., Rao, K.S., Sukla, L., Mishra, B., 2008. Heap bioleaching of chalcopyrite: a review. *Minerals Engineering*. 21, 355-365.

- Pradhan, J.K., Kumar, S., 2012. Metals bioleaching from electronic waste by *Chromobacterium violaceum* and *Pseudomonads sp.* Waste Management and Research. 30, 1151-1159.
- Priya, A., Hait, S., 2017. Comparative assessment of metallurgical recovery of metals from electronic waste with special emphasis on bioleaching. Environmental Science and Pollution Research. 24, 6989-7008.
- Priya, A., Hait, S., 2018. Extraction of metals from high grade waste printed circuit board by conventional and hybrid bioleaching using *Acidithiobacillus ferrooxidans*. Hydrometallurgy. 177, 132-139.
- Priya, A., Hait, S., 2020. Biometallurgical recovery of metals from waste printed circuit boards using pure and mixed strains of *Acidithiobacillus ferrooxidans* and *Acidiphilium acidophilum*. Process Safety and Environmental Protection. 143, 262-272.
- Pronk, J.T., de Bruyn, J.C., Bos, P., Kuenen, J.G., 1992. Anaerobic growth of *Thiobacillus ferrooxidans*. Applied and Environmental Microbiology. 58, 2227-2230
- Qu, Y., Lian, B., Mo, B., Liu, C., 2013. Bioleaching of heavy metals from red mud using *Aspergillus niger*. Hydrometallurgy. 136, 71-77.
- Quatrini, R., Appia-Ayme, C., Denis, Y., Ratouchniak, J., Veloso, F., Valdes, J., Lefimil, C., Silver, S., Roberto, F., Orellana, O., Denizot, F., Jedlicki, E., Holmes, D.S., Bonnefoy, V., 2006. Insights into the iron and sulfur energetic metabolism of *Acidithiobacillus ferrooxidans* by microarray transcriptome profiling. Hydrometallurgy. 83, 263-272.
- Quatrini, R., Escudero, L.V., Moya-Beltrán, A., Galleguillos, P.A., Issotta, F., Acosta, M., Cárdenas, J.P., Nuñez, H., Salinas, K., Holmes, D.S., 2017. Draft genome sequence of *Acidithiobacillus thiooxidans* CLST isolated from the acidic hypersaline Gorbea salt flat in northern Chile. Standards in Genomic Sciences. 12, 1-8.
- Rasoulnia, P., Mousavi, S.M., 2016. Maximization of organic acids production by *Aspergillus niger* in a bubble column bioreactor for V and Ni recovery enhancement from power plant residual ash in spent-medium bioleaching experiments. Bioresource Technology. 216, 729-736.
- Ravindra P., Kodli B., Veera Rao V.P.R., 2015. Effect of Adaptation of *Acidithiobacillus ferrooxidans* on Ferrous Oxidation and Nickel Leaching Efficiency. Advances in Bioprocess Technology. 17-26.
- Rawlings, D.E., 1997. Mesophilic, autotrophic bioleaching bacteria: description, physiology and role. In: Rawlings DE, ed. Biomining: Theory, Microbes and Industrial Processes. Springer-Verlag, Berlin, 229-245.
- Rawlings, D.E., 2005. Characteristics and adaptability of iron- and sulfur-oxidizing microorganisms used for the recovery of metals from minerals and their concentrates. Microbial Cell Factories. 4, 13.
- Rawlings, D.E., Johnson, D.B., 2007 The microbiology of biomining: development and optimization of mineral-oxidizing microbial consortia. Microbiology. 153, 315-324.
- Ren, W., Li, P., Geng, Y., Li, X., 2009. Biological leaching of heavy metals from a contaminated soil by *Aspergillus niger*. Journal of Hazardous Materials. 167, 164-169.

- Rezza, I., Salinas, E., Elorza, M., Tosetti, M., Donati, E., 2001. Mechanisms involved in bioleaching of an aluminosilicate by heterotrophic microorganisms. *Process Biochemistry*. 36, 495-500.
- Rohwerder, T., Gehrke, T., Kinzler, K., Sand, W., 2003. Bioleaching review part A: Progress in bioleaching: fundamentals and mechanisms of bacterial metal sulfide oxidation. *Applied Microbiology and Biotechnology*. 63, 239-248.
- Rojas-Chapana, J.A., Bärtels, C.C., Pohlmann, L., Tributsch, H., 1998. Co-operative leaching and chemotaxis of *Thiobacillus* studied with spherical sulfur/sulfide substrates. *Process Biochemistry*. 33, 239-248.
- Roshani, M., Shojaosadati, S.A., Safdari, S.J., Vasheghani-Farahani, E., Mirjalili, K., Manafi, Z., 2017. Bioleaching of molybdenum by two new thermophilic strains isolated and characterized. *Iranian Journal of Chemistry and Chemical Engineering*. 36, 183-194.
- Roy, J. J., Madhavi, S., Cao, B., 2021. Metal extraction from spent lithium-ion batteries (LIBs) at high pulp density by environmentally friendly bioleaching process. *Journal of Cleaner Production*. 280, 124242.
- Rozas, E. E., Mendes, M. A., Nascimento, C. A. O., Espinosa, D. C.R., Oliveira, R., Oliveira, G., Custodio., M. R., 2017. Bioleaching of electronic waste using bacteria isolated from the marine sponge *Hymeniacidon heliophila* (Porifera). *Journal of Hazardous Materials*. 329, 20-130.
- Ruan, J., Zhu, X., Qian, Y., Hu, J., 2014. A new strain for recovering precious metals from waste printed circuit boards. *Waste Management*. 34, 901-907.
- Sajjad, W., Zheng, G., Din, G., Ma, X., Rafiq, M., Xu, W., 2019. Metals extraction from sulfide ores with microorganisms: the bioleaching technology and recent developments. *Transactions of the Indian Institute of Metals*. 72, 559-579.
- Saleh, D.K., Abdollahi, H., Noaparast, M., Nosratabad, A.F., Tuovinen, O.H., 2019. Dissolution of Al from metakaolin with carboxylic acids produced by *Aspergillus niger*, *Penicillium bilaji*, *Pseudomonas putida*, and *Pseudomonas koreensis*. *Hydrometallurgy*. 186, 235-243.
- Samadzadeh Yazdi, M., Abdollahi, M., Mousavi, S., Khodadadi Darban., 2020. A Comparison of Copper Dissolution in Chalcopyrite Concentrate Bioleaching with *Acidianus Brierleyi* in Different Initial pH Values. *Journal of Mining and Environment*. 11, 753-764.
- Sand, W., Gehrke, T., Jozsa, P-G., Schippers, A., 2001. (Bio)chemistry of bacterial leaching—direct vs indirect bioleaching. *Hydrometallurgy*. 59, 159-175
- Santaolalla A., Gutierrez, J., Gallastegui G., Barona A., Rojo N., 2021. Immobilization of *Acidithiobacillus ferrooxidans* in bacterial cellulose for a more sustainable bioleaching process. *Journal of Environmental Chemical Engineering*. 9, 105283
- Santhiya, D., Ting, Y. P., 2005. Bioleaching of spent refinery processing catalyst using *Aspergillus niger* with high-yield oxalic acid. *Journal of Biotechnology*. 116, 171-184.
- Senophiyah-Mary, J., Loganath, R., Meenambal, T., 2018. A novel method for the removal of epoxy coating from waste printed circuit board. *Waste Management and Research*. 36, 645-652.
- Shabani, M.A., Irannajad, M., Azadmehr, A.R., Meshkini, M., 2013. Bioleaching of copper oxide ore by *Pseudomonas aeruginosa*. *International Journal of Minerals Metallurgy and Materials*. 20, 1130-1133.

- Shah, M.B., Tipre, D.R., Purohit, M.S., Dave, S.R., 2015. Development of two-step process for enhanced biorecovery of Cu–Zn–Ni from computer printed circuit boards. *Journal of Bioscience and Bioengineering*. 120, 167-173.
- Sheng, P.P., Etsell, T.H., 2007. Recovery of gold from computer circuit board scrap using aqua regia. *Waste Management and Research*. 25, 380-383.
- Shenker, M., Hadar, Y., Chen, Y., 1999. Kinetics of iron complexing and metal exchange in solutions by *rhizoferrin*, a fungal siderophore. *Soil Science Society of America Journal*. 63, 1681-1687.
- Shin, D., Jeong, J., Lee, S., Pandey, B., Lee, J-C., 2013. Evaluation of bioleaching factors on gold recovery from ore by cyanide-producing bacteria. *Minerals Engineering*. 48, 20-24.
- Shin, D., Park, J., Jeong, J., Kim, B., 2015. A biological cyanide production and accumulation system and the recovery of platinum-group metals from spent automotive catalysts by biogenic cyanide. *Hydrometallurgy*. 158, 10-18.
- Silvas, F.P.C., Correa, M.M.J., Caldas, M.P.K., de Moraes, V.T., Espinosa, D.C.R., Tenório, J.A.S., 2015. Printed circuit board recycling: physical processing and copper extraction by selective leaching. *Waste Management*. 46, 503-510.
- Singh, A., Manikandan, A., Ravi Sankar, M., Paksirajan, K., Roy, L., 2018. Experimental investigations and surface morphology of bio-micromachining on copper. *Materials Today: Proceedings*. 5, 4225-4234.
- Sodha, A.B., Tipre, D.R., Dave, S.R., 2020. Optimisation of biohydrometallurgical batch reactor process for copper extraction and recovery from non-pulverized waste printed circuit boards. *Hydrometallurgy*. 191, 105170.
- Stott, M.B., Sutton, D.C., Watling, H.R., Franzmann, P.D., 2003. Comparative leaching of chalcopyrite by selected Acidophilic Bacteria and Archaea. *Geomicrobiology Journal*. 20, 215-230.
- Štyriaková, I., Štyriak, I., Nandakumar, M. P., Mattiasson, B., 2003. Bacterial destruction of mica during bioleaching of kaolin and quartz sands by *Bacillus cereus*. *World Journal of Microbiology and Biotechnology*. 19, 583-590.
- Tang, J.A.; Valix, M., 2006. Leaching of low grade limonite and nontronite ores by fungi metabolic acids. *Minerals Engineering*. 19, 1274–1279.
- Temple, K.L., Colmer, A.R., 1951. The autotrophic oxidation of iron by a new bacterium: *Thiobacillus ferrooxidans*. *Journal of Bacteriology*. 62, 605-611.
- Tesfaye, F., Lindberg, D., Hamuyuni, J., Taskinen, P., Hupa, L., 2017. Improving urban mining practices for optimal recovery of resources from e-waste. *Minerals Engineering*. 111, 209-221.
- Thangavelu, V., Tang, J., Ryan, D., Valix, M., 2006. Effect of saline stress on fungi metabolism and biological leaching of weathered saprolite ores. *Minerals Engineering*. 19, 1266-1273.
- Tributsch, H., 2001. Direct vs indirect bioleaching. *Hydrometallurgy*. 59, 177-185.
- Uno, Y., Kaneeda, T., Yokomizo, S., 1993. Fundamental study on biomachining, machining of metals by *Thiobacillus ferrooxidans*. *JSME International Journal*. 39, 837-842.
- Vakilchap, F., Mousavi, S.M., Shojaosadati, S.A., 2016. Role of *Aspergillus niger* in recovery enhancement of valuable metals from produced red mud in Bayer process. *Bioresource Technology*. 218, 991-998.

- Valdés, J., Pedroso, I., Quatrini, R., Dodson, R.J., Tettelin, H., Blake, R., Eisen, J.A., Holmes, D.S., 2008. *Acidithiobacillus ferrooxidans* metabolism: from genome sequence to industrial applications. *BMC Genomics*. 9, 597.
- Valix, M., 2017. Bioleaching of electronic waste: milestones and challenges. In: *Current Developments in Biotechnology and Bioengineering: Solid Waste Management*. Ed: Elsevier. 407-440.
- Van Yken, J., Cheng, K.Y., Boxall, N.J., Nikoloski, A.N., Moheimani, N., Valix, M., Sahajwalla, V., Kaksonen A.H., 2020. Potential of metals leaching from printed circuit boards with biological and chemical lixivants. *Hydrometallurgy*. 196, 105433.
- Velásquez, L., Dussan, J., 2009. Biosorption and bioaccumulation of heavy metals on dead and living biomass of *Bacillus sphaericus*. *Journal of Hazardous Materials*. 167, 713-716.
- Verma P., Sodhi A.K., Bhanot N., 2019. Application of *Aspergillus Niger* for Biomachining of Aluminium Alloy 4004. In: Agnihotri A., Reddy K., Bansal A. (eds) *Sustainable Engineering. Lecture Notes in Civil Engineering*, vol 30. Springer, Singapore.
- Vermeulen, F., Nicolay, X., 2017. Sequential bioleaching of copper from brake pads residues using encapsulated bacteria. *Minerals Engineering*. 106, 39-45.
- Vestola, E.A., Kuusenaho, M.K., Närhi, H.M., Tuovinen, O.H., Puhakka, J.A., Plumb, J.J., Kaksonen, A.H., 2010. Acid bioleaching of solid waste materials from copper, steel and recycling industries. *Hydrometallurgy*. 103, 74-79.
- Vilcáez, J., Suto, K., Inoue, C., 2008. Bioleaching of chalcopyrite with thermophiles: Temperature-pH-ORP dependence. *International Journal of Mineral Processing*. 88, 37-44.
- Vrdoljak, G.A., S.C. Spiller., 2005. Characterization of an Acid Mine Biofilm by Cryo Scanning Electron Microscopy. *Microscopy and Microanalysis*. 11, 292-293.
- Wang, J.W., Bai, J.F., Xu, J.Q., Liang, B., 2009. Bioleaching of metals from printed wire boards by *Acidithiobacillus ferrooxidans* and *Acidithiobacillus thiooxidans* and their mixture. *Journal of Hazardous Materials*. 172, 1100-1105.
- Wang, Y.G., Su, L.J., Zhang, L.J., Zeng, W.M., Wu, J.Z., Wan, L.L., Qiu, G.Z., Chen, X.H., Zhou, H.B., 2012. Bioleaching of chalcopyrite by defined mixed moderately thermophilic consortium including a marine acidophilic halotolerant bacterium. *Bioresource Technology*. 21, 348-354.
- Wang, S., Zheng, W., Chen, L., Mahadevan, G. D., Zhao, F., 2016. Enhanced bioleaching efficiency of metals from e-wastes driven by biochar. *Journal of Hazardous Materials*. 320, 393-400.
- Wang, S., Chen, L., Zhou, X., Yan, W., Ding, R., Chen, B., Wang, C. T., Zhao, F., 2018. Enhanced bioleaching efficiency of copper from printed circuit boards without iron loss. *Hydrometallurgy*. 180, 65-71.
- Watling, H.R., 2006. The bioleaching of sulphide minerals with emphasis on copper sulphides- A review. *Hydrometallurgy*. 84, 81-108.
- Whulanza, Y., Nadhif, H., Istiyanto, J., Supriadi, S., Bachtiar, B., 2016. PDMS surface modification using biomachining method for biomedical application. *Journal of Biomimetics Biomaterials and Biomedical Engineering*. 26, 66-72.
- Widmer, R., Oswald-Krapf, H., Sinha-Khetriwal, D., Schnellmann, M., Böni, H., 2005. Global perspectives on e-waste. *Environmental Impact Assessment Review*. 25, 436-458.

- Wu, H.Y., Ting, Y.P., 2006. Metal extraction from municipal solid waste (MSW) incinerator fly ash—Chemical leaching and fungal bioleaching. *Enzyme and Microbial Technology*. 38, 839-847.
- Wu, X., Hu, Q., Hou, D., Miao, B., Liu, X., 2010. Differential gene expression in response to copper in *Acidithiobacillus ferrooxidans* strains possessing dissimilar copper resistance. *Journal of General and Applied Microbiology*. 56, 491-498.
- Wu, W., Liu, X., Zhang, X., Zhu, M., Tan, W., 2018. Bioleaching of copper from waste printed circuit boards by bacteria-free cultural supernatant of iron–sulfur-oxidizing bacteria. *Bioresources and Bioprocessing*. 5, 10.
- Xenofontos, E., Feidiou, A., Constantinou, M., Constantinides, G., Vyrides, I., 2015. Copper biomachining mechanisms using the newly isolated *Acidithiobacillus ferrooxidans* B1. *Corrosion Science*. 100, 642-650.
- Xia, J-l., Peng, A-a., He, H., Yang, Y., Liu, X-d., Qiu, G-z., 2007. A new strain *Acidithiobacillus albertensis* BY-05 for bioleaching of metal sulfides ores. *The Transactions of Nonferrous Metals Society of China*. 17, 168.
- Xia, M., Bao, P., Liu, A., Wang, M., Shen, L., Yu, R., Liu, Y., Chen, M., Li, J., Wu, X., Qiu, G., Zeng, W., 2018. Bioleaching of low-grade waste printed circuit boards by mixed fungal culture and its community structure analysis. *Resources, Conservation and Recycling*. 136, 267-275.
- Xiang, Y., Wu, P., Zhu, N., Zhang, T., Liu, W., Wu, J., Ping, L., 2010. Bioleaching of copper from waste printed circuit boards by bacterial consortium enriched from acid mine drainage. *Journal of Hazardous Materials*. 184, 812-818.
- Xin, B., Jiang, W., Li, X., Zhang, K., Liu, C., 2012. Analysis of reasons for decline of bioleaching efficiency of spent Zn–Mn batteries at high pulp densities and exploration measure for improving performance. *Bioresource Technology*. 112, 186-192.
- Yamane, L.H., de Moraes, V.T., Espinosa, D.C., Tenório, J.A., 2011. Recycling of WEEE: Characterization of spent printed circuit boards from mobile phones and computers. *Waste Management*. 31, 2553-2558.
- Yang, T., Xu, Z., Wen, J., Yang, L., 2009a. Factors influencing bioleaching copper from waste printed circuit boards by *Acidithiobacillus ferrooxidans*. *Hydrometallurgy*. 97, 29-32.
- Yang, Y., Wang, X., Liu, Y., Wang, S., Wen, W., 2009b. Techniques for micromachining using *Thiobacillus ferrooxidans* based on different culture medium. *Applied Mechanics and Materials*. 16-19, 1053-1055.
- Liu, J., Yang, J., 2011. Leaching copper from shredded particles of waste printed circuit boards. *Journal of Hazardous Materials*. 187, 393-400.
- Yang, Y., Chen, S., Li, S., Chen, M., Chen, H., Liu, B., 2014. Bioleaching waste printed circuit boards by *Acidithiobacillus ferrooxidans* and its kinetics aspect. *Journal of Biotechnology*. 173, 24-30.
- Yang, C., Zhu, N., Shen, W., Zhang, T., Wu, P., 2017. Bioleaching of copper from metal concentrates of waste printed circuit boards by a newly isolated *Acidithiobacillus ferrooxidans* strain Z1. *Journal of Material Cycles and Waste Management*. 19, 247-255.
- Yin, N.H., Sivry, Y., Avril, C., Borensztajn, S., Labanowski, J., Malavergne, V., Lens, P.N.L., Rossano, S., van Hullebusch, E.D., 2014. Bioweathering of lead blast furnace metallurgical

- slags by *Pseudomonas aeruginosa*. International Biodeterioration and Biodegradation. 86, 372-381.
- Yu, R., Liu, Z., Yu, Z., Wu, X., Shen, L., Liu, Y., Zeng, W., 2019. Relationship among the secretion of extracellular polymeric substances, heat resistance, and bioleaching ability of *Metallosphaera sedula*. International Journal of Minerals, Metallurgy and Materials. 26, 1504-1511.
- Zhan, Y., Yang, M., Zhang, S., Zhao, D., Duan, J., Wang, W., Yan, L., 2019. Iron and sulfur oxidation pathways of *Acidithiobacillus ferrooxidans*. World Journal of Microbiology and Biotechnology. 35, 60.
- Zhang, Y., Yang, Y., Liu, J., Qiu, G., 2013. Isolation and characterization of *Acidithiobacillus ferrooxidans* strain QXS-1 capable of unusual ferrous iron and sulfur utilization. Hydrometallurgy. 136, 51-57.
- Zhang, G., Chao, X., Guo, P., Cao, J., Yang, C., 2015. Catalytic effect of Ag⁺ on arsenic bioleaching from orpiment (As₂S₃) in batch tests with *Acidithiobacillus ferrooxidans* and *Sulfobacillus sibiricus*. Journal of Hazardous Materials. 283, 117-22.
- Zhang, X.Q., Li, Y.S., 2017. Changes in shale oil composition and yield after bioleaching by *Acidithiobacillus mucilaginosus* and *thiobacillus ferrooxidans*. Oil Shale. 34, 146.
- Zhang, S., Yan, L., Xing, W., Chen, P., Zhang, Y., Wang, W., 2018. *Acidithiobacillus ferrooxidans* and its potential application. Extremophiles 22, 563-579.
- Zhao, H., Hu, M., Li, Y., Zhu, S., Qin, W., Qiu, G., 2015. Wang, J. Comparison of electrochemical dissolution of chalcopyrite and bornite in acid culture medium. Transactions of Nonferrous Metals Society of China. 25, 303-313.
- Zhao, H., Zhang, Y., Zhang, X., Qian, L., Sun, M., Yang, Y., Zhang, Y., Wang, J., Kim, H., Qiu, G., 2019. The dissolution and passivation mechanism of chalcopyrite in bioleaching: An overview. Minerals Engineering. 136, 140-54.
- Zheng, G., Zhou, L., Wang, S., 2009. An acid-tolerant heterotrophic microorganism role in improving tannery sludge bioleaching conducted in successive multibatch reaction systems. Environmental Science and Technology. 43, 4151-4156.
- Zhou, H.B., Liu, X., Fu, B., Qiu, G., Huo, Q., Zeng, W.M., Liu, J.S.H., Chen, X.H., 2007. Isolation and characterization of *Acidithiobacillus caldus* from several typical environments in China. Journal of Central South University of Technology. 14, 163-169
- Zhou, X., Guo, J., Lin, K., Huang, K., Deng, J., 2013. Leaching characteristics of heavy metals and brominated flame-retardants from waste printed circuit boards. Journal of Hazardous Materials. 246-247, 96-102.
- Zhu, W., Xia, J., Yang, Y., Nie, Z.Y., Zheng, L., Ma, C.Y., Zhang, R.Y., Peng, A., Tang, L., Qiu, G., 2011. Sulfur oxidation activities of pure and mixed thermophiles and sulfur speciation in bioleaching of chalcopyrite. Bioresource Technology. 102, 3877-3882.
- Zhu, N., Shi, C., Shang, R., Yang, C., Xu, Z., Wu, P., 2017. Immobilization of *Acidithiobacillus ferrooxidans* on cotton gauze for biological oxidation of ferrous ions in a batch bioreactor. Biotechnology and Applied Biochemistry. 64, 27-734.
- Zotti, M., Di Piazza, S., Roccoliello, E., Lucchetti, G., Mariotti, M. G., Marescotti, P., 2014. Microfungi in highly copper-contaminated soils from an abandoned Fe-Cu sulphide mine: Growth responses, tolerance and bioaccumulation. Chemosphere. 117, 471-476.

MATERIALS AND GENERAL METHODS

1. MATERIALS

1.1. Microorganisms

The specific bacterium used in this thesis was *Acidithiobacillus ferrooxidans* (*A. ferrooxidans*). It is an aerobic and acidophilic microorganism that preferably grows at pH between 1.5 and 2.5, and is able to survive at high concentrations of heavy metals (David et al., 2008; Almárcegui et al., 2014). This rod-shaped bacterium that was used as a model in the genome sequencing projects has a biosafety level of 1, which means that it is not known to consistently cause disease in immunocompetent adult humans and that presents minimal potential hazard to laboratory personnel and the environment (US Department of Health and Human Services, 2020).

The bacteria were supplied from two different sources depending on the experiment. The *Acidithiobacillus ferrooxidans* ATCC 23270 was kindly provided by the Department of Chemical Engineering and Food Technologies at the University of Cádiz (UCA, Spain). The *Acidithiobacillus ferrooxidans* DSM 14882 strain was acquired from the German collection Leibniz Institute DSMZ-German Collection of microorganisms and Cell Cultures (<https://www.dsmz.de/collection/catalogue>) and it was isolated from an acid bituminous coal mine in Pennsylvania (USA). Both bacteria are the same strain whose designation in the corresponding collection is Strain 14882, NCIMB 8455 or ATCC 23270 (<https://www.dsmz.de/collection/catalogue/details/culture/DSM-14882>).

Additionally, *Gluconacetobacter xylinum* bacteria was used for immobilization experiments. It is a strictly aerobic gram-negative bacterium that grows at temperature ranging between 25 and 30 °C and preferably at pH between 4 and 7. It is one of the most commonly used bacteria for Biocellulose synthesis due to its ability to produce high amount of this polymer in static liquid medium (Nguyen et al., 2008; Vázquez et al., 2013).

1.2. Copper workpieces

Copper workpieces (purity 99.9 %) were prepared in the Department of Mechanical Engineering at the University of the Basque Country (UPV/EHU, Spain) using a REMET TRE100 Evol metallographic saw. Varying dimensions of the workpieces were employed in this work depending on the experiment. In some experiments approximately 15 x 10 x 2 mm measuring workpieces were used with a 2-mm diameter hole drilled in each workpiece (ERLO S-18 dotting equipment) for holding the piece during immersion into the active medium. In other experiments, copper workpieces measuring approximately 32 x 25 x 2 mm of thickness were used. Prior to use, all the workpieces were rinsed with deionized water and ethanol (96 %), and then gently heated to remove surface moisture.

Other materials different from copper pieces are described in the corresponding chapter together with the experimental procedure in particular.

2. GENERAL METHODS

2.1. *Acidithiobacillus ferrooxidans* bacterial growth

A. ferrooxidans cells were cultured in the Lundgren-Silverman medium (Silverman and Lundgren, 1959). This medium is an aqueous solution that contains several inorganic salts, among which ferrous sulfate is used as a source of ferrous iron (Fe^{2+}) (Table 10).

The Lundgren-Silverman solution contains $9 \text{ g Fe}^{2+} \text{ L}^{-1}$, being identified as 9K medium, but other two concentrations (1.5 and $6 \text{ g Fe}^{2+} \text{ L}^{-1}$) have also been tested. The medium is obtained by mixing two solutions: the basal salts containing solution (referenced in Table 10 as S-1) that provides nutrients for bacteria, and the ferrous iron solution (referenced in Table 10 as S-2) that provides the energy source for the proper bacterial growth.

Table 10. Composition of culture medium according to final iron concentration.

	Compounds	Amount
S1	$(\text{NH}_4)_2\text{SO}_4$ (g L^{-1})	3
	$\text{MgSO}_4 \cdot 7\text{H}_2\text{O}$ (g L^{-1})	0.5
	K_2HPO_4 (g L^{-1})	0.5
	KCl (g L^{-1})	0.1
	$\text{Ca}(\text{NO}_3)_2 \cdot 4\text{H}_2\text{O}$ (g L^{-1})	0.01
	H_2O (mL)	700
		7.47 ($1.5 \text{ g Fe}^{2+} \text{ L}^{-1}$, 1.5K medium)
S2	$\text{FeSO}_4 \cdot 7\text{H}_2\text{O}$ (g L^{-1})	29.97 ($6 \text{ g Fe}^{2+} \text{ L}^{-1}$, 6K medium)
		44.80 ($9 \text{ g Fe}^{2+} \text{ L}^{-1}$, 9K medium)
	H_2O (mL)	300

The solutions S-1 and S-2 were prepared separately in beakers of 1 liter, adjusting their pH separately with sulfuric acid (25 %) at 1.7-1.8. After pH adjustment, both solutions were mixed and the final pH was adjusted again, if necessary.

Although this medium can be prepared and stored in the refrigerator, in this study, the culture medium was prepared before use, because the S-2 solution (containing ferrous iron) could be abiotically oxidized into ferric iron, gradually losing the necessary energy source for bacterial growth.

Once the nutrient medium was prepared, it was inoculated with an *A. ferrooxidans* culture in the exponential growth phase (between 2 % and 15 % (v:v) depending on the experiments). Bacterial growth was carried out under varying shaking speeds (130-170 rpm) and 31 °C of temperature until complete oxidation of Fe²⁺ to Fe³⁺ was achieved.

The pH was controlled throughout the culture growth and adjusted when necessary to maintain values around 1.7-1.8.

2.2. Copper mobilization experiments

All the copper solubilization experiments were carried out in two-steps: first, *A. ferrooxidans* culture was grown until the complete oxidation of Fe²⁺ to Fe³⁺ was achieved (step 1), and second, the bioleaching of copper pieces was performed (step 2).

Step 1 involved inoculating the *A. ferrooxidans* culture in the exponential growth phase in a 250 mL conical flask containing the culture medium (1.5-9K depending on the experiment). Bacteria were incubated under shaking conditions at 31 °C. Once the complete amount of Fe²⁺ was oxidized to Fe³⁺, the previously weighted copper workpieces were immersed in the oxidizing medium (step 2). After a certain period of time (depending on the particular experiment) the workpieces were removed from the solution, rinsed with deionized water and ethanol (96 %), dried, and then weighed to SMRR. All the experiments were carried out under non-sterile conditions to simulate an industrial-scale process.

The specific operating conditions of each metal removal experiments will be detailed in the corresponding chapter.

2.3. Determination of the bacterial concentration in the medium

Due to the small size of *A. ferrooxidans* bacteria, a quantitative evaluation of these cells is difficult. Therefore, the Most Probable Number (NMP) technique was used for counting the bacteria in 9K medium (Johnson et al., 2007, Istiyanto et al., 2010, Xenofontos et al., 2015). This technique consists of two main steps. The first step is devoted to preparing a series of dilutions from the original active culture medium. In the second step, these dilutions are incubated paying special attention to the growth that progressively occurs in each one of them. The dilutions that contain microbial cells will present turbidity and a color change. Conversely, in those dilutions where bacterium is inactive or died, the medium will remain transparent. Therefore, the presence of bacteria is determined by the color change in the culture medium.

After being sterilized and washed with deionized water and ethanol, 15 glass tubes of 10 mL capacity were numbered from 1 to 15 according to dilutions.

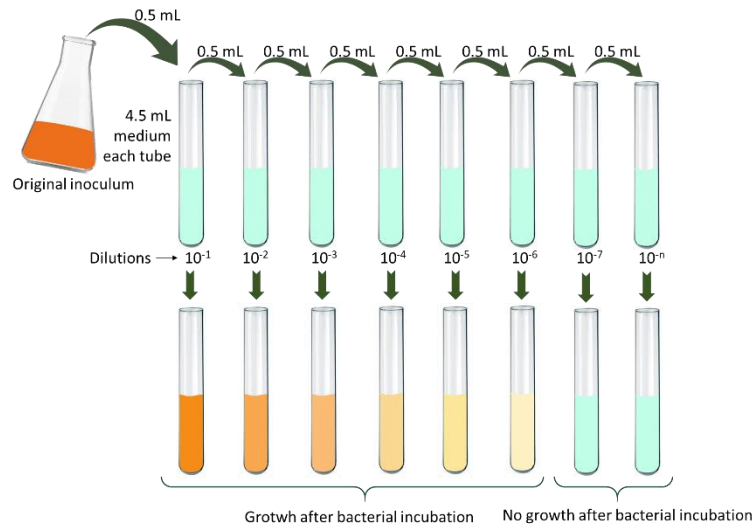


Figure 11. Most probable number (MPN) methodology.

Once the 9K medium was prepared, 4.5 mL was added to each tube. The blank only contained 5 mL of culture medium. Then, 0.5 mL of the grown *A. ferrooxidans* culture medium was added to tube T-1, containing 1:10 dilution accordingly. Subsequently, 0.5 mL was transferred from tube T-1 to T-2 (1:100 dilution). The same procedure was followed from tube T-3 to T-15. The incubation period of the dilutions was carried out at 130 rpm and 31 °C until the number of dilutions presenting turbidity did not kept constant. In this way, the last tube to develop color was considered the one indicating the concentration of bacteria present in the medium (Figure 11). Figure 12 shows the aspect of tubes before and after being incubated for MPN technique.

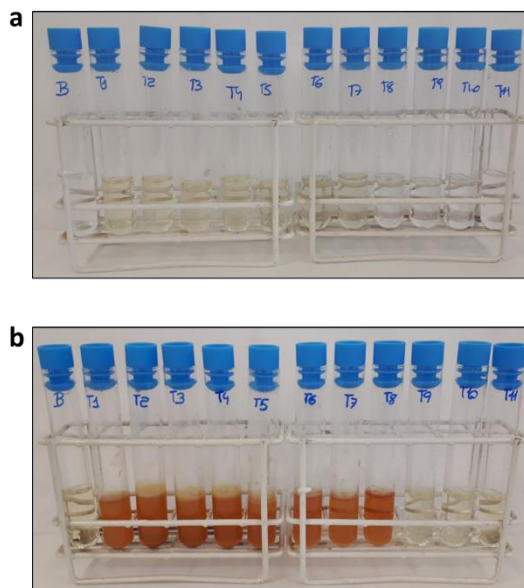


Figure 12. Photographs of the tubes before (a) and after (b) being incubated for the most probable number technique.

2.4. Metal removal rate and specific metal removal rate

The metal removal rate (MRR) and the specific metal removal rate (SMRR) were determined by applying the procedures followed by Jadhav et al. (2013), Muhammad et al. (2015), Diaz-Tena et al. (2016) and Ma et al. (2020). During the copper solubilization tests, each workpiece was regularly taken out from the medium, washed with distilled water and ethanol (96 %), dried and weighed in an analytical balance (Denver instruments, SI-234 230 g/0.1 mg). The MRR and SMRR were calculated as shown in the equations below (Equation 16 and 17):

$$\text{MRR (mg h}^{-1}\text{)} = \frac{\text{Amount of metal removed (mg)}}{\text{Time (h)}} \quad (\text{Eq. 15})$$

$$\text{SMRR (mg h}^{-1}\text{ cm}^{-2}\text{)} = \frac{\text{MRR}}{\text{Area (cm}^2\text{)}} \quad (\text{Eq. 16})$$

2.5. Determination of iron species in solution

The ferrous (Fe^{2+}) and total iron concentration were determined using the 2,2'-dipyridyl molecular absorption spectrophotometry method (adapted from the '3500-Fe B' colorimetric procedure of the Standard Methods for the Examination of Water and Wastewater (Eaton et al., 1998; Diaz-Tena et al., 2016).

The details about the reagents used in this analytical method are shown in Table 11.

Table 11. Reagents used in the colorimetric method for ferrous and total iron determination.

Solution	Composition	Preparation method	Objective
Iron standard solution (0.05 mg L ⁻¹)	Standard iron solution 1 g Fe L ⁻¹ in 2 % HNO ₃	Dilute 5 mL of the standard solution in 100 mL of deionized water	Obtaining the calibration curve
Ammonium acetate / Acetic acid Buffer	Ammonium acetate 98 % Acetic acid glacial 99.8 %	Dissolve 280 g of ammonium acetate in 1 L of deionized water. Add glacial acetic acid until pH 5.5 is reached	Keep the pH stable around 5.5
Hydroxylamine hydrochloride 10 % (w:v)	Hydroxylamine hydrochloride	Dissolve 5.0 g of the salt in 50 mL of deionized water	Reduce Fe ³⁺ to Fe ²⁺
Solution 2.2 dipyridyl 0.5 % (w:v)	2,2'-dipyridyl Ethanol 96 %	Dissolve 0.5 g of the salt in 100 mL of 96 % ethanol (v:v)	React with Fe ²⁺ to give a color complex

It is essential to determine the concentration of both ferric and ferrous iron throughout the process, since both values are indicative of the process progress. Nevertheless, only the ferrous Fe^{2+} ion can be measured by the colorimetric method. Consequently, if the Fe total amount is to be determined, the Fe^{3+} has to be reduced to Fe^{2+} and the original Fe^{2+} and the reduced Fe^{2+} will be quantified simultaneously, rendering the total iron amount. Obviously, the Fe^{3+} concentration will be determined by subtraction.

Prior to the measurement, it was necessary to obtain the calibration curve. The calibration standards of 0, 1, 2, 5 and 10 $\text{mg Fe}^{3+} \text{ L}^{-1}$ were prepared from a certified solution of 0.05 $\text{g Fe}^{3+} \text{ L}^{-1}$ by adding the following solutions to each 50 mL volumetric flask (Figure 13):

- a- the corresponding volume of the 0.05 $\text{mg Fe}^{3+} \text{ L}^{-1}$ solution for each standard
- b- 5 mL of buffer solution (ammonium acetate/acetic acid) to ensure the pH stability during the process
- c- 2 mL of the hydroxylamine hydrochloride 10 % solution to reduce the ferric iron to ferrous iron. Shaking vigorously for 5 min was recommended to ensure the complete reduction of ferric iron. This reagent will only be added if the total Fe amount is to be determined. Obviously, it will not be added for Fe^{2+} determination. The Fe^{3+} concentration will be calculated by subtracting the Fe^{2+} amount to the total concentration.
- d- 2 mL of the dipyriddy solution. All the ferrous iron containing samples developed a red color. All the solutions were stirred for 5 minutes to ensure the complete reaction.
- e- Deionized water to make up to 50 mL.



Figure 13. Iron standards for calibration curve.

The absorbance of all the samples were measured with a visible spectrophotometer Jenway 6305 at a wavelength of 520 nm, using 1 cm and 4.5 mL PMMA cuvettes.

Taking into account the dilution factor, the value of total iron and ferrous iron in the original solution was obtained by Equation 17, where Y is the absorbance value, b the cut-off point between the calibration curve and the vertical axis and a the calibration curve slope.

$$\text{Fe (g L}^{-1}\text{)} = \frac{Y - b}{a} \cdot \frac{50}{1} \cdot \frac{100}{1} \cdot \frac{1 \text{ g}}{1000 \text{ mg}} \quad (\text{Eq. 17})$$

2.6. Metal content analysis (ICP and AAS)

The metal concentration in the leached solutions was measured by ICP-OES plasma spectrometry (Figure 14a). Inductively coupled plasma (ICP) is the ionization source that together with an optical emission spectrophotometer (OES) constitutes the ICP-OES equipment. Specifically, a Perkin Elmer OPTIMA 2000DV equipment with a CETAC U 5000AT + ultrasonic nebulizer was used.

Additionally, Atomic absorption spectroscopy (Figure 14b) is also commonly used in metal mobilization process to analyze metal elements in liquid samples. In this thesis copper and iron content was also quantified in a Perkin Elmer AAnalyst 100 AAS equipment, depending on the experiment.

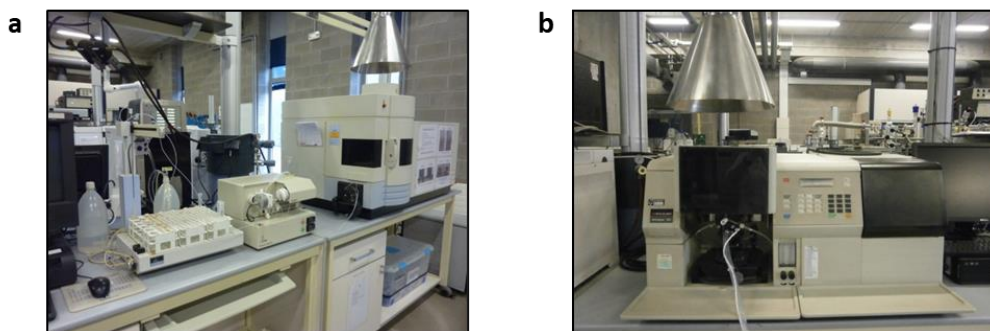


Figure 14. ICP-OES plasma spectrometry (a) and Atomic absorption spectroscopy (b) equipment.

All samples were filtered by a 0.45 μm filter before analysis and the calibration standards were prepared in a matrix as similar as possible to the samples.

2.7. Scanning electron microscopy (SEM)

Regarding the scanning electron microscopy (SEM) imaging, samples were fixed in 2 % glutaraldehyde in 0.1 M cacodylate buffer (pH 7.4), washed in iso-osmolar cacodylate/sucrose buffer, and postfixed in 1 % osmium tetroxide in cacodylate buffer. Samples were then dehydrated through an ethanol series and washed in

hexamethyldisilazane prior to air-drying. Finally, samples were mounted onto stubs and gold-coated using a JEOL fine-coat ion sputter JFC-1100. Samples were visualized and micrographed using a SEM (Hitachi S-4800) at 15 kV accelerating voltage. Those SEM images were obtained by the Sgiker service (Advanced Research Facilities) of the University of the Basque Country (UPV/EHU).

2.8. Other methods

The pH was measured with a Crison Basic 20 pH-meter equipped with a sensION+ 5010T pH electrode. The redox potential was recorded with a Thermo-Orion 920+ instrument equipped with an Orion 9778BNWPO Sur-Flow® electrode.

3. REFERENCES

- Almarcegui, R.J., Navarro, C.A., Paradela, A., Albar, J.P., von Bernath, D., Jerez, C.A., 2014. New copper resistance determinants in the extremophile *Acidithiobacillus ferrooxidans*: a quantitative proteomic analysis. *Journal of Proteome Research*. 13, 946-960.
- Meechan, P.J., Potts, J., 2020. Biosafety in microbiological and biomedical laboratories: United States Department of Health and Human Services, Public Health Service, Centers for Disease Control and Prevention, National Institutes of Health.
- David, D.J., Pradhan, D., Das, T., 2008. Evaluation of iron oxidation rate of *Acidithiobacillus ferrooxidans* in presence of heavy metal ions. *Mineral Processing and Extractive Metallurgy*. 117, 56-61.
- Díaz-Tena, E., Gallastegui, G., Hipperdinger, M., Donati, E. R., Ramírez, M., Rodríguez, A., López de Lacalle, L. N., Elías, A., 2016. New advances in copper biomachining by iron-oxidizing bacteria. *Corrosion Science*. 112, 385-392.
- Eaton, A.D., Clesceri L.S., Greenberg, A.E., Franson, M.A.H., 1998. Standard Methods for the Examination of Water and Wastewater, American Public Health Association, American Water Works Association, Water Environment Federation, Washington DC.
- Istiyanto, J., Ko, T. J., Yoon, I.-C., 2010. A study on copper micromachining using microorganisms. *International Journal of Precision Engineering and Manufacturing*. 11, 659-664,
- Jadhav, U., Hocheng, H., Weng, W.H., 2013. Innovative use of biologically produced ferric sulfate for machining of copper metal and study of specific metal removal rate and surface roughness during the process. *Journal of Materials Processing Technology*. 213, 1509-1515.
- Johnson, D., Warner, R. and Shih, A. J., 2007. Surface roughness and material removal rate in machining using microorganisms. *Journal of Manufacturing Science and Engineering*. 129, 223-227.
- Ma F., Huang H., Cui C., Mater J., 2020. Biomachining properties of various metals by microorganisms. *Process Technology*. 278, 116512.
- Muhammad, I., Sana Ullah, S. M., Sup Han, D., Jo Ko, T., 2015. Selection of optimum process parameters of biomachining for maximum metal removal rate. *International Journal of Precision Engineering and Manufacturing-Green Technology*. 2, 307-313.

Nguyen, V.T., Flanagan, B., Gidley, M.J., Dykes, G.A., 2008. Characterization of cellulose production by a *Gluconacetobacter xylinus* strain from Kombucha. *Current Microbiology*. 57, 449-53.

Silverman M. P., Lundgren D. G., 1959. Studies on the chemoautotrophic iron bacterium *Ferrobacillus ferrooxidans*: I. An improved medium and a harvesting procedure for securing high cell yields. *Journal of Bacteriology*. 77, 642-647.

Song, Y.X., Zhang, H.P., Chon, C.H., Chen, S., Pan X., Li, D.Q., 2010. Counting bacteria on a microfluidic chip. *Analytica Chimica Acta*. 681, 82-86.

Vazquez, A., Foresti, M.L., Cerrutti, P., Galvagno, M., 2013. Bacterial cellulose from simple and low cost production media by *Gluconacetobacter xylinus*. *Journal of Polymers and the Environment*. 21, 545-554.

Xenofontos, E., Feidiou, A., Constantinou, M., Constantinides, G., Vyrides, I., 2015. Copper biomachining mechanisms using the newly isolated *Acidithiobacillus ferrooxidans* B1. *Corrosion Science*. 100, 642-650.

CHAPTER 1.
OPERATION WITH
SUSPENDED BIOMASS

1.1. OBJECTIVE

As far as biomachining and bioleaching processes is concerned, most of the studies in these fields are still carried out in a small scale. Therefore, the larger industrial scale of these bioprocesses is still limited (Díaz-tena et al., 2017; Erust et al., 2021). One of the main drawbacks for continuous operation at high scale, even under optimum operating conditions, is the decrease in the amount of mobilized metal as a consequence of the loss of bio-oxidative activity which can be attributed to the increasing toxicity of the medium (Díaz-Tena et al., 2016; Liang et al., 2018). Another feature to be considered is that the final depleted solution requires adequate (and sometimes complex) treatment before discharge, increasing process cost.

The objective here was to contribute to the design of a bioprocess with suspended biomass that allows the maintenance of the metal removal rate at high values while minimizing the amount of depleted solution. Copper was selected as a representative metal to assess the influence of iron concentration on both suspended *A. ferrooxidans* growth and metal mobilization efficiency, and to determine the contribution of bacteria to the specific metal removal rate (SMRR). Bearing in mind the future industrial applications in bioleaching of metals from electronic waste and biomachining, an alternate process composed of two stages (metal removal + regeneration stage) was searched with the aim of maintaining high SMRR and reusing the solution in semicontinuous operation.

Figure 1.1 shows the outline of the experimental section of this chapter.

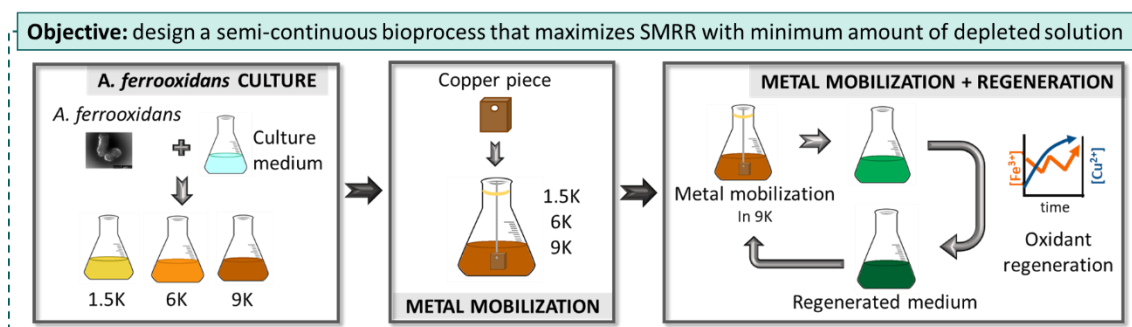


Figure 1.1 . Outline of the experimental section of this chapter.

1.2. MATERIALS AND METHODS

1.2.1. Copper pieces

Copper workpieces (purity 99.9 %) measuring approximately 2 x 10 x 15 mm were cut employing a Remet LS1 metallographic cutting machine with K-type cutting discs. A 2-mm diameter hole was drilled in each workpiece for holding it during immersion into

cell suspension. Before further treatment, they were cleaned and prepared as described in Section 1.2 *Copper workpieces* (materials and general methods).

1.2.2. Microorganisms and culture media

The *A. ferrooxidans* bacterium (ATCC 23270) used for this study was cultured in a Silverman and Lundgren medium (Silverman and Lundgren, 1959) as described in Section 1.1 *Microorganisms* (materials and general methods).

1.2.3. Metal mobilization experiments

Metal mobilization experiments were performed to evaluate the influence of Fe^{2+} concentration on microbial growth (experiment G1), and to record the variation in metal removal over time as function of Fe^{3+} concentration (experiment BM1). In addition, the biomass's contribution to the process was studied by comparing biotic and abiotic experiments using the optimum iron concentration selected in BM1 as the initial energy source for bacterial growth (experiment BM2).

The experiments were carried out in two-stages following the procedure described in Section 2.2. *Copper mobilization experiments* (materials and general methods). First, the medium containing varying concentration of ferrous iron (1.5, 6 and 9K) was inoculated with a 2 % v:v of an *A. ferrooxidans* culture in an exponential growth phase, and each sample was cultured until the complete Fe^{2+} oxidation (step 1). Thus, the treatment solutions were obtained. Once Fe^{2+} was oxidized to Fe^{3+} , a previously weighted copper workpiece was immersed in the treatment solution (step 2). The workpieces were removed from the oxidizing medium on an hourly basis, rinsed with deionized water and ethanol (96 % v:v), dried, and then weighed as described in Section 1.2 *Copper workpieces* (materials and general methods). Thereafter, they were immersed once again in the corresponding culture until the end of each experiment.

Additionally, several abiotic tests were used for comparison purposes (control tests without bacteria). In these assays, the solution containing Fe^{3+} was prepared by filtering the treatment solution obtained as previously described in step 1 (a 0.45 μm polyvinylidene fluoride filter was used). All the experiments were carried out at 31 °C, at a shaking speed of 130 rpm. A pH threshold value of 1.7-1.8 was maintained in both steps by the addition of sulfuric acid (25 % v:v). Each metal mobilization experiment was performed in triplicate. The specifics of each experiment are described below.

1.2.3.1. Effect of iron content on bacterial growth and metal mobilization

The effect of the energy source (iron concentration) on *A. ferrooxidans* growth in step 1 was studied by culturing the bacteria in media with different initial concentrations of

Fe^{2+} (experiment G1): 1.5, 6 and 9 g Fe^{2+} L⁻¹. The influence of the initial biotic Fe^{3+} concentration on metal removal efficiency was also investigated in a three-hour experiment (experiment BM1) by comparing the SMRR recorded during copper solubilization when using the final oxidizing solutions obtained in step 1. In addition, an abiotic three-hour experiment was conducted using the supernatant (SN) obtained by filtering the bacteria from the final solution in step 1 using a 0.45 μm polyvinylidene fluoride filter (experiment SN1). Finally, two additional abiotic assays (B1 and B2) were performed under the same operating conditions to ascertain the effect of dissolved oxygen on the process.

1.2.3.2. SMRR as a function of time during the metal mobilization process

In this experiment, both the oxidizing medium with bacteria (experiment BM2) and after filtration (experiment SN2) were used to estimate the biomass's contribution to the process. An initial concentration of 9 g Fe^{2+} L⁻¹ was selected as the initial energy source for bacterial growth and, once all the iron was biologically transformed into Fe^{3+} , the abovementioned procedure was repeated in a 20-hour experiment. In addition, a blank assay (without bacteria) was conducted following the same strategy and using 9 g Fe^{2+} L⁻¹ (experiment B3) to ascertain the effect of Fe^{2+} on the SMRR. The experimental conditions for bacterial growth, biotic and abiotic metal mobilization experiments, and blanks are summarized in Table 1.1.

Table 1.1. Experimental conditions for bacterial growth, metal mobilization and abiotic assays.

Exp.	Inoculum (v:v)	Initial iron concentration (g L ⁻¹)	Duration of experiment	Study objective
G1	2 % ^a	$[\text{Fe}^{2+}]_0 = 1.5, 6.0, 9.0$	Until complete Fe^{2+} oxidation	Influence of $[\text{Fe}^{2+}]_0$ on bacterial growth.
B1	abiotic	$[\text{Fe}^{2+}]_0 = 1.5, 6.0, 9.0$	120 h	Contribution of dissolved O_2 to Fe^{2+} oxidation.
BM1	2 % ^a	$[\text{Fe}^{3+}]_0 = 1.5, 6.0, 9.0$	3 h	Influence of $[\text{Fe}^{3+}]_0$ on SMRR.
SN1	abiotic	$[\text{Fe}^{3+}]_0 = 1.5, 6.0, 9.0$	3 h	Contribution of $[\text{Fe}^{3+}]_0$ on SMRR in the absence of bacteria.
B2	abiotic	0.0	3 h	Contribution of dissolved O_2 to Cu^0 oxidation.
BM2	2 % ^a	$[\text{Fe}^{3+}]_0 = 9.0$	20 h	Evolution of SMRR over time in the presence of bacteria.
SN2	abiotic	$[\text{Fe}^{3+}]_0 = 9.0$	20 h	Evolution of SMRR over time in the absence of bacteria.
B3	abiotic	$[\text{Fe}^{2+}]_0 = 9.0$	20 h	Contribution of O_2 to Fe^{2+} oxidation and to SMRR.

^aThe inoculum contained an average of 10^8 cells per milliliter.

1.2.4. Alternate process: metal mobilization + regeneration

An experiment particularly focused on setting an alternate process operation which would increase the average SMRR and reduce the amount of depleted treatment solution was carried out, with special attention to the detection of microbial activity inhibition (BM3 experiment). In this assay, biomass was first grown in the 9K medium until all the Fe^{2+} had been oxidized to Fe^{3+} . Second, a copper workpiece was immersed in that medium (*A. ferrooxidans* + 9 g $\text{Fe}^{3+} \text{L}^{-1}$) for a three-hour metal removal process (first stage, MR1), following the abovementioned procedure. The workpiece (Cu^0) was subsequently removed from the biotic medium to let microorganisms regenerate the oxidant (bio-oxidation of Fe^{2+}) (first regeneration stage). Once the regeneration step had been completed, the workpiece was again immersed in the treatment solution for the next three-hour treatment (second stage, MR2), and this sequence was repeated until the time needed for Fe^{2+} re-oxidation doubled the initial one.

1.2.5. Analytical methods

The iron concentration, pH and redox potential were measured following the procedure described in Sections 2.5 *Determination of iron species in dissolution* and 2.8 *Other methods* (materials and general methods). The Most Probable Number (MPN) technique was used to estimate the microbial concentration in the initial inoculum.

Copper concentration in the samples was measured by ICP-OES plasma spectrometry following the procedure described in Section 2.6 *Metal content analysis (ICP and AAS)* (materials and general methods).

The MRR and SMRR were used to quantify treatment efficiency, being calculated as shown in Equations 15 and 16 (materials and general methods).

1.3. RESULTS

1.3.1. Metal mobilization experiments

1.3.1.1. Influence of Fe^{2+} concentration on bacterial growth

A. ferrooxidans is a gram-negative, mesophilic, and extremely acidophilic chemolithotrophic bacterium that uses iron as an electron donor during aerobic respiration, whereby its growth depends on ferrous and ferric iron concentrations ($[\text{Fe}^{2+}]$ and $[\text{Fe}^{3+}]$) (Jadhav et al., 2013). Nevertheless, certain threshold concentrations of these ions depending on the strain may inhibit the biooxidation of Fe^{2+} . As an example, Kawabe et al. (2003) have concluded that the T23-3 strain oxidizes Fe^{2+} in the presence

of 26 g Fe³⁺ L⁻¹, while the ATCC19859 strain is fully inhibited with 16 g Fe³⁺ L⁻¹ under the same operating conditions (30 °C, 120 rpm, pH 1.5).

Regarding Fe²⁺ concentration, Hocheng et al. (2012a) have reported that the BCRC 13820 strain of *A. ferrooxidans* oxidized Fe²⁺ concentrations up to 8 g Fe²⁺ L⁻¹ (30 °C, 150 rpm, initial pH 2.5 without further regulation), even though the cell population hardly grew above 6 g Fe²⁺ L⁻¹. Kim et al. (2002) have concluded that Fe²⁺ concentrations higher than 9 g Fe²⁺ L⁻¹ inhibited the activity of the KCTC 2677 strain of *A. ferrooxidans* (30 °C, 200 rpm, pH 2.0-2.5), which was attributed to the limited ratio between the enzyme capable of oxidizing Fe²⁺ to Fe³⁺ and the amount of substrate (Fe²⁺).

The present study therefore uses 1.5, 6 and 9 g Fe²⁺ L⁻¹ as energy source for *A. ferrooxidans* (ATCC 23270) growth in order to ascertain the concentration that optimizes the metal mobilization process when solubilizing copper. Figure 1.2 shows aspect of the culture medium before and after the incubation period of *A. ferrooxidans* bacteria for 1.5, 6 and 9K media.

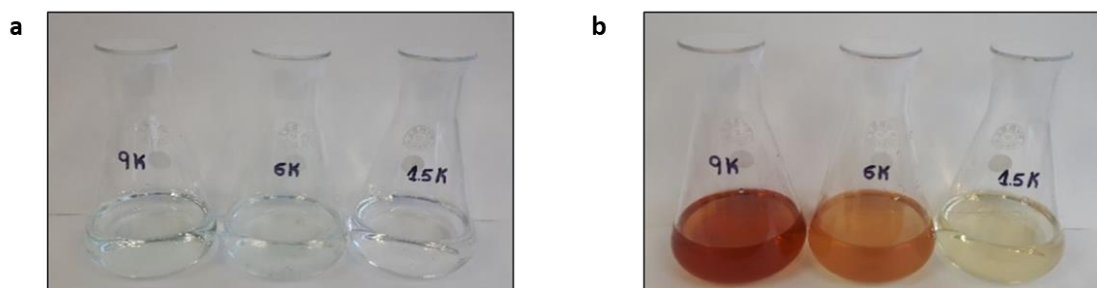


Figure 1.2. Culture medium before (a) and after (b) the growth period of *A. ferrooxidans* bacteria for 9, 6 and 1.5K media.

As shown in Figure 1.3a, the concentration of Fe³⁺ did not start to increase considerably until 19, 23, and 30 h for the medium containing 1.5, 6 and 9 g Fe²⁺ L⁻¹, respectively. This behavior was attributed to the lag phase stage which was dependent on the initial available concentration of Fe²⁺ (Mousavi et al., 2006). The redox potential increased accordingly in the three cultures until it peaked at around 600 mV, corresponding to the complete bio-oxidation of Fe²⁺ to Fe³⁺ (Figure 1.3b). The total time required for the complete oxidation of Fe²⁺ to Fe³⁺ depended on the initial concentration of Fe²⁺ ([Fe²⁺]₀), and 53, 76 and 120 h were needed when the microorganisms were cultured in 1.5K, 6K and 9K medium, respectively (Figure 1.3).

The culturing times recorded in this study were lower than those reported by Díaz-Tena et al. (2016), who have established an incubation period of 87 h for the same bacterial strain with an initial concentration of 6 g Fe²⁺ L⁻¹ and a pH of 1.8. Conversely, Jadhav et al. (2013) have registered a period of 54 h for the total oxidation of 9 g Fe²⁺ L⁻¹, although the strain inoculated in that study (*A. ferrooxidans* BCRC 13823) recorded its maximum

yield at 150 rpm and pH 2.5, with these conditions being significantly different to the ones used here.

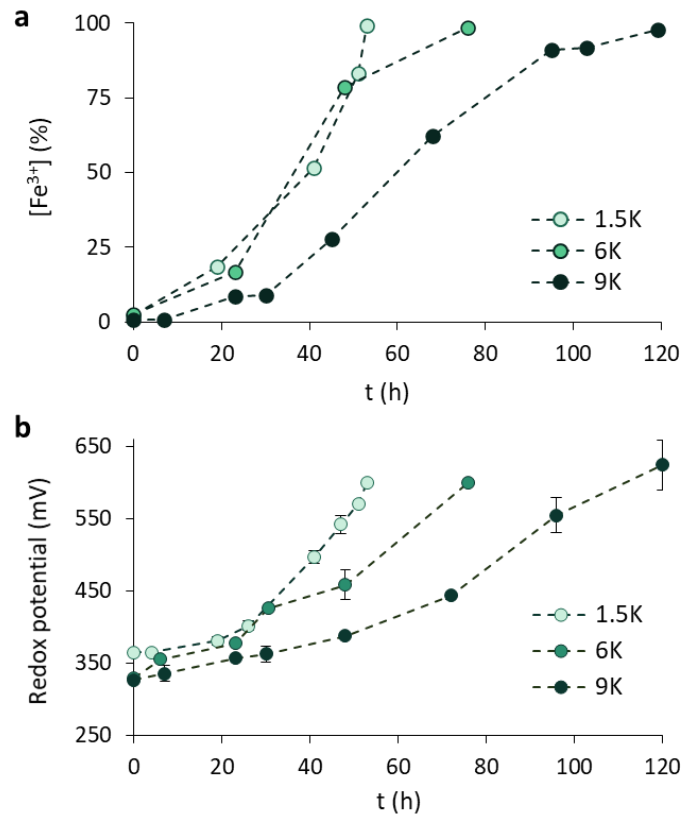


Figure 1.3. Evolution of the $[\text{Fe}^{3+}]$ (a) and the redox potential (b) during the incubation period in medium containing 1.5, 6 and 9 $\text{g Fe}^{2+} \text{L}^{-1}$.

The color of the culture medium changed through the incubation period from transparent to an intense red color when all the Fe^{2+} was oxidized to Fe^{3+} . Figure 1.4 shows this variation through time when using 9K medium as a representative example of the progress of the process.



Figure 1.4. Color variation of the culture medium during the oxidation of Fe^{2+} into Fe^{3+} by means of *A. ferrooxidans* bacteria in 9K medium.

The biological oxidation of Fe^{2+} to Fe^{3+} during the incubation period generates energy and consumes hydrogen ions (Equation 1). The increase in the pH at the beginning of

the experiment (lag phase) was moderate due to low bacterial activity (Figure 1.5). Conversely, this parameter increased more acutely during the exponential growth phase, being the total amount of sulfuric acid consumed for maintaining a pH threshold value of 1.7 threefold higher in the 9K medium than in the 1.5K one.

This acidic pH in the cultures was crucial for preventing the iron from precipitating as jarosite ($MFe_3(SO_4)_2(OH)_6$, where $M: Na^+, NH_4^+, Ag^+$ or H_3O^+), as also reported by other authors (Daoud et al., 2006; Xenofontos et al., 2015; Liu et al., 2020). A huge accumulation of jarosite precipitates could reduce the diffusion of reactants and products which could lead to a reduction in the dissolved ferric iron availability (van Hille et al., 2010). Yu et al. (2011) found that jarosite produced by bacterial oxidation formed a barrier layer which severely inhibit the bioleaching of chalcopyrite. Similarly, Sasaki et al. (2009) reported poor copper recoveries which they attributed to jarosite precipitation.

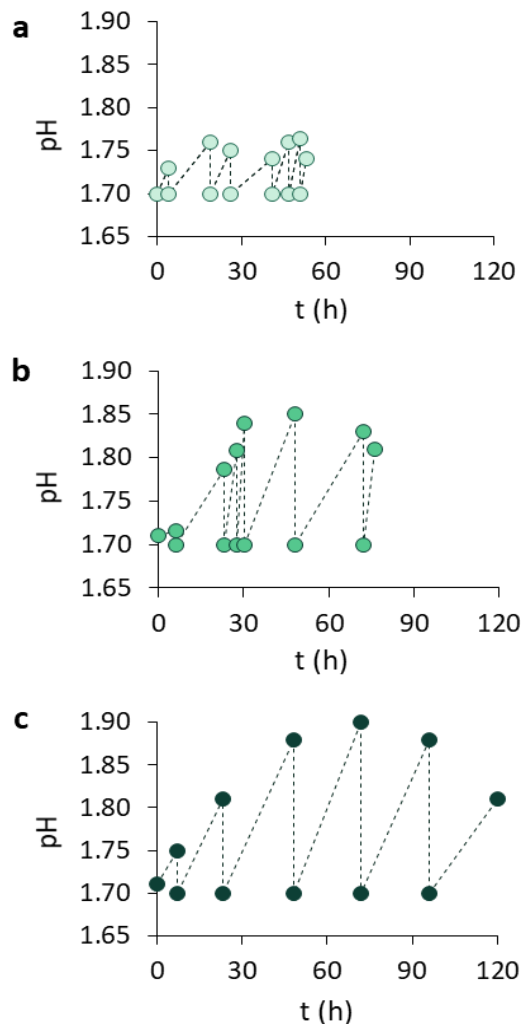


Figure 1.5. Evolution of pH during the incubation period in the medium containing 1.5 g Fe²⁺ L⁻¹ (a), 6 g Fe²⁺ L⁻¹ (b) and 9 g Fe²⁺ L⁻¹ (c). The pH was readjusted to 1.7 after each analysis.

The Fe^{2+} oxidation rate as defined by Blanch and Clark (1996) (during the bacterial exponential growth phase) was 2.8 times lower in the culture with an initial ferrous iron concentration of $1.5 \text{ g Fe}^{2+} \text{ L}^{-1}$ ($0.036 \text{ g Fe}^{2+} \text{ L}^{-1} \text{ h}^{-1}$) than in the 9K medium ($0.101 \text{ g Fe}^{2+} \text{ L}^{-1} \text{ h}^{-1}$). Considering that the inoculum was the same for the three experiments, this behavior could be attributed to the higher cell density in the 9K medium (10^8 cells mL^{-1} in 9K medium vs 10^7 cells mL^{-1} in 1.5K medium), which is consistent with the literature (Muhammad et al., 2015; Díaz-Tena et al., 2018). Díaz-Tena et al. (2018) have observed a linear relationship between the initial Fe^{2+} concentration (3, 6 and $9 \text{ g Fe}^{2+} \text{ L}^{-1}$) and the oxidation rate by *A. ferrooxidans* DSM 14882 cultured in MAC medium at $30 \text{ }^\circ\text{C}$, 180 rpm, and pH 1.5. Similarly, Kim et al. (2002) have reported a positive correlation between those parameters up to $9 \text{ g Fe}^{2+} \text{ L}^{-1}$ in a study carried out with *A. ferrooxidans* KCTC 2677 cultivated in a 9K medium ($30 \text{ }^\circ\text{C}$, 200 rpm), while higher concentrations appeared to inhibit the reaction.

Under the experimental conditions in the abiotic assay (experiment B1), neither the redox potential nor the pH changed significantly (data not shown). As far as the redox potential is concerned, after 120 h in the absence of microorganisms, low increments of 23, 50 and 62 mV were registered in the 1.5K, 6K and 9K cultures, respectively. This variation was attributed to the poor oxidation of the ferrous ion by the dissolved oxygen in the medium, being the low solubility of oxygen at $31 \text{ }^\circ\text{C}$ (7.5 ppm).

1.3.1.2. Influence of Fe^{3+} concentration on SMRR

The efficiency of copper solubilization can vary substantially with different strains of *A. ferrooxidans* (Xenofontos et al., 2015). Consequently, the recommended value of the initial concentration of Fe^{3+} for the maximum copper removal reported in the literature is very variable. In this study, three-hour experiments were carried out using pre-grown cultures (experiment BM1) and culture supernatants (experiment SN1) containing 1.5, 6 and $9 \text{ g Fe}^{3+} \text{ L}^{-1}$, in order to select the initial concentration of Fe^{3+} that maximizes copper solubilization when using the *A. ferrooxidans* ATCC 23270 strain under the described operating conditions. Initial concentrations of Fe^{3+} higher than $9 \text{ g Fe}^{3+} \text{ L}^{-1}$ were not assayed due to the drawbacks reported by other authors, such as the deficient quality of the surface finish in biomachining experiments (Jadhav et al., 2013) and jarosite precipitation (Nazari et al., 2014). Additionally, Kawabe et al. (2003) have reported that the Fe^{2+} oxidation activity of three *A. ferrooxidans* strains (ATCC23270, ATCC 19859, and T23-3) is reduced by more than half at Fe^{3+} concentrations above $14 \text{ g Fe}^{3+} \text{ L}^{-1}$ due to competitive inhibition.

The results obtained in the blank assays (experiments B2 and B3) confirmed that the dissolved oxygen (as oxidant) made a negligible contribution to copper leaching, both in the presence of Fe^{2+} (first 3 h in experiment B3; $< 2.0 \%$ of the SMRR achieved in the

biotic BM2 experiment) and in the total absence of iron (experiment B2; < 0.5 % of the SMRR obtained in the biotic BM1 experiment). Fe^{3+} was therefore concluded to be the main oxidant responsible for copper leaching, in agreement with other studies (Xenofontos et al., 2015; Lambert et al., 2015).

The presence of microorganisms improved the process efficiency, as the total Cu amount solubilized in the 6K and 9K biotic systems was 10 % and 25 % higher, respectively, than the amount dissolved in the absence of microorganisms (Table 1.2). By contrast, Cu removal after three hours in the 1.5K solution was similar in both cases, which is indicative of the poor oxidation activity attributed to the lower biomass concentration at low iron concentrations (78.1±4.8 and 75.5±1.8 mg Cu for the biotic and abiotic 1.5K experiments, respectively).

Table 1.2. Total copper amount removed in the biotic (BM1) and abiotic (SN1) experiments after the three-hour immersion of a copper piece.

Initial Fe^{3+} concentration (g Fe^{3+} L ⁻¹)	Experiment BM1 (biotic medium) (mg Cu)	Experiment SN1 (abiotic medium) (mg Cu)
1.5	78.1±4.8	75.5±1.8
6	254.5±8.2	231.0±16.3
9	358.4±25.9	287.0±19.7

The total amount of copper solubilized per square centimeter in the 6K and 9K biotic solutions was 12-13 % higher than in the absence of microorganisms (69.2±1.0 vs. 61.6±1.0 mg cm⁻² in the 6K; 102.3±5.9 vs. 90.1±3.2 mg cm⁻² in the 9K solution), with the bacteria's effect being greater than that described by other authors. For example, Xenofontos et al. (2015) have reported that the bacterial contribution only accounted for an increase of 5.7 % in the removed copper (from 15.9 mg cm⁻² to 16.8 mg cm⁻²) after 6 h with an initial concentration of 6.5 g Fe^{3+} L⁻¹. Likewise, Lambert et al. (2015) have reported that this difference never exceeded 7-8 % during the first 10 h in assays performed with initial iron concentrations up to 7 g Fe^{3+} L⁻¹.

Regarding SMRR, the most significant difference between the biotic (BM1) and abiotic (SN1) assays was recorded for the 9 g Fe^{3+} L⁻¹ initial concentration during the first two hours of operation (Figure 1.6). The high SMRR value in the biotic medium could be attributed to the presence of sufficient amounts of extracellular polymeric substances (EPSs) with attached Fe^{3+} ions, enhancing the catalytic oxidation of Fe^{2+} , and thus the recovery of the oxidant and the amount of metal mobilization. Sand and Gehrke (2006)

have concluded that strains of *A. ferrooxidans* with a high amount of Fe^{3+} ions in their EPSs recorded greater Fe^{2+} oxidation activity than those with a lower Fe^{3+} concentration.

In the particular case of metal sulfides, some authors have observed that EPSs, composed mainly of neutral sugars and lipids, provide a controlled reaction layer that concentrates Fe^{3+} ions by complexation through uronic acids or other metabolites on the compound surface, increasing effective Fe^{3+} concentration in the attachment points and recording a 20-100 times enhancement over chemical leaching (Kinzler et al., 2003; Silva et al., 2015).

Figure 1.6 shows that the maximum SMRR (SMRR_{max}) values were recorded within the first hour, and then the rate decreased over time. The SMRR_{max} obtained here is consistent with those described in the literature for experiments using either *A. ferrooxidans* cultures or a cell-free culture supernatant (Table 1.3). It is noteworthy that the SMRR_{max} recorded in the biotic 9K experiment ($40 \text{ mg h}^{-1} \text{ cm}^{-2}$) was slightly higher than that reported by Jadhav et al. (2013) with the strain BCRC 13823 and an initial concentration of $40 \text{ g FeSO}_4 \text{ L}^{-1}$. Consequently, the 9K medium was selected for subsequent experiments in this study.

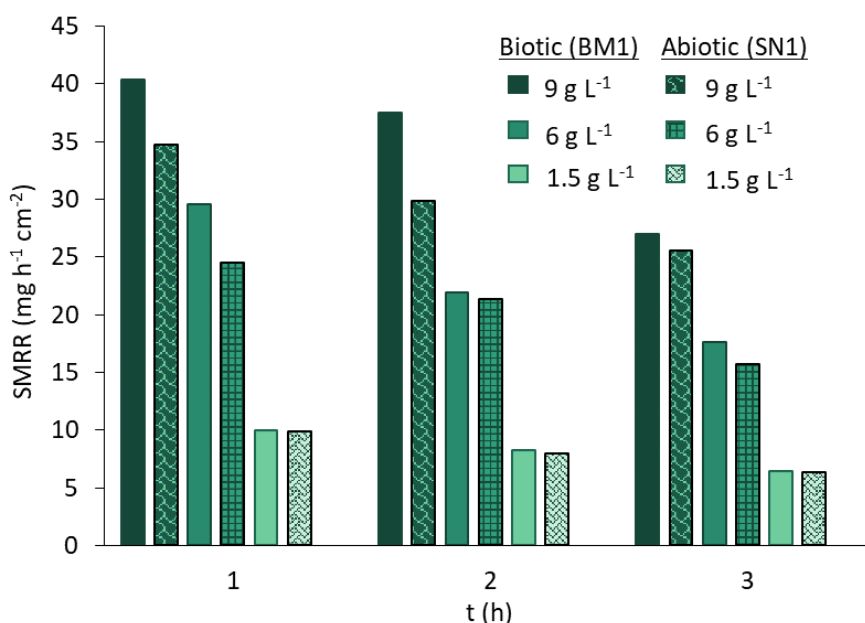


Figure 1.6. Variation of the SMRR during the three-hour experiment for the three initial Fe^{3+} concentrations ($9, 6$ and $1.5 \text{ g Fe}^{3+} \text{ L}^{-1}$).

Regardless of the metal removal rate recorded in the experiments, the $\text{Fe}^{3+}/\text{Fe}^{2+}$ ratio followed a similar evolution in all cases and, after the three-hour immersion of a copper piece in the oxidant medium, the Fe^{3+} content decreased to $55 \pm 4 \%$ of its initial value in both biotic and abiotic assays (BM1 and SN1 experiments respectively).

Table 1.3. Maximum SMRR values obtained in the literature and in this study when using different initial concentrations of Fe³⁺ at T= 30-31 °C).

SMRR _{max} (mg Cu h ⁻¹ cm ⁻²)	<i>A. ferrooxidans</i> strain	[Fe ³⁺] _{t=0} (g L ⁻¹)	pH	Reference
Biotic experiments				
2	ATCC 23270	0.6	1.8	Díaz-Tena et al., 2016
10	ATCC 23270	1.5	1.7	This study
10	Isolated from acidic pit water	5.0	1.8	Ma et al., 2020
22	ATCC 23270	6.0	1.8	Díaz-Tena et al., 2016
30	ATCC 23270	6.0	1.7	This study
40	ATCC 23270	9.0	1.7	This study
36	BCRC 13823	14.7	2.5 ^a	Jadhav et al., 2013
Abiotic experiments				
10	ATCC 23270	1.5	1.7	This study
16	BCRC 13823	3.7	2.5 ^a	Jadhav et al., 2013
5.4	BCRC 13820	4.0	2.5 ^a	Hocheng et al., 2012b
28	ATCC 23270	6.0	1.7	This study
28	ATCC 23270	9.0	1.7	This study
40	BCRC 13823	14.7	2.5 ^a	Jadhav et al., 2013

^aThis value corresponds solely to the initial pH.

1.3.1.3. SMRR as a function of time during metal mobilization process

Several authors have studied the variation in the SMRR over time using different *A. ferrooxidans* strains and operating conditions (Istiyanto et al., 2010; Xenofontos et al., 2015; Díaz-Tena et al., 2018). Nevertheless, the literature on the effect of microbial presence on metal leaching by comparing biotic and abiotic experiments over prolonged periods of time is scarce.

In this study, after 20 h of operation the total copper mobilization was 55 % higher in the biotic system (1043±14 mg) than in the abiotic one (672±12 mg) (Figure 1.7a). Assuming that all the dissolved copper was in the Cu²⁺ ionic form, a final concentration of 7.6 g Cu²⁺ L⁻¹ and 4.9 g Cu²⁺ L⁻¹ was reached in the reactor with and without microorganisms, respectively. The evolution of the Fe³⁺/Fe²⁺ ratio over time is shown in Figure 1.7a, as this ratio plays a key role in overall metal removal kinetics by influencing the rate of the chemical process (metal dissolution) and the biologically catalyzed process (oxidant bio-regeneration). During the first four hours of operation, the ratio

quickly decreased due to Fe^{3+} consumption in the copper oxidation process, with this ion being the acceptor that simultaneously received electrons from the metal.

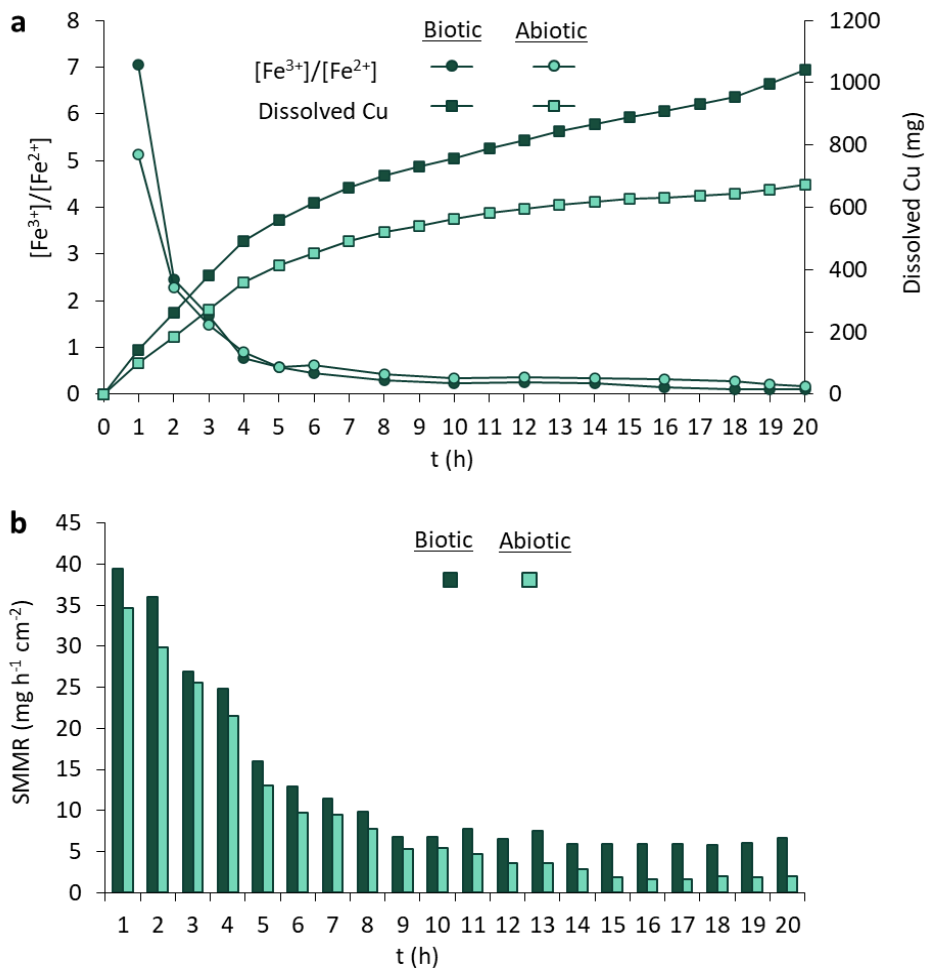


Figure 1.7. Evolution of dissolved copper and $[\text{Fe}^{3+}]/[\text{Fe}^{2+}]$ ratio (a), and SMRR (b) throughout time.

Nevertheless, from hour 8 onwards, the ratio remained almost constant for the biotic and abiotic systems, which can be explained by the limited rate of electron transfer, as suggested by Vargas et al. (2014). As far as the biotic system is concerned, when the rate of electron transfer from copper metal to Fe^{3+} (rate of Fe^{2+} produced in the chemical process) equaled the rate of electron transfer from Fe^{2+} to O_2 (rate of Fe^{2+} consumption in the biological process) a pseudo steady-state was reached, and the amount of $\text{Fe}^{3+}/\text{Fe}^{2+}$ was therefore expected to remain constant. However, the abiotic system recorded a similar trend with even slightly higher $\text{Fe}^{3+}/\text{Fe}^{2+}$ ratio values during the final hours of the experiment, which means that Fe^{3+} consumption was lower, resulting in a lower amount of copper dissolved.

As shown in Figure 1.7b, during the first four hours the SMRR decreased in both reactors more significantly, in agreement with the results recorded in the previous three-hour

experiment. Afterwards, from 5 to 8 h the metal solubilization process slowed down in the two assays, and the SMRR value fell to $8 \text{ mg h}^{-1} \text{ cm}^{-2}$. Finally, the SMRR value became almost constant at an average value of $6.5 \pm 0.7 \text{ mg h}^{-1} \text{ cm}^{-2}$ from hour 9 onwards for the biotic system (BM2), whereas this value was $1.8 \pm 0.2 \text{ mg h}^{-1} \text{ cm}^{-2}$ from 15 h onwards for the abiotic assay (SN2). Thus, the difference between the SMRR in both assays became constant beyond 15 h, with the SMRR in the biological reactor being almost four times higher than in the abiotic assay. These results are consistent with those reported by Istiyanto et al. (2007), who have concluded that the reduction in the MRR (mg h^{-1}) is inversely proportional to machining time, and not simply linear. These authors have observed that the decrease in the MRR in a reactor containing *A. ferrooxidans* ATCC 21834 is almost negligible from hour 12 onwards.

A slight variation in the SMRR was observed in experiment B3, where copper extraction from the workpiece was induced by the spontaneous oxidation of Fe^{2+} to Fe^{3+} in the presence of the oxygen dissolved in the acidic medium. In this experiment, the SMRR increased with operation time to an average of $1.8 \pm 0.3 \text{ mg h}^{-1} \text{ cm}^{-2}$ for the 10-20-h period. This value is almost identical to that recorded in experiment SN2 from 15 h onwards, which means the leaching process in the absence of bacteria (SN2) seems to be limited by the re-oxidation of Fe^{2+} to Fe^{3+} assisted by the oxygen dissolved in the medium. According to these results, after 15 h of treatment, 65 % of the SMRR recorded in the microorganism-containing reactor (BM2) was attributed to the presence of bacteria, whose catalytic action greatly enhanced the electron transfer process.

1.3.2. Alternate process: metal mobilization + regeneration

As concluded in the previous section, microorganism-assisted metal mobilization performed better than abiotic process. Nevertheless, the SMRR decreased significantly after three-hours of treatment, which would be a technical drawback when longer operation time is required, for example, to engrave specific geometries on a copper piece in biomachining application. Thus, the alternative proposed here was to treat the metal piece in consecutive three-hour leaching stages. In this approach, the reuse of the solution (after regeneration) in several metal mobilization stages is essential for the system's sustainability. Therefore, the efficiency of the regenerated solution in consecutive treatment stages was studied and the criteria for the solution to be considered "exhausted" was defined.

Figure 1.8a shows the SMRR during six metal mobilization + regeneration stages. In addition, Figure 1.8b provides a detailed view of the variation in Fe^{3+} and Cu^{2+} concentrations in the medium during stages MR1 and MR2 and the first regeneration stage.

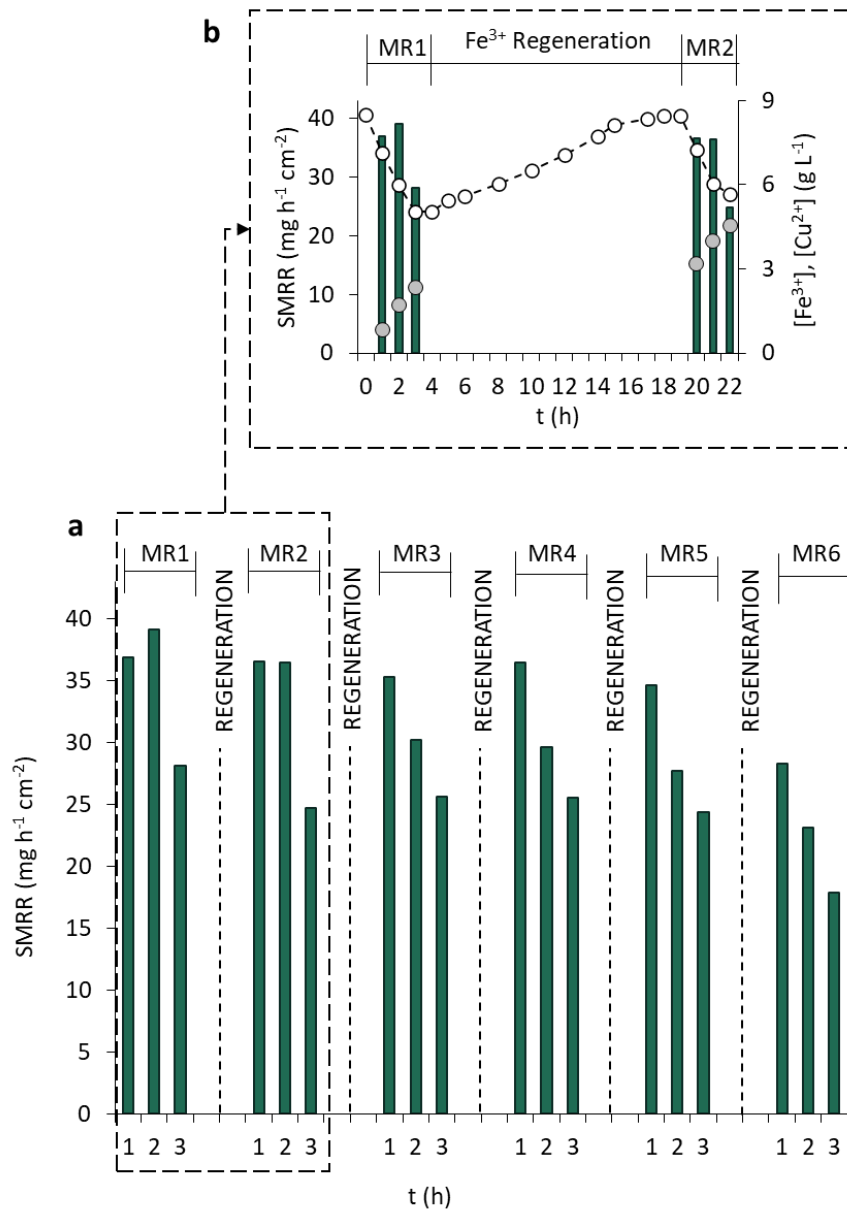


Figure 1.8. SMRR as a function of time during six three-hour metal removal stages (a); variation in SMRR (bars), $[\text{Cu}^{2+}]$ (grey dots) and $[\text{Fe}^{3+}]$ (white dots) during two successive treatment stages (MR1 and MR2) and the oxidant regeneration step (b).

The trend in the SMRR during each three-hour treatment was similar in all the stages (MR1-MR6). It is noteworthy that the SMRR_{max} remained almost constant ($36.0 \pm 0.9 \text{ mg h}^{-1} \text{cm}^{-2}$) in MR1- MR5 stages, and decreased in MR6 by about 22 % of the initial value. The stages MR1 and MR2 recorded a slightly better performance than the successive ones in terms of total Cu removal, and the amount of copper dissolved (calculated as the average for each 3 h period) remained in the $97\text{-}104 \text{ mg cm}^{-2}$ range (Figure 1.9). In MR3 to MR5, this value was almost constant ($89.9 \pm 2.7 \text{ mg cm}^{-2}$), and in MR6 this value was 33 % lower than that recorded in MR1. These accumulated values were significantly

higher than those recently reported by Ma et al. (2020) using an *A. ferrooxidans* strain isolated from acidic pit water taken from an iron mine in China. These authors have reported a removal of copper of approximately 60 mg cm^{-2} after an eight-hour leaching experiment using 5 g L^{-1} of iron as energy source ($30 \text{ }^\circ\text{C}$, 160 rpm , $\text{pH } 1.8$).

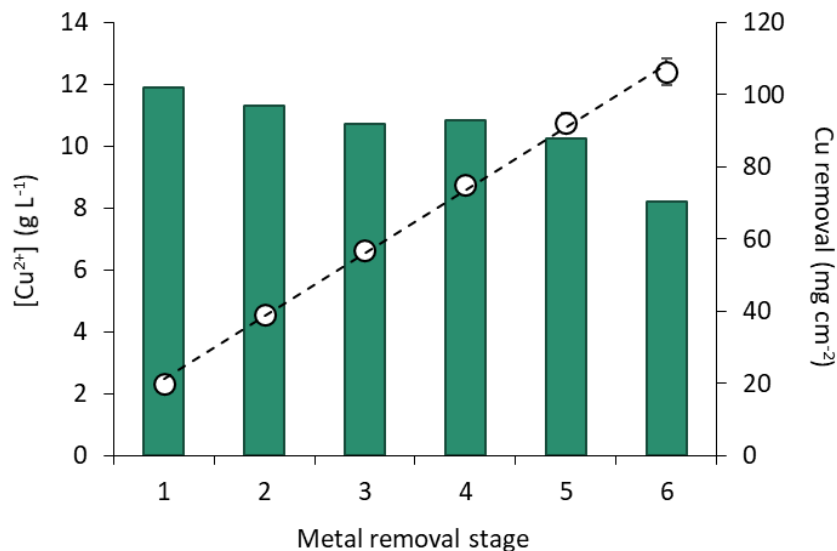


Figure 1.9. Copper solubilization in consecutive treatment stages (columns, right axis) and accumulated copper concentration in the solution (white dots, left axis).

Overall, the proposed system design being comprised of three-hour copper mobilization stages in consecutive operation (with intermediate regeneration stages) significantly improved the average SMRR for copper extraction in comparison to continuous operation (Section 1.3.1.3 *SMRR as a function of time during the metal mobilization process*). Indeed, the total amount of removed copper in 5 consecutive stages (15 h of treatment) (471.6 mg cm^{-1}) was 52.4 % higher than the metal amount extracted during 15 h in continuous operation (224.6 mg cm^{-1}). This means that the time for extracting a certain amount of copper can be considerably shortened in the consecutive stage mode, with the positive perspective for sustainability and industrial implementation of the process.

Regarding the cumulative copper concentration shown in Figure 1.9, this parameter increased linearly with treatment time and, consequently, with stage number ($[\text{Cu}^{2+}]$ (g L^{-1}) = $2.03 \cdot \text{stage number} + 0.466$; $R^2 = 0.9980$). In this experiment, the final concentration recorded after six metal mobilization stages was $12.4 \text{ g Cu}^{2+} \text{ L}^{-1}$, and the total mass of copper removed from the workpiece throughout the whole experiment was 1.57 g.

Figure 1.10 shows the solutions after six metal mobilization + regeneration stages.



Figure 1.10. Resulting solutions after six metal mobilization + regeneration stages (in duplicate).

A low concentration of dissolved copper in the medium is essential for *A. ferrooxidans* growth, as high concentration of this metal leads to the denaturation of the proteins and nucleic acids necessary for metabolic activities (Valix et al., 2017), inhibiting bacterial activity, and thus halting the whole process. The results recorded here confirmed that the loss of bacterial activity due to the increasing Cu^{2+} concentration in the medium impaired the activity of *A. ferrooxidans* strain ATCC 23270. Nevertheless, under these particular operating conditions, it was not until the dissolved Cu^{2+} concentration was higher than 10.7 g L^{-1} (recorded at the end of MR5) that biomass activity was more severely affected, slowing the bacterial Fe^{2+} re-oxidation rate, and thus reducing the SMRR. The inhibitory copper concentration depends both on the bacterial strain and on the operating conditions. However, the maximum dissolved copper concentration before bacterial inhibition detected in this study was slightly higher than that reported by other authors for other *A. ferrooxidans* strains. Thus, Díaz-Tena et al. (2016) have observed a 63 % reduction in *A. ferrooxidans* ATCC 23270 activity for oxidizing Fe^{2+} ions in the presence of $6.1 \text{ g Cu}^{2+} \text{ L}^{-1}$ ($30 \text{ }^\circ\text{C}$, 130 rpm, pH 1.8), and Cho et al. (2008) have evidenced that the oxidation capacity of Fe^{2+} by the *A. ferrooxidans* ATCC 19859 strain was completely annulled by a Cu^{2+} concentration above 10.8 g L^{-1} ($30 \text{ }^\circ\text{C}$, 200 rpm, pH 2.0).

Regarding the reduction in the waste solution generation, the results showed that microorganisms effectively re-oxidized the Fe^{2+} generated in the metal solubilization stage (Figure 1.11), which allowed the solution reuse and reagent consumption saving. Nevertheless, the medium's increasing toxicity was responsible for the longer time required for the complete bio-regeneration of the oxidant solution in the consecutive regeneration steps (Figure 1.11).

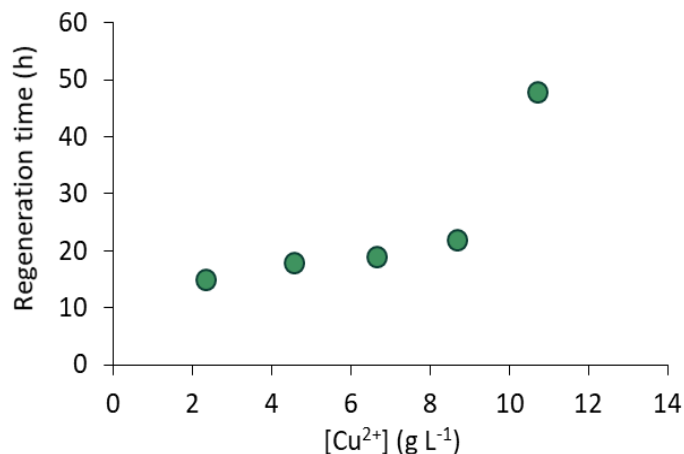


Figure 1.11. Regeneration time as a function of the copper concentration in the medium.

Figure 1.11 shows the linear increase in the time needed for complete Fe²⁺ re-oxidation or regeneration ($t_{\text{regen}} \text{ (h)} = 1.04 \cdot [\text{Cu}^{2+}] \text{ (g L}^{-1}\text{)} + 12.72$; $R^2 = 0.969$) until it sharply increased after MR5 ($[\text{Cu}^{2+}] = 10.7 \text{ g L}^{-1}$), when the time needed was 3.2 times higher than that required in the first regeneration stage ($[\text{Cu}^{2+}] = 2.3 \text{ g L}^{-1}$). The final cumulative concentration of Cu²⁺ (12.4 g L^{-1}) was not considered to be the toxic limit for biomass activity, as the bio-regeneration of the oxidant still took place in the solution after MR6. Nevertheless, the bio-regeneration time was longer than 90 h and it was considered too long for an industrial application.

The results obtained in this study suggest that the alternate mode could be successfully implemented at industrial scale by installing two (or more) treatment lines in parallel when using suspended biomass. Thus, the metal pieces (or metal containing wastes) could be consecutively immersed in the regenerated solution of each line without waiting for the oxidant recovery.

The operation mode proposed in this study is a relevant contribution for the sustainable application of this metal solubilization process to new sectors, as it prolongs the use of the solutions (and consequently reduces liquid waste generation), and improves process performance until the toxicity limit is reached.

1.4. CONCLUSIONS

This chapter has focused on studying the aspects that can contribute to the efficient solubilization of copper in microorganism-assisted processes with suspended biomass. An alternate procedure for enhancing the oxidant bioregeneration and maintaining high SMRR was sought.

As far as the influence of the iron concentration is concerned, the 9 K medium (containing 9 g L^{-1}) was concluded to be the optimum one for both *A. ferrooxidans* ATCC

23270 growth (Fe^{2+}) and copper solubilization (Fe^{3+}). Under the operating conditions, the Fe^{2+} oxidation rate in the 9K medium during microbial growth ($0.101 \text{ g Fe}^{2+} \text{ L}^{-1} \text{ h}^{-1}$) was 2.8 times higher than that recorded in the presence of $1.5 \text{ g Fe}^{2+} \text{ L}^{-1}$ ($0.036 \text{ g Fe}^{2+} \text{ L}^{-1} \text{ h}^{-1}$), rendering a higher concentration of Fe^{3+} available in the subsequent step for copper solubilization. Similarly, the presence of microorganisms improved the copper solubilization process efficiency in comparison to the biotic experiment, as the total Cu amount leached in the 9K biotic system was 25 % higher than that in absence of microorganisms.

The SMRR peaked during the first hour (SMRR_{max} of $40 \text{ mg Cu h}^{-1} \text{ cm}^{-2}$) and decreased significantly after 3-4 hours. After 15 h, 65 % of the SMRR was attributed to the re-oxidation of Fe^{2+} to Fe^{3+} due to bacterial activity, but the SMRR values recorded after 15 h in both biotic ($6.5 \pm 0.7 \text{ mg Cu h}^{-1} \text{ cm}^{-2}$) and abiotic samples ($1.8 \pm 0.2 \text{ mg Cu h}^{-1} \text{ cm}^{-2}$) were too low for industrial application.

The SMRR decrease after the first hours of treatment could be a technical drawback when longer operation time is required. Therefore, an alternate process in stages (metal solubilization during 3 hours followed by oxidant regeneration) has been proposed with the aim of maintaining high SMRR and reusing the solution in semicontinuous operation. The amount of metal mobilized in 5 consecutive stages (471.6 mg cm^{-1}) was 52.4 % higher than the amount obtained in the continuous operation for the same treatment time (15 h) (224.6 mg cm^{-1}). The inclusion of an oxidant regenerating stage between two consecutive metal solubilization stages contributed to prolonging the solution lifespan. Nevertheless, the regeneration time increased threefold compared to the first regeneration stage when the copper concentration in the medium was $0.7 \text{ g Cu}^{2+} \text{ L}^{-1}$. This alternate design allows the reduction of both the treatment time and the amount of depleted solution, which enhances the sustainability of the process.

1.5. REFERENCES

- Blanch H.W., Clark D.S., Biochemical Engineering, Marcel Dekker Inc., New York, 1996.
- Cho K. S., Ryu H. W., Choi H. M., 2008. Toxicity Evaluation of Complex Metal Mixtures Using Reduced Metal Concentrations: Application to Iron Oxidation by *Acidithiobacillus ferrooxidans*. Journal of Microbiology and Biotechnology. 18, 1298-1307.
- Daoud J., Karamanev D., 2006. Formation of jarosite during Fe^{2+} oxidation by *Acidithiobacillus ferrooxidans*. Minerals Engineering. 19, 960-967.
- Díaz-Tena E., Gallastegui G., Hipperdinger M., Donati E. R., Ramírez M., Rodríguez A., López de Lacalle L. N., Elías A., 2016. New advances in copper biomachining by iron-oxidizing bacteria. Corrosion Science. 112, 385-392.
- Díaz-Tena E., Gallastegui G., Hipperdinger M., Donati E. R., Rojo N., Santaolalla A., Ramirez M., Barona A., Elías A., 2018. Simultaneous Culture and Biomachining of Copper in MAC

- Medium: A Comparison between *Acidithiobacillus ferrooxidans* and *Sulfobacillus thermosulfidooxidans*. ACS Sustainable Chemistry and Engineering. 6, 17026–17034.
- Hocheng H., Chang J. H., Hsu H.S., Han H. J., Chang Y. L., Jadhav U. U., 2012a. Metal removal by *Acidithiobacillus ferrooxidans* through cells and extra-cellular culture supernatant in biomachining. CIRP Journal of Manufacturing Science and Technology. 5, 137-141.
- Hocheng H., Chang J., Jadhav U. U., 2012b. Micromachining of various metals by using *Acidithiobacillus ferrooxidans* 13820 culture supernatant experiments. Journal of Cleaner Production. 20, 180-185.
- Istiyanto J., Ko T. Jo, Yoon C., 2010. A study on copper micromachining using microorganisms. International Journal of Precision Engineering and Manufacturing. 11, 659-664.
- Jadhav U., Hocheng H., Weng W., 2013. Innovative use of biologically produced ferric sulfate for machining of copper metal and study of specific metal removal rate and surface roughness during the process. Journal of Materials Processing Technology. 213, 1509-1515.
- Kawabe Y., Inoue C., Suto K., Chida T., 2003. Inhibitory effect of high concentrations of ferric ions on the activity of *Acidithiobacillus ferrooxidans*. Journal of Bioscience and Bioengineering. 96, 375-379.
- Kim I., Jang H., Lee J. U., 2002. Kinetics of Fe²⁺ Oxidation by *Acidithiobacillus ferrooxidans* Using Total Organic Carbon Measurement. Journal of Microbiology and Biotechnology. 12, 268-272.
- Kinzler K., Gehrke T., Telegdi J., Sand W., 2003. Bioleaching—a result of interfacial processes caused by extracellular polymeric substances (EPS). Hydrometallurgy. 71, 83-88.
- Lambert F., Gaydardzhiev S., Léonard G., Lewis G., Bareel P., Bastin D., 2015. Copper leaching from waste electric cables by biohydrometallurgy. Minerals Engineering. 76, 38-46.
- Liang G., Lin W., He Q., Liu W., Zhou Q., 2018. Mechanism of energy metabolism for adapted *Acidithiobacillus ferrooxidans* to copper resistance. Environmental Progress and Sustainable Energy. 38, 13054.
- Liu R., Wang W., Zhou W., Cheng H., Zhou H., 2020. Acid catalysis coupling bioleaching for enhancement of metals removal from waste resin powder. Journal of Cleaner Production. 247, 119-130.
- Ma F., Huang H., Cui C., Mater J., 2020. Biomachining properties of various metals by microorganisms. Process Technology. 278, 116512.
- Mousavi, S.M., Yaghmaei, S., Salimi, F., Jafari, A., 2006. Influence of process variables on biooxidation of ferrous sulfate by an indigenous *Acidithiobacillus ferrooxidans*. Part I: flask experiments. Fuel. 85, 2555-2560.
- Muhammad I., Sana Ullah S. M., Sup Han D., Jo Ko T., 2015. Selection of optimum process parameters of biomachining for maximum metal removal rate. International Journal of Precision Engineering and Manufacturing - Green Technology. 2, 307-313.
- Nazari B., Jorjani E., Hani H., Manafi Z., Riahi A., 2014. Formation of jarosite and its effect on important ions for *Acidithiobacillus ferrooxidans* bacteria. Transactions of Nonferrous Metals Society of China. 24, 1152-1160.

- Sand W., Gehrke T., 2006. Extracellular polymeric substances mediate bioleaching/biocorrosion via interfacial processes involving iron(III) ions and acidophilic bacteria. *Research in Microbiology*. 157, 49-56.
- Sasaki, K., Nakamuta, Y., Hirajima, T., Tuovinen, O.H., 2009. Raman characterization of secondary minerals formed during chalcopyrite leaching with *Acidithiobacillus ferrooxidans*. *Hydrometallurgy*. 95, 153-158.
- Silva R. A., Park J., Lee E., Park J., Choi S. Q., Kim H., 2015. Influence of bacterial adhesion on copper extraction from printed circuit boards. *Separation and Purification Technology*. 143, 169-176.
- Silverman M. P., Lundgren D. G., 1959. Studies on the chemoautotrophic iron bacterium *Ferrobacillus ferrooxidans*: I. An improved medium and a harvesting procedure for securing high cell yields. *Journal of Bacteriology*. 77, 642-647.
- Singh A., Manikandan N. A., Sankar M. R., Pakshirajan K., Roy L., 2018. Experimental Investigations and Surface Morphology of Bio-Micromachining on Copper. *Materials Today: Proceedings*. 5, 4225-4234.
- Valix M., Wong J.-C., Tyagi D., Pandey A., 2017. Bioleaching of Electronic Waste: Milestones and Challenges. (Eds.), *Current Developments in Biotechnology and Bioengineering: Solid Waste Management*, Elsevier 407-442.
- van Hille, R.P., van Zyl, A.W., Spurr, N.R.L., Harrison, S.T.L., 2010. Investigating heap bioleaching: effect of feed iron concentration on bioleaching performance. *Minerals Engineering*. 23, 518-525.
- Vargas T., Davis-Belmar C.S., Cárcamo C., 2014. Biological and chemical control in copper bioleaching processes: When inoculation would be of any benefit? *Hydrometallurgy*. 150, 290-298.
- Xenofontos E., Feidiou A., Constantinou M., Constantinides G., Vyrides I., 2015. Copper biomachining mechanisms using the newly isolated *Acidithiobacillus ferrooxidans* B1. *Corrosion Science*. 100, 642-650.
- Yu, R., Zhong, D., Miao, L., Wu, F., Qiu, G., Gu, G., 2011. Relationship and effect of redox potential, jarosites and extracellular polymeric substances in bioleaching chalcopyrite by *Acidithiobacillus ferrooxidans*. *Transactions of Nonferrous Metals Society of China*. 21, 1634-1640.

CHAPTER 2.
OPERATION WITH
IMMOBILIZED BIOMASS

2.1. OBJECTIVE

One of the main drawbacks that hinders the implementation of biomachining and bioleaching at industrial scale is the limited oxidant bioregeneration rate due to the poor bacterial cell density in the reactor when using cell suspension (Long et al., 2004; Akhlaghi, 2019). However, this problem could be overcome by immobilizing the biomass on suitable support materials which would lead to an increase in bacterial density and, hence, to the improvement of the global performance of the bioreactor (Gomez et al., 2000; Nie et al., 2015; Zhu et al., 2017).

Several authors have reported the suitability of *A. ferrooxidans* bacteria for cell immobilization based on its natural tendency to grow on surfaces (Jaisankar and Modak, 2009; Zhu et al., 2017; Akhlaghi, 2019). However, the support material should be carefully selected, taking into account critical parameters such as cell adherence and/or high porosity (Giaveno et al., 2008). Additional indispensable properties of these materials are: insolubility in liquid solutions, non-toxicity for microorganisms and good mechanical and chemical stability. They must also withstand the levels of pH, temperature and agitation used in the bioleaching and biomachining processes (Martins et al., 2013). Finally, it should be pointed out that different carriers exert different influence on the deposition of jarosite (Zhu et al., 2017).

Even though the influence of operating parameters such as shaking mode and speed, iron concentration or copper concentration toxicity have already been reported in literature when using cell suspension (Cabrera et al., 2005; Mousavi et al., 2006), comparative studies on the optimization of the process with immobilized biomass are scarce. In addition, the ratio between nutrient media volume and the amount of support material has to be carefully selected, as it leads to different patterns of support material-media contact, which affects ferric iron productivity (Jaisankar and Modak, 2009).

The objective of this chapter was to explore the potential of different support materials for *A. ferrooxidans* immobilization (biocellulose -BC-, polyvinyl alcohol -PVA-, cellulose triacetate -CTA- and chitosan -CH-). After a preliminary selection, the research focused on the use of biocellulose (BC) for the preparation of an innovative active material able to oxidize Fe^{2+} to Fe^{3+} . In addition, the operating conditions (shaking mode and speed, initial Fe^{2+} concentration, and nutrient media volume to amount of support ratio) that improve the process performance were selected. The effect of additional aspects on the process was also assessed, such as the increasing concentration of dissolved copper and the storage of the active material. Finally, a series of comparative tests were carried out using PVA under the optimal conditions selected for BC.

Figure 2.1 shows the outline of the experimental section of this chapter

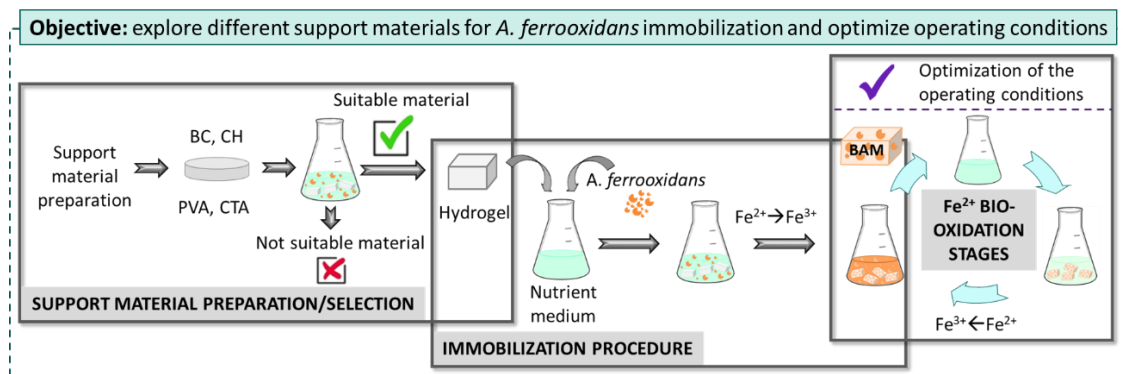


Figure 2.1. Outline of the experimental section of this chapter.

2.2. MATERIALS AND METHODS

2.2.1. Microorganism and culture medium

The microorganism strain used in this study was *A. ferrooxidans* DSM 14882. The cells were cultured in the medium developed by Silverman and Lundgren (1959), using 6 and 9 g $Fe^{2+} L^{-1}$ (6K and 9K medium, respectively) as initial iron concentration depending on the experiment. *Gluconacetobacter xylinum* strain was used for bacterial cellulose production. The details regarding both the media and the bacteria are described in Section 1.1 *Microorganisms* (materials and general methods).

2.2.2. Synthesis of the support materials

Bacterial cellulose or Biocellulose (BC), polyvinyl alcohol (PVA), cellulose triacetate (CTA) and chitosan (CH) were preliminarily selected to be tested as potential support materials for bacterial immobilization. Figure 2.2 shows the molecular structure of those materials.

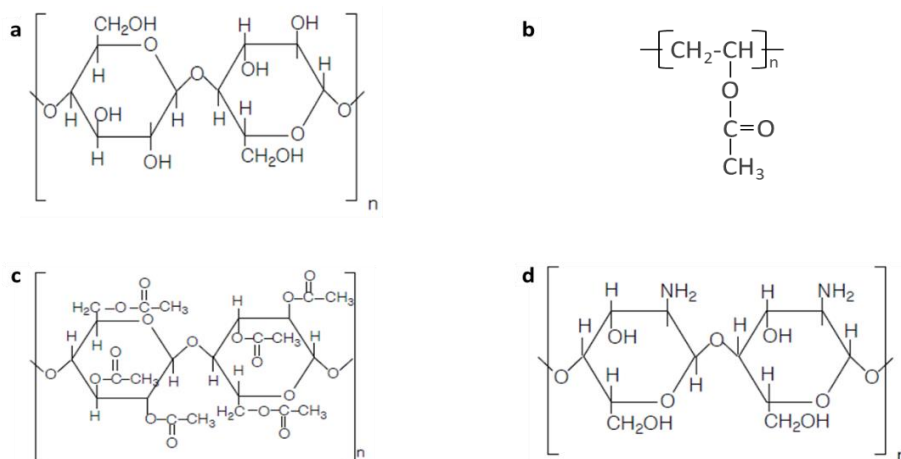


Figure 2.2. Molecular structure of bacterial cellulose (BC) (a), polyvinyl alcohol (PVA) (b), cellulose triacetate (CTA) (c) and chitosan (CH) (d).

BC is a tridimensional natural nanofiber network produced by microorganisms with a high specific surface. It exhibits outstanding qualities, such as a highly porous network structure, biocompatibility, and good mechanical and chemical stability (Azeredo et al., 2019; de Oliveira et al., 2021). Being synthesized by bacteria, it can be obtained with the desired size and shape.

PVA is a bioplastic derived from the hydrolysis, alcoholysis or aminolysis of polyvinyl acetate. It is a highly biodegradable thermoplastic polymer and easily soluble in water due to its crystalline structure. It stands out for its flexibility and high chemical resistance and for being a barrier for gases and aromas (Hammannavar and Lobo, 2018; Abrial et al., 2020).

CTA is a chemical compound obtained by treating cellulose where all cellulose hydroxyl groups are replaced by acetyl groups. It is commonly used to elaborate membranes characterized by well-defined pores (Sikorski et al., 2004; Nabili et al., 2017). Two different CTA-based support materials were tested: modified CTA membrane and CTA spheres.

CH is a natural biopolymer that is obtained from the partial deacetylation of chitin. This is a very abundant polysaccharide in nature and is obtained from the shell or exoskeleton of crustaceans, fungi and insects, generally as a by-product of fishing industries. It is insoluble in water with a high molecular weight, nontoxic and biodegradable biopolymer (Muxika et al., 2017; Bakshi et al., 2020).

2.2.2.1. Bacterial cellulose

Bacterial cellulose hydrogel was biosynthesized in the laboratory by *Gluconacetobacter xylinus* bacterial strain. It was obtained by adding 1 % inoculum of *Gluconacetobacter xylinus* bacteria to the medium containing panela and pineapple dissolved in water (13 % w:v). The culture was incubated under static conditions at 28 °C, until the desired thickness of the pellicle was reached after 25 days (the incubation time can be adjusted to obtain the necessary thickness). In this study, BC membranes with a 0.7 cm thickness were used. The pH was adjusted to 3.5 by the addition of acetic acid (CH₃COOH) (Retegi et al., 2010).

After biosynthesis, BC pellicle was washed with a 2 % w:v solution of sodium hydroxide (NaOH) for 24 h at room temperature and orbital shaking. Finally, it was rinsed with deionized water several times until the complete neutralization of the BC membrane (Gutierrez et al., 2013). After the purification process, a completely white bacterial cellulose membrane was obtained (Figure 2.3).

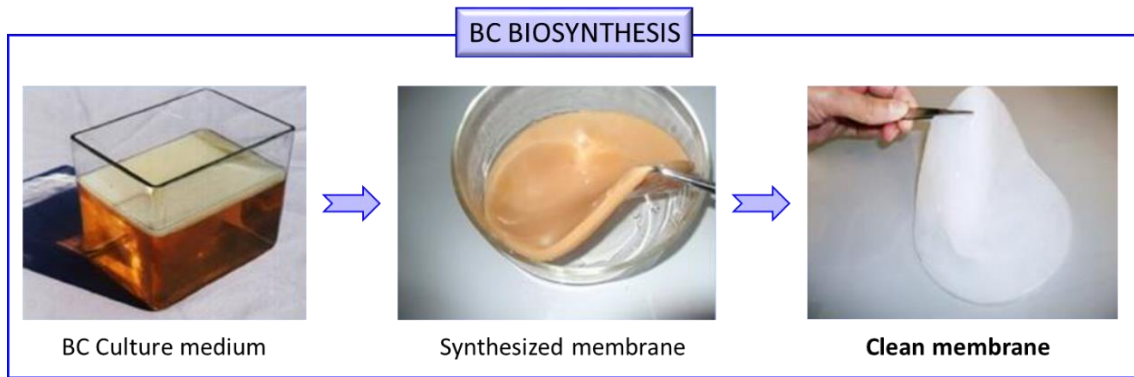


Figure 2.3. Culture medium and synthesized BC membrane.

2.2.2.2. Polyvinyl alcohol

PVA hydrogel was prepared using powder PVA (M_w 130000 g mol⁻¹, Sigma-Aldrich Corporation). First, 2.5, 5 and 10 % w:w PVA solutions were prepared by dissolving PVA in deionized water at 95 °C under vigorous stirring for 3 h. The homogenous PVA solution was subsequently placed into a petri dish and cooled at room temperature. Then, two different techniques were used for synthesizing PVA hydrogels: Freeze-Thawing and Freeze-Drying.

In the Freeze-Thawing method (Hassan and Peppas, 2000), previously obtained PVA solutions were subjected to 24 h freezing at -21 °C and 3 h of thawing at 25 °C for a total of 3 cycles. The Freeze-Thaw cycling promotes the crystallization of PVA domains, which results in a strong hydrogel formation with high mechanical stability and good properties such as viscoelasticity (Peppas and Scott, 1992; Vrana et al., 2009). During the freezing the PVA domains get closer due to the formation of frozen water, allowing the formation of cross-links (Holloway et al., 2013). After thawing, these PVA domains result in non-covalent bond formation between the polymer chains (Ou et al., 2017).

Figure 2.4 schematically shows the Freeze-Thawing process for PVA labeled samples.

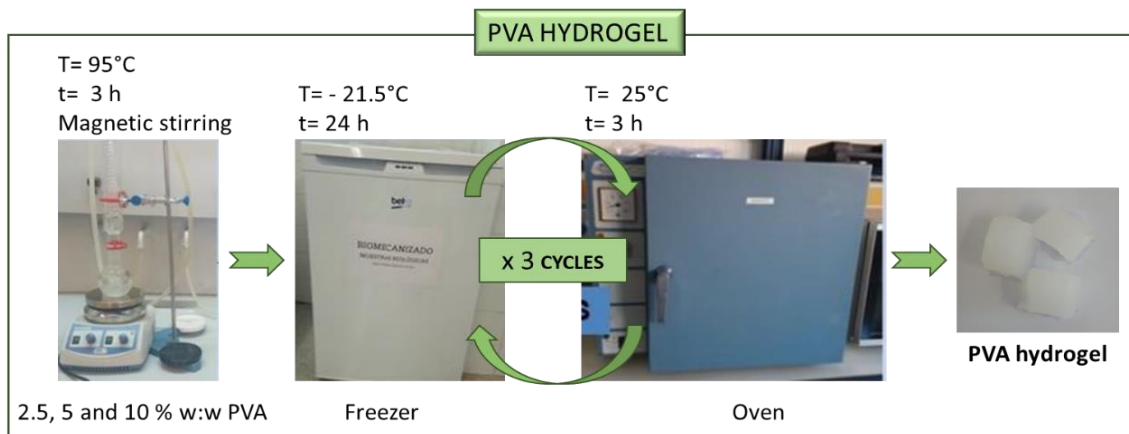


Figure 2.4. PVA hydrogel preparation process using Freeze-Thawing technique.

In the Freeze-Drying method the PVA solutions were frozen for 24 h at $-21.5\text{ }^{\circ}\text{C}$ and subsequently placed in a lyophilization equipment (model Alpha 1_4LD (Martin Christ)) at $-85\text{ }^{\circ}\text{C}$ and 0.1 mbar. Figure 2.5 shows the scheme of the process. The samples obtained were labeled L-PVA, referring to lyophilized PVA. In this technique only samples of 2.5 and 5 % w:w by mass were prepared, since 10 % w:w concentration was too high for the resulting material to be porous enough for the desired application.

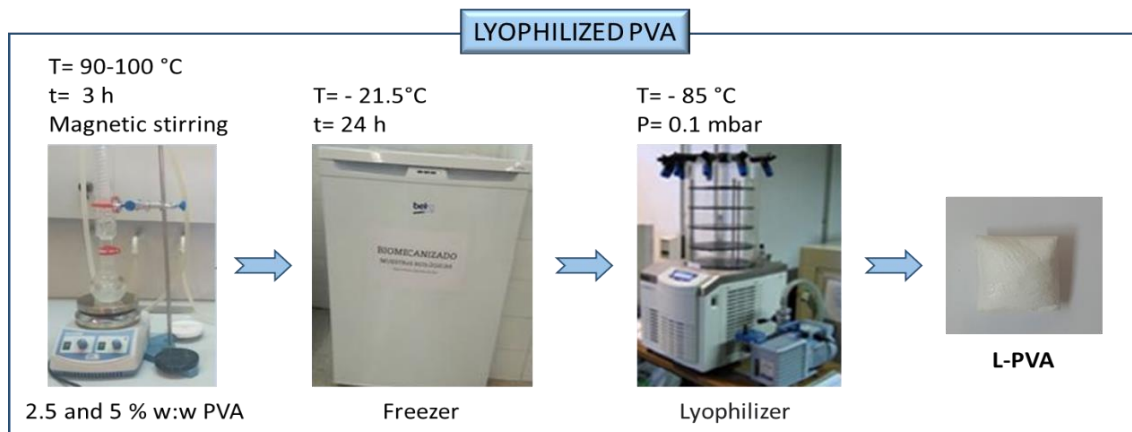


Figure 2.5. Lyophilized PVA (L-PVA) preparation process using Freeze-Drying technique.

2.2.2.3. Modified cellulose triacetate membrane

A modified CTA membrane was fabricated by an adaptation of the method published by Kaiser et al. (2017). The solution of the triacetate cellulose biopolymer was prepared with acetone as solvent because it is insoluble in water but soluble in organic solvents. CTA (Sigma Aldrich) was dissolved in 300 mL of acetone (99.5 %, Panreac) and kept in a closed container under stirring conditions for 24 h thus obtaining a solution with a 10 % w:v concentration. Afterwards, the solution was transferred to a container with 20.5 g of calcium carbonate (99.5 %, Panreac) and 8.8 g of glycerol (99 %, 98.09 g mol^{-1} , Labkem). It was then vigorously mixed in a blender for 5 min. Finally, the mixture was introduced into a closed container.

Afterwards, two water baths containing 0.25 M HCl (99 %, Panreac) and deionized water, respectively, were prepared in order to completely dissolve both calcium carbonate and glycerol. The obtained liquid polymer was spread on a flat glass of 1-2 mm of thickness and it was dried for 5 min approximately. After this time, it was carefully immersed in the HCl bath for 10 min, and bubble formation on the surface was observed, due to the dissolution of calcium carbonate with the consequent CO_2 release. The obtained membrane was introduced then into the deionized water bath for another 10 min. Finally, it was extracted and placed on absorbent paper, until a dry porous membrane was obtained. The material obtained was labelled M-CTA. Figure 2.6 shows the scheme of the procedure carried out for the synthesis of the M-CTA membrane.

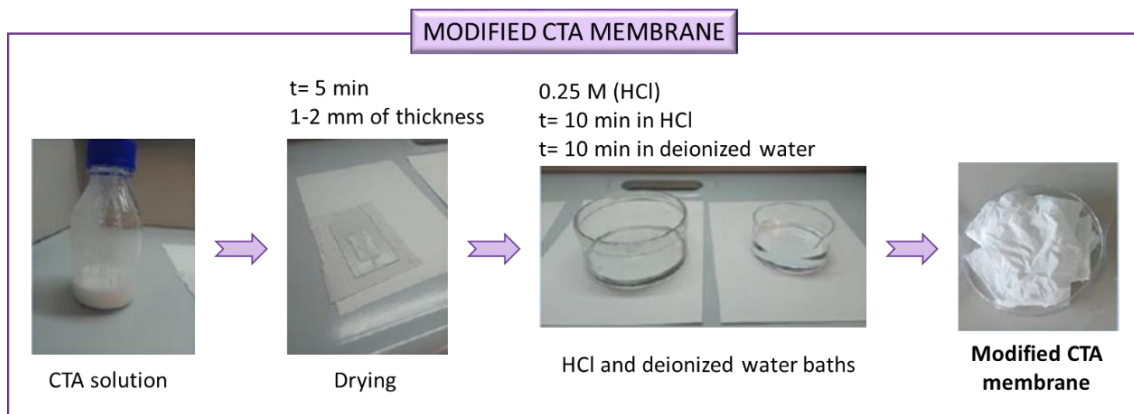


Figure 2.6. Preparation process of modified CTA membrane (M-CTA).

2.2.2.4. Cellulose triacetate spheres

The fabrication of the CTA spheres was carried out as follows. Once the abovementioned CTA solution (10 % w:v) was completely dissolved, a certain quantity of the prepared solution was introduced for 10 s into a beaker containing deionized water at 95 °C. The observed bubbling caused by the evaporation of the acetone allowed the formation of the pores. Afterwards, the solution was removed from the beaker, the spheres were manually rounded, and they were placed in an oven (Selecta P model) at 45 °C until the total evaporation of acetone. This support material was labelled B-CTA. Figure 2.7 shows the scheme of the preparation process.

Finally, the spheres were weighed and measured for classification according to size. For this study, the spheres with an average surface area of $4.6 \pm 0.4 \text{ cm}^2$ were selected.

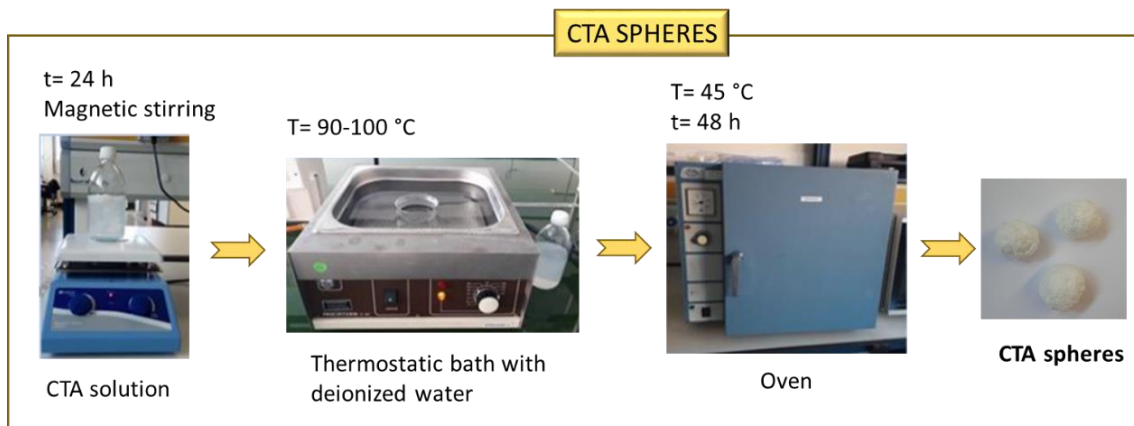


Figure 2.7. Preparation process of CTA spheres (B-CTA).

2.2.2.5. Chitosan

The chitosan solution was prepared by dissolving 2.45 g of chitosan (Aldrich's, medium molecular weight) in 120 g of a solvent solution containing deionized water and acetic

acid at 2 % w:v (99.8 %, Honeywell). The mixture was maintained in a closed container under stirring for 24 h. Then, it was poured into a Petri dish and placed in the freezer at $-21.5\text{ }^{\circ}\text{C}$. After 24 h the samples were extracted from the freezer and two different procedures were carried out. In the first one, the sample was just kept at room temperature. This chitosan material was identified as CH. In the second treatment, the frozen sample was lyophilized obtaining the so-called lyophilized chitosan material (L-CH, Figure 2.8).

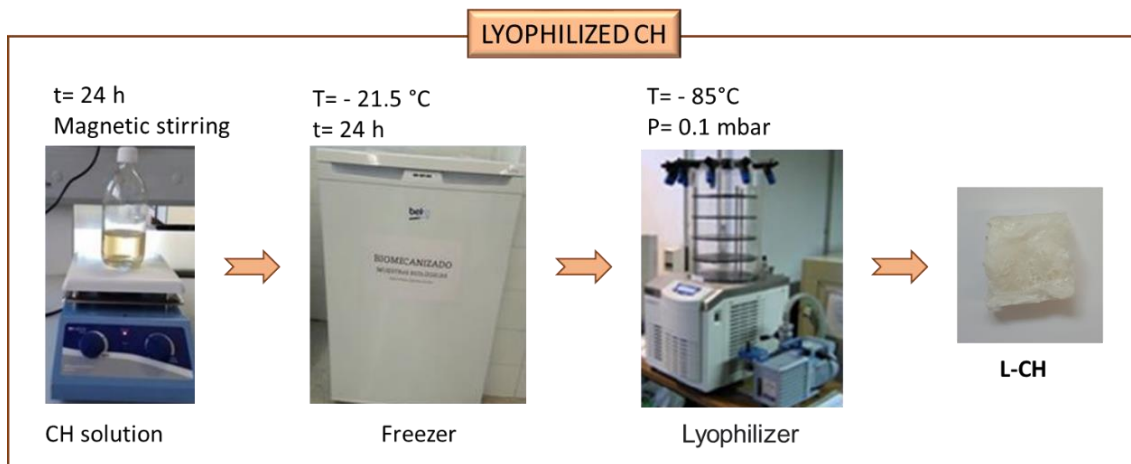


Figure 2.8. Preparation process of lyophilized chitosan L-CH.

2.2.3. Pre-treatment of the support material

The four synthesized materials, namely bacterial cellulose (BC), polyvinyl alcohol (PVA), cellulose triacetate (CTA) and chitosan (CH) were tested as immobilization support materials in this study.

As far as BC and PVA hydrogels are concerned, they were cut into rectangular parallelepiped pieces, rendering an external surface area (ESA) of $4.8\pm 0.4\text{ cm}^2$. CTA spheres were rounded to a mean diameter of $1.21\pm 0.05\text{ cm}$ which corresponds to an ESA of $4.6\pm 0.4\text{ cm}^2$. CH and modified CTA membrane support materials were prepared trying to maintain the same ESA area.

It should be noted that the presence of trace amounts of the reagents used for the synthesis of the materials could hinder microbial growth, thereby making the cleaning of all the support materials mandatory before bacterial immobilization. Therefore, the pieces were rinsed with deionized water at 130 rpm and $31\text{ }^{\circ}\text{C}$ for 1 h. This process was repeated twice and subsequently the same protocol was carried out (twice) replacing the deionized water by fresh nutrient medium (6K or 9K depending on the experiment). Finally, pieces of the different support materials were immersed in fresh nutrient medium for 24 h (130 rpm, $31\text{ }^{\circ}\text{C}$).

2.2.4. The design of a decision-making protocol

A decision-making protocol was designed to study the viability of the synthesized materials in bacterial immobilization procedures. Therefore, the main objective of this protocol was to assess the materials' suitability for microbial immobilization for its application in the metal removal process. Figure 2.9 shows the lay-out of the decision-making protocol.

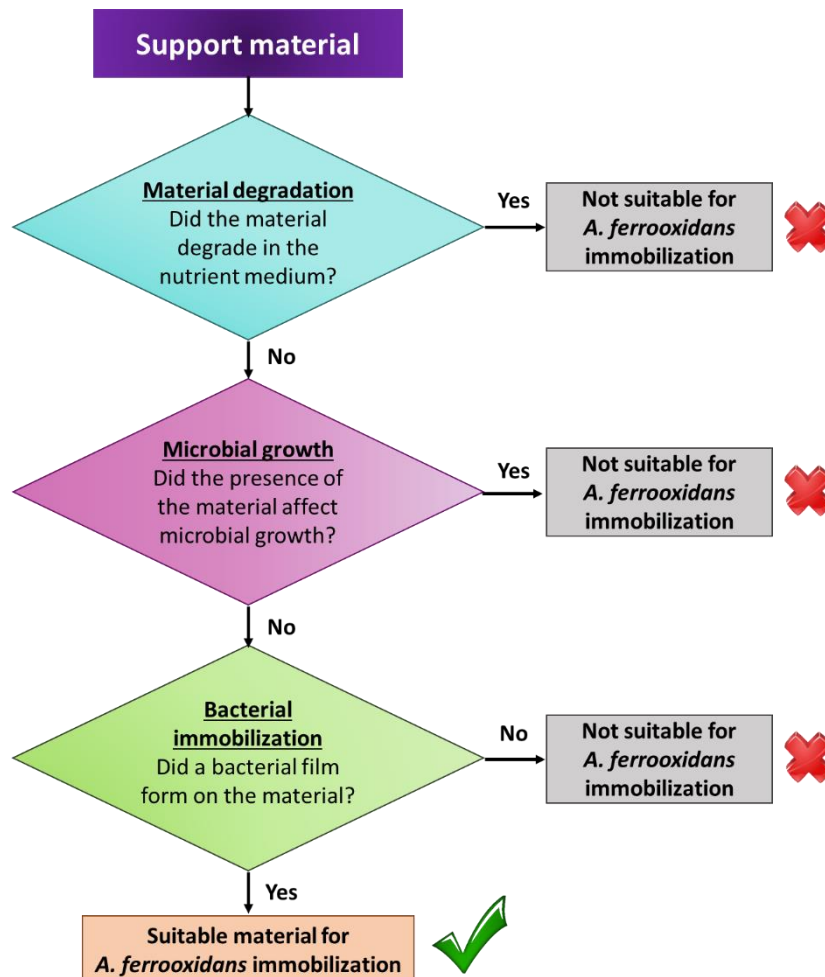


Figure 2.9. Decision-making protocol.

In the first stage, the possible degradation when being immersed in 9K medium (without bacterial inoculation) was tested by introducing the materials into the aforementioned solution under shaking conditions for 1 day (130 rpm, 31 °C). They were directly discarded when the physical integrity was not maintained and, otherwise, they proceeded to the next stage.

The second stage consisted of evaluating whether the materials exerted any adverse influence on microbial growth. Bearing in mind this objective, an immobilization test was carried out by inoculating *A. ferrooxidans* bacteria (5 % v:v of culture in the

exponential growth phase) in the 9K culture medium in the presence of each support (130 rpm, 31 °C).

The last stage was focused on assessing the microbial colonization. Once the materials were proved not to be degraded by the medium and not to impair microbial growth, the supports already exposed to biomass in the previous step were cleaned using fresh medium and then cultured in 9K medium without further bacterial inoculation. In case of successful Fe²⁺ oxidation by the “active material”, the supports were concluded to be favorable for *A. ferrooxidans* immobilization. If not, they were definitively disregarded for further experimentation. Thus, it was assumed that the microbial film was active if, after the immobilization procedure, the freshly fed Fe²⁺ was oxidized into Fe³⁺ without further inoculation.

2.2.5. Selection of the inoculum percentage

As this chapter is focused on the immobilization procedure of the *A. ferrooxidans* bacteria, it was considered relevant to investigate the optimum amount of inoculum that shortened the incubation period while ensuring an adequate bacterial growth. Thus, different percentages (2, 5 and 10 %) of an *A. ferrooxidans* culture in an exponential growth phase were inoculated in 250 mL Erlenmeyers containing 150 mL of the 6K culture medium (6 g Fe²⁺ L⁻¹). The experiments were carried out at 31 °C and shaking speed of 130 rpm. A pH threshold value of 1.8 was maintained by the addition of sulfuric acid (25 % v:v).

2.2.6. Suitability of bacterial cellulose as support material for *A. ferrooxidans* immobilization

Among the suitable materials selected according to the decision-making protocol previously described in Figure 2.9., BC has not yet been proposed as support for *A. ferrooxidans* immobilization. Consequently, it was selected for the experiments focused on selecting the most adequate operating conditions for obtaining and using an Active Bacterial Cellulose (A-BC) capable of transforming the ferrous iron dissolved in the nutrient medium into ferric iron. The particular interest on BC hydrogel lied in its outstanding properties as a viable support material and its novel use for this application.

2.2.6.1. Preparation of the Active Bacterial Cellulose (A-BC)

The procedure to obtain the A-BC started with the immersion of the BC pieces into an Erlenmeyer flask containing the nutrient medium (6K and 9K depending on the experiment), and then the *A. ferrooxidans* bacteria (5 % v:v of a culture in an exponential growth phase) was inoculated and cultured at 31 °C and pH 1.8 (adjusted with sulfuric

acid 25 % v:v). This immobilization step was carried out in duplicate under low-demanding conditions until the complete oxidation of Fe^{2+} (shaking rate of 130 rpm and a Nutrient medium volume (mL) to external surface area (cm^2) (NMV:ESA) ratio of 1:0.2). Thus, biologically active biocellulose (A-BC) was obtained (Figure 2.10).

2.2.6.2. Effect of operating parameters on Fe^{2+} bio-oxidation

The previously prepared A-BC material was used in several experiments with the objective of ascertaining the effect of the shaking mode (orbital vs linear), NMV:ESA ratio (in the 1:0.1-1:0.6 range), initial Fe^{2+} concentration (6 vs 9 $\text{g Fe}^{2+} \text{ L}^{-1}$) and shaking speed (130 vs 170 rpm) on the iron bio-oxidation performance. The experimental conditions are detailed in Table 2.1. During the experiments, the pH was adjusted to 1.8 with sulfuric acid (25 % v:v) and the temperature was maintained at 31 °C. All the BC pieces were incubated until 100 % Fe^{2+} contained in the nutrient medium was oxidized.

Table 2.1. Experimental conditions for the iron bio-oxidation experiments using the A-BC pieces at 31 °C and pH 1.8.

Experiment	Shaking mode	Operation parameter		
		NMV:ESA ratio (mL:cm ²)	Dissolved [Fe^{2+}] (g L ⁻¹)	Shaking speed (rpm)
Shaking mode	Orbital	1:0.2	6	130
	Linear			
NMV:ESA ratio	Orbital	1:0.1	6	130
		1:0.2		
		1:0.3		
		1:0.6		
Dissolved [Fe^{2+}]	Orbital	1:0.6	6	130
			9	
Shaking speed	Orbital	1:0.6	9	130
				170

In all the experiments (except for the shaking mode experiment) the same A-BC pieces were used in two consecutive bio-oxidation stages under the same operating conditions (Figure 2.10). This procedure allowed to study the activity of the material in successive stages and to identify the possible problems that could arise from its long-term use.

In addition, control tests were conducted using 6K and 9K medium inoculated with 5 % v:v of *A. ferrooxidans* culture in exponential growth phase but without hydrogel pieces.

Figure 2.10 illustrates the scheme of the whole process including A-BC preparation and the subsequent bio-oxidation stages.

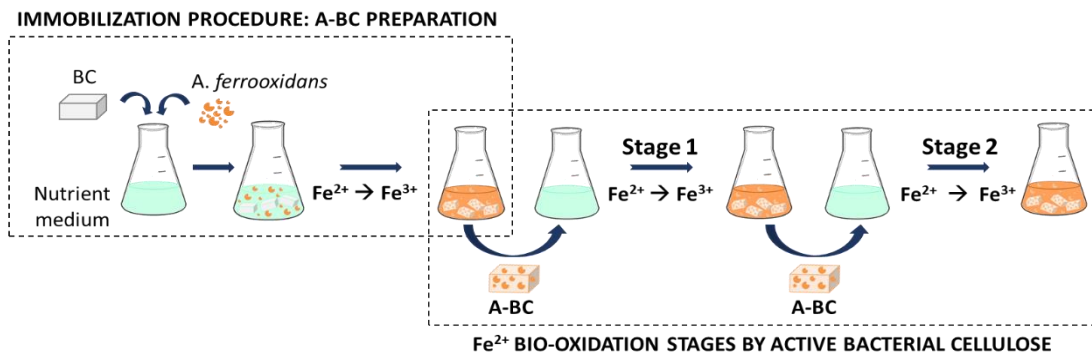


Figure 2.10. Scheme of bacterial immobilization procedure and subsequent oxidation stages.

2.2.6.3. Influence of dissolved copper concentration on bacterial immobilization and subsequent iron bio-oxidation stages

The influence of the presence of dissolved copper (Cu^{2+}) on the preparation of A-BC was tested, as increasingly dissolved metal concentration originated throughout the processes is known to affect bacterial activity and survival (Liang et al., 2018). Thus, the protocol described in Section 2.2.6.1 *Preparation of the Active Bacterial Cellulose (A-BC)* was repeated using 9K medium, 1:0.6 NMV:ESA ratio, and variable concentrations of dissolved copper (from 0 to $40 \text{ g Cu}^{2+} \text{ L}^{-1}$).

The BAM pieces were labelled as “A-BCX” being X the concentration of dissolved copper. Several consecutive bio-oxidation stages were carried out for each copper concentration with the active materials pieces, and the time required for complete iron oxidation in each stage was recorded.

In addition, the ability of immobilized *A. ferrooxidans* to adapt to the presence of dissolved copper was tested by immersing the A-BC15 pieces into the medium with increasing Cu^{2+} concentrations (20, 25 and $30 \text{ g Cu}^{2+} \text{ L}^{-1}$) in several consecutive bio-oxidation assays. Table 2.2 shows the whole procedure particularly applied to the sample A-BC15.

Table 2.2. Copper concentration in the medium during A-BC15 preparation and subsequent bio-oxidation stages with the sample A-BC15.

Stages	$[\text{Cu}^{2+}]$ (g L^{-1})
A-BC15 preparation	15
S1-S4	15
S5-S7	20
S8	25
S9	30

The operating conditions in those experiments were 31 °C, pH 1.8 and orbital shaking at 170 rpm.

2.2.6.4. Influence of active BC storage on bacterial activity

The proper preservation of the biologically active material (A-BC) would allow its storage for further use, which would contribute to facilitate the future full-scale application. The influence of two storage temperatures (4 and 22 °C) on the recovery of the activity of the A-BC after the storage period was assessed as follows. First, several A-BC pieces underwent two iron bio-oxidation stages using 1:0.1, 1:0.2 and 1:0.3 NMV:ESA ratios (31 °C, pH 1.8, 130 rpm of orbital shaking). The A-BC pieces for each ratio were then divided into two sets and stored in wet conditions (in fresh 6K medium) at 4 °C and at 22 °C, respectively. After 15 days, the A-BC pieces were transferred to an Erlenmeyer flask containing 6K fresh medium (without further inoculation) and incubated in two consecutive bio-oxidation cycles under the same operating conditions used before storage (31 °C, pH 1.8, orbital shaking, 130 rpm).

The long-term storage (6 months) at 4 °C was also studied by repeating the abovementioned procedure. In this case, a single iron bio-oxidation stage was carried out after storage. The operating conditions used in the tests before and after storage were those selected from the results obtained in the experiments described in *Section 2.2.6.2. Effect of operating parameters on Fe²⁺ bio-oxidation.*

2.2.6.5. Biocellulose cleaning and reuse

The strategy of washing the A-BC pieces covered with jarosite for removing the precipitate and re-using the cleaned BC for subsequent bacterial immobilization procedures was tested, in order to expand the life-span of the support material and reduce both A-BC preparation time and reagent consumption.

Biocellulose pieces containing precipitated jarosite were introduced in a 50 mL Erlenmeyer flask and covered with 20 mL of 10 % w:v oxalic acid solution for 1 h (W1). Then, the oxalic medium was removed and 20 mL of fresh oxalic acid were added in two consecutive washing stages (W2-W3). The experiment was carried out at 25 °C and 150 rpm to ensure an adequate shaking speed with the objective of cleaning of the material.

Once the cleaning operation was concluded, the BC pieces were immersed in fresh 9K medium and inoculated with a 5 % v:v of *A. ferrooxidans* culture in the exponential growth phase to assess the possibility of reusing the biopolymer again as support material. Once the first bio-oxidation stage was completed, the BC pieces were re-immersed in fresh 9K medium with no further inoculation to check if the attached bacteria were able to successfully oxidize the Fe²⁺. The immobilization procedure after

washing the BC was carried out under the previously selected optimum conditions (31°C, 170 rpm, 9K medium, pH 1.8).

An additional experiment was carried out to ascertain if the microorganism were able to survive after the successive cleaning cycles with oxalic acid. Thus, the clean BC pieces were cultured in fresh 9K medium without inoculation under the same operating conditions. The progress of the Fe²⁺ oxidation was recorded as indicative of the microbial activity.

2.2.7. Comparison of BC and PVA as support materials

Once the operating conditions for preparing the active material were optimized with the BC, the same procedure was applied to the PVA hydrogel in order to compare the viability of both materials in the immobilization and subsequent Fe²⁺ bio-oxidation processes. In addition, the influence of the presence of dissolved copper (Cu²⁺) on the Fe²⁺ oxidation with A-BC and Active PVA (A-PVA) was also tested. The pieces were labelled with A-BCX and A-PVAX for BC and PVA hydrogels respectively, being X the concentration of dissolved copper.

2.2.8. Analytical methods

Iron concentration and pH were monitored throughout the process by following the procedure described in Sections 2.5 *Determination of iron species in dissolution* and 2.8 *Other methods* (materials and general methods).

For scanning electron microscopy (SEM) imaging, samples were adequately prepared following the procedure described in Section 2.7. *Scanning electron microscopy (SEM)* (materials and general methods).

The Fourier transform infrared spectrum (FTIR) was used to analyze and characterize the jarosite precipitates. It was registered using a Nicolet Nexus FTIR spectrometer with a Golden Gate (Specac) ATR sampling accessory in the range of 4000-750 cm⁻¹ (32 scans).

2.3. RESULTS

2.3.1. Selection and characterization of suitable materials for *A. ferrooxidans* immobilization

A. ferrooxidans has reportedly been immobilized on non-bio-based and bio-based support materials. Amongst the first ones, activated carbon (Ginsburg and Karamanev, 2007), glass beads (Gomez et al., 2000), polyurethane foam (Mesa et al., 2004; Jaisankar and Modak, 2009), PVA (Yujian et al., 2006), and clay tiles (Donati, 2008) can be mentioned. Regarding the bio-based materials, cotton gauze (Nie et al., 2015; Zhu et al.,

2017; Vermeulen and Nicolay, 2017), hemp fibers (Akhlaghi, 2019) and chitosan (Giaveno et al., 2008) have been used. Inorganic support materials and synthetic polymers (within the non-bio-based classification) exhibit high rigidity and chemical resistance, but they are not biocompatible, and some of them have been reported to be impractical at industrial scale (Pogliani and Donati, 2000; Yujian et al., 2006; Junfeng et al., 2007; Westman et al., 2012; Cheng et al., 2013). In recent years, the use of natural (bio-based) carriers is prevailing for biotechnological applications, as they cause fewer disposal concerns and promote the circular economy (Dzionic et al., 2016; Rodríguez et al., 2020). Nevertheless, the main disadvantages of those materials, such as poor mechanical strength and durability, need to be overcome for their implementation in full-scale processes (Yujian et al., 2006).

As far as this study is concerned biocellulose (BC), chitosan (CH), polyvinyl alcohol (PVA) and cellulose acetate (CTA) were selected to analyze and compare their suitability as support materials for *A. ferrooxidans* immobilization.

Table 2.3 shows the results obtained after applying the decision-making protocol summarized in Figure 2.9 to the selected materials.

Table 2.3. Selection of suitable materials for *A. ferrooxidans* immobilization.

Material	Material degradation	Influence on microorganism's growth	Successful bacterial immobilization	Suitable material
PVA hydrogel (PVA) ^a	No	No	Yes	<input checked="" type="checkbox"/>
Lyophilized PVA (PVA)	No	No	No	<input type="checkbox"/>
BC hydrogel (BC)	No	No	Yes	<input checked="" type="checkbox"/>
Modified CTA Membrane (M-CTA)	Yes	-	-	<input type="checkbox"/>
CTA beads (B-CTA) ^b	No	No	Yes	<input checked="" type="checkbox"/>
CH hydrogel (CH)	Yes	-	-	<input type="checkbox"/>
Lyophilized CH (L-CH)	No	Yes	No	<input type="checkbox"/>

^a10, 5 and 2.5 % w:w concentrations are included.

^bA large amount of precipitate was deposited during the immobilization process, so it was discarded for further experiments.

Two hydrogels, PVA and BC, were the only ones fulfilling all the requirements, as they allowed the effective immobilization of the bacteria while maintaining their physical integrity (Figure 2.11).

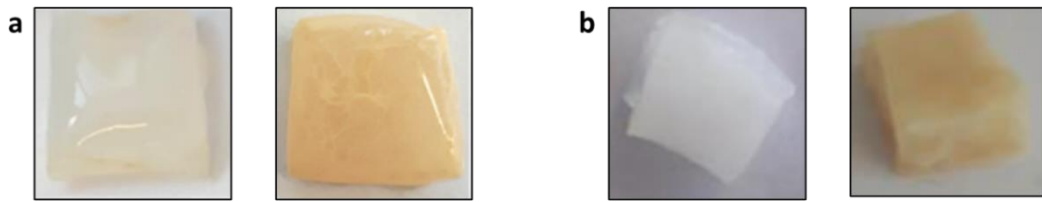


Figure 2.11. Selected support materials before (left) and after (right) being submerged in the 9K medium: BC (a) and PVA 10 % w:w (b).

On the contrary, the rest of the materials were discarded for further experiments, since they did not show adequate characteristics for this application. CH and M-CTA were affected by the 9K medium under the selected operating conditions (pH 1.8, 31 °C, 170 rpm) (Figure 2.12a-c). The degradation of L-CH took place at a longer term and thus it halted microorganism's growth in the second stage of the protocol. Regarding L-PVA, bacteria were not successfully immobilized (Figure 2.12d). Finally, it should be pointed out that even though the bacteria were successfully immobilized on B-CTA beads, a large amount of precipitate was deposited on the surface of this material (Figure 2.12e). This phenomenon could negatively affect the availability of iron in the medium and, hence, this support was also discarded for further studies.

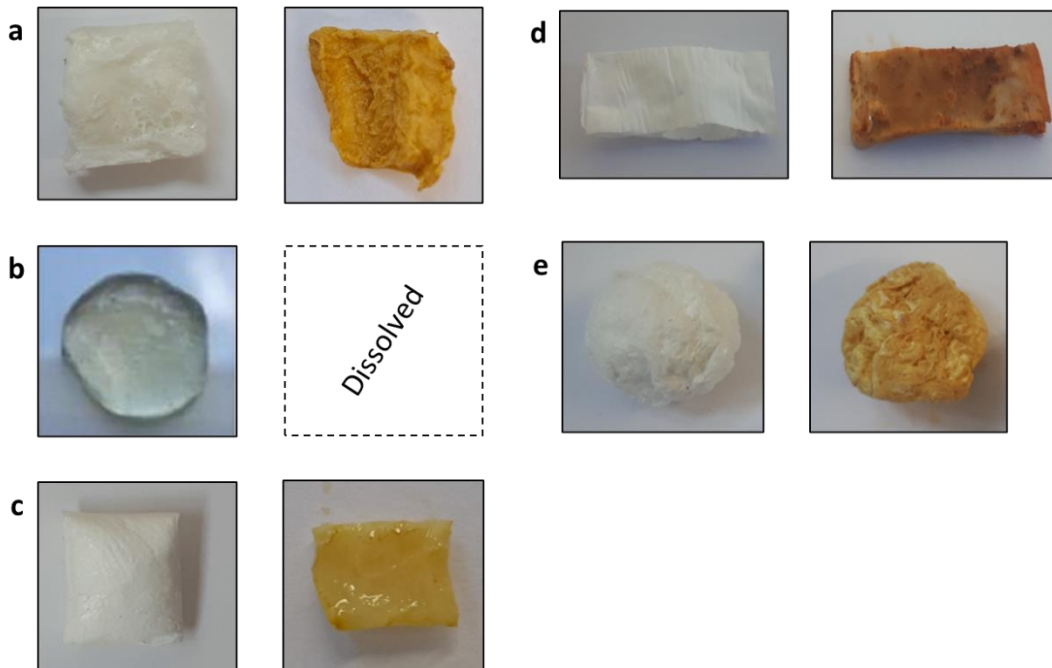


Figure 2.12. Discarded support materials before (left) and after (right) being submerged in the 9K medium: L-PVA (a), CH (b), L-CH (c), M-CTA (d) and B-CTA (e).

The morphology of selected hydrogels was studied by SEM. Figure 2.13 shows the SEM surface image of PVA hydrogels at different concentrations (2.5, 5 and 10 % w:w). As it is well-known, the final properties of PVA hydrogels can be controlled by varying both freeze thaw cycles and polymer concentration. In this study, hydrogels with three different polymer concentrations were subjected to 3 freeze-thaw cycles. At low magnification (Figure 2.13 right), only 2.5 % w:w showed a gel porosity. On the contrary, high magnification images (Figure 2.13 left) confirmed microporous internal structure for all PVA hydrogels. The effect of increasing initial PVA concentration on the pore size can be clearly observed. The smallest pores were detected for 10 % w:w hydrogel and both the pore size and porosity increased at lower PVA concentration.

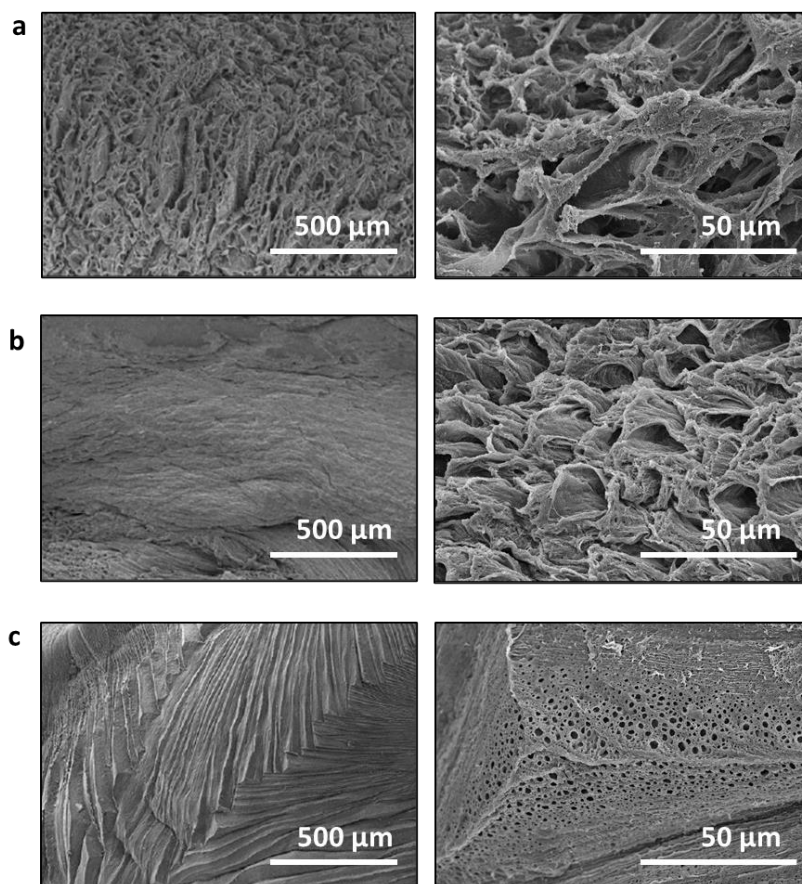


Figure 2.13. SEM image at low (right) and high magnification (right) of PVA hydrogels at different weight concentrations: 2.5 % (a), 5 % (b) and 10 % (c).

Morphology of the BC hydrogel was also investigated. BC hydrogel was characterized as a 3D network structure composed by long cellulose nanofibers (Figure 2.14a). The width of nanofibers was around 60-120 nm. The cross-sectional image of this material (Figure 2.14b) revealed a multilayer structure directly associated with the layer-by-layer growth that takes place during the bacterial cellulose biosynthesis.

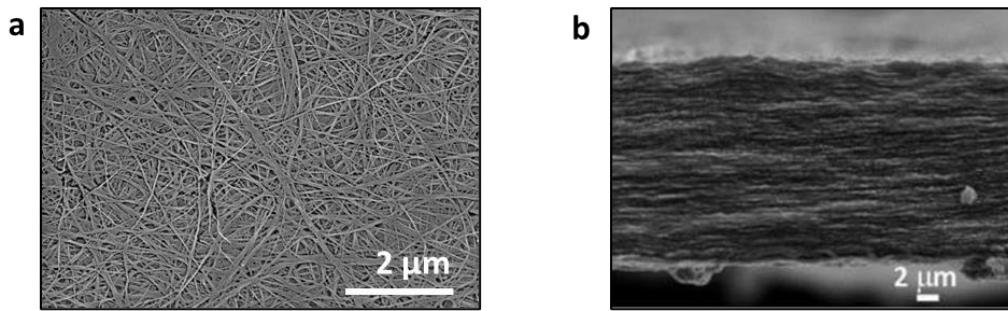


Figure 2.14. SEM images of BC top surface (a) and b) cross-section image (b).

In addition to the favorable characteristics for bacterial immobilization due to its highly porous network structure, BC is a biomaterial susceptible to sterilization and manipulation, and shows good mechanical and chemical stability (Junfeng et al., 2007; de Oliveira et al., 2021). This material is free of the lignin, hemicelluloses, and pectin normally present in plant-derived celluloses, thereby reducing the consumption of the chemicals required for cellulose purification and reducing the overall production cost and environmental impact (Azeredo et al., 2019). This combination of properties has resulted in the use of this material in many fields of application (i.e., electronics, food packaging, tissue engineering, carriers for drug delivery, enzyme immobilization, etc.) (Wu and Lia, 2008; Trovatti et al., 2011; Azeredo et al., 2019). Nevertheless, its application in bioleaching processes has not yet been reported and, thus, it was selected for further studies.

2.3.2. Selection of the inoculum percentage

The selection of the adequate amount of inoculum to be added to the medium containing the support material is crucial for the success of the immobilization procedure. If that amount is too low, the bacterial attachment is expected to be very poor. Conversely, too high values are not recommended for feasible application at industrial scale (Rastegar et al., 2015). Thus, three immobilization tests with inoculum percentages of 2 %, 5 % and 10 % v:v were carried out at 31 °C and pH 1.8, using an initial iron concentration of 6 g Fe²⁺ L⁻¹.

The results in Figure 2.15 showed that the time for the complete Fe²⁺ oxidation (as an indicative of *A. ferrooxidans* growth) decreased 10 % and 20 % when the percentage of inoculum was increased from 2 % to 5 % and to 10 %, respectively. Therefore, it was concluded that the time required to complete the Fe²⁺ biooxidation decreased as the inoculum amount was increased.

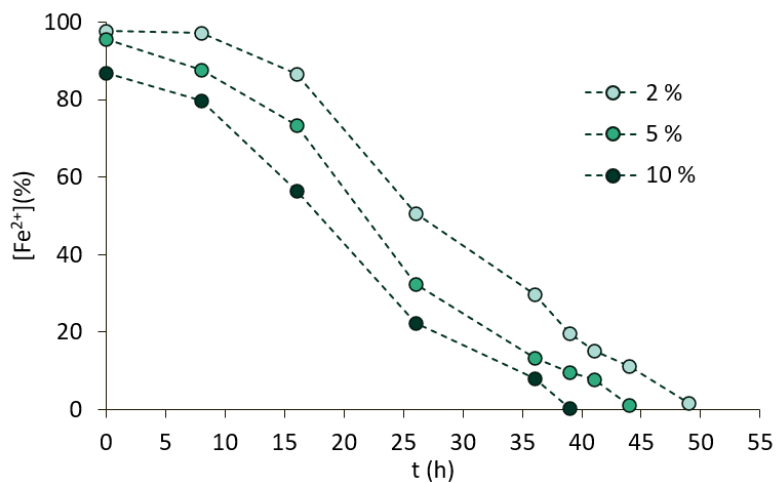


Figure 2.15. Evolution of Fe^{2+} (%) during the incubation period with 2 %, 5 %, 10 % v:v inoculum percentages.

However, although the biooxidation process was 5 hours shorter when the inoculum percentage was increased from 5 to 10 %, iron loss was more intense at high values, probably due to jarosite precipitation. Thus, 5.0 % and 3.6 % iron precipitated when 10 % and 5 % inoculum was added to the culture medium, respectively (precipitation was calculated as the difference between the initial and final total iron concentration). Thus, 5 % of inoculum percentage was selected for further studies in this work.

2.3.3. Suitability of bacterial cellulose as support material for *A. ferrooxidans* immobilization

Cellulose is the most abundant natural biopolymer on earth, and although plants are the major sources of these compounds, various bacteria are able to produce a polymer that is structurally similar to plant cellulose, albeit with superior physicochemical properties (de Oliveira et al., 2021). Even though the outstanding combination of properties of BC has resulted in its use in many fields of application, its use in bioleaching and biomachining processes has not yet been reported. Therefore, the feasibility of this material for *A. ferrooxidans* immobilization was searched.

2.3.3.1. Preparation of the Active Bacterial Cellulose

The distinctive multilayer crosslinked 3D network of BC fibers observed by SEM (Figure 2.16a) conferred this hydrogel a highly porous structure for cell attachment. Its biosynthesis in the laboratory allowed selecting the desired thickness, which in this study was 0.7-0.8 mm.

Once the BC pieces were immersed in the inoculated solution for A-BC preparation, the material changed color from white to reddish due to Fe^{3+} formation, and an inorganic

precipitate was observed on the material's surface by SEM analysis (Figure 2.16b). This deposit of jarosite has often been reported to precipitate in this medium and to be an effective adsorbent for bacteria, contributing to biofilm formation (Pogliani and Donati, 2000; Junfeng et al., 2007; Chowdhury and Ojumu, 2014). Bearing in mind that several authors have proposed that the bacteria are first wrapped by EPS and then embedded in aggregates of deposited jarosite, the visualization of individual cells by SEM photograph could be hindered by the deposit (Harneit et al., 2006, Lei et al., 2009; Africa et al., 2010, Mulopo and Schaefer, 2015). Pogliani and Donati (2000) observed that bacterial populations immobilized by jarosite precipitation were not easily leached, indicating the biofilm's strong attachment to the deposit.

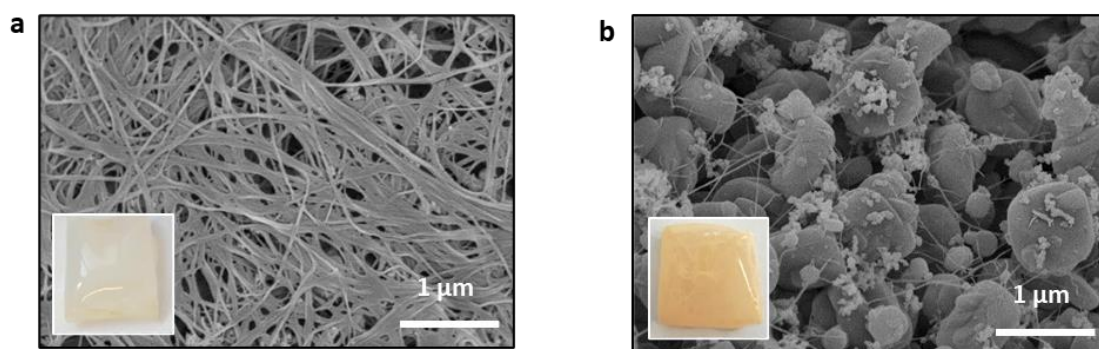


Figure 2.16. Picture and SEM photograph of the pretreated biocellulose (a) and the surface of the biologically active bacterial cellulose (A-BC) obtained after the immobilization protocol (b).

Under the low-demanding operating conditions selected for the preparation of A-BC, the bacteria required 79 h and 97 h for the complete bio-oxidation of 6 and 9 g Fe²⁺ L⁻¹, respectively. *A. ferrooxidans* immobilization on different solid supports has already been studied by other authors in order to increase the bio-oxidation rates of Fe²⁺ during the metal removal processes. Although the accurate comparison of the performance of the BC with other support materials reported in the literature is not feasible due to the influence of the bacterial strain and particular operating conditions, Table 2.4 summarizes the results reported for several *A. ferrooxidans* strains immobilization under similar pH and temperature conditions. Fe²⁺ oxidation occurred faster during bacterial immobilization on BC than when using non-biobased materials such as nickel alloy fiber (Gomez et al., 2000) and monolithic particles (Kahrizi et al., 2008). For example, the time needed for 95 % conversion in the reactors containing 6 g Fe²⁺ L⁻¹ was slightly lower than that reported by Kahrizi et al. (2008) for a similar initial Fe²⁺ concentration (6.7 g Fe²⁺ L⁻¹) when immobilizing *A. ferrooxidans* DSM 584 in a monolithic reactor using a twofold higher inoculum percentage (Table 2.4). These authors have reported that it took 72 h to convert 95 % of the initial Fe²⁺ concentration, which is 7 % longer than that needed

in this study for the same iron conversion (62 h). BC also recorded a better performance during immobilization when compared to sulfonated polystyrene-divinylbenzene copolymer (SlufSDVB), sulfonated polystyrene-divinylbenzene copolymer with granular activated carbon (SulfSCVB-GAC), and polyurethane foam (PUF) (Koseoglu-Imer and Keskinler, 2013). Thus, the time needed to fully convert the Fe^{2+} was three to four times shorter despite this study's higher iron concentration (6 and 9 vs 5 $\text{g Fe}^{2+} \text{ L}^{-1}$), lower inoculum percentage (5 % vs 10 %), and lower temperature (30 °C vs 35 °C) (Koseoglu-Imer and Keskinler, 2013).

Table 2.4. Time required for the bio-oxidation of the Fe^{2+} during the immobilization of *A. ferrooxidans* on different support materials (pH = 1.6-2.0 and T = 30-31 °C).

Support material	<i>A. ferrooxidans</i> strain	Time (h)	$[\text{Fe}^{2+}]_0$ (g L^{-1})	Conversion ^a (%)	Reference
Nickel alloy fibre	Isolated from Rio Tinto mines ^b	65 ^c	2	100	(Gomez et al., 2000)
Hemp fibres	PTCC 1646	34	5	80-90	(Akhlaghi, 2019)
Monolithic particles	DSM 584	72 ^c	6.7	95	(Kahrizi et al., 2008)
Chitosan beads	DSM 11477	58	9	100	(Giaveno et al., 2008)
Cotton gauze	CCTCC M2013102 ^d	48	9	100	(Zhu et al., 2017)
Activated carbon		56 ^c			
Zeolite		56 ^c			
Biocellulose	DSM 14882	79	6	100	This study
		97	9		

^aPercentage of initial Fe^{2+} converted to Fe^{3+} when the experiment was considered to be completed.

^bThe strain has the same properties and characteristics as NCIMB 9490.

^cGraphically inferred.

^dIsolated from acid mine drainage collected from a local pyrite mine in Guangdong, People's Republic of China.

After the bacterial immobilization procedure, and despite the acidic pH and orbital shaking, the material maintained its physical integrity, which was attributed to the outstanding mechanical properties conferred by its 3D network structure and morphology (Tercjak et al., 2015; de Oliveira et al., 2021). Therefore, BC proved to be a suitable material for the immobilization of *A. ferrooxidans*.

2.3.3.2. Effect of operating parameters on Fe^{2+} bio-oxidation

2.3.3.2.1. Shaking mode

The shaking of the bacterial suspended cultures has a positive impact on growth rate, as it provides better aeration and higher availability of oxygen and nutrients (Juergensmeyer et al., 2007). Two shaking systems can be used: linear reciprocal movement or orbital movement, being the latter one more widely used (Klöckner and Büchs, 2012). In this study, both shaking modes were compared and, as a result, the bio-oxidation time needed for the complete oxidation of $6\text{ Fe}^{2+}\text{ L}^{-1}$ by A-BC in a NMV:ESA 1:0.2 ratio was found to decrease a 40 % when the reactors were shaken using the orbital mode in contrast to the horizontal shaking ($43.5\pm 0.7\text{ h}$ vs. $73.0\pm 4.2\text{ h}$). Therefore, the orbital shaking mode was selected for further studies.

2.3.3.2.2. Nutrient medium volume (mL) to external surface area (cm^2) ratio

Bacterial density plays a crucial role in the bioleaching and biomachining processes since it determines ferric iron productivity and, hence, bio-oxidation time (Jaisankar and Modak, 2009; Zhu et al., 2017). Therefore, increasing the amount of active material inside the reactor will obviously reduce the time necessary for the complete Fe^{2+} oxidation. Nevertheless, according to Jaisankar and Modak (2009), different NMV:ESA ratios could lead to different patterns of material-media contact, which could affect ferric iron productivity (Fe^{3+} produced per medium volume and time). Therefore, the influence of the amount of A-BC on Fe^{2+} bio-oxidation was analyzed by increasing the NMV:ESA ($mL:cm^2$) ratio. Figure 2.17 (left axis) shows the time required by the A-BC to oxidize $6\text{ g Fe}^{2+}\text{ L}^{-1}$ in two consecutive bio-oxidation stages (S1 and S2) using different NMV:ESA ($mL:cm^2$) ratios. The time recorded when using the cell suspension culture (control) and the average Fe^{3+} productivity (right axis) for each ratio are also shown.

When comparing the time recorded for the complete Fe^{2+} bio-oxidation in A-BC preparation step and A-BC bio-oxidation stages (S1-S2) for the same NMV:ESA ratio ($1:0.2\text{ mL:cm}^2$), it was concluded that the process was significantly shorter in the latter case, as it was reduced almost to a half (45 % reduction). Junfeng et al. (2007) observed the same reduction percentage between bacterial immobilization on ceramic beads and the first bio-oxidation stage using the active material. The behavior is also in agreement with the results obtained when using *A. ferrooxidans* (DSM 584) immobilized on a monolithic reactor by Kahrizi et al. (2008), who reported a 33 % reduction of the bio-oxidation time in the second and third batch cultures compared to the time needed during the immobilization step. Similarly, Akhlaghi (2019) reported a 38 % reduction of this parameter when using hemp fibers as immobilization material.

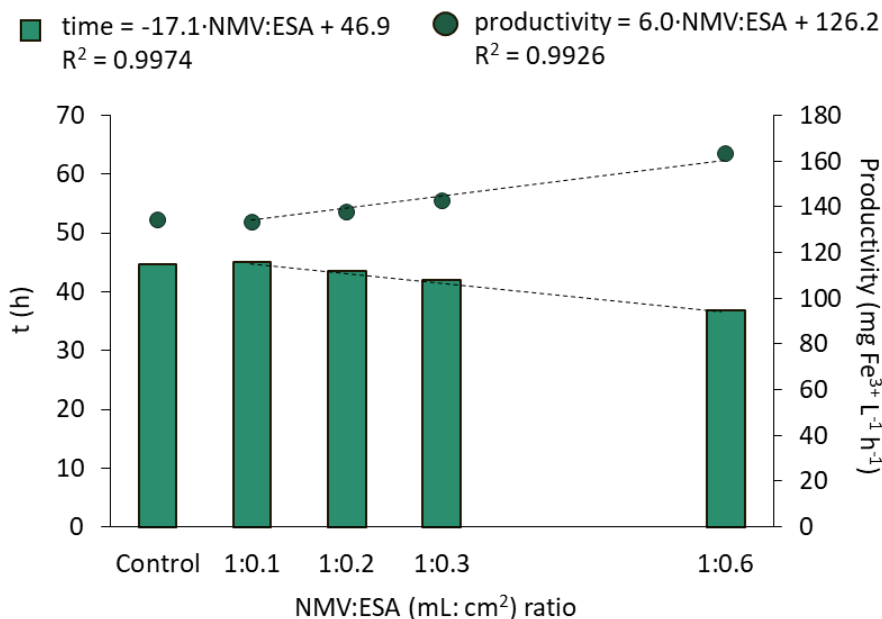


Figure 2.17. Average time required for the complete Fe^{2+} bio-oxidation in two consecutive stages (left axis) and average Fe^{3+} productivity (right axis) for different NMV:ESA (mL:cm²) ratios when using A-BC pieces.

When comparing the time recorded for the complete Fe^{2+} bio-oxidation in A-BC preparation step and A-BC bio-oxidation stages (S1-S2) for the same NMV:ESA ratio (1:0.2 mL:cm²), it was concluded that the process was significantly shorter in the latter case, as it was reduced almost to a half (45 % reduction). Junfeng et al. (2007) observed the same reduction percentage between bacterial immobilization on ceramic beads and the first bio-oxidation stage using the active material. The behavior is also in agreement with the results obtained when using *A. ferrooxidans* (DSM 584) immobilized on a monolithic reactor by Kahrizi et al. (2008), who reported a 33 % reduction of the bio-oxidation time in the second and third batch cultures compared to the time needed during the immobilization step. Similarly, Akhlaghi (2019) reported a 38 % reduction of this parameter when using hemp fibers as immobilization material.

It is noteworthy that there were not significant differences between the bio-oxidizing time for S1 and S2 at each NMV:ESA ratio (individual data not shown), and thus only average results are plotted in Figure 2.17. A similar finding was observed by other authors, who reported constant bio-oxidation times after the first immobilization batch on support materials such as cotton gauze (Nie et al., 2015) or nickel alloy fiber (Gomez et al., 2000).

Conversely, the NMV:ESA ratio influenced the Fe^{2+} bio-oxidation time. In this study, the time required for full Fe^{2+} conversion at a 1:0.1 NMV:ESA ratio was similar to that achieved when cells were grown in suspension (5 % v:v of inoculum). By contrast, this

parameter decreased linearly with the A-BC loading for a selected nutrient medium volume (Figure 2.17), which was attributed to a higher initial cell density. In general terms, there was a 19 % reduction in the time required for the complete Fe^{2+} bio-oxidation between the reactors with a 1:0.6 and a 1:0.1 NMV:ESA ratio. This difference between samples was more significant when comparing the percentage of Fe^{2+} converted during the process. For example, after 33 h, the sample with a 1:0.6 NMV:ESA ratio reached a 90 % Fe^{2+} conversion while only the 60 % was transformed in the case of the 1:0.1 relationship in the same period. The average Fe^{3+} productivity increased with the NMV:ESA ratio. These results are in agreement with those presented by Jaisankar and Modak (2009), who also reported that lower (media volume):(support material) ratios require longer times for complete iron oxidation and render lower productivities when using biologically active polyurethane foam pieces (BAPUF). By contrast, Pogliani and Donati (2000) found that average Fe^{3+} productivity was very similar for cultures with densities of glass beads of 1, 5, 10 and 15 %, which was attributed to low amounts of bacteria attached to the glass beads.

The results obtained in this experiment led to the conclusion that the highest NMV:ESA ratio tested (1:0.6) was the most favorable when using A-BC for *A. ferrooxidans* immobilization, as the time for Fe^{2+} bio-oxidation was significantly reduced and the average productivity increased compared to samples with lower NMV:ESA ratios and cell suspension cultures (control). Additionally, the suspension of A-BC in the media was uniform and the system was adequately shaken. Higher ratios were discarded because more active material pieces in the medium volume might have adverse effects, such as the difficulty for effective shaking or the excessive loss of iron (precipitated as jarosite) on the material's surface. Therefore, 1:0.6 NMV:ESA ratio was selected for further experiments.

2.3.3.2.3. Fe^{2+} concentration

Besides facilitating biomass handling and reducing iron bio-oxidation time, the use of A-BC can enhance the metal removal process performance if higher iron concentrations are bio-oxidized in shorter treatment times (compared to cell suspension cultures). Thus, in this study the influence of Fe^{2+} concentration (6 vs. 9 $\text{g Fe}^{2+} \text{ L}^{-1}$) in the bio-oxidation time required by A-BC was studied using the selected NMV:ESA ratio (1:0.6 mL:cm^2). Higher iron concentrations were not studied as they can exert an inhibitory effect on the activity of immobilized *A. ferrooxidans*, as concluded by Junfeng et al. (2007) and Jaisankar and Modak (2009).

The time required by A-BC for the complete bio-oxidation of Fe^{2+} remained almost constant in two successive stages in the presence of 6 (36.8 ± 1.6 h) and 9 $\text{g Fe}^{2+} \text{ L}^{-1}$ (47.0 ± 1.7 h) (calculated as the average value for two consecutive stages). Conversely,

oxidation time decreased 18 % and 28 % for the 6K and 9K media, respectively, in comparison to the cell suspension mode. In addition, the highest Fe^{3+} average productivity was recorded in the samples with 9K medium ($190 \text{ mg Fe}^{3+} \text{ L}^{-1} \text{ h}^{-1}$), being this value a 16 % and 39 % higher than that obtained in the samples with 6K medium ($163 \text{ mg Fe}^{3+} \text{ L}^{-1} \text{ h}^{-1}$) and the 9K control ($136 \text{ mg Fe}^{3+} \text{ L}^{-1} \text{ h}^{-1}$), respectively.

The use of A-BC in a 1:0.6 NMV:ESA ratio was especially recommended for an initial concentration of $9 \text{ g Fe}^{2+} \text{ L}^{-1}$, as the bio-oxidation time was reduced and Fe^{3+} productivity was increased compared to cell suspension growth using the same initial Fe^{2+} concentration. In addition, Fe^{3+} productivity was higher than that recorded with A-BC in the 6K medium, which means that a higher amount of the oxidant would readily become available in the medium. It could lead to a higher metal removal rate in any bioleaching and biomachining process, being of great interest for future industrial applications.

2.3.3.2.4. Shaking speed

Many authors have demonstrated the influence of shaking speed in bacterial activity during bioleaching and biomachining processes (Ting et al., 2000; Jadhav et al., 2013; Xenofontos et al., 2015; Singh et al., 2018; Chakankar et al., 2019). However, scarce data have been reported about the influence of this parameter on bacterial immobilization and on the time needed by the active material for Fe^{2+} bio-oxidation in subsequent stages. In this study two shaking speeds were tested at the optimum operating conditions (NMV:ESA ratio = 1:0.6, $[\text{Fe}^{2+}] = 9 \text{ g L}^{-1}$): 130 and 170 rpm. Higher shaking speed values were not evaluated since excessively vigorous shaking could damage the integrity of the material and, therefore, reduce the lifespan of A-BC.

In this study, A-BC preparation time significantly decreased from 63.7 ± 2.3 to 44 ± 0.1 h when the shaking speed was increased from 130 to 170 rpm (Table 2.5). This result was attributed to a more efficient oxygenation and contact between the support material and the culture medium. As far as biobased materials are concerned, Giaveno et al. (2008) have reported a Fe^{2+} bio-oxidation time of 60 h (graphically inferred) in the first colonization stage of *A. ferrooxidans* DSM11477 on cross-linked chitosan beads at 180 rpm ($9 \text{ g Fe}^{2+} \text{ L}^{-1}$, $30 \text{ }^\circ\text{C}$, $\text{pH} = 1.8$). When cotton gauze was used, it took 48 h to successfully immobilize *A. ferrooxidans* CCTCC M2013102 at 165 rpm ($9 \text{ g Fe}^{2+} \text{ L}^{-1}$, $30 \text{ }^\circ\text{C}$, $\text{pH} = 2.0$). Zhu et al. (2017) have concluded that this support material needed a shorter immobilization time than zeolite and activated carbon because the biocompatibility and biosorption capacity of cellulose favored the process (Zhu et al., 2017). Thus, the lower oxidation times shown in Table 2.5 could be attributed to the structural and particular properties of BC in comparison with plant cellulose (de Oliveira et al., 2021). After bacterial immobilization, the Fe^{2+} bio-oxidation time decreased compared to the A-BC

preparation step, probably due to the formation of a denser biofilm during the first bio-oxidation stage (Table 2.5).

Table 2.5. Influence of shaking speed on bio-oxidation time during both A-BC preparation and A-BC use in two consecutive stages.

Shaking speed (rpm)	Fe ²⁺ bio-oxidation time (h)	
	preparation	use
130	63.7±2.3	47.5±2.0
170	44.0±0.1	40.0±0.6

The advantageous results and the fact that material integrity was not affected during the experiments at 170 rpm supported the selection of this shaking speed for further experiments.

2.3.3.3. Influence of dissolved copper concentration on bacterial immobilization and subsequent iron bio-oxidation stages

Several studies have reported that the inhibitory effect of dissolved copper in the medium varies between unadapted and adapted bacteria, as well as among *A. ferrooxidans* strains (Liang et al., 2010; Martinez-Bussenius et al., 2016; Liang et al., 2018). In this study, the influence of dissolved copper on *A. ferrooxidans* activity was studied during the A-BC preparation and the subsequent bio-oxidation stages (S1-S4) under the previously selected operating conditions (1:0.6 NMV:ESA ratio, 9 g Fe²⁺ L⁻¹, 170 rpm orbital shaking).

The active material was prepared in several bioreactors in the presence of different copper concentrations ranging from 5 to 20 g Cu²⁺ L⁻¹. The absence of dissolved copper was used as the control sample.

The time required for the complete bio-oxidation during the immobilization period increased linearly ($R^2 = 0.9839$) as the dissolved copper concentration increased from 5 to 20 g Cu²⁺ L⁻¹ (Figure 2.18). Thus, the bio-oxidation time in the presence of 20 g Cu²⁺ L⁻¹ was 3.1-fold longer than for the control sample during bacterial immobilization stage.

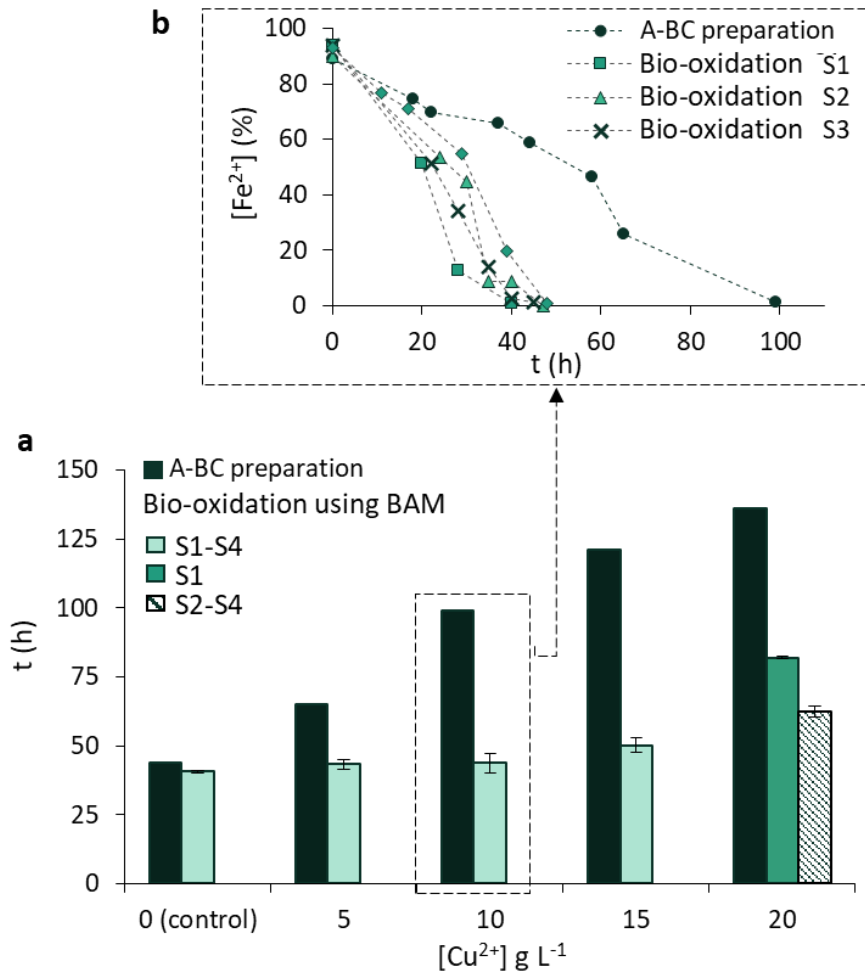


Figure 2.18. Fe^{2+} bio-oxidation time during A-BC preparation and subsequent bio-oxidation stages at different Cu^{2+} concentrations (a) and evolution of Fe^{2+} concentration in the reactor with $[Cu^{2+}] = 10 g L^{-1}$ (b).

It is noteworthy that when the same A-BC pieces were used for four consecutive bio-oxidation stages (S1-S4) the average process time decreased considerably compared to the A-BC preparation time (Figure 2.18), which was attributed to bacterial adaptation to the metal. Slight variations were recorded among the A-BC5, A-BC10 and A-BC15 samples, and the average value (46.4 ± 4.3 h) was only 14 % higher than that recorded in the copper-free sample (control sample). Another salient result obtained in these samples is that the bio-oxidation time for the four cycles was very similar in all cases, as shown in upper Figure 2.18 for the concentration of $10 g Cu^{2+} L^{-1}$ as a representative example.

As far as the results for the A-BC sample with $20 g Cu^{2+} L^{-1}$ are concerned, the time for complete Fe^{2+} bio-oxidation gradually decreased until 64 % reduction was recorded in stages S2-S4, compared to the A-BC preparation step (Figure 2.18). This response was attributed to the activity inhibition that might be due to the presence of $20 g Cu^{2+} L^{-1}$.

Bacterial inactivation was even more severe in the presence of 30 and 40 g $\text{Cu}^{2+} \text{L}^{-1}$, as the amount of oxidized Fe^{2+} during BAM30 and BAM40 preparation was only 30 % after a prolonged period of 140 h (when the experiment was concluded).

Figure 2.19 shows the aspect of the culture medium with A-BC before and after Fe^{2+} bio-oxidation in the presence of different concentrations of dissolved copper (0-20 g $\text{Cu}^{2+} \text{L}^{-1}$).

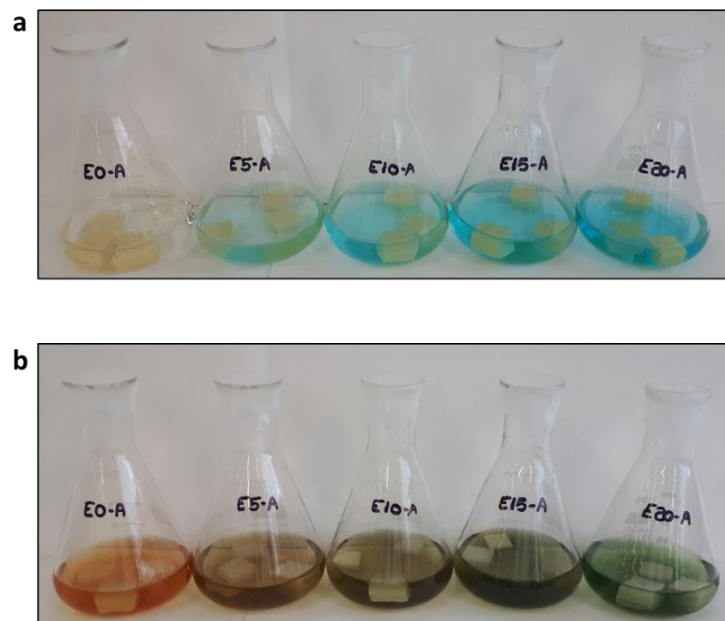


Figure 2.19. Reactors with A-BC before (a) and after (b) Fe^{2+} bio-oxidation in the presence of different concentrations of dissolved copper (0-20 g $\text{Cu}^{2+} \text{L}^{-1}$).

Based on the promising results with the A-BC samples, the ability of immobilized *A. ferrooxidans* to adapt to the presence of even higher concentrations of dissolved copper was explored by exposing the sample A-BC15 to Cu^{2+} concentrations up to 30 g $\text{Cu}^{2+} \text{L}^{-1}$ in several consecutive bio-oxidation steps.

Thus, bacterial resistance and adaptation were verified when the A-BC15 sample was finally able to successfully oxidize all the Fe^{2+} in the presence of 30 g $\text{Cu}^{2+} \text{L}^{-1}$ in 89.0 ± 1.0 h (Table 2.6). Although the bio-oxidation time increased with the dissolved copper concentration (time = $7.5 \cdot [\text{Cu}^{2+}] + 66.2$, $R^2 = 0.9941$, $[\text{Cu}^{2+}]$ range = 20-30 g $\text{Cu}^{2+} \text{L}^{-1}$), the values were significantly lower than those obtained in the A-BC preparation step using unadapted bacteria in the presence of 20 g $\text{Cu}^{2+} \text{L}^{-1}$. These results are consistent with those reported by Liang et al. (2018), who have concluded that adapted *A. ferrooxidans* has a relatively higher Fe^{2+} oxidation rate during the process than unadapted bacteria.

Table 2.6. Fe²⁺ bio-oxidation time of sample A-BC15 when exposed to higher dissolved copper concentrations.

Stage	[Cu ²⁺] (g L ⁻¹)	Fe ²⁺ bio-oxidation time (h)
Immobilization	15	121.0±0.5
S1-S4	15	50.3±2.8
S5-S7	20	74.0±3.6
S8	25	80.5±0.5
S9	30	89.0±1.0

The inhibitory copper concentration achieved in this study for *A. ferrooxidans* DSM 14882 is higher or similar to those reported in literature for other strains. For example, Mykytchuk et al. (2011) obtained that the copper tolerance for six *A. ferrooxidans* strains cultivated in suspension ranged from 0.3 to 9.5 g Cu²⁺ L⁻¹. Similarly, Orellana and Jerez (2011) reported that a 50 % inhibition of growth was registered when unadapted ATCC23270 cells were grown in 0.6 g Cu²⁺ L⁻¹ and, conversely, an equivalent percentage of inhibition was observed for ATCC53993 at a concentration of 6.5 g Cu²⁺ L⁻¹. Additionally, Oetiker et al. (2018) reported that strain ATCC 53993 still actively expressed the proteins related to the RND efflux systems at 12.7 g Cu²⁺ L⁻¹. Higher inhibitory concentrations were achieved by Novo et al. (2000) who reported an oxygen uptake inhibition in the 40-80 % range for eight *A. ferrooxidans* strains cultivated in the presence of 25.4 g Cu²⁺ L⁻¹.

2.3.3.4. Material integrity

The maintenance of the material's physical integrity after successive bio-oxidation stages is crucial to ensure process efficiency and avoid issues in its long-term use. Conventionally, bio-based support materials have a shorter lifespan and deteriorate more easily than inorganic ones in biological systems (Lebrero et al., 2014). Nevertheless, they have the advantage of being biodegradable, which contributes to the process sustainability and waste reduction. In this study, the material maintained its physical integrity (corroborated by visual inspection) despite being subjected to extreme acidic conditions (pH 1.8) and vigorous shaking (170 rpm) during several successive stages.

During the process, a precipitate appeared on the surface of the A-BC (Figure 2.20a), which was identified as jarosite by FTIR analysis according to the most distinctive bands in the FTIR spectrum (Figure 2.20b) (Giaveno et al., 2008). Zhu et al. (2017) have

reported that different carriers have different effects on the adsorption of this precipitate. Figure 2.20c (right) shows that when the cells were grown in suspension, the jarosite adhered to the Erlenmeyer walls, but in the presence of A-BC pieces, it was adsorbed on the surface of the support material. Cotton gauze reportedly had the same ability to retain this precipitate, probably due to its similar nature (Zhu et al., 2017). Nevertheless, jarosite precipitation should be controlled by pH adjustment to avoid the loss of iron (oxidant) in the leaching solution, despite its positive effect on biofilm formation.

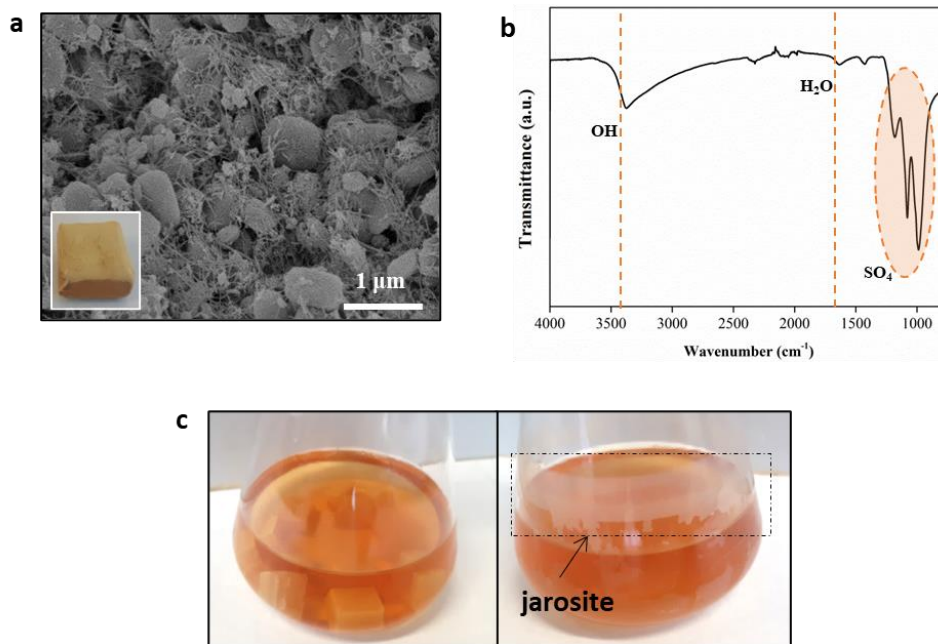


Figure 2.20. Picture and SEM photograph of A-BC after several bio-oxidation stages (a), FTIR analysis of the jarosite (b), and two Erlenmeyers with A-BC pieces and suspended cells respectively (c).

The optimum operating conditions for the successful *A. ferrooxidans* immobilization on BC and the successful use of A-BC pieces are summarized in Table 2.7.

Table 2.7. Optimum operating conditions for A-BC preparation and use.

Parameter	Shaking mode and speed (rpm)	NMV:ESA ratio (mL:cm ²)	[Fe ²⁺] (g L ⁻¹)
Optimum value	Orbital, 170 rpm	1:0.6	9

2.3.3.5. Influence of BAMs storage on bacterial activity

Industrial activity may require stopping and restarting the reactors due to changes in the operation procedure, scheduled or unexpected shutdowns, cleaning, etc. Therefore, the

storage of the immobilized bacteria may be of great interest for shortening the re-start operation (Donati, 2008; Jaisankar and Modak, 2009). In this study, the influence of storage temperature on A-BC reactivation was studied.

The A-BC pieces recovered their oxidizing activity very rapidly after 15 days of storage, regardless of the temperature, and this activity remained practically constant in all the samples in two consecutive Fe^{2+} oxidation stages (Table 2.8). This behavior is consistent with the results reported by other authors studying different support materials (Gomez et al., 2000; Donati, 2008; Akhlaghi, 2019), and it has been attributed to the wet storage mode, as bacteria use carbon dioxide and other vital nutrients available in the liquid medium for their survival (Jaisankar and Modak, 2009; Akhlaghi, 2019).

Table 2.8. Fe^{2+} oxidation time required by A-BC after 15 days of storage (average of two successive bio-oxidation cycles).

NMV:ESA ratio (mL:cm ²)	Fe^{2+} bio-oxidation time (h)		
	Before storage	After 15 days at 4 °C	After 15 days at 22 °C
1:0.1	45.0±1.4	50.5±3.5	51.0±7.1
1:0.2	43.5±0.7	43.5±0.7	49.5±2.1
1:0.3	42.0±1.8	40.5±0.7	41.5±2.1

In addition, after being 6 months stored at 4 °C, the A-BC pieces were able to recover their activity. The active material required 51 % more time to completely bio-oxidize the iron compared to the time required before storage (40 h vs. 82 h). Nevertheless, the long-term storage of the A-BC could have operational benefits, such as the reduction of the total time for re-starting the reactor (no need of BC fabrication and immobilization).

The results achieved in this study confirm that the bacteria maintained their oxidative capacity during storage (Donati, 2008; Jaisankar and Modak, 2009), which is of great interest for industrial applications where the installation/process could be temporarily halted.

2.3.3.6. Reuse of BC as support material after washing

Massive jarosite precipitation is an undesired effect that can impair bacterial activity and inactivate the active support material. Thus, the removal of the jarosite precipitated on the surface of A-BC pieces may allow the reuse of this material in latter bacterial immobilization processes, avoiding the use of freshly synthesized BC. This would

contribute to extend the lifespan of the BC as support material and, thus, to the sustainability of the process.

After three washing cycles employing oxalic acid 10 % w:v, the progressive color change of the A-BC pieces revealed the removal of jarosite from the biopolymer (Figure 2.21a-d).

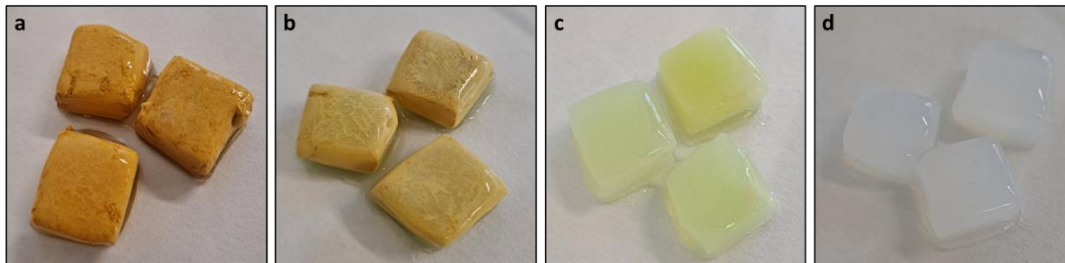


Figure 2.21. BC pieces after use in the iron oxidation process but before washing with oxalic acid (a) and after W1 (b), W2 (c) and W3 (d) washing cycles, respectively.

Once the BC pieces were cleaned, it took almost 10 days for the remaining bacteria to oxidize Fe^{2+} (the medium was not reinoculated). Nevertheless, when cells were inoculated, the cleaned BC pieces were able to immobilize bacteria again as the iron bio-oxidation time required by the newly prepared A-BC pieces was 46 h. This time was only 4.3% higher than that achieved when using A-BC obtained from fresh BC.

In summary, this acid washing not only removed the jarosite precipitate but also destroyed the biomass. Nevertheless, it rendered a “clean” material that could be reused and reinoculated, prolonging its lifespan. Thus, the viability of reusing this hydrogel for *A. ferrooxidans* immobilization after jarosite removal by a cleaning process with oxalic acid was demonstrated.

2.3.4. Comparison of BC and PVA as support material

The rate of the biological Fe^{2+} oxidation depends on several factors (bacterial strain, support material, operating conditions, etc.) and, hence, the accurate comparison of the results achieved when using the BC with those reported in the literature for other support materials is not feasible. Thus, a series of tests were carried out using PVA hydrogel (2.5, 5 and 10 % w:v), the second suitable material selected in Section 2.3.1 *Selection and characterization of suitable materials for A. ferrooxidans immobilization*, under the optimum operating conditions set for the BC (1:0.6 NMV:ESA ratio, 9 g Fe^{2+} L⁻¹, 170 rpm orbital shaking).

A. ferrooxidans bacteria were successfully immobilized on both hydrogels (BC and PVA), as two bio-oxidation stages (S1 and S2) were satisfactorily carried out using the active materials in the absence of further microbial inoculation (Figure 2.22).

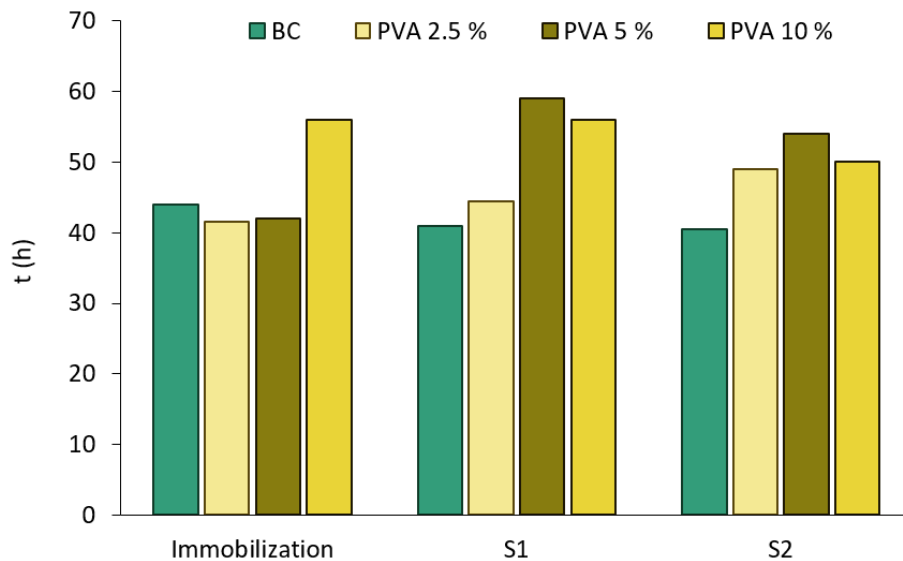


Figure 2.22. Fe^{2+} bio-oxidation time during BAM (BC and 2.5, 5 and 10 % PVA) preparation and subsequent bio-oxidation stages (S1 and S2).

Regarding the immobilization stage, the time needed for the complete iron oxidation when using BC and 2.5 and 5 % PVA varied very slightly (42-44 h), and this value was ~ 20 % higher when using 10 % PVA. The microbial activity in this stage rendered an increasing concentration of Fe^{3+} in the solution, which was responsible for the materials changing color from bright white to brown/yellowish (Figure 2.23).

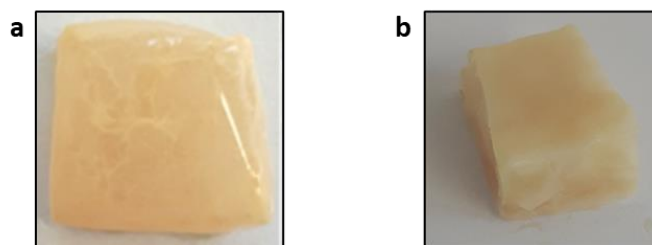


Figure 2.23. Biologically active materials after the immobilization procedure: A-BC (a) and 10 % A-PVA (b).

Two different behaviors were also registered for the successive oxidation stages (S1 and S2) when using A-PVA (Figure 2.22). As far as 10 % A-PVA is concerned, it was concluded that there were not significant differences between the oxidation time for S1 and S2, in accordance with the results obtained when using BC (Figure 2.22). However, the Fe^{2+} bio-oxidation rate was faster with A-BC than with 10 % A-PVA, which was attributed to its 3D network structure which favored cell immobilization. Conversely, the iron oxidation rate slowed down as the number of stages increased when 2.5 % and 5 % A-PVA were used. This behavior was attributed to the difference in the structure of the

materials, as the smaller pores generated in the 10 % PVA could allow the generation of a more stable biofilm (greater adhesion of the cells) compared to 2.5 and 5 % PVA materials. On the contrary, the bigger pores observed in the 2.5 and 5 % PVA samples could have resulted in the washing of microorganisms between successive oxidation stages and, therefore, these materials were discarded for its further use. Figure 2.24 shows the Biologically active materials, A-BC and A-PVA (2.5, 5 and 10 % w:w), after successive Fe^{2+} oxidation stages.

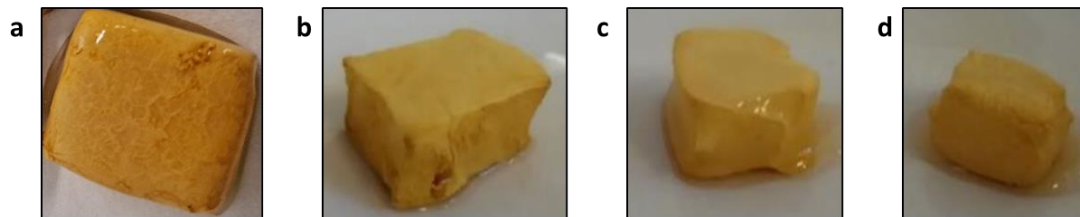


Figure 2.24. Biologically active materials after successive Fe^{2+} oxidation stages: A-BC (a), 10 % A-PVA (b), 5 % A-PVA (c) and 2.5 % A-PVA (d).

The 2.5, 5 and 10 % PVA samples exhibited better results than those obtained by Long et al. (2004) who have immobilized *A. ferrooxidans* by PVA–boric acid method. These authors reported that long time (7 days) was necessary for the first iron oxidation cycle, then decreasing to 72 and 48 h for the second and third oxidation cycles, respectively. Furthermore, problems associated with this method have been reported, such as the toxicity of saturated boric acid, which is difficult to remove and the agglomeration of the PVA beads (Lozinsky and Plieva, 1998; Yujian et al., 2006). Yujian et al. (2007) found a decrease in bacterial activity, which they attributed to the possible toxicity of saturated boric acid to microorganisms. Although the latter one can be avoided by adding sodium alginate (Yujian et al., 2007; Idris et al., 2008; Zain et al., 2011), this techniques are still less cleaner and sustainable than the method presented in this work to obtain the PVA hydrogel. The iterative freeze-thaw technique provides the possibility to cross-link an aqueous solution of PVA without leaving chemical remnant in the gel matrix (El-Naas et al., 2013).

The influence of dissolved copper on iron bio-oxidation time when using A-BC and 10 % A-PVA is shown in Figure 2.25a. All the 10 % A-PVA samples required longer times for the complete iron transformation in the presence of dissolved copper than in its absence (control), regardless of copper concentration. It is noteworthy that this value remained almost constant (70.6 ± 3.1 h) in the samples containing 5-15 $\text{g Cu}^{2+} \text{ L}^{-1}$. However, it was considerably longer than that obtained when employing A-BC under the same operating conditions (46.4 ± 4.3 h). The highest copper concentration tested (20 $\text{Cu}^{2+} \text{ L}^{-1}$) had a negative influence on the activity of both 10 % A-PVA and A-BC, as the time needed for the complete iron bio-oxidation increased markedly in both cases. The variation in Fe^{3+}

concentration with time for the control sample is plotted in Figure 2.25b as a representative example.

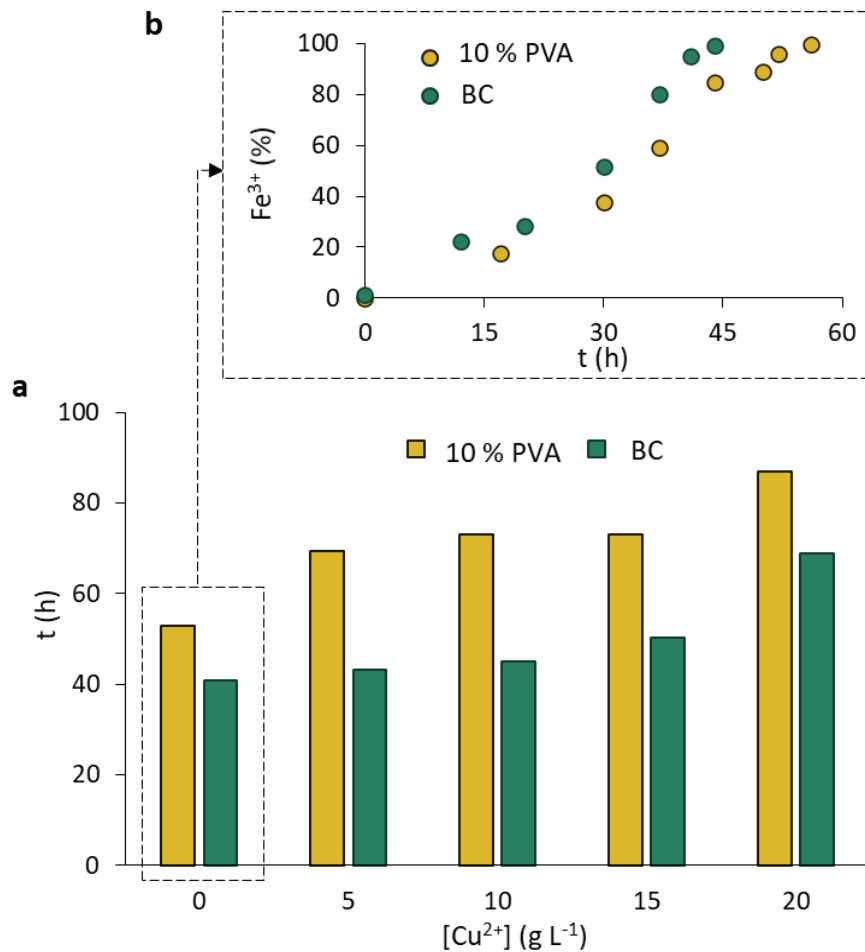


Figure 2.25. Fe^{2+} bio-oxidation time at different Cu^{2+} concentrations (a) and evolution of Fe^{3+} concentration in the control reactor (b) when using A-BC and A-PVA.

In summary, the 10 % PVA fabricated using the freeze-thawing method showed suitable characteristics for the preparation of an active support material to be used in metal removal processes. In addition, although the presence of copper in the solution has been reported to halt the process, the microbial activity in the active 10 % A-PVA was not fully inhibited even at 20 $g Cu^{2+} L^{-1}$. Nevertheless, BC hydrogel was selected as the most suitable support material for *A. ferrooxidans* immobilization due to the faster iron oxidation (even in the presence of increasing dissolved copper concentrations) and the maintenance of its integrity throughout the process during consecutive bio-oxidation stages.

2.4. CONCLUSIONS

The use of immobilized biomass in substitution to cell suspension is a promising strategy for improving the performance of the metal mobilization processes that are assisted by microorganisms. In this chapter, several materials (biocellulose -BC-, polyvinyl alcohol -PVA-, cellulose triacetate -CTA-, and chitosan -CH-) were fabricated to be tested as supports for *A. ferrooxidans* immobilization. Only BC and PVA hydrogels synthesized in the laboratory were proven to be suitable for this purpose, as they were not degraded in the 9K medium, they did not interfere bacterial growth, and the two active materials were able to re-oxidize the Fe^{2+} to Fe^{3+} without further inoculation. The novel BC was finally selected for further experiments based on its outstanding properties, such as highly porous network structure, very good mechanical properties, and chemical stability.

Once a decision was made on the support material, the best operating conditions for reducing the iron bio-oxidation time and increasing the Fe^{3+} productivity with the active biocellulose (A-BC) were determined in several experiments. The results showed that the optimum values were as follows: 1:0.6 for the NMV:ESA ratio, 170 rpm for the orbital shaking, and 9 g $\text{Fe}^{2+} \text{ L}^{-1}$ for the energy source solution. Under these conditions, the time required for complete oxidation of Fe^{2+} was reduced by a 30 % when compared with the cell suspension.

As far as the influence of dissolved copper is concerned, the time required by the A-BC for the complete bio-oxidation during the immobilization period increased linearly as long as the dissolved copper concentration increased from 5 to 20 g $\text{Cu}^{2+} \text{ L}^{-1}$. Thus, the bio-oxidation time in the presence of 20 g $\text{Cu}^{2+} \text{ L}^{-1}$ was 3.1-fold longer than for the control sample (0 g $\text{Cu}^{2+} \text{ L}^{-1}$). Conversely, when the same A-BC pieces were used in consecutive stages, only slight variations were recorded among the samples containing 5-15 g $\text{Cu}^{2+} \text{ L}^{-1}$. In this case, the average value of the oxidation time (46.4 ± 4.3 h) was only 14 % higher than that achieved in the copper-free sample. When A-BC was consecutively exposed to higher concentrations of the metal, it was finally able to successfully oxidize all the Fe^{2+} in the presence of 30 g $\text{Cu}^{2+} \text{ L}^{-1}$ in 89.0 ± 1.0 h.

The maintenance of the physical integrity of the A-BC during the whole experimentation, the ease of handling, and the ability to recover its original activity after storage at 4°C were other advantages verified in the study.

In summary, BC was concluded to be a suitable support material for bioregenerating the oxidant (Fe^{3+}) in copper solubilization processes. Besides its efficiency in this novel application, this hydrogel can be biosynthesized in the desired size and shape, and the generation of spent support material can be avoided as it is biodegradable.

2.5. REFERENCES

- Abral, H., Atmajaya, A., Mahardika, M., Hafizulhaq, F., Kadriadi, Handayani, D., Sapuan, S.M., Ilyas, R.A., 2020. Effect of ultrasonication duration of polyvinyl alcohol (PVA) gel on characterizations of PVA film. *Journal of Materials Research and Technology*. 9, 2477-2486.
- Africa, C.J., Harrison, S.T.L., Becker, M., van Hille, R.P., 2010. In situ investigation and visualisation of microbial attachment and colonization in a heap bioleach environment: The novel biofilm reactor. *Minerals Engineering*. 23, 486-491.
- Akhlaghi, N., 2019. Hemp fibres as novel green support material for immobilization of *Acidithiobacillus ferrooxidans*. *International Journal of Engineering*. 32, 1225-1230.
- Azeredo, H.M.C., Barud, H., Farinas, C.S., Vasconcellos, V.M., Claro, A.M., 2019. Bacterial cellulose as a raw material for food and food packaging applications. *Frontiers in Sustainable Food Systems*. 3, 1-14.
- Bakshi, P.S., Selvakumar, D., Kadirvelu, K., Kumar, N.S., 2020. Chitosan as an environment friendly biomaterial - a review on recent modifications and applications. *International Journal of Biological Macromolecules*. 150, 1072-1083.
- Cabrera, G., Gómez, J.M., Cantero, D., 2005. Influence of heavy metals on growth and ferrous sulphate oxidation by *Acidithiobacillus ferrooxidans* in pure and mixed culture. *Process Biochemistry*. 40, 2683-2687.
- Cacicedo M.L., Castro M.C., Servetas I., Bosnea L., Boura K., Tsafrakidou P., 2016. Progress in bacterial cellulose matrices for biotechnological applications. *Bioresource Technology*. 213, 172-180.
- Chakankar, M., Su, C.H., Hocheng, H., 2018. Leaching of metals from end-of-life solar cells. *Environmental Science and Pollution Research*. 26, :29524-29531.
- Cheng, R., Zhou, W., Lin, L., Xie, T., Zhang, Y., 2013. Removal of high concentrations of H₂S from simulated natural gas by *Acidithiobacillus ferrooxidans* immobilized on polyurethane foam. *Journal of Chemical Technology and Biotechnology*. 88, 975-978.
- Chowdhury, F., Ojumu, T.V., 2014. Investigation of ferrous-iron biooxidation kinetics by *Leptospirillum ferriphilum* in a novel packed-column bioreactor: Effects of temperature and jarosite accumulation. *Hydrometallurgy*. 141, 36-42.
- de Oliveira Barud, H.G.; da Silva, R.R.; Borges, M.A.C.; Castro, G.R.; Ribeiro, S.J.L.; da Silva Barud, H., 2021. Bacterial Nanocellulose in Dentistry: Perspectives and Challenges. *Molecules*. 26, 49.
- Donati, E.R. 2008. Ferrous iron oxidation by *Acidithiobacillus ferrooxidans* immobilized on refractory clay tiles. *Open Biotechnology Journal*. 2, 190-194.
- Dzionek, A., Wojcieszynska, D., Guzik, U., 2016. Natural carriers in bioremediation: a review. *Electronic Journal of Biotechnology*. 23, 28-36.
- El-Naas, M.H., Mourad, A-H.I., Surkatti, R., 2013. Evaluation of the characteristics of polyvinyl alcohol (PVA) as matrices for the immobilization of *Pseudomonas putida*. *International Biodeterioration and Biodegradation*, 85, 413-420.
- Fernandes, I.d.A.A.; Pedro, A.C.; Ribeiro, V.R.; Bortolini, D.G.; Ozaki, M.S.C.; Maciel, G.M., Haminiuk, C.W.I., 2020. Bacterial cellulose: From production optimization to new applications. *International Journal of Biological Macromolecules*. 164, 2598-2611.

- George, J., Sajeevkumar, V.A., Kumar, R., Ramana, K.V., Sabapathy, S.N., Bawa, A.S., 2008. Enhancement of thermal stability associated with the chemical treatment of bacterial (*Gluconacetobacter xylinus*) cellulose. *Journal of Applied Polymer Science*. 108, 1845-1851.
- Giaveno, A., Lavallo, L., Guibal, L., Donati, E., 2008. Biological ferrous sulfate oxidation by *A. ferrooxidans* immobilized on chitosan beads. *Journal of Microbiological Methods*. 72, 227-234.
- Ginsburg, M.A., Karamanev, D., 2007. Experimental study of the immobilization of *Acidithiobacillus ferrooxidans* on carbon based supports. *Biochemical Engineering Journal*. 36, 294-300.
- Gomez, J.M., Cantero, D., Webb, C., 2000. Immobilization of *Thiobacillus ferrooxidans* cells on nickel alloy fibre for ferrous sulphate oxidation. *Applied Microbiology and Biotechnology*. 54, 335-340.
- Gutierrez, J., Fernandes, S.C.M., Mondragon, I., Tercjak, A., 2013 Multifunctional hybrid nanopapers based on bacterial cellulose and sol-gel synthesized titanium/vanadium oxide nanoparticles. *Cellulose*. 20, 1301-1311.
- Hammanavar, P.B., Lobo, B., 2018. Experimental study of the microstructure and optical properties of PVA–PVP blend filled with lead nitrate. *Materials Today: Proceedings*. 5, 2677-2684.
- Harneit, K., Göksel, A., Kock, D., Klock, J.H., Gehrke, T., Sand, W., 2006. Adhesion to metal sulfide surfaces by cells of *Acidithiobacillus ferrooxidans*, *Acidithiobacillus thiooxidans* and *Leptospirillum ferrooxidans*. *Hydrometallurgy*. 83, 245-254.
- Hassan, C.M., Peppas, N.A., 2000. Structure and applications of poly (vinyl alcohol) hydrogels produced by conventional crosslinking or by freezing/thawing methods. *Advances in Polymer Science*. 153, 37-65.
- Holloway, J.L., Lowman, A.M., Palmese, G.R., 2013. The role of crystallization and phase separation in the formation of physically cross-linked PVA hydrogels. *Soft Matter*. 9, 826-833.
- Idris, A., Zain, N.A.M., Suhaimi, M.S., 2008. Immobilization of Baker's yeast invertase in PVA–alginate matrix using innovative immobilization technique. *Process Biochemistry*. 43, 331-338.
- Jadhav, U., Umesh, U., Hocheng, H., Weng, W.-H., 2013. Innovative use of biologically produced ferric sulfate for machining of copper metal and study of specific metal removal rate and surface roughness during the process. *Journal of Materials Processing Technology*. 213, 1509-1515.
- Jaisankar, S., Modak, J.M., 2009. Ferrous iron oxidation by foam immobilized *Acidithiobacillus ferrooxidans*: experiments and modeling. *Biotechnology Progress*. 25, 1328-1342.
- Juergensmeyer, M.A., Nelson, E.S., Juergensmeyer, E.A., 2007. Shaking alone, without concurrent aeration, affects the growth characteristics of *Escherichia coli*. *Letters in Applied Microbiology*. 45, 179-183.
- Junfeng, Y., Guoliang, L., Wei, C., 2007. Ferrous sulphate oxidation using *Acidithiobacillus ferrooxidans* cells immobilized in ceramic beads. *Chemical and Biochemical Engineering Quarterly*. 21, 175-179.

- Kahrizi, E., Alemzadeh, I., Vossoughi, M., 2008. Bio-oxidation of ferrous ions by *Acidithiobacillus ferrooxidans* in a monolithic bioreactor. *Journal of Chemical Technology and Biotechnology*. 84, 504-510.
- Kaiser, A., Stark, W.J., Grass, R.N., 2017. Rapid production of a porous cellulose acetate membrane for water filtration using readily available chemicals. *Journal of Chemical Education* 94, 483-487.
- Klößner, W., Büchs, J., 2012. Advances in shaking technologies. *Trends in Biotechnology*. 30, 307-314.
- Koseoglu-Imer, D.Y., Keskinler, B., 2013. Immobilization of *Acidithiobacillus ferrooxidans* on sulfonated microporous poly (styrene-divinylbenzene) copolymer with granulated activated carbon and its use in bio-oxidation of ferrous iron. *Materials Science and Engineering C*. 33, 53-58.
- Lebrero, R., Estrada, J.M., Muñoz, R., Quijano, G., 2014. Deterioration of organic packing materials commonly used in air biofiltration: effect of VOC-packing interactions. *Journal of Environmental Management*. 137, 93-100.
- Lei, J., Huaiyang, Z., Xiaotong, P., Zhonghao, D., 2009. The use of microscopy techniques to analyze microbial biofilm of the bio-oxidized chalcopyrite surface. *Minerals Engineering*. 22, 37-42.
- Liang, G. B., Mo, Y. W., & Zhou, Q. F., 2010. Novel strategies of bioleaching metals from printed circuit boards (PCBs) in mixed cultivation of two acidophiles. *Enzyme and Microbial Technology*. 47, 322-326.
- Liang, G., Lin, W., He, Q., Liu, W., Zhou, Q., 2018. Mechanism of energy metabolism for adapted *Acidithiobacillus ferrooxidans* to copper resistance. *Environmental Progress and Sustainable Energy*. 38, 13054.
- Long, Z., Huang, Y. H., Cai, Z. L., Cong, W., Ouyang, F., 2004. Immobilization of *Acidithiobacillus ferrooxidans* by a PVA-boric acid method for ferrous sulphate oxidation. *Process Biochemistry*. 39, 2129-213.
- Lozinsky, V.I., Plieva, F.M., 1998. Poly(vinyl alcohol) cryogels employed as matrices for cell immobilization. 3. Overview of recent research and developments. *Enzyme and Microbial Technology*. 23, 227-242.
- Martinez-Bussenius, C., Navarro, C.A., Orellana, L., Paradela, A., Jerez, C.A., 2016. Global response of *Acidithiobacillus ferrooxidans* ATCC 53993 to high concentrations of copper: a quantitative proteomics approach. *Journal of Proteomics*. 145, 37-45.
- Martins, S.C.S., Martins, C.M., Santaella, S.T., 2013. Immobilization of microbial cells: a promising tool for treatment of toxic pollutants in industrial wastewater. *African Journal of Biotechnology*. 12, 4412-4418.
- Mesa, M.M., Andrades, J.A., Maćias, M., Cantero, D., 2004. Biological oxidation of ferrous iron: study of bioreactor efficiency. *Journal of Chemical Technology and Biotechnology*. 79, 163-170.
- Mousavi, S.M., Yaghmaei, S., Salimi, F., Jafari, A., 2006. Influence of process variables on biooxidation of ferrous sulfate by an indigenous *Acidithiobacillus ferrooxidans*. Part I: flask experiments. *Fuel*. 85, 2555-2560.

- Mulopo, J., Schaefer, L., 2015. Biological regeneration of ferric (Fe³⁺) solution during desulphurisation of gaseous streams: effect of nutrients and support material. *Water Science and Technology* 71, 1672-1678
- Muxika, A., Etxabide, A., Uranga, J., Guerrero, P., De La Caba, K., 2017. Chitosan as a bioactive polymer: Processing, properties and applications. *International Journal of Biological Macromolecules*. 105, 1358-1368.
- Mykytczuk, N. C. S., Trevors, J. T., Foote, S. J., Leduc, L. G., Ferroni, G. D., Twine, S. M., 2011. Proteomic insights into cold adaptation of psychrotrophic and mesophilic *Acidithiobacillus ferrooxidans* strains. *Antonie van Leeuwenhoek*. 100, 259-277.
- Nabili, A., Fattoum, A., Brochier-Salon, M-C., Bras, J., Elaloui, E., 2017. Synthesis of cellulose triacetate-I from microfibrillated date seeds cellulose (*Phoenix dactylifera* L.). *Iranian Polymer Journal*. 26, 137-147.
- Nie, H.Y., Zhu, N.W., Cao, Y.L., Xu, Z.G., Wu, P.X., 2105. Immobilization of *Acidithiobacillus ferrooxidans* on cotton gauze for the bioleaching of waste printed circuit boards. *Applied Microbiology and Biotechnology*. 177, 675-688.
- Novo, M. T., da Silva, A. C., Moreto, R., Cabral, P. C., Costacurta, A., Garcia, O. Jr, Ottoboni, L. M., 2000. *Thiobacillus ferrooxidans* response to copper and other heavy metals: growth, protein synthesis and protein phosphorylation. *Antonie van Leeuwenhoek, International Journal of General and Molecular Microbiology*. 77, 187-19.
- Oetiker, N., Norambuena, R., Martínez-bussenius, C., Navarro, C.A., Amaya, F., Álvarez, S.A., Paradela, A., Jerez, C.A., 2018. Possible role of envelope components in the extreme copper resistance of the biomining *Acidithiobacillus ferrooxidans*. *Genes*. 9, 347.
- Oliver-Ortega, H., Geng, S., Espinach, F., Oksman K. X., Vilaseca, F., 2021. Bacterial cellulose network from kombucha fermentation impregnated with emulsion-polymerized poly(methyl methacrylate) to form na
- Orellana, L.H., Jerez, C.A., 2011. A genomic island provides *Acidithiobacillus ferrooxidans* ATCC 53993 additional copper resistance: a possible competitive advantage. *Applied Microbiology and Biotechnology*. 92, 761-767.
- Ou, K., Dong, X., Qin, C., Ji, X., He, J., 2017. Properties and toughening mechanisms of PVA/PAM double-network hydrogels prepared by freeze-thawing and anneal-swelling. *Materials Science and Engineering C*. 77, 1017-1026.
- Peppas, N.A., Scott, J.E., 1992. Controlled release from poly(vinyl alcohol) gels prepared by freezing-thawing processes. *Journal of Controlled Release*. 18, 95-100.
- Pogliani, C., Donati, E., 2000. Immobilization of *Thiobacillus ferrooxidans*: importance of jarosite precipitation. *Process Biochemistry*. 35, 997-1004.
- Rajwade, J. M., Paknikar K. M., Kumbhar, J. V., 2015. Applications of bacterial cellulose and its composites in biomedicine. *Applied Microbiology and Biotechnology*. 99, 2491-2511.
- Rastegar, S.O., Mousavi, S.M., Shojaosadati, S.A., Sarraf Mamoor, R., 2015. Bioleaching of V, Ni, and Cu from residual produced in oil fired furnaces using *Acidithiobacillus ferrooxidans*. *Hydrometallurgy*. 157, 50-59.
- Retegi, A., Gabilondo, N., Peña, C., Zuluaga, R., Castro, C., Ganán, P., de La Caba, K., Mondragon I., 2010. Bacterial cellulose films with controlled microstructure-mechanical property relationships. *Cellulose*. 17, 661-669.

- Rodríguez, A., Gea, T., Sánchez, A., Font X., 2020. Agro-wastes and Inert Materials as Supports for the Production of Biosurfactants by Solid-state Fermentation. *Waste and Biomass Valorization*. 12, 1963-1976.
- Sikorski, P., Wada, M., Heux, L., Shintani, H., Stokke, B.T., 2004. Crystal structure of cellulose triacetate I. *Macromolecules*. 37, 4547-4553.
- Silverman, M.P., Lundgren, D.G., 1959 Studies on the chemoautotrophic iron bacterium *Ferroobacillus ferrooxidans*: I. An improved medium and a harvesting procedure for securing high cell yields. *Journal of Bacteriology*. 77, 642-647.
- Singh, A., Manikandan, N. A., Sankar, M. R., Pakshirajan, K., Roy, L., 2018. Experimental investigations and surface morphology of bio-micromachining on copper. *Materials Today: Proceedings*. 5, 4225-4234.
- Tercjak, A., Gutierrez, J., Barud, H.S., Domenegueti, R.R., Ribeiro, S.J.L., 2015. Nano- and macroscale structural and mechanical properties of in situ synthesized bacterial cellulose/PEO-b-PPO-b-PEO biocomposites. *ACS Applied Materials and Interfaces*. 7, 4142-4150.
- Ting, Y.P., Kumar, S., Rahman, M., Chia, B.K., 2000. Innovative use of *Thiobacillus ferrooxidans* for the biological machining of metals. *Acta Biotechnologica*. 20, 87-96.
- Trovatti, E., Serafim, L.S., Freire, C.S.R., Silvestre, A.J.D., Neto, C.P., 2011. Gluconacetobacter sacchari: an efficient bacterial cellulose cell-factory. *Carbohydrate Polymers*. 86, 1417-1420.
- Vasconcelos, N.F., Andrade, F.K., de Araújo, L.V.P., Vieira, R.S., Vaz, J.M., Chevallier, P., Mantovani, D., de Fátima Borges, M., de Freitas Rosa, M., 2020. Oxidized bacterial cellulose membrane as support for enzyme immobilization: properties and morphological features. *Cellulose*. 27, 3055-3083.
- Vermeulen, F., Nicolay, X., 2017. Sequential bioleaching of copper from brake pads residues using encapsulated bacteria. *Minerals Engineering*. 106, 39-45.
- Vrana, N.E., O'Grady, A., Kay, E., Cahill, P.A., Mc Guinness, B., 2009. Cell encapsulation within PVA-based hydrogels via freeze-thawing: a one-step scaffold formation and cell storage technique. *Journal of Tissue Engineering and Regenerative Medicine*. 3, 567-72.
- Wang, S., Li, T., Chen, C., Kong, W., Zhu, S., Dai, J., Diaz, A.J., Hitz, E., Solares, S.D., Li, T., Hu, L., 2018. Transparent, anisotropic biofilm with aligned bacterial cellulose nanofibers. *Advanced Functional Materials*. 28, 1707491.
- Westman, J.O., Ylittervo, P., Franzén, C.J., Taherzadeh, M.J., 2012. Effects of encapsulation of microorganisms on product formation during microbial fermentations. *Applied Microbiology and Biotechnology*. 96, 1441-1454.
- Wu, S.C., Lia, Y.K., 2008. Application of bacterial cellulose pellets in enzyme immobilization. *Journal of Molecular Catalysis B: Enzymatic*. 54, 103-108.
- Xenofontos, E., Feidiou, A., Constantinou, M., Constantinides, G., Vyrides, I., 2015. Copper biomachining mechanisms using the newly isolated *Acidithiobacillus ferrooxidans* B1. *Corrosion Science*. 100, 642-650.
- Yujian, W., Xiaojuan, Y., Hongyu, L., Wei, T., 2006 Immobilization of *Acidithiobacillus ferrooxidans* with complex of PVA and sodium alginate. *Polymer Degradation and Stability*. 91, 2408-2414.

Yujian, W., Xiaojuan, Y., Wei, T., Hongyu, L., 2007. High-rate ferrous iron oxidation by immobilized *Acidithiobacillus ferrooxidans* with complex of PVA and sodium alginate. *Journal of Microbiological Methods*. 68, 212-7.

Zain, N.A.M., Suhaimi, M.S., Idris, A., 2011. Development and modification of PVA-alginate as a suitable immobilization matrix. *Process Biochemistry*. 46, 2122-2129.

Zhu, N., Shi, C., Shang, C. R., Yang, Z., Xu, Z., Wu, P., 2017. Immobilization of *Acidithiobacillus ferrooxidans* on cotton gauze for biological oxidation of ferrous ions in a batch bioreactor. *Biotechnology and Applied Biochemistry*. 64, 727-734.

CHAPTER 3.
APPLICATION 1: BIOMACHINING OF
COPPER PIECES FOR THE FABRICATION
OF MICROFLUIDIC DEVICES

3.1. OBJECTIVE

The need to move towards a more sustainable manufacturing has focused attention on biological metal removal (biomachining) for the generation of simple patterns used in micro-devices industry (Hocheng et al., 2012; Muhammad et al., 2018). When applied to the engraving of geometries on metal surfaces, this process is characterized by micromachining pieces with no thermal damage or residual stress, and without exerting a cutting force (Muhammad et al., 2015; Díaz-Tena et al., 2017). In addition, it has been reported to be less energy demanding, have lower cost and be more ecofriendly than conventional mechanical and chemical machining processes (Watling, 2006; Kumar and Yaashikaa, 2020).

The bio-manufacturing of metal pieces with different patterns or geometries has already been reported in literature (Hocheng et al., 2012; Díaz-Tena et al., 2014; Muhammad et al., 2015; Muhammad et al., 2018). Nevertheless, as far as microfluidic devices are concerned, this technology has only been used for polydimethylsiloxane (PDMS) surface modification in order to create an irregular pattern for cell adhesion enhancement (Whulanza et al., 2016). Therefore, to the best of the authors' knowledge, the biomachining of metal molds for the manufacturing of PDMS microfluidic devices is a novelty that can contribute to the sustainable production of consumer goods.

This chapter focuses on the development of a biomachining process for manufacturing well-defined microfluidic structures on a copper piece. Then, the generated molds were used for the fabrication of functional PDMS microfluidic devices. The bio-regeneration and the subsequent re-use of the biomachining solution in consecutive mold-etching stages was fully characterized with the aim of achieving a repetitive mold-etching procedure, which enhanced the full process sustainability by extending the life-span of the biomachining solution.

Figure 3.1 shows the outline of the experimental section of this chapter.

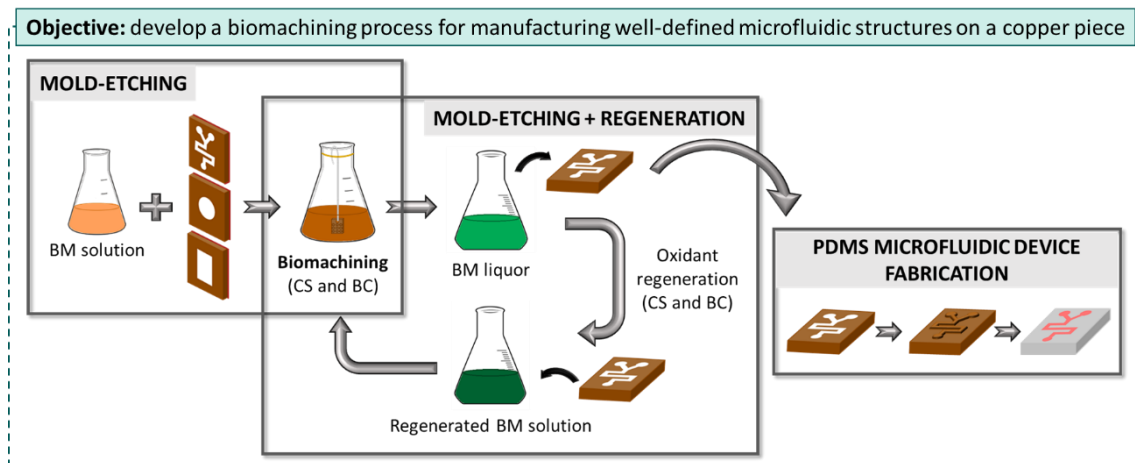


Figure 3.1. Outline of the experimental section of this chapter.

3.2. MATERIALS AND METHODS

3.2.1. Microorganisms and biomachining solution

The microorganism used in this study was *A. ferrooxidans* DSM 14882 strain. This bacterium's cells were cultured in the medium developed by Silverman and Lundgren (1959) as described in Section 1.1 *Microorganisms* (materials and general methods) using $9 \text{ g Fe}^{2+} \text{ L}^{-1}$ (9K medium) as initial iron concentration.

The biomachining solution (BM solution) was prepared by inoculating a 5 % of *A. ferrooxidans* DSM 14882 in the exponential growth phase to the nutrient medium and culturing it until the complete oxidation of Fe^{2+} to Fe^{3+} . In this study the bacterial growth was carried out in an orbital incubator (Shaking Incubator 211B) at 130 rpm and $31 \text{ }^\circ\text{C}$, and the solution pH was adjusted to 1.8 with sulfuric acid (25 % v:v).

An abiotic machining solution (M solution) was used in the control tests for comparison purposes. It was obtained by filtering the BM solution with a $0.45 \text{ }\mu\text{m}$ polyvinylidene fluoride filter for bacterial removal.

3.2.2. Workpiece preparation

3.2.2.1. Workpiece dimensions and preparation

Flat copper workpieces of $32 \times 25 \times 2 \text{ mm}$ and 99.9 % purity (Figure 3.2a) were cut in the Department of Mechanical Engineering at the University of the Basque Country (UPV/EHU, Spain) using a REMET TRE100 Evol metallographic saw.

The workpieces were prepared according to a novel coating process based on the combination of a Pressure Sensitive Adhesive (PSA) mask and a lacquer to ensure that only the side with the geometry to be engraved was exposed to the BM solution. Thus, the PSA mask was adhered to the surface of the piece to be biomachined. The opposite surface of the piece was protected with a coating material (lacquer) in order for the oxidizing solution to only remove the metal from the uncovered area (Figure 3.2b). The preparation of the piece is described in the next sections.

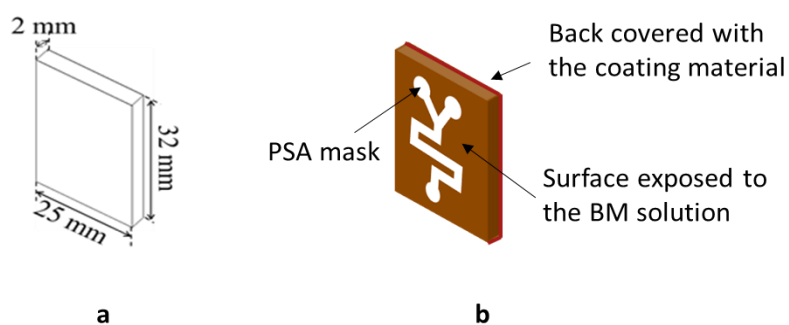


Figure 3.2. Copper workpiece: dimensions (a) and preparation (b).

3.2.2.2. Geometries to be biomachined

Three geometries were designed to be engraved on the copper workpieces: a circle of 10 mm diameter (Figure 3.3a), a microfluidic serpentine channel (72 mm total length x 2 mm width) (Figure 3.3b) that included an inlet circle and two outlet circles of 3 mm diameter, and a rectangular structure (20 mm length x 7 mm width) (Figure 3.3c). A mask with the desired geometry was cut by Graphtec cutting Plotter CE6000-40 (CPS Cutter Printer Systems, Spain) on sheets of PSA layers (127 μm thick ARcare[®] 8939 white PSA, Adhesive Research, Ireland).

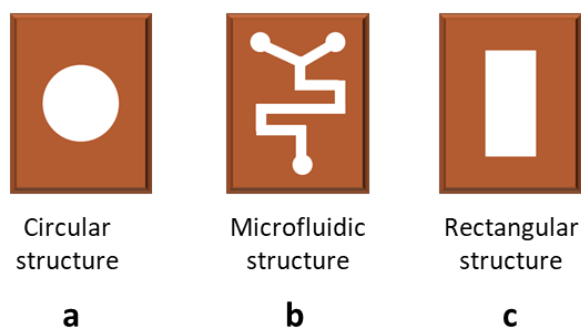


Figure 3.3. Selected geometries for micro-etching: circle (a), microfluidic structure with serpentine channel (b), and rectangular structure (c).

Each copper workpiece was rinsed with deionized water and ethanol (96 %) and gently wiped to remove surface moisture. Then, the mask adhesive (circle, serpentine channel or rectangle) was stuck to one surface.

3.2.2.3. Selection of the coating material for surface protection

Two epoxy resin coating materials (lacquers) were tested: MAT1- lacquer for bulbs MONGAY, S.A. (red color) and MAT2- TASOVISION protective and insulating lacquer (transparent) (Figure 3.4).



Figure 3.4. Coating materials for surface protection: bulb lacquer (left) and insulating protective lacquer (right).

Several experiments were carried out with the two coating materials (MAT-1 and MAT-2) with the final aim of assessing their effectiveness in protecting the workpieces' back surface from etching and ascertaining their possible inhibition effect on bacterial growth. The material to be protected in these experiments was a rod glass (inert material), as any other metallic material could interfere the process (Figure 3.5a).

Thus, two glass rods were coated with the aforementioned materials (red MAT-1 and transparent MAT-2) (Figure 3.5b). The rods were immersed by suspension into 150 mL of 9K medium containing a 5 % v:v *A. ferrooxidans* inoculum. The Erlenmeyers containing the rods were incubated under the same operating conditions as in the bacterial incubation experiments (3.2.1. *Microorganisms and biomachining solution*), until all the Fe^{2+} was oxidized into Fe^{3+} (Figure 3.5c). An Erlenmeyer solely containing inoculated culture medium (without any rod immersed) was the control sample. Once all the ferrous iron was oxidized, the coated rods were maintained submerged in the BM medium during 24 hours to ascertain whether the coatings were reactive with the oxidizing agent (Fe^{3+}).

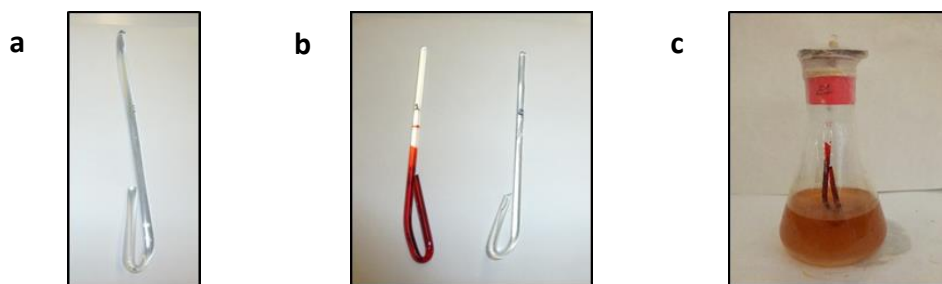


Figure 3.5. Glass rod prior to use (a), glass rods with the two coating materials (b) and assay system (c).

The evolution of iron species (total, Fe^{2+} and Fe^{3+}) and pH were measured throughout the experiment as described in Sections 2.5 *Determination of iron species in dissolution* and 2.8 *Other methods* (materials and general methods). In addition, the weight loss of the coated rods was measured after immersion in the BM solution during 4 and 24 h.

3.2.3. Mold-etching using cell suspension

A suspension culture was used to study the influence of treatment time on the SMRR and mold height. In addition, the re-use of the BM solution in consecutive mold-etching stages and its influence on process performance was assessed.

3.2.3.1. Influence of treatment time on mold-etching

The relationship among the biomachining time, the SMRR and the height of the engraved structure was studied in two etching experiments. First, two copper

workpieces (Cu⁰) masked with the circular geometry were immersed in 150 mL of the BM and M solution, respectively, for 7 hours. After several time intervals (Table 3.1), the workpieces were removed from the treatment solution, rinsed with ethanol (96 %) and deionized water, dried, weighed (Denver instruments, SI-234) and immersed again in the same solution. The abiotic machining experiment was carried out as a control test in order to compare the variation of SMRR and height with the results achieved in the biotic assay.

Table 3.1. Immersion times in the mold-etching experiments.

Engraved structure	Treatment time (h)	Observations
Circular structure	7	Intermediate extractions after 0.25, 0.50, 0.75, 1, 2, 3, 4, 5 and 6 h
Microfluidic structure	0.25, 0.50, 1, 2, 6	Without intermediate extractions

In a second experiment using the mask with the microfluidic structure, five different copper workpieces were covered with the PSA serpentine channel (Figure 3.3b) and each piece was subjected to one of following treatment times: 0.25, 0.5, 1, 2 and 6 h (Table 3.1). This assay was carried out with no intermediate extractions in order to simulate a real mold manufacturing process.

Both experiments were carried out in an orbital incubator (Shaking Incubator 211B) at 130 rpm and 31 °C. The pH was measured and adjusted to 1.8 during the process, if necessary, by the addition of sulfuric acid (25 % v:v).

Assays with circular and microfluidic structures were carried out in triplicate and duplicate, respectively, and under non-sterile conditions to simulate a real-scale treatment.

3.2.3.2. Extension of the lifespan of the BM solution

Copper workpieces masked with the microfluidic channel were selected to ascertain the ability of *A. ferrooxidans* to re-oxidize the Fe²⁺ generated during mold-etching, and to study the influence of the regenerated BM solution on both the average specific metal removal rate (SMRR_{av}) and the engraved height after successive mold-etching + regeneration cycles. In this study, the two-stage metal removal procedure described in Chapter 1 was modified for its use in the manufacture of metallic molds. Thus, stage 1 involved mold-etching (biomachining), and was carried out under the same experimental conditions described in Section 3.2.3.1 *Influence of treatment time on mold-etching*. After the set treatment time (t = 0.25, 0.50, 2 and 6 h), each workpiece

(Cu⁰) was removed from the BM solution to let the microorganisms regenerate the oxidant (stage 2). Once this stage was completed, the same copper workpiece was immersed again in the regenerated BM solution for the next mold-etching step. The process was repeated until the time needed for Fe²⁺ re-oxidation doubled that recorded in the first regeneration step.

3.2.4. Mold-etching using immobilized biomass

The influence of using immobilized bacteria (instead of cell suspension) on the SMRR_{av} and the height of the engraved structure was studied.

Based on the results achieved in Chapter 2, bacterial cellulose (BC) was selected as the support material for *A. ferrooxidans* immobilization. This hydrogel was synthesized and pretreated following the procedure described in Sections 2.2.2. *Synthesis of the support materials* and 2.2.3. *Pre-treatment of the support material* (Chapter 2). Afterwards, the bacterial immobilization procedure was carried out under the optimal operating conditions selected in Chapter 2: orbital shaking at 170 rpm, 31 °C and 1:0.6 nutrient medium volume (mL):exposed surface area (cm²) ratio (NMV:ESA) in 9K medium. This stage proceeded until 100 % Fe²⁺ contained in the nutrient medium was oxidized to Fe³⁺. The pH was adjusted to 1.8 with sulfuric acid (25 % v:v) throughout the incubation period.

Copper workpieces were masked with the rectangular structure shown in Figure 3.3c and the back covered with the protective lacquer. Then, they were subjected to four mold-etching + regeneration cycles as described in Section 3.2.3.2. *Extension of the lifespan of the BM solution*. The selected etching time was 2 hours.

Two experimental configurations were tested.

- Configuration 1 (BM-BC_{IN}): The copper piece etching was carried out by immersing the masked pieces into the BM solution containing the active BC (A-BC). The metal removal was, thus, carried out in the presence of the A-BC pieces. After the selected treatment time, the copper piece was extracted to allow the A-BC regenerate the medium for successive biomachining stages.
- Configuration 2 (BM- BC_{OUT}): The copper removal stage (biomachining stage) was carried out using the biologically oxidized medium (medium containing Fe³⁺) in the absence of A-BC. After the treatment time, the copper piece was extracted and the BM medium was regenerated by introducing the A-BC pieces in the solution.

The biomachining + regeneration process was also carried out using a cell suspension as a control test (BM-Susp). Thus, the masked copper workpiece was subjected to the same two-stage process.

The biomachining and regeneration stages were carried out at 170 rpm (Shaking Incubator 211B) and 31 °C. The pH was measured and adjusted to 1.8 during the process, if necessary, by the addition of sulfuric acid (25 % v:v).

Table 3.2 summarizes the operating conditions for each experimental configuration.

Table 3.2. Experimental conditions in metal removal experiments when using A-BC and cell suspension (control).

Experiment	Etching stage	Regeneration stage	Operating conditions
BM-BC _{IN}	BM solution + A-BC	A-BC	Treatment time: 2 h 170 rpm, 31°C, pH 1.8
BM- BC _{OUT}	BM solution (abiotic)	A-BC	
BM-Susp	BM solution + suspended cells	Suspended cells	

3.2.5. Fabrication of the PDMS devices

Once the copper mold etching was completed, the PSA mask was removed from the surface and the metal piece was placed inside of a poly(methyl methacrylate) (PMMA) gasket. The gasket, consisting of two different PMMA substrates glued with a transparent PSA layer, was grafted by a CO₂ Laser System (VERSA Laser, VLS2.30 Desktop Universal Laser System equipped with one 10.6 μm CO₂ laser source ranging in power from 10 to 30 watts). A 1.1 mm thick PMMA substrate (ME303010, clear, Goodfellow) was cut (37 mm length x 30 mm width) and used as the bottom base of the device. A 4 mm thick PMMA substrate (PLEXIGLAS®, Evonik Industries AG) used as the gasket walls delimited an internal space of 32 mm length x 25 mm width in order to place the metal mold inside. The transparent PSA layer (146 μm thick ARcare® 90880, Adhesive Research, Ireland) used to attach the two pieces of PMMA was cut by the same Graphtec cutting Plotter as the previous described PSA.

The PDMS devices were fabricated by casting, placing the copper mold inside of the PMMA gasket. The curing agent and the polymer-base (SYLGARD 184 silicone elastomer kit, Farnell, Spain) were mixed (1:10 proportion) and degassed in a vacuum desiccator (PolyLab, Spain) for 30 min to remove air bubbles. Once degassed, the PDMS mixture was poured onto the gasket and placed at 70 °C in a STZ 5.4 mini oven (FALC, Italy) for 2 h, in order to completely cross-link the PDMS. The resulting PDMS device was peeled off from the mold and three through-holes were punched in the inlet and outlets of the device, using a 3.0 mm diameter Harris Uni-core puncher (Sigma Aldrich, Spain) to enable the load of the sample.

The microchannel was closed using a transparent PSA layer (50 μm thick ARcare[®] 92712, Adhesive Research, Ireland) as a bottom base of the device. The resulting PDMS device was degassed in a RVR003H-01 Vacuum Chamber (Dekker Vacuum Technologies, USA) for 1 h at 0.7 mbar in order to remove the air inside the material. Afterwards, the PDMS device was placed under atmospheric pressure again and a sample (water + red dye) was added to the inlet. The PDMS was able to absorb air from the closed serpentine structure, moving the liquid sample through the entire channel.

3.2.6. Analytical methods

Iron concentration and pH were monitored throughout the process by following the procedure described in Sections 2.5 *Determination of iron species in dissolution* and 2.8 *Other methods* (materials and general methods). The MRR and SMRR were used to quantify treatment efficiency, being calculated as shown in Equations 15 and 16 (materials and general methods).

$$\text{MRR (mg h}^{-1}\text{)} = \frac{\text{Amount of metal removed (mg)}}{\text{Time (h)}} \quad (\text{Eq. 15})$$

$$\text{SMRR (mg h}^{-1}\text{ cm}^{-2}\text{)} = \frac{\text{MRR}}{\text{Area (cm}^2\text{)}} \quad (\text{Eq. 16})$$

The height of the micro-etched structures was measured using a stylus profilometer (DektakXT, Germany) (Figure 3.6). Video was recorded using mobile OnePlus 6T, 1080p at 30fps.

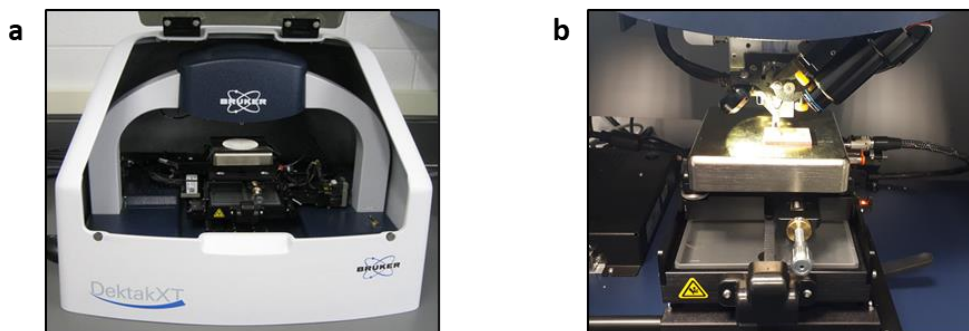


Figure 3.6. Stylus profilometer (DektakXT) (a) and workpiece height measurement with profilometer (b).

3.3. RESULTS

The constant search for alternative technologies that reduce the economic cost and environmental impact of conventional machining processes have led to the application of bioleaching principles to the generation of microstructures to be used in different fields, such as microelectromechanical systems. Thus, the viability of using this technology for creating simple microstructures such as circular and triangular dimples, circular micro pillars, and linear, square and rectangular micro-patterns on metal surfaces has been already studied by some authors (Hocheng et al., 2012; Istiyanto et al., 2012; Muhammad et al., 2018). Nevertheless, the fabrication of metallic molds for their use in the fabrication of microfluidic devices has not been investigated to date.

The use of microfluidic devices offers a wide range of advantages over conventional analytical tools (Aaron et al., 2013). Their diversity of applications plays an important role in the progress of many research fields, which precise of unconventional chemical, biological and engineering operations. Moreover, from the device fabrication point of view, there are many techniques and materials available to manufacture optimized devices and face the vast number of application requirements (Chiu et al., 2017).

Since their introduction in 1998 (Xia and Whitesides, 1998), soft-lithography techniques have been employed for the development of microfluidic devices, especially for polydimethylsiloxane (PDMS) chips (Lunelli et al., 2020; Teo et al., 2020). Thanks to its multiple properties, including high flexibility, biocompatibility and oxygen permeability, PDMS molding by soft-lithography is still the most standardized method for the manufacture of microfluidic devices (Torino et al., 2018; Gao et al., 2019). However, the process of mold fabrication by soft-lithography is tedious, since requires many fabrication steps (surface cleaning and treatment, spin coating, soft bake, UV exposure, post exposure bake and development) and involves the use of cleanroom facilities; therefore, other rapid prototyping techniques for molding of polymeric materials is in continuous exploration (Gale et al., 2018).

Despite the progresses made on eliminating the use of specialized facilities at a research level, the microfluidics industry still requires the use of highly resistant molds to enable the manufacturing of large number of devices. Therefore, in order to improve these manufacture techniques, new methods able to reduce production times and costs are ambioned in mold fabrication. New materials like 3D resins (Ferraz et al., 2020), polymers (Speller et al., 2019; Tsao and Wu, 2020) and metals (Azarsa et al., 2020) have been investigated for the fabrication of molds and, due to the development of the manufacturing techniques, these new molds have been tested to generate more efficient production processes.

In particular, metal molds are being found to be the most resistant; however, their design could only be carried out using machining techniques (Azarsa et al., 2020). The machining of metals can be achieved by three different processes: mechanical, chemical and biological. The physical and chemical machining (micro-milling, micro-EDM, chemical-etching...) are aggressive methods that could harm the metallurgical properties of the mold and, in a more important extend, generate environmental issues due to the hazardous materials and chemicals needed and generated during the fabrication process of the required molds. In addition, the aggressive treatment makes more laborious the control of the thickness of the layer eroded from the surface, hindering the standardization of the process for microfluidics applications (Pandey and Shan, 2012). Conversely, biological metal machining has been proposed as a potential alternative to these techniques due to its capability to obtain molds with good surface quality and without any thermal or structural damage on the metallic workpieces (Istiyanto et al., 2010; Diaz-Tena et al., 2018). Thus, in this study biomachining has been proposed as a sustainable alternative to the conventional mold production techniques.

3.3.1. Workpiece preparation: an alternative to the traditional techniques

Photolithography, the most used covering alternative in the preparation of pieces for the biomachining process, consists of covering the piece with a photoresist resin for “printing” the pattern of the geometry from a photomask. This photomask lets the light remove the resin only from the exposed areas and only resin free parts are biomachined (Hocheng et al., 2012; Istiyanto et al., 2012). One drawback of mask-based photolithography method is that it requires the use of expensive masks and custom-made optical components. Additionally, the photoresins that are formulated for photolithography require severe post-processing conditions (Liaros and Fourkas, 2019).

In this study, the use of lacquers and PSA adhesives is proposed to cover the areas of the workpieces not to be biomachined and thus, ensure that only the side with the geometry to be engraved was exposed to the BM solution. These materials are easily available and do not require sophisticated equipment for their use, so they would be a fast and economical alternative to photolithography. However, its composition could interfere with the activity of the biomass. Therefore, it was necessary to assess their effectiveness in protecting the workpiece’ surface from etching and to ascertain their possible inhibition effect during bacterial growth. Figure 3.7 shows the evolution of Fe^{2+} during the *A. ferrooxidans* incubation period in the presence and the absence of the two studied lacquers.

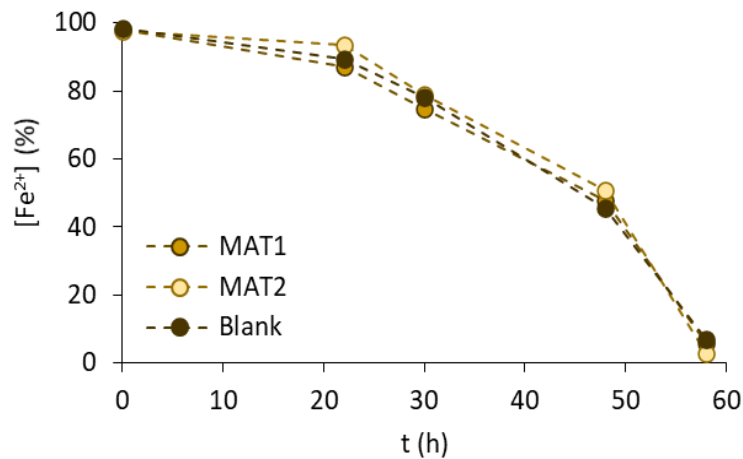


Figure 3.7. Evolution of Fe^{2+} (%) during the *A. ferrooxidans* incubation period in the presence and the absence of the two studied lacquers.

Regarding the synthetic lacquers, the decrease in Fe^{2+} concentration through the incubation period showed the same pattern for the two samples containing the coated glass rod and the blank, revealing that the protective materials (MAT1 and MAT2) did not interfere the process or halt the bacterial activity (Figure 3.7).

Almost no iron variation was observed during the experiment in any case since only 1.3 and 1.7 % of total iron was lost during biomachining experiments for MAT1 and MAT2, respectively. Both coating materials were concluded to be suitable for protecting the surface from engraving. Nevertheless, the colorless MAT2 (insulating lacquer) was difficult to visually distinguish and, thus, red light bulb lacquer (MAT1) was chosen for further mold-etching studies carried out in this work. Likewise, the PSA adhesives were proven not to be detached from the workpiece after up to 30 hours of treatment and to successfully cover the desired surface.

As a conclusion, the lacquer + PSA adhesive combination resulted to be a feasible, biocompatible and fast method for surface protection in biomachining applications.

3.3.2. Mold-etching using cell suspension

The influence of biomachining time on the SMRR and on the structure's height was studied, with the aim of defining the mathematical equation to calculate the treatment time required to obtain a fixed mold height. In addition, a process comprising consecutive mold-etching and BM solution regeneration stages was proposed in order to improve system's sustainability.

3.3.2.1. *Specific metal removal rate and structure's height as a function of treatment time*

The relationship between biomachining time and SMRR or height/depth values of the developed structures has been studied by several authors (Muhammad et al., 2015; Istiyanto et al., 2018; Singh et al., 2018). Although the SMRR has been found to be maximum during the first hour (Chapter 1), it is necessary to explore the evolution of this parameter during variable treatment times in order to obtain molds with adequate channel heights for certain applications. Therefore, the influence of engraving pieces during periods shorter and longer than 1 hour on the SMRR and on the channel height were studied in this chapter.

As a preliminary step in the design of the bacteria-assisted mold-etching process, a circle was first selected to ascertain the efficiency of the system to engrave this simple geometry while maintaining the original dimensions of the circle through treatment time. The diameter of the circular structure measured after the selected etching time (7 h) remained practically invariable in both the biotic (0.98 ± 0.01 cm) and the abiotic (0.97 ± 0.01 cm) tests and thus the process was considered not to affect the original geometry.

Regarding SMRR and structure's height, treatment time was determinant for assessing the system's response. The results shown in Figure 3.8a-b are in accordance with those presented in Chapter 1, as a SMRR peak value was registered during the first hour of treatment. Diaz-Tena et al. (2016) also registered maximum values after 1 h of copper biomachining with *A. ferrooxidans* DSM 14882, reporting a SMRR of $23.5 \text{ mg h}^{-1} \text{ cm}^{-2}$ and $19.5 \text{ mg h}^{-1} \text{ cm}^{-2}$ for biotic and abiotic samples, respectively ($6 \text{ g Fe}^{3+} \text{ L}^{-1}$, $30 \text{ }^\circ\text{C}$ and 130 rpm). In this study, when the biomachining time was 15, 30, 45 and 60 min, the maximum SMRR remained almost constant in the $20.8\text{-}22.1 \text{ mg h}^{-1} \text{ cm}^{-2}$ range both in the presence and in the absence of microorganisms (Table 3.3, Figure 3.8a). In this period, the accumulated mass of copper and engraved height increased linearly with treatment time, and the etching rate was $18.8 \text{ } \mu\text{m h}^{-1}$ ($R^2 = 0.967$) and $18.6 \text{ } \mu\text{m h}^{-1}$ ($R^2 = 0.968$) in the biotic and abiotic samples, respectively (Table 3.3, Figure 3.8a).

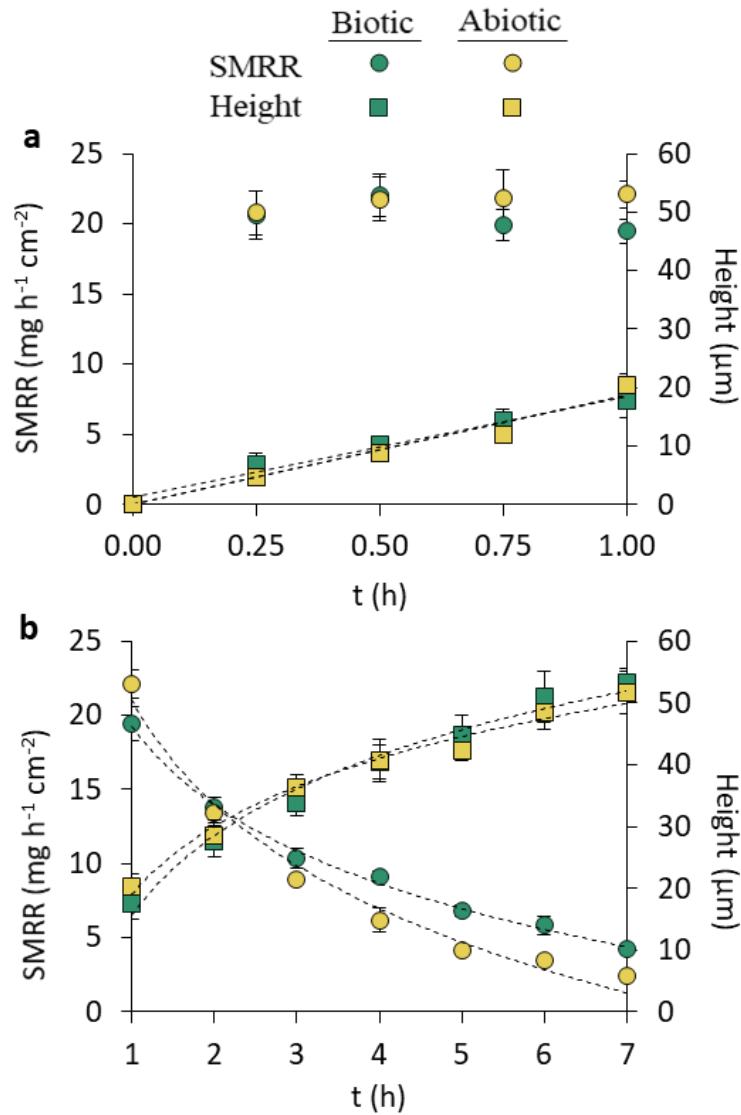


Figure 3.8. Variation of SMRR and height of the engraved structures with treatment time: 0-1 h (a) and 1-7 h (b).

Table 3.3. SMRR (mg h⁻¹ cm⁻²), structure's height (Ht, μm), and removed copper (mCu, mg) variation according to the two treatment time intervals (h) for the circular geometry.

Time	Biomachining	R ²	Machining	R ²
0-1 h	SMRR = 20.5±0.1	--	SMRR = 21.6±0.6	--
	Ht = 18.8·t	0.9675	Ht = 18.6·t	0.9678
	m _{Cu} = 458.9·t	0.9141	m _{Cu} = 439.7·t	0.9205
1-7 h	SMRR = -7.6·ln t + 19.3	0.9141	SMRR = -10.2·ln t + 21.0	0.9827
	Ht = 18.7·ln t + 15.7	0.9816	Ht = 15.9·ln t + 19.0	0.9811
	m _{Cu} = 261.5·ln t + 479.0	0.9844	m _{Cu} = 205.2·ln t + 530.3	0.9844

Conversely, in the 1-7 h range, the SMRR decreased following a logarithmic trend, and the height and accumulated copper mass increased accordingly (Table 3.3, Figure 3.8b). The reduction in the SMRR can be attributed to the combination of decreasing Fe^{3+} and increasing Cu^{2+} concentration in the solution, as well as hydrolysis (Istiyanto et al., 2010). These results are consistent with those achieved in Chapter 1, and those reported by Istiyanto et al. (2010) who have also concluded that metal removal rate is inversely proportional to the machining time, but not simply linear, when copper pieces were biomachined in 9K medium (35 °C, 120 rpm).

Figure 3.9 shows the solution's color progression during the 7 h biomachining experiment. The increasing concentration of dissolved copper is responsible for the solution color.

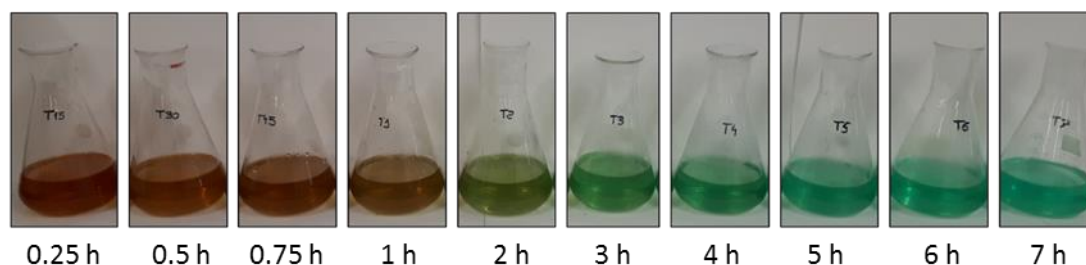


Figure 3.9. Resulting solutions after 0.25 to 7 h biomachining treatment.

The difference in the SMRR achieved in the biotic and the abiotic process during the first two hours was not relevant ($\leq 5\%$). Despite the high difference in the standard reduction potentials of oxygen and copper ($\text{O}_2/\text{H}_2\text{O} = 1.23\text{ V}$ vs. $\text{Cu}^{2+}/\text{Cu}^0 = 0.34\text{ V}$), copper oxidation by dissolved oxygen has been reported not to be the most important mechanism of the solubilization of this metal, probably due to the low oxygen solubility in water and gas-liquid mass transfer limitations (Lambert et al., 2015). This limitation has also been confirmed from the results achieved in Chapter 1. Thus, the contribution of this parameter on the process was considered negligible. In fact, the ability of the biologically generated abiotic solution (M solution) to biomachine copper pieces corroborated the significant contribution of Fe^{3+} as oxidizing agent to the process through the indirect mechanism (Xenofontos et al., 2015). This process requires an intermediate redox couple (i.e. $\text{Fe}^{2+}/\text{Fe}^{3+}$) which is able to solubilize pure copper according to Equation 7 (described in materials and general methods).

Then, *A. ferrooxidans* bacterium uses the simultaneously generated Fe^{2+} as energy source and bio-oxidizes it to Fe^{3+} (Equation 8, described in materials and general methods). According to literature, during the oxidation process most of the electrons (95 %) enter the downhill electron pathway. Thus, they enter the cytoplasm through the

cell membrane, transport to oxygen and react with protons to generate water; simultaneously a proton gradient is formed by pumping the protons out of the membrane (Ingledew, 1982, Valdés et al., 2008).

In the presence of bacteria, the abovementioned reactions can lead to a cyclic process in which copper is dissolved and Fe^{3+} bio-oxidized until the environmental conditions (pH, dissolved copper concentration, etc.) inhibit bacterial activity. Nevertheless, the biological Fe^{3+} regeneration (Equation 8) has been reported to be slower than Fe^{3+} consumption (Equation 7) (Lambert et al., 2015).

This can explain the results obtained in the shortest treatment times (< 2 h) in which the SMRR was not greatly affected by the presence of microorganisms. Interestingly, after 3 h of biomachining the SMRR was higher in the biotic than in the abiotic samples, which was attributed to the higher Fe^{3+} availability due to the continuous microbial regeneration of the oxidant iron species. This difference increased until hour 5, after which the SMRR remained 1.7-fold higher in the biotic process. These results support the conclusion obtained in Chapter 1 regarding that the indirect mechanism plays an important role in the process.

Albeit the non linear variation of the SMRR throughout the whole process, the average MRR (MRR_{av}) has been calculated in order to compare the results obtained in this work with those reported by other authors. For the biotic sample, the MRR_{av} value after 7 h ($96.8 \text{ mg Cu h}^{-1}$) was higher than that obtained by Ting et al. (2000). These authors have reported a value of 20 and 17 mg h^{-1} for mild steel and copper, respectively ($4 \text{ g Fe}^{3+} \text{ L}^{-1}$, pH 2, $30 \text{ }^\circ\text{C}$, 120 rpm, 3 % inoculum). Regarding the abiotic assay, a MRR_{av} value of $121.3 \text{ mg Cu h}^{-1}$ was obtained in this experiment after 4 h of treatment. This value was considerably higher than that reported by Jadhav et al. (2013) who registered a MRR of $18.97 \text{ mg Cu h}^{-1}$ after 4 h when employing an abiotic medium obtained by filtering an *A. ferrooxidans* cell suspension ($40 \text{ g FeSO}_4 \text{ L}^{-1}$, pH 2.5, $30 \text{ }^\circ\text{C}$ and 150 rpm). After 7 hours of treatment, the accumulated copper removal was 106.3 and 96.7 mg cm^{-2} in the biomachining and the abiotic machining treatment, respectively. These values were significantly higher than those obtained by Ma et al., (2020), who reported the elimination of 61 mg Cu cm^{-2} after 8 hours of biomachining ($30 \text{ }^\circ\text{C}$, pH 1.8, 160 rpm, 3 g Fe L^{-1}).

Regarding the mold height, final values of 53.3 ± 2.4 and $51.7 \pm 3.4 \text{ } \mu\text{m}$ were achieved after 7 hours in the biotic and abiotic experiment, respectively. These results cannot be accurately compared with the ones reported by other authors, as most biomachining studies describe the generation of cavities with different shapes (circles, lines, etc.) and, thus, depth values are reported (instead of height values). In addition, the results depend on operating parameters such as initial iron concentration or shaking speed.

Nevertheless, for comparison purposes, Table 3.4 shows some height and depth values found in bibliography when using *A. ferrooxidans* for copper biomachining.

Table 3.4. Height and depths values (μm) reported in bibliography by other authors.

Geometry	Height/depth (μm) (biomachining time)	Shaking speed	Author
Lines	80 (48 h)	Static conditions	Istiyanto et al., 2011
Circular gear	48 (24 h)	Static conditions	Istiyanto et al., 2012
Line	74.75 (4 h)		
Circle	61.75 (4 h)	150 rpm	Hocheng et al., 2012
Square	60.45 (4 h)		
Crescent dimples	14.65 (20 min)		
Circular dimples	13.98 (20 min)	170 rpm	Muhammad et al., 2018
Circular micro pillars	9.56 (100 min)		
Circle	51.1 (7 h)		
Microfluidic geometry	65.3 (6 h)	130 rpm	This study

In another experiment, five treatment times, specifically 0.25, 0.50, 1, 2 and 6 h, were selected to verify that the two-trend behavior observed with the circular geometry remained invariant when engraving the microfluidic structure, and to ascertain the equations that would allow to define the treatment time needed to achieve a desired structure's height. In this case, five pieces were selected and they were independently immersed in the BM solution for the selected time (without intermediate extractions). For comparison purposes, data plotted in Figure 3.8 were used to calculate the average SMRR (SMRR_{av}) for the same time intervals (0.25, 0.50, 1, 2 and 6 h) for the experiment carried out with the circular geometry. The comparison between SMRR_{av} in the samples with the circular geometry and the microfluidic channels is shown in Figure 3.10.

In accordance to the results obtained with the circular geometry, the maximum SMRR_{av} obtained when engraving the microfluidic channel was recorded during the first hour and it maintained approximately constant at $23.5 \text{ mg h}^{-1} \text{ cm}^{-2}$. Then, it decreased in a logarithmic trend along time, regardless of the shape of the structure. The fitting equations are $\text{SMRR}_{\text{av}} = -5.2 \cdot \ln(t) + 20.6$ ($R^2 = 0.9979$) and $\text{SMRR}_{\text{av}} = -6.4 \cdot \ln(t) + 23.1$ ($R^2 = 0.9993$), for the circle and microfluidic channel, respectively.

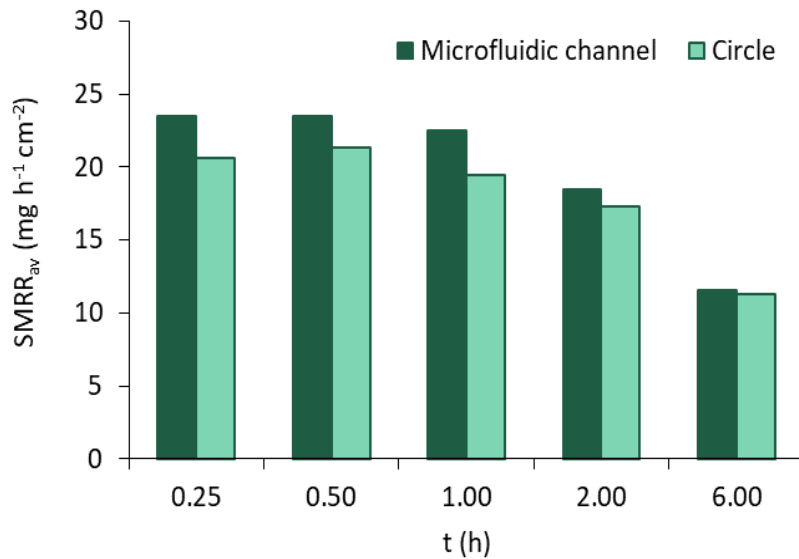


Figure 3.10. SMRR_{av} in the samples with the circular geometry and the microfluidic channels.

Regarding the height of the molds, greater values were achieved in the experiments carried out using the microfluidic structure than the circular geometry. As an example, after 6 h of biomachining the microchannel's height ($63.5 \pm 5.1 \mu\text{m}$) was 28 % greater than the circle's ($51.1 \pm 4.1 \mu\text{m}$). This was attributed to the slightly higher SMRR_{av} during the first hours and the smaller surface area exposed to the solution due to the area covered by the mask.

The equations that allow predicting the treatment time (t, h) required to obtain a serpentine channel mold with a certain engraved height (Ht, μm) were calculated for each interval (Equations 3.1 and 3.2):

$$t = 0-1 \text{ h} \quad t = 0.047 \cdot Ht \quad (R^2=0.9912) \quad \text{Eq. 3.1}$$

$$t = 1-7 \text{ h} \quad t = 0.564 \cdot e^{0.036 \cdot Ht} \quad (R^2=0.9994) \quad \text{Eq. 3.2}$$

These equations provide a simple tool to easily determine the biomachining time for obtaining a desired engraved height in a microfluidic structure. Using the previous equations for mold biomachining could result in a longer total time for the process than the expected using other techniques; however, an exhaustive control during the entire process by qualified personnel or the use of a clean room facility are not necessary, a fact that drastically reduces the total costs of the process. Thus, the biologically assisted etching method was concluded to be low time consuming for the laboratory personnel and with no need of supplementary pre-treatments. In addition, an accurate control of the resulting structure can be obtained because this procedure enabled the measure of the structures at every moment during every mold-etching step.

On the contrary, in some process such as soft-lithography, the user could only measure the shape of the structure at the end, not allowing rectifications in case of possible mistakes.

Figure 3.11 shows the molds manufactured after 0.25, 0.5, 2 and 6 h of biomachining, corresponding to a height of 4.7 ± 0.4 , 11.0 ± 2.3 , 34.1 ± 4.7 and 65.3 ± 5.1 μm , respectively.

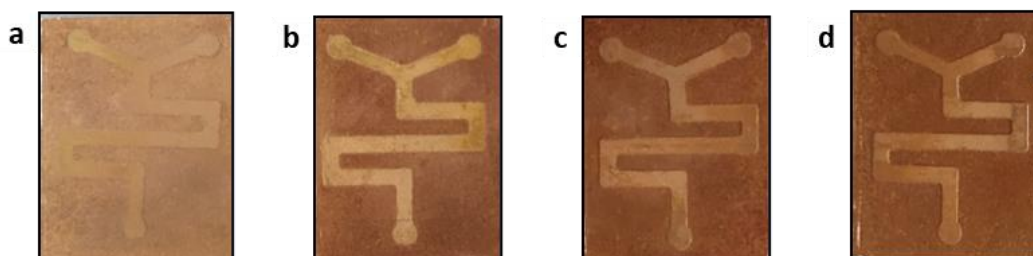


Figure 3.11. Molds for the fabrication of microfluidic devices obtained after 15 min (a), 30 min (b), 2 h (c) and 6 h (d) of biomachining.

3.3.2.2. Prolonging the BM solution lifespan for a more sustainable process

The fabrication of PDMS microfluidic devices would greatly benefit from obtaining a metallic mold of the desired height minimizing the time invested and the economic and environmental costs of the process. To this end, extending the lifespan of the BM solution is an alternative that would reduce the consumption of chemical reagents and the management cost of the exhausted solution, thus having a positive impact on the sustainability of the biomachining process and circular economy.

The use of the regenerated BM solution for biomachining rendered similar results to those obtained in the single stage assay employing fresh solution. As observed in Figure 3.12a, it is particularly remarkable that the SMRR_{av} remained invariant for each treatment time in several consecutive mold-etching stages using the regenerated BM solution, which is of great interest for ensuring that the same amount of copper will be dissolved when a piece is exposed to the solution for a certain treatment time.

In this study, the SMRR_{av} was maximum and remained constant at 24.3 ± 0.6 $\text{mg h}^{-1} \text{cm}^{-2}$ in 7 consecutive mold-etching steps when the treatment lasted less than 1 h (Figure 3.12a). In longer treatments, 17.7 ± 1.4 and 10.9 ± 0.4 $\text{mg h}^{-1} \text{cm}^{-2}$ were removed in the 2 h (average of 6 consecutive stages) and 6 h (average of 5 consecutive stages) biomachining, respectively. These results confirm that the equations proposed to predict the time needed to obtain a mold with a certain height for the fabrication of PDMS devices (Equations 3.1 and 3.2) are applicable when both fresh and regenerated BM solution are employed.

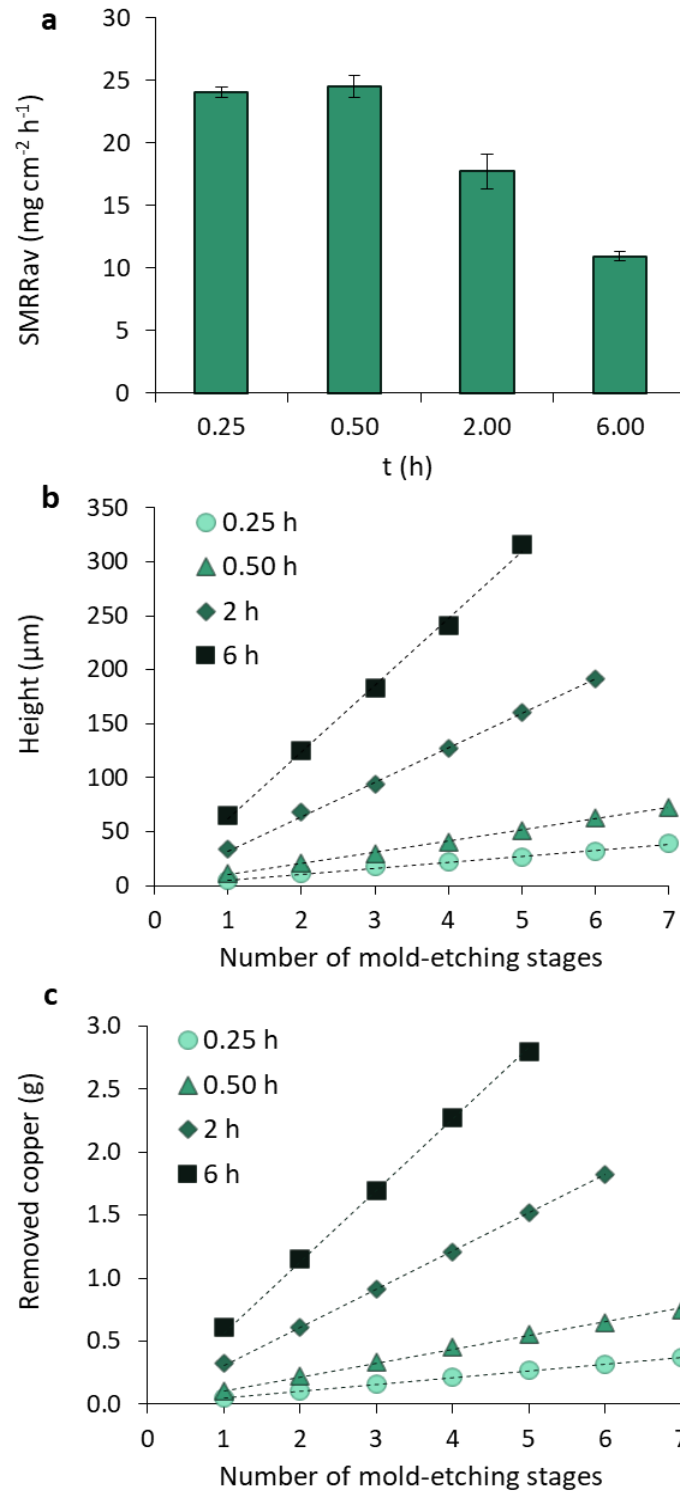


Figure 3.12. Average SMRR for each selected treatment time (a), and variation of mold's height (b) and removed copper (c) with the number of mold-etching stages.

The linear regression equations that fit the data plotted in Figures 3.12b and 3.12c are summarized in Table 3.5.

Table 3.5. Linear equations that correlate mold's height (μm) and removed copper mass (m_{Cu} , g) with the number of mold-etching stage (N).

Treatment time (h)			
0.25	0.50	2	6
Ht = 5.4·N	Ht = 10.3·N	Ht = 32.0·N	Ht = 62.0· N
R ² =0.9959	R ² =0.9992	R ² =0.9988	R ² =0.9983
$m_{\text{Cu}} = 0.05 \cdot N$	$m_{\text{Cu}} = 0.11 \cdot N$	$m_{\text{Cu}} = 0.30 \cdot N$	$m_{\text{Cu}} = 0.56 \cdot N$
R ² =0.9999	R ² =0.9996	R ² =0.9999	R ² =0.9998

In accordance with these results, the increase in the structure's height remained practically constant for each mold-etching time throughout the experiment (5.2 ± 1.2 , 10.1 ± 0.9 , 32.2 ± 4.1 and $63.3 \pm 7.8 \mu\text{m}$ for the 0.25, 0.5, 2 and 6-h treatment) and, consequently, this parameter increased linearly as the consecutive etching stages progressed (Figure 3.12b). The accumulated amount of removed copper is shown in Figure 3.12c. The average copper mass dissolved in each mold-etching step was 52.6 ± 2.5 , 106.9 ± 9.8 , 313.2 ± 23.2 and $571.1 \pm 34.5 \text{ mg}$, and thus, assuming that all the removed copper was in the solution, the metal concentration at the end of the experiment (after several treatment + regeneration stages) would be 2.8, 5.8, 13.5 and $20.6 \text{ g Cu}^{2+} \text{ L}^{-1}$ for the 0.25, 0.50, 2 and 6 h treatment, respectively.

The inclusion of a regeneration step was proven to be a successful strategy for the recovery of the oxidizing capacity of the BM solution. After each mold-etching stage, microorganisms were able to re-oxidize all the Fe^{2+} in the BM solution and, thus, after each regeneration step, all the iron was in the Fe^{3+} form, ready to be used in the next treatment. Figure 3.13a shows the variation of Fe^{3+} in the sample treated for 2 h in 6 mold-etching + regeneration stages, as a representative example of the process. The regeneration time increased with the amount of Fe^{2+} to be re-oxidized (3.13b). As an example, after the first 6 h mold-etching stage the regeneration time was 3.4-fold higher than the time needed in the 0.25 h treatment.

Likewise, this parameter also increased with the number of treatment stages in all samples, as higher amounts of dissolved copper in the medium affected the process. The time needed to re-oxidize the BM solution used in the 0.25 mold-etching assay increased 30 % between the first and last regeneration stage. Thus, copper concentration lower than 3 g L^{-1} was concluded to slightly affect the ability of *A. ferrooxidans* DSM 14882 to re-oxidize the Fe^{2+} present in the BM solution under the selected operating conditions. The equations summarized in Table 3.6 allowed the estimation of the regeneration time according to the copper concentration.

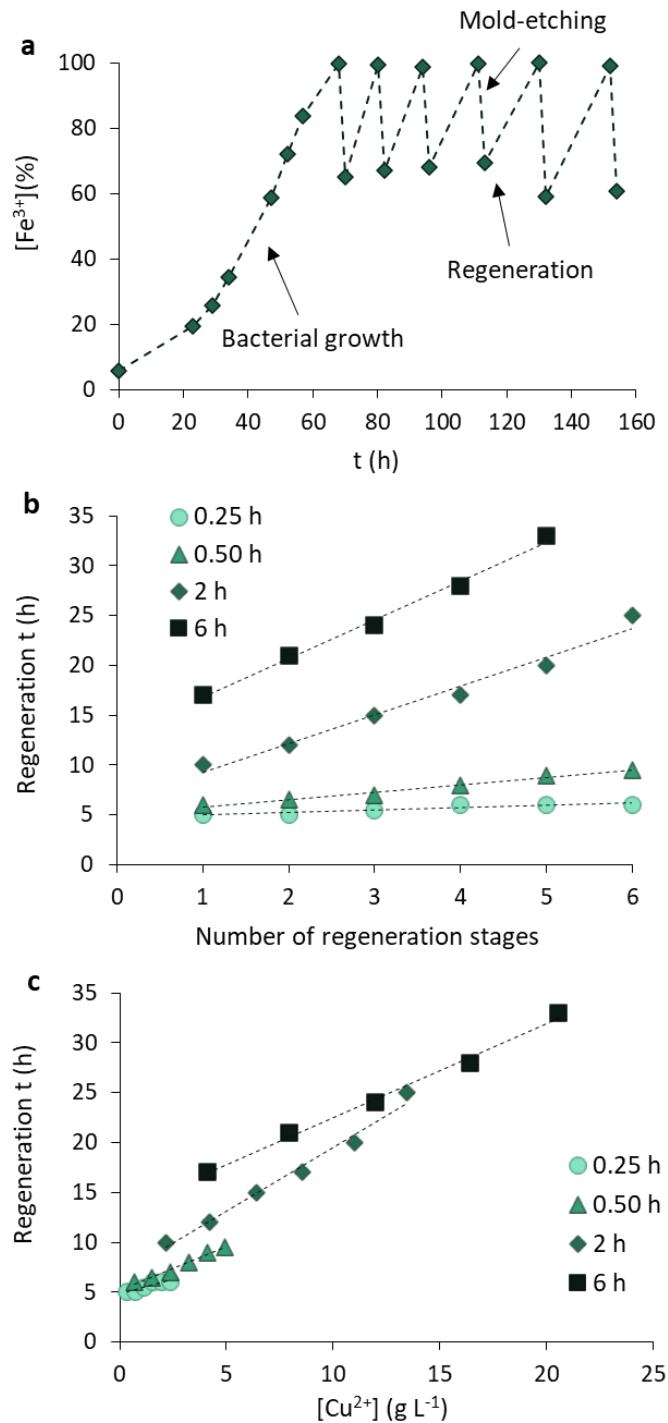


Figure 3.13. Variation of Fe^{3+} concentration during the successive mold-etching (2 h) and regeneration stages (a), and the regeneration time with stage number (b) and with copper concentration (c).

Conversely, higher copper concentrations affected more severely the biological iron oxidation process, and the time needed to regenerate the BM solution increased linearly with the metal concentration for each selected treatment time (0.5, 2.0 and 6.0 h) (Figure 3.13c).

The equations summarized in Table 3.6 allowed the estimation of the regeneration time according to the copper concentration.

Table 3.6. Relationship between the regeneration time (t_{regen} , h) and the concentration of dissolved copper (Cu, g L⁻¹).

Treatment time (h)			
0.25	0.50	2	6
$t_{\text{regen}} = 4.7 + 0.6 \cdot \text{Cu}$	$t_{\text{regen}} = 5.2 + 0.9 \cdot \text{Cu}$	$t_{\text{regen}} = 6.7 + 1.3 \cdot \text{Cu}$	$t_{\text{regen}} = 13.1 + 0.9 \cdot \text{Cu}$
$R^2=0.8537$	$R^2=0.9830$	$R^2=0.9833$	$R^2=0.9940$

Valix (2017) found that high concentrations of dissolved copper led to the denaturation of the proteins and nucleic acids necessary for the bacterial metabolic activities inhibiting, thus, the bacterial activity. However, the results obtained in this study showed that, after subjecting the bacteria to the presence of increasing concentrations of dissolved copper, the biomass was able to tolerate up to 20.6 g Cu²⁺ L⁻¹. Albeit bacterial activity was not completely inhibited at this copper concentration, the time needed for Fe²⁺ re-oxidation after the last 6 h mold-etching stage ($t_{\text{regen}} = 33$ h) doubled the value for the first regeneration ($t_{\text{regen}} = 17$ h).

These results are in agreement with those obtained in Chapter 2 where it was concluded that increasing concentrations of dissolved copper slowed down bacterial activity if the microorganisms were not previously adapted to the metal presence. Many authors have studied the resistance capacity of *A. ferrooxidans* bacteria to different copper concentrations and the maximum tolerance for different bacterial strains to this metal reportedly ranged between 0.6 and 25 g Cu L⁻¹ (Leduc et al., 1997; Das et al., 1998; Novo et al., 2000; Wu et al., 2010; Cabrera et al., 2015). A complete inhibition of *A. ferrooxidans* bacterial activity by a Cu²⁺ concentration above 10.8 g L⁻¹ was found by Cho et al. (2008). Similarly, Díaz-Tena et al., (2016) observed a drastic reduction in the Fe²⁺ bacterial oxidation in the presence of 6.1 g Cu²⁺ L⁻¹. Additionally, Mykytczuk et al. (2011) have founded a copper tolerance ranging between 0.3 to 9.5 g Cu²⁺ L⁻¹ for six *A. ferrooxidans* strains.

From the obtained results a mold etching process to obtain molds for the fabrication of microfluidic devices is proposed. Thus, once the etching treatment is completed, the solution bioregenerated by bacteria allows its reuse in successive treatment stages, leading to a cyclical process capable of producing molds with different engraved heights or geometries. The reuse of the BM solution in several consecutive etching stages lead to a successful fabrication of metallic molds, contributing to the sustainability of the process both from an environmental and economic point of view.

Figure 3.14 shows the schematics of the proposed etching + regeneration process.

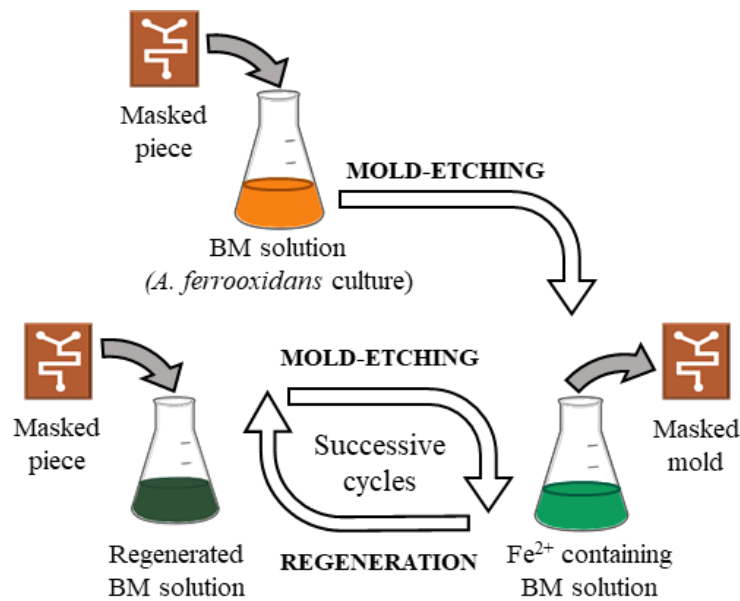


Figure 3.14. Schematic of the etching + regeneration process for engraving of microfluidic structures.

3.3.3. Biomachining with immobilized biomass

As concluded in Chapter 2, biomass immobilization on suitable support materials can increase the production of ferric iron and therefore reduce the iron bio-oxidation time. However, the research on how immobilized biomass can improve the SMRR and engraved heights is scarce.

Thus, the use of *A. ferrooxidans* bacteria immobilized on bacterial cellulose (A-BC) was studied in order to ascertain if it was of any benefit for the process efficiency after several consecutive etching + regeneration cycles. The ability of the biologically active material to regenerate the biomachining solution in the presence of increasing concentration of dissolved copper was also investigated. A simple geometry (rectangle) and 2 h treatment time were selected.

As far as the $SMRR_{av}$ is concerned, two different behaviors were recorded in the samples without and with active material (BM-susp vs BM-BC_{IN}/BM-BC_{OUT}). When the biomachining process was carried out in the presence of suspended biomass (BM-susp), the $SMRR_{av}$ remained practically constant in the 4 mold-etching stages (data not shown), as also concluded in μ n 3.3.2.2. *Prolonging the BM lifespan for a more sustainable process*. However, the average value calculated in this cell suspension experiment ($21.8 \pm 1.8 \text{ mg Cu h}^{-1} \text{ cm}^{-2}$) was higher than reported in Section 3.3.2.2. *Prolonging the BM solution lifespan for a more sustainable process* ($17.7 \pm 1.4 \text{ mg Cu h}^{-1} \text{ cm}^{-2}$) which was attributed to the higher shaking speed (130 vs 170 rpm).

Conversely, in the samples containing active material a maximum $SMRR_{av}$ value was reached in the first stage, regardless of the operation mode ($SMRR_{av} = 19.2 \pm 1.2 \text{ mg Cu h}^{-1} \text{ cm}^{-2}$ in the BC_{OUT} experiment and $20.7 \pm 2.9 \text{ mg Cu h}^{-1} \text{ cm}^{-2}$ in the BC_{IN} experiment) (Figure 3.15). Afterwards, the value slightly decreased and kept approximately constant at $17.23 \pm 0.3 \text{ mg Cu h}^{-1} \text{ cm}^{-2}$ in three consecutive mold-etching stages when the immobilized biomass was periodically removed from the solution (BC_{OUT} experiment) (Figure 3.15). By contrast, when the biomachining process was carried out in the presence of the immobilized biomass ($BM-BC_{IN}$), the $SMRR_{av}$ progressively decreased until a final value of $14.8 \pm 2.1 \text{ mg Cu h}^{-1} \text{ cm}^{-2}$ was achieved after 4 etching stages (Figure 3.15). This behavior can be attributed to a worse contact between the surface of the copper workpiece and the oxidant due to the presence of A-BC inside the reactor.

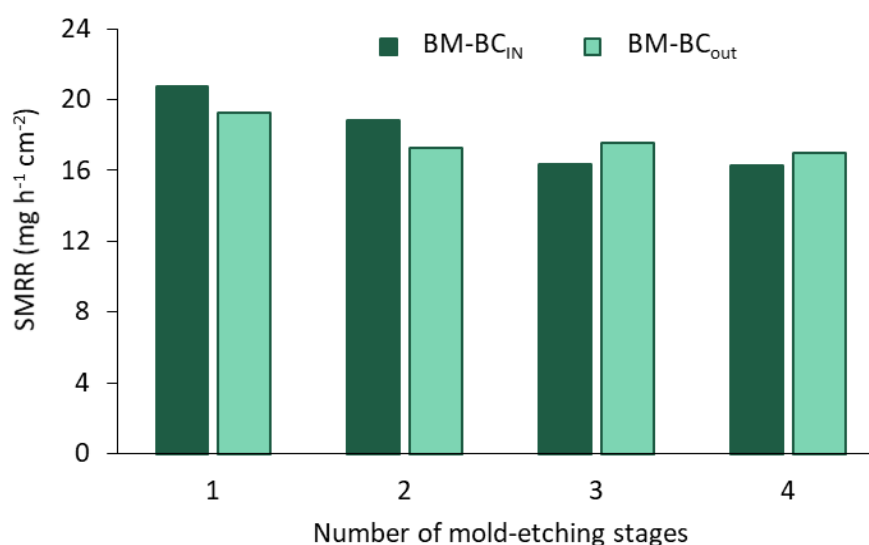


Figure 3.15. Evolution of SMRR for the experiments with immobilized biomass.

The evolution of structure's height, the removed copper amount and the time needed for Fe^{2+} re-oxidation in each regeneration stage throughout the consecutive mold-etching stages for each experiment are plotted in Figures 3.16a-c.

The structure's height (Figure 3.16a) and the removed copper amount (Figure 3.16b) increased linearly as the consecutive etching stage progressed. Regarding mold's height, greater values were achieved in the experiments carried out using the suspended biomass, being this value 1.1 and 1.2 times higher than the value achieved in the molds obtained in $BM-BC_{IN}$ and $BM-BC_{OUT}$ experiments, respectively (data not shown). At the end of the experiments, after four mold-etching + regeneration stages, a total height of 104.4 ± 8.8 , 99.3 ± 4.0 and $118.4 \pm 3.2 \mu\text{m}$ was obtained in $BM-BC_{IN}$, $BM-BC_{OUT}$ and $BM-Susp$ biomachined samples, respectively.

Table 3.7 shows the linear equations that relate the mentioned parameters.

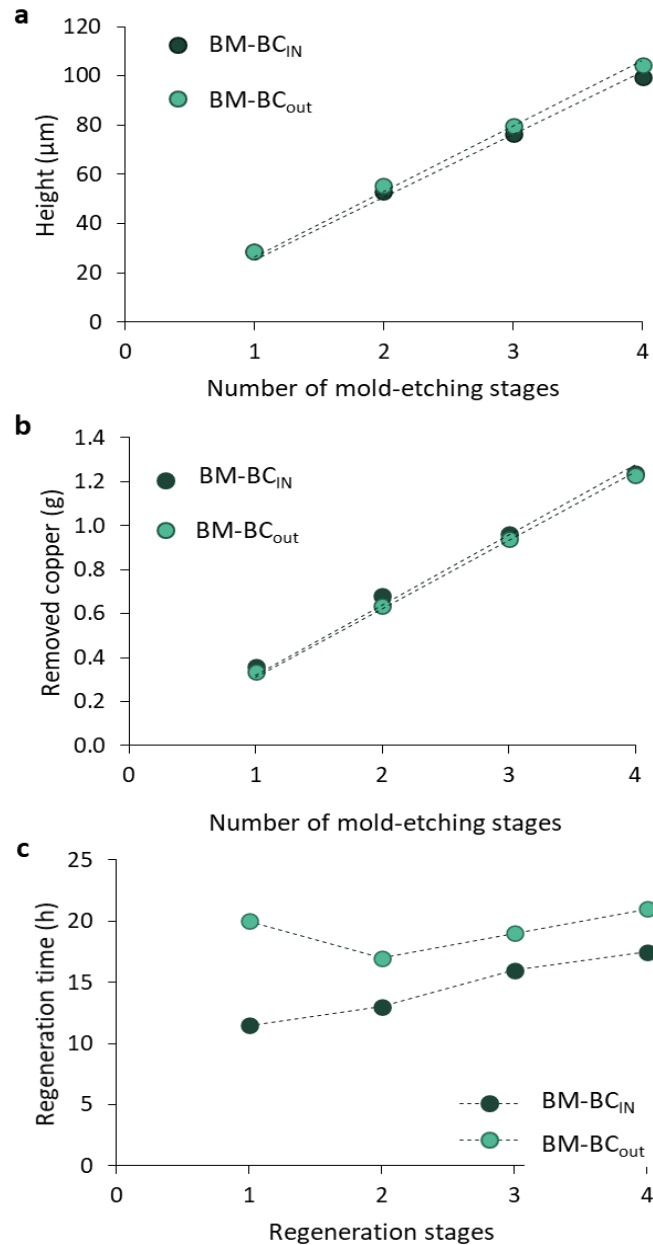


Figure 3.16. Evolution of structure's height (a) and removed copper mass throughout the consecutive mold-etching stages (b), and time needed for Fe²⁺ oxidation after each regeneration stage (c) for BM-BC_{IN} and BM-BC_{OUT}.

Table 3.7. Linear equations that correlate the height of the structure (Ht, μm) and the amount of copper removed (m_{Cu}, g) with the number of mold-etching stages (N).

Experiment	Equation	R ²
BM-BC _{IN}	Ht = 25.381·N	0.9924
	m _{Cu} = 0.319·N	0.9985
BM-BC _{OUT}	Ht = 26.528·N	0.9957
	m _{Cu} = 0.311·N	0.9980

The total amount of copper dissolved at the end of the experiment (4 mold-etching stages) was 1.2 ± 0.1 , 1.2 ± 0.1 and 1.5 ± 0.1 g for BM-BC_{IN}, BM-BC_{OUT} and BM-Susp, respectively (Figure 3.16b). Thus, assuming all the removed copper was dissolved in the medium, the metal concentration at the end of the experiment was 12.4, 12.7 and 14.8 g Cu²⁺ L⁻¹ for BM-BC_{IN}, BM-BC_{OUT} and BM-Susp samples, respectively.

As expected, increasing Cu concentrations prolonged the re-oxidation process in the regenerations stage when using immobilized biomass. After each etching stage, immobilized *A. ferrooxidans* bacteria were able to re-oxidize Fe²⁺ to Fe³⁺, allowing the BM solution to be re-used in new treatment cycles (Figure 3.16c). Nevertheless, shorter regeneration times were required when the copper biomachining was carried out in the presence of A-BC (Figure 3.16c). It took 42 % longer to complete the Fe²⁺ re-oxidation in the presence of almost the same copper concentration (3.6 and 3.3 g Cu²⁺ L⁻¹ in the BM-BC_{IN} and BM-BC_{OUT} reactors, respectively) when the active material was removed during the biomachining stage in comparison to the reactors where the copper dissolution was carried out in the presence of A-BC.

This behavior was attributed to the adaptation of the immobilized microorganisms to the presence of the metal when the biomachining was carried out with the active material. On the contrary, when the A-BC pieces were reintroduced in the copper containing reactor, the bacteria required longer time to adapt to the medium, which slowed down the oxidant regeneration process. These results are in agreement with those obtained in Chapter 2, where it was concluded that the oxidation time in the presence of increasing concentrations of dissolved copper decreased considerably when the active material had already been exposed to the metal. For example, when culturing A-BC in the presence of 20 g Cu²⁺ L⁻¹, the complete Fe²⁺ oxidation was reduced 46 % when comparing adapted (A-BC previously cultured in the presence of 15 g Cu²⁺ L⁻¹) and non adapted (not previously exposed to copper) active material.

Thus, as the A-BC adapted to the presence of increasing copper concentrations, the time required to re-oxidize the Fe²⁺ after the fourth mold-etching stages was 17 % longer in BM-BC_{OUT} than in BM-BC_{IN}. These results are in agreement with those reported by other authors who have suggested that the tolerance of microorganisms to different metals can be increased if they are adapted to the metal presence during growth (Ilyas et al., 2007; Ravindra et al., 2015; Pourhossein and Mousavi, 2018; Liang et al., 2019).

In these experiments, the difference in the regeneration time between the immobilized and suspended biomass was not remarkable (data not shown). Nevertheless, the benefit of using immobilized microorganisms lies in the ease of handling (feeding and replacing) of the biomass in large-scale operation.

Figure 3.17 shows the photographs of the biomachining solution after several mold-etching + regeneration stages in the BM- BC_{IN} experiment.

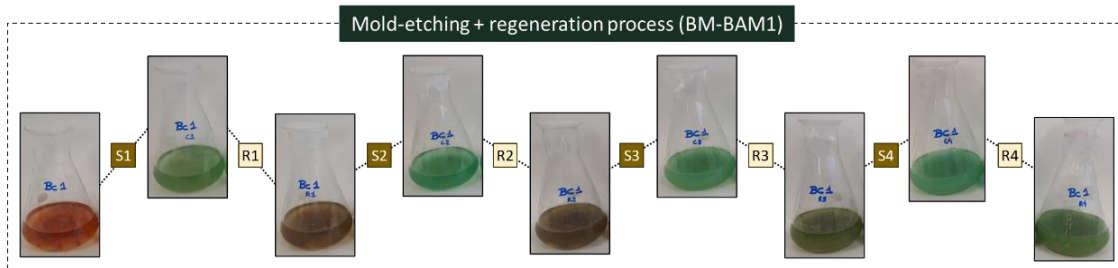


Figure 3.17. Photographs of the biomachining solution during the BM- BC_{IN} experiment (where S_x is the number of the mold-etching stage and R_x the corresponding regeneration stage).

The regeneration time was affected when the active material was removed during the biomachining stages and reintroduced for the regeneration stages, probably due to the sudden exposure to increasing concentrations of dissolved copper. Therefore, in view of the obtained results, it is proposed for further studies the possibility of storing the A-BC in the presence of a certain dissolved copper concentration (5 g Cu L⁻¹, for example) while carrying out the biomachining stage, to prevent microorganism's shock when being reintroduced into the reactor containing increasing dissolved copper concentrations.

3.3.4. Fabrication of PDMS devices

Once the biomachining process was completed, the resulting molds could be used for the manufacture of PDMS devices. The microfluidic devices were fabricated using the protocol presented in the Section 3.2.5 *Fabrication of the PDMS devices* (Figure 3.18a). The final structure of a PDMS microfluidic device fabricated from a workpiece mold biomachined for 6 etching stages of 6 h (36 treatment h), with a channel height of 316.9±5.4 μm is presented in the Figure 3.18a-3 as a proof of concept. Similar devices were obtained with the molds obtained by the other biomachining times investigated.

It is worth to mention here that, due to the high roughness of the surface obtained by the biomachining process, it was difficult to bond the PDMS replica to other PDMS or glass surface, even after plasma treatment of both surfaces. Therefore, the PDMS replica was closed using a PSA layer as a bottom base of the device. No leaching was observed for any of the devices investigated, using this fabrication protocol.

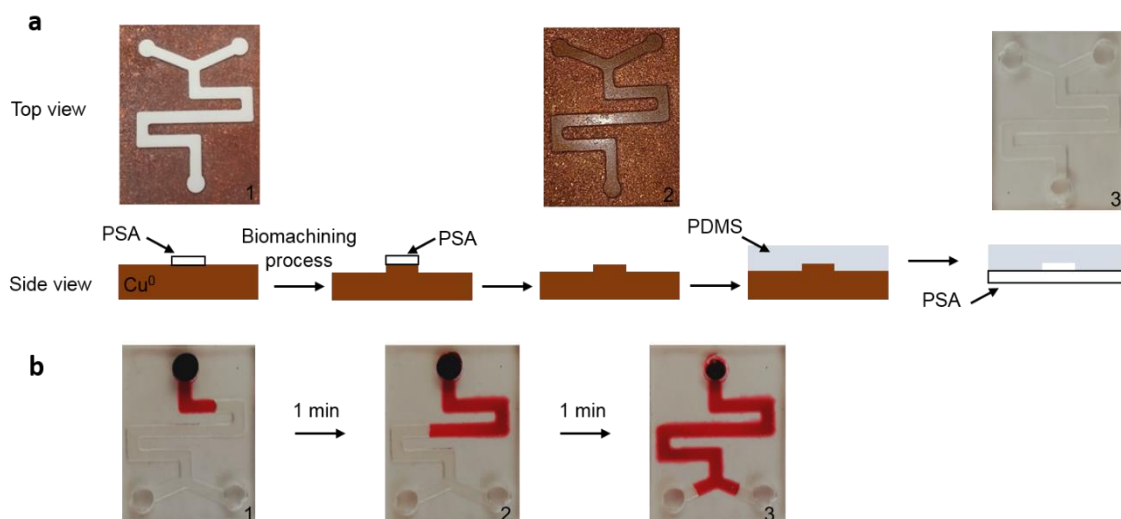


Figure 3.18. Fabrication (a) and performance (b) of a hybrid PDMS/PSA microfluidic device ($316.9 \pm 5.4 \mu\text{m}$ height) fabricated using a mold obtained after 36 h of biomachining.

Then, the degasification of the microfluidic device was performed in order to generate a self-powered microfluidic device, which is able to move the liquid in the microchannel by degass-driven flow (Liang et al., 2011). Later, a colored solution was placed at the inlet of the device and the liquid was observed to advance through the entire serpentine in less than 3 min, see [Video](#). This result demonstrated that, despite the use of a hydrophobic substrate for the base (the PSA layer) that increases the flow resistance, the fluidic properties of the device were verified. Figure 3.18b shows three snapshots of the movement of the red colored solution over time, though a $316.9 \pm 5.4 \mu\text{m}$ height micro-channel obtained after a 6 h machining process. The robustness of the resulting metallic molds allowed the generation of multiple microfluidic devices, with the exact microchannel dimensions, by a very repetitive fabrication process.

Finally, it should be pointed out that biomachining permitted the creation of more durable molds since metallic components are more robust than other materials such as polymers, *e.g.* SU8. In addition, this process did not require the need of any cleanroom facilities, without the limitation of conventional lithography fabrication conditions. Moreover, by just replacing the mask at different steps of the process could lead to the creation of more complex structures than the one presented here, obtaining microstructures of different heights in the same mold. This is possible thanks to the ability of the technique to control the metal removal rate with high precision at the micrometer level in short-period of time.

3.4. CONCLUSIONS

This chapter has focused on studying the biomachining process as a sustainable alternative to the traditional techniques for manufacturing well-defined microfluidic structures on metal pieces. It was used to engrave copper molds with the final objective of elaborating functional PDMS microfluidic devices.

The first stage of the biomachining of copper pieces was the selective protection of the surface not to be engraved. This requirement was fulfilled with the combination of one common lacquer (red light bulb lacquer) and a PSA adhesive, being a feasible and efficient alternative that did not damage bacterial activity.

Copper removal presented two distinct behaviors during mold biomachining using cell suspension: it was maximum in the 0-1 h range ($SMRR_{av} = 20-22 \text{ mg h}^{-1} \text{ cm}^{-2}$) and, afterwards, it decreased with a logarithmic trend. The equations that allow predicting the treatment time required for obtaining a serpentine channel mold (height) were determined for the two trends. They proved to be a simple tool to select the immersion time needed to obtain the desired structure ($t = 0-1 \text{ h}$, $t = 0.047 \cdot \text{height}$; $t = 1-7 \text{ h}$, $t = 0.564 \cdot \exp(0.036 \cdot \text{height})$).

The inclusion of a regeneration step was proven to be a successful strategy for the recovery of the oxidizing capacity of the BM solution after successive mold-etching stages and, hence, it allowed to extend solution lifespan and reduce the consumption of chemical reagents. It is noteworthy that the use of the regenerated BM solution rendered similar results to those achieved with the fresh BM medium in terms of $SMRR_{av}$ and mold height. Nevertheless, the increasing dissolved copper concentration affected the time needed for ion re-oxidation. Despite the fact that concentrations lower than $3 \text{ g Cu}^{2+} \text{ L}^{-1}$ Cu did not severely impact the regeneration process, the re-oxidation time increased linearly at higher metal concentrations.

The $SMRR_{av}$ and height values were similar when using suspended or immobilized biomass. Nevertheless, the additional benefit of the latter one would lie in the ease of handling the biomass in large-scale operation. Another benefit is that shorter regeneration times were required when the copper biomachining was carried out in the presence of the active biocellulose.

In summary, the proposed process has proved to be a feasible and sustainable technology for this application. In addition, several advantages can be highlighted, such as: a clean room facility is not necessary (which reduces the total costs of the process), the process is less time-consuming for the laboratory personnel in comparison to other conventional manufacturing techniques, and the height of the resulting structure can be measured at any moment during the mold-etching step.

3.5. REFERENCES

- Aaron, M. Streets, A.M., Huang, Y., 2013. Chip in a lab: Microfluidics for next generation life science research. *Biomicrofluidics*. 7, 011302.
- Azarsa, E., Jeyhani, M., Ibrahim, A., Tsai, S.S.H., Papini, M., 2020. A novel abrasive water jet machining technique for rapid fabrication of three-dimensional microfluidic components. *Biomicrofluidics*. 14, 044103.
- Cabrera, G., Gómez, J.M., Cantero, D., 2005. Influence of heavy metals on growth and ferrous sulphate oxidation by *Acidithiobacillus ferrooxidans* in pure and mixed culture. *Process Biochemistry*. 40, 2683-2687.
- Chiu, D.T., de Mello, A.J., Di Carlo, D., Doyle, P.S., Hansen, C., Maceiczky, R.M., Wootton, R.C.R., 2017. Small but Perfectly Formed? Successes, Challenges, and Opportunities for Microfluidics in the Chemical and Biological Sciences. *Chem*, 2, 201-223.
- Cho K. S., Ryu H. W., Choi H. M., 2008. Toxicity Evaluation of Complex Metal Mixtures Using Reduced Metal Concentrations: Application to Iron Oxidation by *Acidithiobacillus ferrooxidans*. *Journal of Microbiology and Biotechnology*. 18, 1298-1307.
- Das, A., Modak, J.M., Natarajan, K.A., 1998. Surface chemical studies of *Thiobacillus ferrooxidans* with reference to copper tolerance. *Antonie Van Leeuwenhoek*. 73, 215-222.
- Díaz-Tena E, Gallastegui G, Barona A, Rodríguez A, López de Lacalle, L. N., Elías A., 2017. Biomachining: metal etching via microorganisms. *Critical Reviews in Biotechnology*. 37,323-332.
- Díaz-Tena, E., Gallastegui, G., Hipperdinger, M., Donati, E. R., Ramírez, M., Rodríguez, A., López de Lacalle, L. N., Elías, A., 2016. New advances in copper biomachining by iron-oxidizing bacteria. *Corrosion Science*. 112, 385-392.
- Díaz-Tena, E., Gallastegui, G., Hipperdinger, M., Donati, E. R., Rojo, N., Santaolalla, A., Ramírez, M., Barona, A., Elías, A., 2018. Simultaneous culture and biomachining of copper in MAC medium: a comparison between *Acidithiobacillus ferrooxidans* and *Sulfobacillus thermosulfidooxidans*. *ACS Sustainable Chemistry and Engineering*. 6, 17026-17034.
- Díaz-Tena, E., Rodríguez-Ezquerro, A., López de Lacalle, Marcaide, L. N., Gurtubay L., Elías, A., 2014. A sustainable process for material removal on pure copper by use of extremophile bacteria. *Journal of cleaner production*. 84, 752-760.
- Ferraz, M.D.M.M., Nagashima, J.B., Venzac, B., Le Gac, S., Songsasen, N., 2020. 3D printed mold leachates in PDMS microfluidic devices. *Scientific Reports*. 10, 994.
- Gale, B.K., Jafek, A.R., Lambert, C.J., Goenner, B.L., Moghimifam, H., Nze, U.C., Kamarapu, S.K., 2018. A Review of Current Methods in Microfluidic Device Fabrication and Future Commercialization Prospects. *Inventions*. 3, 60.
- Gao, Y., Stybayeva, G., Revzin, A., 2019. Fabrication of composite microfluidic devices for local control of oxygen tension in cell cultures. *Lab on a Chip*, 19, 306-315.
- Hocheng, H., Chang, J., Jadhav, U.U., 2012c. Micromachining of various metals by using *Acidithiobacillus ferrooxidans* 13820 culture supernatant experiments. *Journal of Cleaner Production*. 20, 180-185.
- Ilyas, S., Anwar, M.A., Niazi, S.B., Ghauri, M.A., 2007. Bioleaching of metals from electronic scrap by moderately thermophilic acidophilic bacteria. *Hydrometallurgy*. 88, 180-188.

- IngledeW, W.J., 1982. *Thiobacillus ferrooxidans*. The bioenergetics of an acidophilic chemolithotroph. *Biochimica et Biophysica Acta*. 683, 89-117.
- Istiyanto J., Dwi Muhadiyantoro D., Whulanza Y., 2018. Modification of surface roughness for a narrow path microfluidic application. *AIP Conference Proceedings* 1983, 040012.
- Istiyanto, J., Kim, M.Y., Ko, T.J., 2011. Profile characteristics of biomachined copper. *Microelectronic Engineering*. 88, 2614-2617.
- Istiyanto, J., Ko, T.J., Yoon, I.C., 2010. A study on copper micromachining using microorganisms. *International Journal of Precision Engineering and Manufacturing*. 11, 659-664.
- Istiyanto, J., Saragih, A.S., Ko, T.J., 2012. Metal based micro-feature fabrication using biomachining process. *Microelectronic Engineering*. 98, 561-565.
- Jadhav, U., Hocheng, H., Weng, W.H., 2013. Innovative use of biologically produced ferric sulfate for machining of copper metal and study of specific metal removal rate and surface roughness during the process. *Journal of Materials Processing Technology*. 213, 1509-1515.
- Juergensmeyer, M.A., Nelson, E.S., Juergensmeyer, E.A., 2007. Shaking alone, without concurrent aeration, affects the growth characteristics of *Escherichia coli*. *Letters in Applied Microbiology*. 45, 179-183.
- Junfeng, Y., Guoliang, L., Wei, C., 2007. Ferrous sulphate oxidation using *Acidithiobacillus ferrooxidans* cells immobilized in ceramic beads. *Chemical and Biochemical Engineering Quarterly*. 21, 175-179.
- Kadivar, S., Pourhossein, F., Mousavi, S.M., 2021. Recovery of valuable metals from spent mobile phone printed circuit boards using biochar in indirect bioleaching. *Journal of Environmental Management*. 280, 111642.
- Kaksonen, A.H., Lavonen, L., Kuusenaho, M.K., Kolli, A., Närhi, H.M., Vestola, E.A., Puhakka, J.A., Tuovinen, O.H., 2011. Bioleaching and recovery of metals from final slag waste of the copper smelting industry. *Minerals Engineering*. 24, 1113-1121.
- Kumar, P.S., Yaashikaa, P.R., 2020. Recent trends and challenges in bioleaching technologies. In *Biovalorisation of Waste to Renewable Chemicals and Biofuels*; Rathinam, N.K., Sani, R.K., Eds.; Elsevier: Amsterdam, The Netherlands, 373-388.
- Lambert, F., Gaydardzhiev, S., Léonard, G., Lewis, G., Bareel, P.F., Bastin, D., 2015. Copper leaching from waste electric cables by biohydrometallurgy. *Minerals Engineering*. 76, 38-46.
- Leduc, L.G., Ferroni, G.D., Trevors, J.T., 1997. Resistance to heavy metals in different strains of *Thiobacillus ferrooxidans*. *World Journal of Microbiology and Biotechnology*. 13, 453-455.
- Liang, D. Y., Tentori, A. M., Dimov, I. K. Lee, L. P., 2011. Systematic characterization of degas-driven flow for poly(dimethylsiloxane) microfluidic devices. *Bio microfluidics*. 5, 024108
- Liang, G., Lin, W., He, Q., Liu, W., Zhou, Q., 2018. Mechanism of energy metabolism for adapted *Acidithiobacillus ferrooxidans* to copper resistance. *Environmental Progress and Sustainable Energy*. 38, 13054.
- Liaros, N., Fourkas, J.T., 2019. Ten years of two-color photolithography. *Optical Materials Express*. 9, 3006-3020.
- Lunelli, L., Barbaresco, F., Scordo, G., Potrich, C., Vanzetti, L., Marasso, S. L., Cocuzza, M., Pirri, C.F., Pederzoli, C., 2020. PDMS-Based Microdevices for the Capture of MicroRNA Biomarkers. *Applied Sciences*. 10, 3867.

- Ma F., Huang H., Cui C., Mater J., 2020. Biomachining properties of various metals by microorganisms. *Process Technology*. 278, 116512.
- Muhammad, I., Khatoon, T., Ullah, S. M. S., Ko, T. J., 2018. Development of Empirical Model for Biomachining to Improve Machinability and Surface Roughness of Polycrystalline Copper. *International Journal of Precision Engineering and Manufacturing-Green Technology*. 5, 201-209.
- Muhammad, I., Sana Ullah, S. M., Sup Han, D., Jo Ko, T., 2015. Selection of optimum process parameters of biomachining for maximum metal removal rate. *International Journal of Precision Engineering and Manufacturing-Green Technology*. 2, 307-313.
- Mykytczuk, N. C. S., Trevors, J. T., Ferroni, G. D., Leduc, L. G., 2011. Cytoplasmic membrane response to copper and nickel in *Acidithiobacillus ferrooxidans*. *Microbiological Research*. 166, 186-206.
- Nie, H.C.Y., Zhu, N., Wu, P., Zhang, T., Zhang, Y., Xing, Y., 2015. Isolation of *Acidithiobacillus ferrooxidans* strain Z1 and its mechanism of bioleaching copper from waste printed circuit boards. *Journal of Chemical Technology and Biotechnology*. 90, 714-721.
- Novo, M. T., da Silva, A. C., Moreto, R., Cabral, P. C., Costacurta, A., Garcia, O. Jr, Ottoboni, L. M., 2000. *Thiobacillus ferrooxidans* response to copper and other heavy metals: growth, protein synthesis and protein phosphorylation. *Antonie van Leeuwenhoek, International Journal*. 77, 187–19.
- Pandey, P., Shan, H., 2012. *Modern Machining Processes*. Tata McGraw-Hill Publishers, India (2012 Ed.).
- Pogliani, C., Donati, E., 2000. Immobilization of *Thiobacillus ferrooxidans*: importance of jarosite precipitation. *Process Biochemistry*. 35, 997-1004.
- Pourhossein, F., Mousavi, S.M., 2018. Enhancement of copper, nickel, and gallium recovery from led waste by adaptation of *Acidithiobacillus ferrooxidans*. *Waste Management*. 79, 98-108.
- Ravindra, P., Kodli, B., Veera, V.P.R., 2015. Effect of Adaptation of *Acidothiobacillus ferrooxidans* on Ferrous Oxidation and Nickel Leaching Efficiency. In: Ravindra P. (eds) *Advances in Bioprocess Technology*. Springer, Cham.
- Rohwerder, T., Gehrke, T., Kinzler, K., Sand, W., 2003. Bioleaching review part A: Progress in bioleaching: fundamentals and mechanisms of bacterial metal sulfide oxidation. *Applied Microbiology and Biotechnology*. 63, 239-248.
- Santaolalla, A., García, J., Rojo, N., Barona, A., Gallastegui, G., 2020. Viability of two alternatives for treating waste solutions from the biomachining process. *Journal of Cleaner Production*. 270, 122549.
- Silverman, M. P., Lundgren, D. G., 1959. Studies on the chemoautotrophic iron bacterium *Ferroobacillus ferrooxidans*: I. An improved medium and a harvesting procedure for securing high cell yields. *Journal of Bacteriology*. 77, 642-647.
- Singh, A., Manikandan, A., Ravi Sankar, M., Paksirajan, K., Roy, L., 2018. Experimental investigations and surface morphology of bio-micromachining on copper. *Materials Today: Proceedings*. 5, 4225-4234.

- Speller, N.C., Morbioli, G.G., Cato, M.E., Cantrell, T.P., Leydon, E.M., Schmidt, B.E., Stockton, A.M., 2019. Cutting Edge Microfluidics: Xurography and a Microwave. *Sensors and Actuators B: Chemical*. 291, 250-256.
- Teo, A.J.T., Malekpour-galogahi, F., Sreejith, K.R., Takei, T., Nguyen, N.-T., 2020. Surfactant-free, UV-curable core-shell microcapsules in a hydrophilic PDMS microfluidic device. *AIP Advances*. Volume 10, 065101.
- Ting, Y.P., Kumar, S., Rahman, M., Chia, B.K., 2000. Innovative use of *Thiobacillus ferrooxidans* for the biological machining of metals. *Acta Biotechnologica*. 20, 87-96.
- Torino, S., Corrado, B., Iodice M., Coppola, G., 2018. PDMS-Based Microfluidic Devices for Cell Culture. *Inventions*. 3, 65.
- Tsao, C.-W., Wu, Z.-K., 2020. Polymer Microchannel and Micromold Surface Polishing for Rapid, Low-Quantity Polydimethylsiloxane and Thermoplastic Microfluidic Device Fabrication. *Polymers*. 12, 2574.
- Valdés, J., Pedroso, I., Quatrini, R., Dodson, R.J., Tettelin, H., Blake, R., Eisen, J.A., Holmes, D.S., 2008. *Acidithiobacillus ferrooxidans* metabolism: from genome sequence to industrial applications. *BMC Genomics*. 9, 597-620.
- Valix, M., 2017. Bioleaching of electronic waste: milestones and challenges. In: *Current Developments in Biotechnology and Bioengineering: Solid Waste Management*. Ed: Elsevier. 407-440.
- Vigneshwaran, S.S., Ramakrishnan, R., ArunPrakash, C., Sashank, C., 2018. Biomachining—a new approach for micromachining of metals. In: *AIP Conference Proceedings, 1943*, 1. AIP Publishing, 020059.
- Watling, H.R., 2006. The bioleaching of sulphide minerals with emphasis on copper sulphides- A review. *Hydrometallurgy*. 84, 81-108.
- Whulanza, Y., Nadhif, H., Istiyanto, J., Supriadi, S., Bachtiar, B., 2016. PDMS surface modification using biomachining method for biomedical application. *Journal of Biomimetics Biomaterials and Biomedical Engineering*. 26, 66-72.
- Wu, X., Hu, Q., Hou, D., Miao, B., Liu, X., 2010. Differential gene expression in response to copper in *Acidithiobacillus ferrooxidans* strains possessing dissimilar copper resistance. *Journal of General and Applied Microbiology*. 56, 491-498.
- Xenofontos, E., Feidiou, A., Constantinou, M., Constantinides, G., Vyrides, I., 2015. Copper biomachining mechanisms using the newly isolated *Acidithiobacillus ferrooxidans* B1. *Corrosion Science*. 100, 642-650.
- Xia, Y., Whitesides, G.M., 1998. SOFT LITHOGRAPHY. *Annual Review of Materials Research*, 28, 153-184.
- Yang, Y., Wang, X., Liu, Y., Wang, S., Wen, W., 2009b. Techniques for micromachining using *Thiobacillus ferrooxidans* based on different culture medium. *Applied Mechanics and Materials*. 16-19, 1053-105.
- Ye, M., Li, G., Yan, P., Ren, J., Zheng, L., Han, D., Sun, S., Huang, S., Zhong, Y., 2017. Removal of metals from lead-zinc mine tailings using bioleaching and followed by sulfide precipitation. *Chemosphere*. 185, 1189-1196.

Zhan, Y., Yang, M., Zhang, S., Zhao, D., Duan, J., Wang, W., Yan, L., 2019. Iron and sulfur oxidation pathways of *Acidithiobacillus ferrooxidans*. *World Journal of Microbiology and Biotechnology*. 35, 60.

Zhu, N., Shi, C., Shang, R., Yang, C., Xu, Z., Wu, P., 2017. Immobilization of *Acidithiobacillus ferrooxidans* on cotton gauze for biological oxidation of ferrous ions in a batch bioreactor. *Biotechnology and Applied Biochemistry*. 64, 27-734.

CHAPTER 4.
APPLICATION 2: BIOLEACHING
OF METALS FROM PCBs

4.1. OBJECTIVE

A printed circuit board (PCB) is the integral piece of any electronic equipment whose function is to mechanically support and electrically connect electronic components using conductive pathways, tracks or signal traces etched from copper sheets laminated onto a non-conductive substrate. Bearing in mind the metal rich composition of the PCBs, this waste material can be as a secondary source of valuable metals (urban mining) and it can offer an entrepreneurial opportunity in the metal sales market.

Some metal recycling technologies applied to the wastes from electronic and electrical equipment (WEEE), such as pyrometallurgical and hydrometallurgical processes, have been extensively investigated in literature (Moltó et al., 2011; Silveira et al., 2015; Gautam et al., 2018; Ippolito et al., 2021). Chemical leaching stands out among the latter ones, employing mineral acids (hydrochloric acid, sulfuric acid or nitric acid) together with strong oxidants (hydrogen peroxide, ferric chloride or chlorine) for metal extraction from PCBs (Birloaga and Vegliò., 2016). However, given the environmental impact caused by the high consumption of reagents, industries are progressively being forced to move toward greener extraction technologies, such as bio-metallurgical processes (Diaz-Tena et al., 2017). Based on microorganisms' ability to bioregenerate the oxidants, bioleaching has become an efficient and affordable alternative to the conventional technologies but intensive research is still necessary before industrial implementation (Priya and Hait, 2017; Díaz-Martínez et al., 2019).

This chapter focuses on the recovery of metallic elements (particularly copper) contained in mobile phone PCBs by bioleaching process. Two different PCB pre-treatments were tested: grinding and removal of epoxy cover (without grinding). Then, one step and two step bioextractions were carried out with the pretreated samples. Additional chemical leaching assays were also conducted for comparison purposes and the reagents ferric iron (to simulate the real bioleaching media) and sulfuric acid (to analyze its contribution to the bioprocess performance) were selected for these experiments. Finally, a preliminary design of a lab-scale plant for metal removal from PCBs was outlined.

Figure 4.1 shows the outline of the experimental section of this chapter.

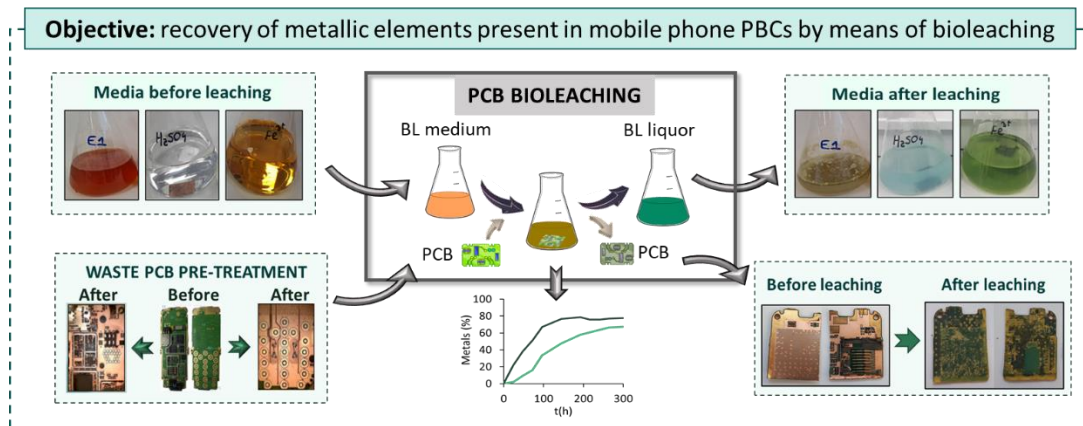


Figure 4.1. Outline of the experimental section of this chapter.

4.2. MATERIAL AND METHODS

4.2.1. Microorganism and culture medium

The strain *A. ferrooxidans* DSM 14882 used for this study was cultured in a Silverman and Lundgren 9K medium (Silverman and Lundgren, 1959) as described in Section 1.1 *Microorganisms* (materials and general methods).

4.2.2. PBC samples

Obsolete mobile phones manufactured by Nokia between 2000 and 2011 were collected. This trademark was selected to delimit the commercialized models, although the necessary amount of Nokia phones of the same model with identical PCB were not available at the moment of this study. Therefore, similar models were chosen.

The dismantling and separation of the PCBs from the mobile phones were carried out manually (Figure 4.2). The average weight of the PCBs was 15.9 ± 5.7 g, which represents approximately 19 % of the total average weight of the standard mobile phone (82.6 ± 10.2 g).

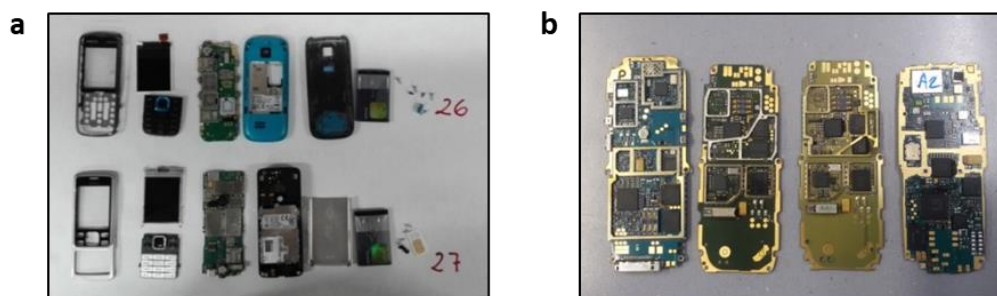


Figure 4.2. Dismantling of mobile phones (a) and printed circuit boards (PCBs) (b).

4.2.3. Sample conditioning

Two different alternatives for facilitating the metal (copper) biorecovery from the PCB samples were tested: 1) mechanical grinding without any further treatment (powder PCB) and, 2) chemical removal of the epoxy cover without grinding (entire PCB).

4.2.3.1. Sample grinding

Five PCB pieces were cut into irregular squares and introduced into a RETSCH SM 2000 mill, with a 4 mm mesh (Figure 4.3). The sample was consecutively crushed with a 1.25 and 0.75 mm mesh, to obtain a sample as homogeneous as possible.



Figure 4.3. RETSCH SM 2000 mill.

4.2.3.2. Removal of the epoxy layer

Solutions containing NaOH and solvents like ethanol, acetone, tween-80, carbinol, benzyl alcohol or dimethylacetamide, among others, have been proposed for the removal of the epoxy coating from PCBs (Adhapure et al., 2014; Jadhav and Hocheng, 2015; Yildirim et al., 2015; Sodha et al., 2020; Rao et al., 2020). However, NaOH is the most widely one used in literature for the epoxy cover removal from PCBs.

Therefore, in this work, a concentrated solution of sodium hydroxide (NaOH 10 M) was used to get the protective layers of epoxy resin apart from the other materials. This pre-treatment was carried out by immersing the PCB on NaOH 10 M solution under stirring conditions for 3-4 days.

4.2.4. Bioleaching experiments

4.2.4.1. One-step bioleaching experiment

Biotic leaching experiments were carried in 1 L Erlenmeyer containing 300 mL of 9K medium (Fe^{2+}) in which a 5 % v:v of *A. ferrooxidans* in an exponential growth phase was inoculated. About 1.22 g of the PCB powder sample (equivalent to 3.5 g L^{-1} pulp density)

were added to one Erlenmeyer, while a piece of the entire PCB (1.5 g) without the epoxy cover (equivalent to 4.0 g L⁻¹ pulp density) was introduced into another Erlenmeyer. Both reactors were incubated at 31 °C and 130 rpm for 18 days. Samples were collected from the medium on a regular basis to analyze metal content after filtration. An abiotic (blank) assay was also conducted in the same conditions but without inoculation as a control test.

4.2.4.2. Two-step bioleaching experiment

Two-stage bioleaching experiment was carried out according to the procedure described in Section 2.2. *Copper mobilization experiments* (materials and general methods). Thus, the medium containing 9 g Fe²⁺ L⁻¹ was inoculated with a 5 % v:v of the *A. ferrooxidans* culture in an exponential growth phase and it was incubated until the complete oxidation of the Fe²⁺ (Step 1). Once Fe²⁺ was oxidized to Fe³⁺, a 2 g PCB piece was immersed in the bioleaching solution (BL solution) (step 2). A blank experiment was also conducted using the supernatant obtained in the first step by filtering the medium with 0.45 µm polyvinylidene fluoride filter. The bioleaching experiments were carried out at 31 °C and 130 rpm for 11 days.

4.2.5. Chemical leaching experiment

Hydrometallurgical processes have been extensively employed for metal dissolution from PCBs (Birloaga et al., 2013; Jadhav and Hocheng, 2016; Gautam et al., 2018; Rao et al., 2021). Therefore, an experiment with chemical Fe³⁺ media (not biologically generated) as leaching reagent was carried out for comparison purposes. Bearing in mind that the sulfuric acid (H₂SO₄) was used for the pH control in the biotic leaching, another experiment was performed with the objective of assessing the contribution of this acid in the process performance. Thus, an abiotic leaching medium containing H₂SO₄ 2 % v:v was prepared and subsequently, the PCB pieces were immersed into 300 mL of this acid solution at 30 °C and 150 rpm for 300 h.

4.2.6. Preliminary design of a bioleaching reaction system

The aim of this section was to design a complete bioleaching system at lab-scale in order to facilitate further studies on scaling. On the basis of the experimental results, the fundamental lay-out consisted of three continuous stirred-tank reactors (CSTR), two of them devoted to the oxidant bioregeneration and the other one to the leaching process. All the ancillary elements, control devices and connections were included in the design.

4.2.7. Analytical methods

Metal content in the samples was measured by ICP-OES plasma spectrometry according to the procedure described in Section 2.6 *Metal content analysis (ICP and AAS)*. Prior to the analysis, the PCB finest fraction (<0.75 mm) was digested in aqua regia (HNO₃:HCl, 1:3 v:v) for quantifying metal composition. This fraction was selected because particle size lower than 0.84 mm has been reported to account for 42.6 % of the copper in crushed PCBs (Gu et al., 2014). Two different weight:volume (w:v) ratios were tested to guarantee acid enough for the total digestion of the sample: 1:40 and 1:80 (in duplicate). Thus, about 0.5 g were weighted and then, 20 mL or 40 mL aqua regia were added for 48 h. A blank sample for each ratio was also prepared (without PCB powder). The equipment for the digestion was Ethos Advanced microwave (Figure 4.4).

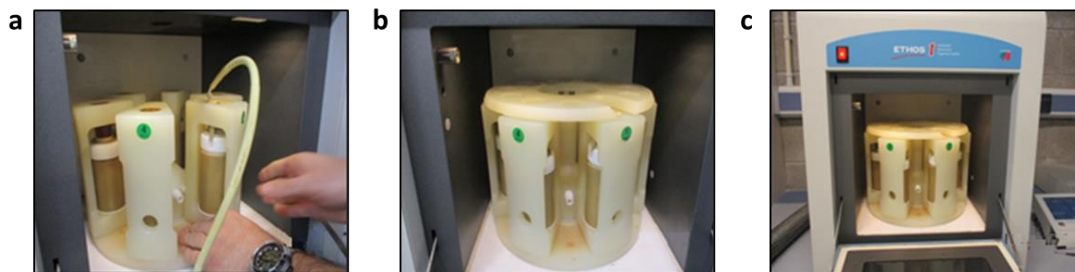


Figure 4.4. Detail of the container placement in the digester carousel.

The samples and the two blanks were digested at 150 °C for 3 h, and after cooling they were filtered (Whatman 424 filter paper) and diluted with 2 % nitric acid (Figure 4.5). The average residual amount of the samples that remained unsolved was lower than 5 % of the original weight in all cases.

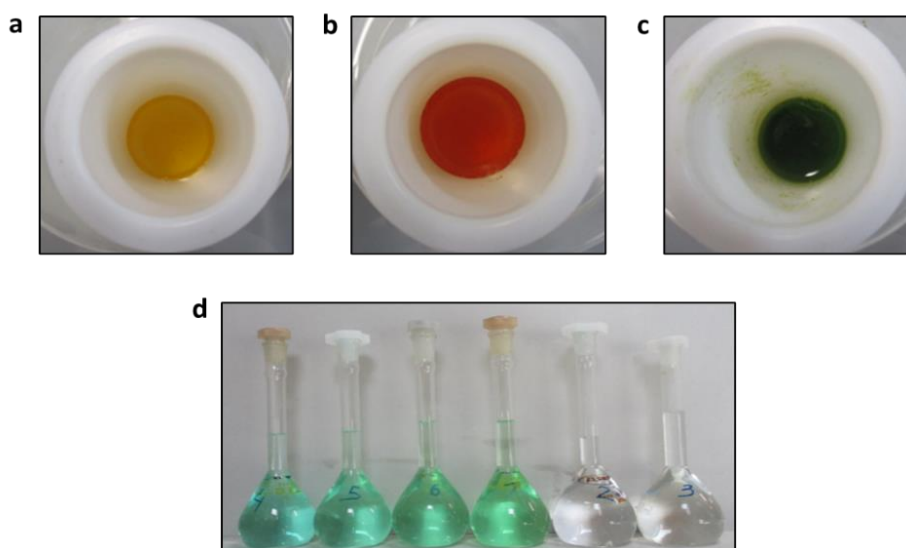


Figure 4.5. Digested samples: blank for 1:40 ratio (a); blank for 1:80 ratio (b); PCB sample (c); final solutions after dilution with nitric acid (d).

The energy dispersive X-ray fluorescence (EDXRF) provides a rapid and non-destructive method for the analysis of trace and major elements and presents the results in real time. In this work, a Fischerscope XDAL desktop EDXRF equipment was used, available at the Sgiker center of the University of the Basque Country (UPV / EHU) and it was applied on an entire PCB and on the PCB powder.

Iron concentration and pH were monitored throughout the process by following the procedure described in Sections 2.5 *Determination of iron species in dissolution* and 2.8 *Other methods* (materials and general methods).

4.3. RESULTS

4.3.1. Pretreatment of the PCBs

The smallest the particle size in the PCB grinded samples, the greater the *surface area* for contact between the powder and the leaching solution (Yang et al., 2017; Sethurajan and van Hullebusch, 2019). Oliveira et al. (2010) recommended a particle size range between 0.3 and 1.5 mm for bioleaching assays, as sieving to too small particle size can lead an important loss of the material (Isildar et al., 2016).

The picture of each fraction (>1.25 mm, 1.25-0.75 mm, and < 0.75 mm) after grinding is shown in Figure 4.6. The total weight loss was about 15 %.



Figure 4.6. Pulverized PCB sample according to particle size: > 1.25 mm (a), 1.25-0.75 mm (b), and < 0.75 mm (c) (1:30 augmentation).

The particle-size distribution (Figure 4.7) revealed that, after grinding, about 60 % of the crushed sample was in the smallest fraction (smaller than 0.75 mm). This fraction was used for subsequent bioleaching tests as it is within the size range most frequently selected by other authors in literature (0.5-2 mm) (Silvas et al., 2015; Isildar et al., 2016; Joshi et al., 2017).

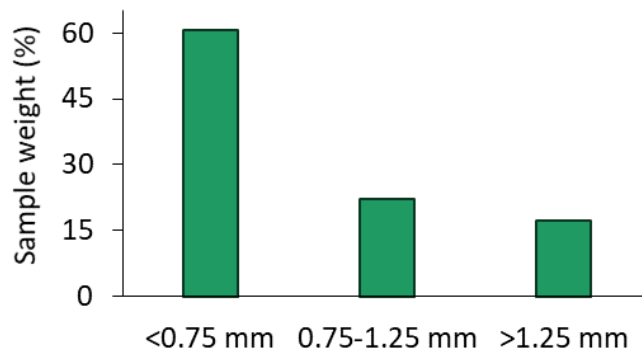


Figure 4.7. Particle-size distribution of pulverized PCB.

A major part of the PCBs' metallic fraction is covered by a layer that makes difficult the proper contact between the leaching medium and the metals in entire pieces. As far as epoxy coating removal is concerned, some authors have studied the efficiency of different pre-treatment methods (Senophiyah-Mary et al., 2018; Moyo et al., 2020). Chemical methods involve the use of chemical reagents, such as solvents for the surface coating removal, which can possibly facilitate the delamination of the metal and fibre glass layers (Moyo et al., 2020). Senophiyah-Mary et al. (2018) have studied the efficiency of different pre-treatment methods for epoxy coating removal from PCBs. These authors found that the complete removal of the epoxy cover was only achieved with NaOH solutions and with sulfuric and nitric acids. Nevertheless, the acidic solutions were not considered because they can promote the partial dissolution of metals together with the layer. Moyo et al. (2020) have also reported best results when employing NaOH. In this study, the use of NaOH 10 M allowed the complete removal of this coating, as observed in Figure 4.8.



Figure 4.8. Mobile phone PCB before and after treatment with a 10 M NaOH solution.

4.3.2. Metal composition of the PCBs

PCBs are very heterogeneous in terms of size, shape and elements, and, thus, its composition is also expected to be variable (Hadi et al., 2015, Monneron-Enaud et al., 2020). Table 4.1 shows the metal content in the PCBs (expressed in mg g^{-1} PCB powder

sample) reported by several authors, including major and some minor but interesting metals (such as Ag, Pt and Au with high market price). As a representative example of the high variability in the composition of the PCBs, the results for the major metal (Cu) vary from 66.5 to 566.8 mg g⁻¹ PCB. The considerable variations in the metallic compositions of PCBs can be attributed to the different models, the changes in the manufacturing process and the technical innovations in the sector (Isildar et al., 2016; Hubau et al., 2019).

Table 4.1. Metal concentration (mg g⁻¹ PCB) of mobile's PCBs reported in literature and market price according to the London Metal Exchange (LME, € kg⁻¹).

Cu	Ni	Sn	Zn	Al	Pb	Pd	Au	Pt	Ag	Reference
234.7	23.5	–	–	–	9.9	0.3	0.6	0.03	3.3	Ogunniyi et al., 2009
351	–	40	–	–	27	–	1.2	–	–	Ha et al., 2010
378.1	25.4	25.5	18.2	6.1	–	12.3	0.9	–	0.5	Kasper et al., 2011
660	23	–	–	–	–	–	0.45	–	–	Kim et al., 2011
344.9	26.3	–	–	–	18.7	–	<0.01	–	2.1	Yamane et al., 2011
566.8	–	14	2.2	14.2	–	0,1	0.21	–	1	Tripathi et al., 2012
428	6	26	0.1	–	0.6	0.096	1.4	0.04	2.3	Kim et al., 2013
388.7	17.3	24.9	3.3	9.6	16.7	0.14	1.6	–	3.98	Le et al., 2013
360	8.55	–	7.96	6.66	12.07	0.64	0.1	–	0.28	Shah et al., 2014
66.5	13.9	–	3.8	31.2	9.2	–	1.8	–	3.6	Arshadi and Mousavi, 2015
319.5	27.1	17.8	11.9	111.1	–	–	–	–	3.4	Calgaro et al., 2015
230.1	11.5	–	3	10.3	1.2	–	0.32	–	–	Isildar et al., 2016
408	3,9	16	4,1	–	13.6	0.05	0.065	–	1.06	Xiu et al., 2015
342.7	11.6	19.3	5.5	19.1	3.7	0.1	1.05	0.0043	2.6	Holgersson et al., 2018
390.4	11.5	28.9	–	1.3	16.1	0.1	0.8	–	0.2	Benzal et al., 2020
Price (€ kg⁻¹)										
6.1	14.1	17.9	2.4	1.9	2.1	82918.7	56891.1	30298.3	645.9	LME

In this study, among the wide variety of metals contained in the PCBs from mobile phones, Cu, Fe, Al, Pb, Zn, Ni, Sb, Pd and Sn were selected to be quantified in the crushed PCB sample with a particle size lower than 0.75 mm. As expected, the major element is copper with an average content of 435±54 mg g⁻¹ PCB, followed by Al, Fe and Ni. This




content is even higher than the pure copper amount contained in ores such as chalcopyrite (34.5 %). The copper concentration in the samples of this work was very high and close to the one reported by Xiu et al. (2015). The Ni and Zn contents are very similar to those obtained by Isildar et al. (2016) and Holgersson et al. (2018) (Table 4.1). The results in mg metal g⁻¹ PCB are summarized in Table 4.2.

Table 4.2. Average metal content in PCBs in this study (mg metal g⁻¹ PCB).

Element	Content
Cu	435.0±54.0
Fe	12.6±0.2
Al	19.6±0.9
Ni	11.4±1.1
Zn	4.4±1.1
Pb	5.9±1.4
Pd	0.6±0.1
Sb	0.4±0.1
Sn	32.9±3.7

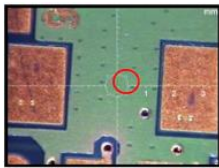
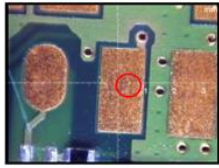
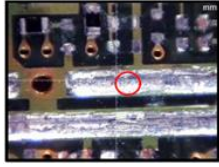

In the PCB powder, the crushing process rendered a heterogeneous final sample. Thus, three different points were analyzed by EDXRF (Table 4.3). It was concluded that the most fibrous and smaller part would correspond to the non-metallic fraction of the original PCBs. In this sample, the presence of mixed metal/non-metal particles (for example Cu/Br) can be observed, which represents a difficulty for their separation (Table 4.3).

Table 4.3. Results of the EDXRF analysis of different areas of the PCB powder.

Zone	Image	Results	Observations
1 st point		Cu (%): 33.15 Br (%): 42.99 Ca (%): 18.46	Mixed Cu/resin particle. The Cu is found underneath the green non-metallic particles. The bromine comes from the epoxy resin cover (green).
2 nd point		Cu (%): 54.91 Ni (%): 41.22	Metallic particle.
3 th point		Cu (%): 85.14 Br (%): 9.59	Copper particle with part of the epoxy resin embedded in a small proportion.

Regarding the non-crushed samples, the presence of Pb in some areas analyzed by EDXRF can be attributed to the use of a soft solder for joining the pieces (Table 4.4.). This solder is usually a metal alloy with a low melting point and it is composed of tin (66 % w) and lead (33 % w). The RoHS Directive (entered into force on July 1, 2006), restricts the use of six substances, including lead, in the electronics industry. However, this metal was found in these PCB samples because the phones were manufactured before 2006. The presence of copper as the major component was clearly sustained both in visible parts and in parts covered by the epoxy resin.

Table 4.4. Results of the EDXRF analysis of different areas of the entire PCB.

Zone	Image	Results	Observations
Green surface		Cu (%): 42.20 Br (%): 40.90	Non-metallic surface area: The bromine comes from the epoxy resin cover (green) and, Cu is in the layer underneath.
Uncovered surface		Cu (%): 52.70 Ni (%): 44.10 Au (%): 3.20	Metallic surface area: It contains Cu and Ni as major elements.
Welding points		Sn (%): 49.93 Pb (%): 33.96	Metallic surface area: It contains the conventional metals used in welding, being Sn the major one.
Connectors		Sn (%): 70.36 Pb (%): 25.40	Metallic surface area: It contains Sn as a main component (characteristic shine).

4.3.3. Bioleaching experiments

Several studies have explored the bioleaching of PCBs in either one- or two-step processes (Choi et al., 2004; Shah et al., 2014; Yang et al., 2014; Khatri et al., 2018). Similarly, in this study, two experimental approaches were employed for applying the bioleaching to the recovery of metals from PCBs: a) the addition of the PCB samples together with the inoculated culture (one-step bioleaching) or b) using the biogenic ferric iron produced during bacterial incubation (step 1) for metal dissolution (step 2) (two-step bioleaching).

4.3.3.1. One-step bioleaching experiment

Monneron-Enaud et al. (2020) have proved the efficiency of the bioleaching process for the dismantling of the PCBs subassemblies (resistors, capacitors, diodes...). Other authors have demonstrated the efficiency of metal bioleaching when PCB powder is employed (Zhu et al., 2011; Isildar et al., 2016; Priya and Hait, 2018; Arshadi and Yaghmaei, 2020). Nevertheless, only a few references have been found about the use of entire PCB pieces for this process (Adhapure et al., 2014; Chandane et al., 2020; Sodha et al., 2020).

One-step bioleaching experiments in 9K medium (containing Fe^{2+}) were conducted with the PCB powder sample (pulverized) and the entire PCB sample without the epoxy cover (non-pulverized). The rationale of selecting the Fe^{2+} containing medium was to let the microbes generate the oxidant for metal slow removal and to detect a possible inhibitory effect. The evolution of copper leaching is shown in Figure 4.9.

The pulverized sample rendered a higher removal efficiency than the non-pulverized one after 336 h of treatment (Figure 4.9). These results are in agreement with those reported by Joshi et al. (2017), who have also obtained better results when employing the PCB powder. It was attributed to the higher surface area in the crushed sample. Copper removal was faster for the pulverized sample during the first 150 h, being the difference in the bioleaching efficiency between both samples more noticeable during this period. At the end of the experiment, 78.3 % and 67.9 % Cu was removed using the pulverized or non-pulverized samples, respectively.

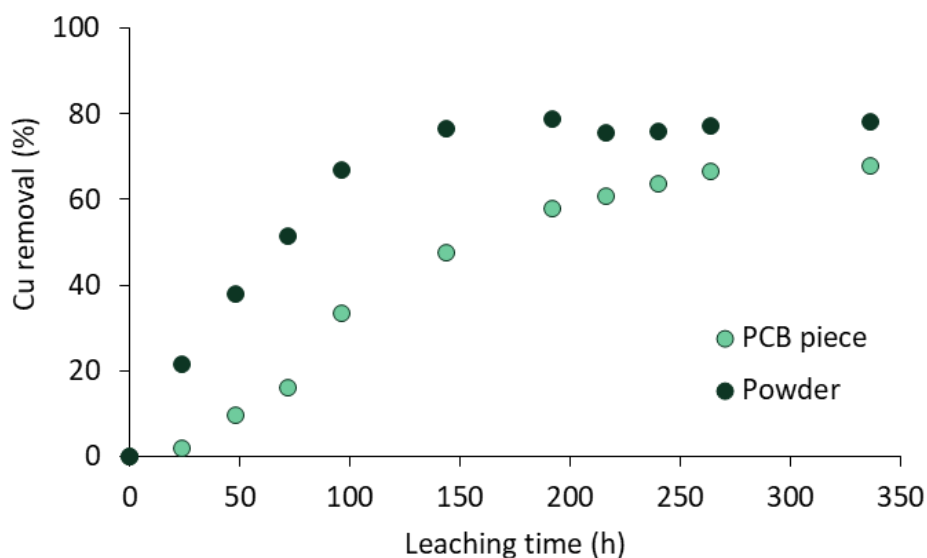


Figure 4.9. Copper removal efficiency during the bioleaching experiments for the PCB powder samples and the entire PCB piece without epoxy layer.

Regarding the PCB powder, the Cu leaching efficiency was higher than that reported by Adhapure et al. (2014) who have obtained a removal amount of 536 mg L⁻¹ of Cu in 9K medium when immersing PCB pieces (4 cm x 2.5 cm) after 240 h of bioleaching. These authors have registered the maximum copper leaching efficiency after 192 hours of treatment. On the contrary, in this work 1267 mg L⁻¹ of Cu were removed after 340 hours of treatment and the maximum copper bioleaching efficiency was recorded after 144 h approximately.

Other authors analyzed the copper bioleaching efficiency when using pulverized PCB under different conditions. For example, Zhu et al. (2011) have obtained leaching efficiencies of 94 %, 93.1 % 94.2 % and 73.3 % when 4, 8, 12 and 14 g PCB powder L⁻¹ pulp densities were employed, respectively after 192 h of bioleaching. Thus, these authors have recorded the maximum leaching efficiency when adding lower PCB pulp densities to the 9K medium (4 g PCB powder L⁻¹). The results obtained in this study were lower than those showed by Zhu et al. (2011), which could be attributed to the difference in the inoculum percentage (10 % vs 2 % used in this work). Conversely, Yang et al. (2017) reported a copper removal of 92 % when an initial pulp density of 4 g PCB powder L⁻¹ was used (10 % of *A. ferrooxidans* inoculum, pH 2.0, 9 g Fe²⁺ L⁻¹). This value was considerably higher than the one obtained in this study (68 % Cu recovery). The difference in obtained results can be attributed to the variability of the PCB pieces.

Although the biotic assays demonstrated the effectiveness of the Cu leaching, it is noticeable that other minor metals could be simultaneously bioleached such as nickel, zinc or lead, among others. Comparative values obtained at the end of the experiment for Zn, Ni and Pb are shown in Table 4.5.

Table 4.5. Metal removal values obtained for Cu, Zn, Ni, and Pb.

Metal	PCB piece	PCB powder
Cu (%)	68	78
Ni (%)	37	54
Zn (%)	53	34
Pb (%)	3	14

During PCB powder bioleaching, Ni, Pb and Zn extracted amount reached a maximum and then, decreased (data not shown). Joshi et al. (2017) also recorded an abrupt increase in Cu, Zn and Pb leaching efficiencies with the subsequent decrease when

employing non-pulverized PCBs. It was attributed to the possible precipitation of these metals (Brand et al., 2001, Ilyas et al., 2013, Adhapure et al., 2013).

Similarly to this work, these authors obtained slightly better bioleaching efficiencies with pulverized PCB compared to non-pulverized ones after 336 h. Shah et al. (2014) have reported that the amounts of Cu, Zn and Ni extracted by one-step bioleaching after 360 h were 87.50 %, 85.67 % and 81.87 % (9 g Fe L^{-1} , 1 g e-waste, 150 rpm at $32 \pm 2^\circ\text{C}$).

Although the grinded sample performed better in terms of copper removal efficiency, pulverization pre-treatment entails an important cost (high energy consumption) and generates particulate matter that can be dangerous for human health. Moreover, the use of non-pulverized sample without the epoxy cover can facilitate the management and separation of PCBs from leachate, as well as providing a “cleaner” medium for microbial activity with less amount of organic compounds (Ueoka et al., 2016). Thus, the treatment of entire PCB pieces for the epoxy cover removal was selected as the most practical PCB pre-treatment for further bioleaching experiments.

4.3.3.2. Two-step bioleaching experiment

Most studies on PCB bioleaching use pulverized samples and one-step process for metal extraction (Yang et al., 2009; Arshadi and Mousavi, 2015; Joshi et al., 2017; Wu et al., 2018; Hubau et al., 2018; Benzal et al., 2020). Studies treating entire PCBs in a two-stage bioleaching process are scarce. Hence, in the present study, the bioleaching process was carried out by immersing the PCB piece in the previously obtained BL solution by *A. ferrooxidans* bacteria. Figure 4.10 shows the results of copper removal from PCBs by BL solution (biotic).

The two-step bioleaching process rendered high copper removal efficiency (Figure 4.10a). During the first 150 h, higher results were obtained in biotic samples (pieces and biomass together) than those obtained in the abiotic test (data not shown). These results are in accordance with those obtained in previous Chapters, where the better performance was attributed to the higher Fe^{3+} availability due to the continuous microbial regeneration of the oxidant iron species. The difference between both values decreased from hour 200 onwards, when a similar amount of copper was removed in both biotic and abiotic tests.

Evolution of Fe through the bioleaching process is shown in Figure 4.10b. An initial increase in the total iron concentration was registered, probably related to the contribution of the dissolution of Fe contained in the PCB sample. However, the subsequent decrease of this parameter (together with a pH increase) was attributed to jarosite precipitation. According to the results obtained in previous Chapters, this precipitation phenomena can be related both to an increment in the pH and to the biofilm formation in biotic samples.

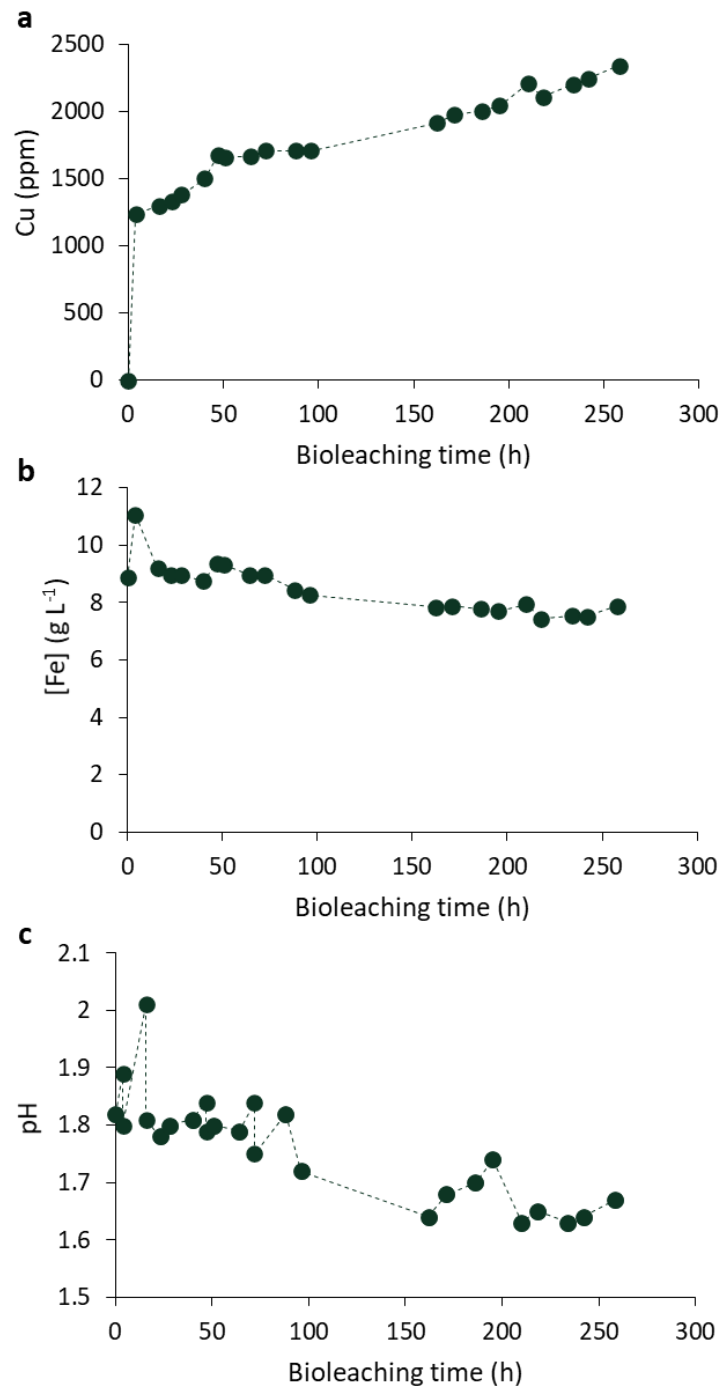


Figure 4.10. Copper removal efficiency (a), total iron concentration evolution (b) and pH evolution (c) during the two-step bioleaching experiment.

The immersion of the PCB piece in the bioleaching medium resulted in the slight rise of the pH during the first hours (Figure 4.10c). This behavior could be attributed to the alkaline condition of the PCB. These results are in agreement with those reported by Yang et al. (2009) and Arshadi and Mousavi (2015) who have observed an increment in the solution pH during the metal dissolution from the PCB. During the last hours of the

experiment, pH slightly decreased and maintained in the 1.6-1.8 range. A total amount of 82 % of copper was dissolved by the end of the assay (300 hours).

Figure 4.11 shows the BL solution and the PCB piece before and after the bioleaching process.

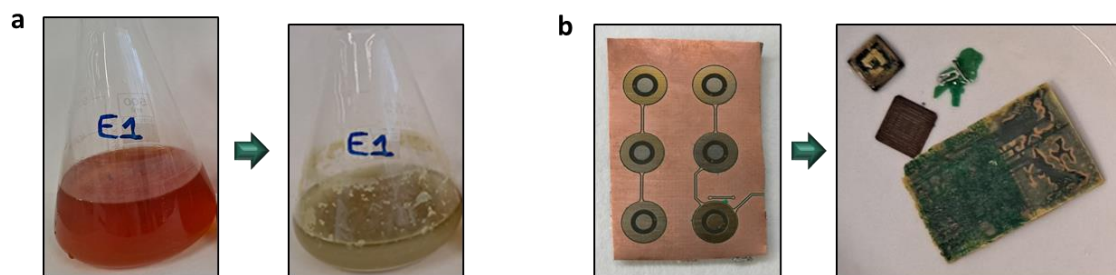


Figure 4.11. BL solution (a) and PCB pieces (b) before and after bioleaching.

Metal removal values for Ni and Zn in two-step bioleaching process are shown in Figure 4.12. Bearing in mind the initial metal content obtained after PCB characterization, a total amount of 32 and 3 % and 2.5 % of Ni, Zn and Pb were removed, respectively.

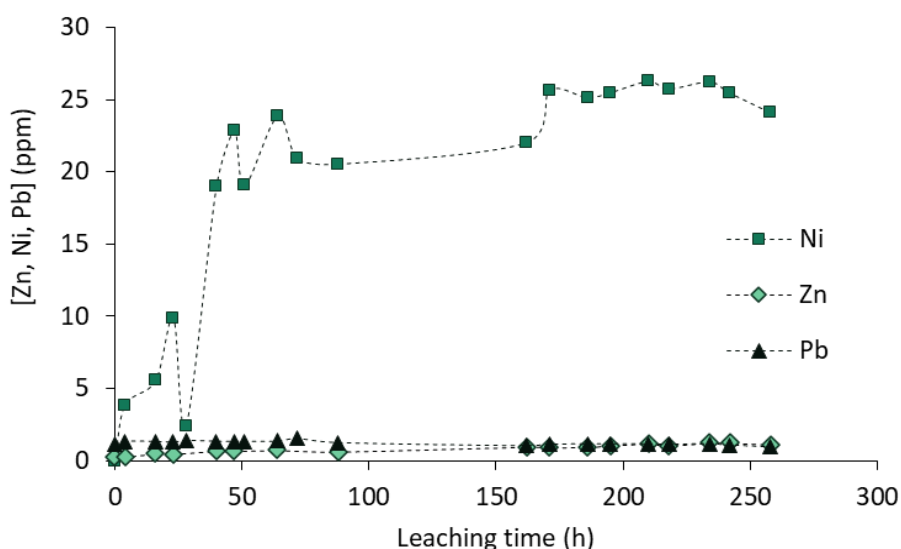


Figure 4.12. Zn, Ni and Pb removal during the two-step bioleaching experiments.

The leaching yields recorded in the present study for Cu, Ni, Zn were lower than the results reported by other authors (Yang et al., 2009; Van Yken et al., 2020). Shah et al. (2014) have reported a difference of 10 % of leached copper after 6 days of two-step bioleaching process (99 % and 89 % in the presence and absence of biomass, respectively). These results are in accordance with those reported by Khatri et al. (2018) who have also obtained low leaching efficiencies when employing pulverized PCB powder in both one step and two step bioleaching experiments.

4.3.4. Chemical leaching experiments

Metal leaching from mobile phone's PCBs can also be performed in total absence of biomass by hydrometallurgical methods (with strong acids and no biotic ferric iron) (Tuncuk et al., 2012; Jadhav and Hocheng, 2015; Patel et al., 2017; Hossain et al., 2018). Despite many other strong acids can be selected for chemical leaching, sulfuric acid was chosen because this compound has rendered good results for controlling the pH during the oxidant bioregeneration and for avoiding iron precipitation as jarosite in previous Chapters.

The removal efficiency of Cu, Zn, Ni and Fe from entire PCBs after 300 h when employing chemical (non-bioregenerated) Fe^{3+} is shown in Figure 4.13. In this study 1977, 1168, 53 and 218 ppm were removed for Cu, Fe, Ni and Zn, respectively after 300 h of leaching. Comparing these results with those obtained when employing BL solution, a similar amount of copper was dissolved in both leaching media until 200 h. Then, after 250 h, 15.7 % more copper was removed in BL solution compared to the abiotic chemical one.

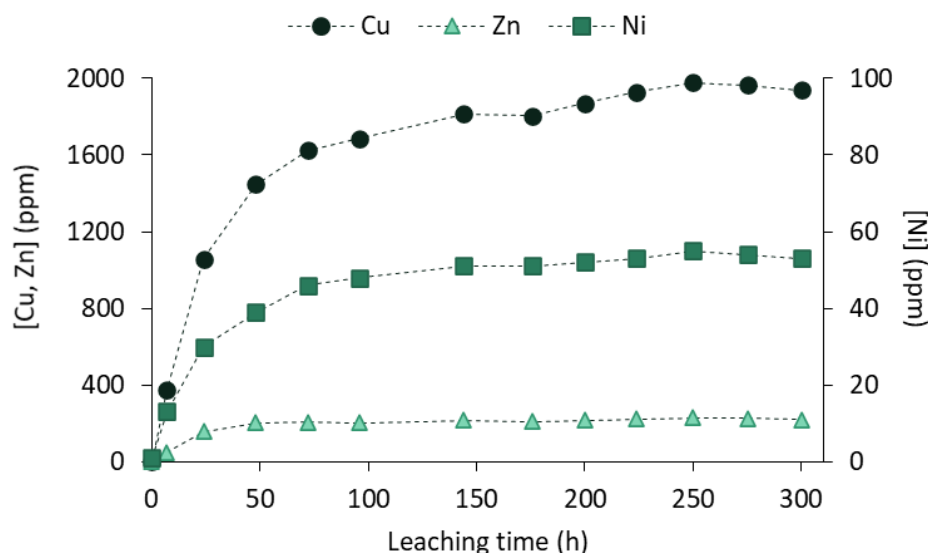


Figure 4.13. Extracted amount of copper, nickel and zinc from PCB in Fe^{3+} medium.

Conversely, a higher amount of Zn (228 ppm) was removed in the chemical leaching than in the BL solution. Nevertheless, the highest Ni removal was obtained in the biotic experiment (1.1-fold-higher than the obtained with chemical Fe^{3+} , respectively). Such behavior was likely attributed to the variation in the metal content of each sample as, the large heterogeneity of the entire PCBs may lead to large variation of sample composition (Khatri et al., 2018; Hubau et al., 2018; Van Yken et al., 2020).

Khatri et al. (2018) have reported a removal efficiency of 90, 49 and 69 % for Cu, Zn and Ni, respectively, when employing ferric sulphate as leaching agent after 9 days (60 g L⁻¹ ferric sulphate, 150 rpm and 30 ± 2 °C).

The chemical leaching accounted for the 76 % of the copper in the solution while the efficiency of the two-step bioleaching process was 83 %. Therefore, the biogenic ferric iron produced by *A. ferrooxidans* bacteria was concluded to be an additional oxidant source that supported the metal solubilization in contrast to the limited amount of oxidant in the chemical leaching.

The extracted amounts of Cu, Ni, Zn and Fe from PCBs when employing H₂SO₄ as the sole leaching agent are plotted in Figure 4.14. Up to 1168, 1000, 23, 21 and 5 ppm were leached for Cu, Fe, Ni, Zn and Al and, as expected, the highest removal efficiency was found for copper.

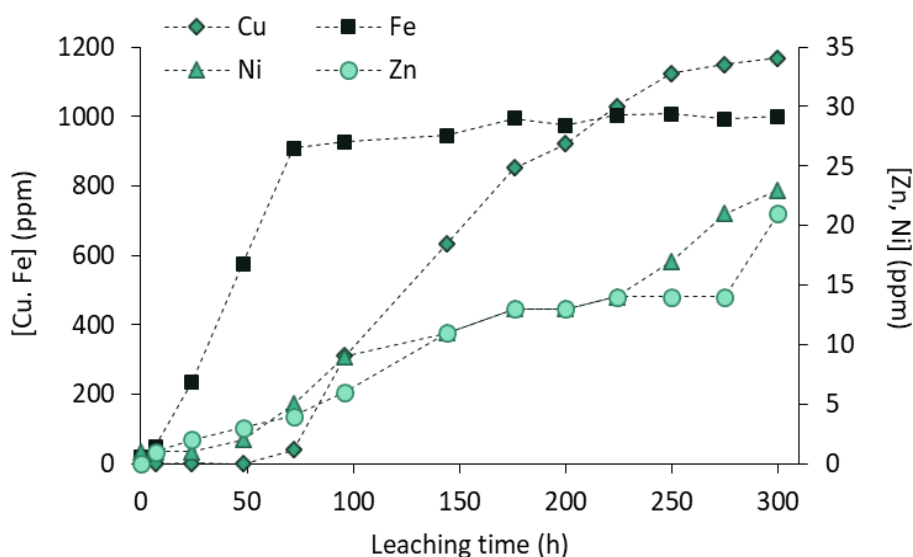


Figure 4.14. Amounts of Cu, Ni, Zn and Fe extracted from PCBs when employing H₂SO₄ as leaching agent.

Jadhav and Hocheng (2015) have analyzed the effect of five different acids (HCl, HNO₃, H₂SO₄, C₂H₄O₂ and C₆H₈O₇) in metal leaching efficiencies from PCBs. Similarly to this study, they used PCB pieces previously treated with 10 M NaOH for the complete removal of the epoxy layer. Hydrogen chloride was concluded to be the best leaching agent as it was capable to remove 100 % of Cu, Zn, Sn, Ni, Pb, Fe, Al, Ag, Au and Pd after 22 h of treatment when treating 4 cm × 4 cm PCB pieces. Nevertheless, lower solubilization percentage was achieved with sulfuric acid, as only 8.8 % of copper was removed after 96 hours. These results are similar to those obtained in this work for the same treatment time, as 10 % of copper was removed from the PCB within 96 h, being this value 40 % after 300 h.

Although HNO_3 has been proposed as another suitable oxidant (Patel et al., 2017), it has not been used intensively because it is more expensive than other alternatives (i.e. HCl or H_2SO_4). Additional reagents such as citric acid or acetic acid have also been disregarded due to poor metal solubilization (Jadhav and Hocheng, 2015).

Chandane et al. (2020) have found that increasing volumes of H_2O_2 (30 %) added to the medium decreased the time required to remove copper from PCBs when treating 2 cm × 2 cm pieces and using sulfuric acid generated by *A. acidophilum* bacteria. These authors have obtained 100 % of copper removal in only 4 h when adding 15 mL of H_2O_2 to the medium. This extraordinary result was attributed to the combination of H_2O_2 together with the acidic media which improved the oxidation potential in the leaching process (Birloaga et al., 2014).

Jadhav and Hocheng (2016) have concluded that it took only 4 hours to remove several metals from the PCB pieces (4 cm x 4 cm) when using a mixture of citric acid (1 M) and H_2O_2 (5.85 %) as leaching agents. Thus, 116.56, 33.20, 9.40 and 0.84 mg g⁻¹ of Cu, Zn, Ni and Fe, respectively were removed. The leaching values reported by these authors in 4 h are higher in comparison to those obtained in this work after 7 h of leaching treatment (0, 0.16, 0.16 and 7.75 mg g⁻¹ for Cu, Zn, Ni and Fe, respectively with H_2SO_4).

The photographs of the Fe^{3+} solution and the PCB piece before and after chemical treatment are shown in Figure 4.15. Similarly, Figure 4.16 shows the solution and the PCB when H_2SO_4 is used as leaching medium.

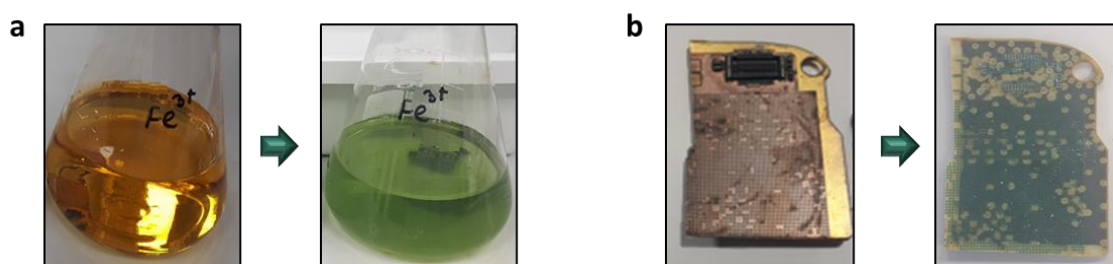


Figure 4.15. The leaching solution when using Fe^{3+} as oxidant (a) and the PCB piece (b) before and after treatment.

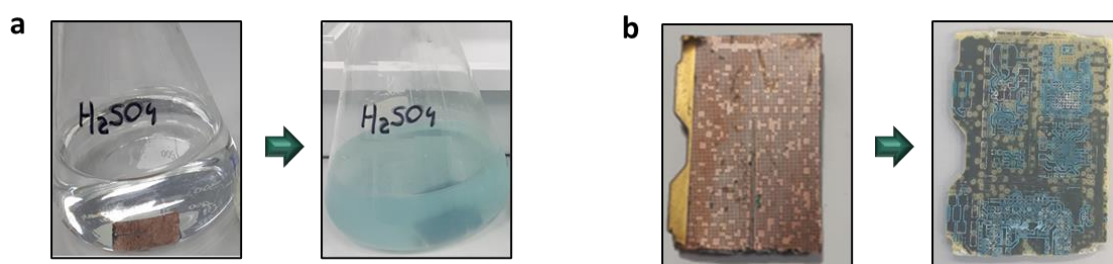


Figure 4.16. The leaching solution when using H_2SO_4 (a) and the PCB piece (b) before and after treatment.

In general terms, higher leaching efficiencies were obtained when using ferric iron in all cases, as up to 40 % more copper was extracted with Fe^{3+} than with the acid by the end of the assay. The highest difference was found for Zn, because almost 90 % more zinc was removed with ferric iron. As far as nickel is concerned, the extracted amount with iron (53 ppm) doubled the result for the acid (23 ppm).

Regarding aluminum extraction, about 5 ppm Al were removed with sulfuric acid while no amount was detected in the leachate obtained with ferric iron (data not shown). These results are consistent with those reported by Van Yken et al. (2020) who have also concluded that ferric iron had no significant impact on aluminum leaching.

After 300 h of treatment, 189.8 and 315.1 mg g^{-1} of Cu were extracted when employing H_2SO_4 and Fe^{3+} media, respectively. On the contrary, lower removal efficiencies of Ni and Zn were achieved (3.7 and 8.6 mg Ni g^{-1} PCB and 3.4 and 35.4 mg Zn g^{-1} PCB with H_2SO_4 and Fe^{3+} media, respectively).

The results obtained in this experiment led to the conclusion that the contribution of sulfuric acid to bioleaching process is almost negetable during the first 100 hours and started to be more significant thenceforth.

Table 4.6 summarized leaching efficiencies for several metals reported in the literature, including biotic and abiotic tests.

Table 4.6. Leaching efficiencies for several metals reported in the literature when treating PCB pieces.

Process	Conditions	Recovered metals	Leaching agent	Leaching efficiency	Reference
Bioleaching	Size: 12 cm x 6 cm Pre-treated with 10M NaOH 200 mL, 15% inoc., 120 rpm, 30°C	Cu, Zn, Ni, Pb	Modified 9K medium	940, 239, 72.7 3.53 mg L ⁻¹ of Cu, Zn, Ni, Pb, respectively in 240 h	Adhapure et al., 2014
Bioleaching	Size: 4 cm x 2.5 cm Pre-treated with 10M NaOH 1 L, 15% inoc., 50 rpm, 30°C,	Cu, Zn, Ni, Pb	Modified 9K medium	536, 152, 35.64 and 0.31 mg L ⁻¹ of Cu, Zn, Ni, Pb, respectively in 240 h	Adhapure et al., 2014
Leaching	Size: 4 cm x 4 cm Pre-treated with 10M NaOH 100 mL, 150 rpm at room temp.	Cu, Zn, Sn, Ni, Pb, Fe, Al, Ag, Pd, Au	HCl	100 % of all metals in 22h	Jadhav and Hocheng, 2015
			HNO ₃	100 % of all metals in 96 h	
			H ₂ SO ₄	8.8 % of Cu in 96 h	
			C ₂ H ₄ O ₂	9.89 % of Cu in 96 h	
Leaching	Size: 2 cm x 2 cm, 6 cm x 6 cm Pre-treated with 10M NaOH 150 mL, 150 rpm at room temp.	Cu, Zn, Sn, Ni, Pb, Fe, Al, Ag, Pd, Au	HCl	100 % of all metals in 8 h (2cmx2cm)	Jadhav and Hocheng, 2015
				100 % of all metals in 25 h (6cmx6cm)	
Leaching	Size: 4 cm x 4 cm Pre-treated with 10M NaOH 100 mL, static conditions, 30°C	Cu, Fe, Zn, Ni, Sn, Pb, Al, Ag, Pd, Au	C ₆ H ₈ O ₇ + H ₂ O ₂	100 % of all metals in 4 h	Jadhav and Hocheng, 2016
Bioleaching	Size: 5.6 cm x 2.6 cm Pre-treated with NaOH 200 mL, 180 rpm, 30°C	Cu, Zn, Pb	Modified 9K medium	70 % Cu, 55 % Zn and 0.5 % Pb	Joshi et al., 2017
Leaching	10 g small pieces Pre-treated with NaOH 100 mL, 60°C	Cu, Zn, Fe, Pb	HNO ₃	19000, 5.5, 2.04, 0.47 mg L ⁻¹ of Cu, Zn, Fe, Pb, respectively in 1 h	Gautam et al., 2018
Leaching	Size: 2 cm x 2 cm Pre-treated with 10M NaOH 100 mL, 30°C	Cu	Biogenerated H ₂ SO ₄ + H ₂ O ₂	100 % of Cu in 4 h (60 mL H ₂ SO ₄ + 20 mL H ₂ O ₂)	Chandane et al., 2020
Bioleaching	Size: 19 cm x 15 cm Pre-treated with 2M NaOH 100 mL, 10% inoc., 180 rpm, 30°C	Cu	SDB1 medium	> 99 % Cu in 48 h	Sodha et al., 2020
Bioleaching	Size: 2.5 cm x 3 cm Pre-treated with 10M NaOH 350 mL, 2% inoc., 130 rpm, 31°C	Cu, Ni, Zn, Pb	9K medium (Fe ²⁺)	68 % Cu, 36.7 % Ni, 53 Zn and 2.9 % Pb in 336 h	This study
Bioleaching	Size: 2.6 cm x 2.1 cm Pre-treated with 10M NaOH 350 mL, 2% inoc., 130 rpm, 31°C	Cu, Ni, Zn, Pb	9K medium (Fe ³⁺)	82 % Cu, 32 % Ni, 4 % Zn and 3 % Pb in 280 h	This study
Leaching	Size: 2.5 cm x 3 cm Pre-treated with 10M NaOH 350 mL., 150 rpm, 30°C, 300 h	Cu, Ni, Zn, Fe	H ₂ SO ₄	1168, 23, 21, and 981 mg L ⁻¹ of Cu, Ni, Zn, and Fe, respectively in 300 h	This study
			Fe ³⁺	1939, 53, 218 and 667 mg L ⁻¹ of Cu, Ni, Zn, Fe respectively in 300 h	

4.3.5. Preliminary design of a bioleaching reaction system

4.3.5.1. Bioleaching assembly

The conclusions hereby obtained can be applied to the design of an assembly for treating PCBs in a bioleaching reaction system. The scale-up of any reaction system can cover three levels: lab-scale, pilot-scale and semi-industrial/industrial scale. This classification is based on the bioreactor volume which is related to the technical/practical knowledge progress (know-how) and the bioprocess purpose (fermentation, cell growth, tissue culture, ore treatment...). As far as PCB biotreatment is concerned, most studies report a bioleaching reactor volume ranging from small scale (250 ml) to higher scale (10 L), but the practical cases for larger industrial scale bioleaching of WEEE are still very limited (Baniyadi et al., 2019; Erust et al., 2021).

This Section is devoted to the preliminary design of a lab-scale bioleaching system treating PCBs for copper recovery in a semi-continuous mode. The novelty of this design is that it is composed of two sections: the biological reaction system and the leaching system. The first one comprises two bioreactors (BR1 and BR2) that hold the biomass immobilized on a novel support material: bacterial cellulose. The second section contains the leaching reactor (LR). The general flowchart from WEEE collection to treatment is shown in Figure 4.17, where the selection of the entire PCB pieces (without crushing) and the highly concentrated NaOH pretreatment can be underlined.

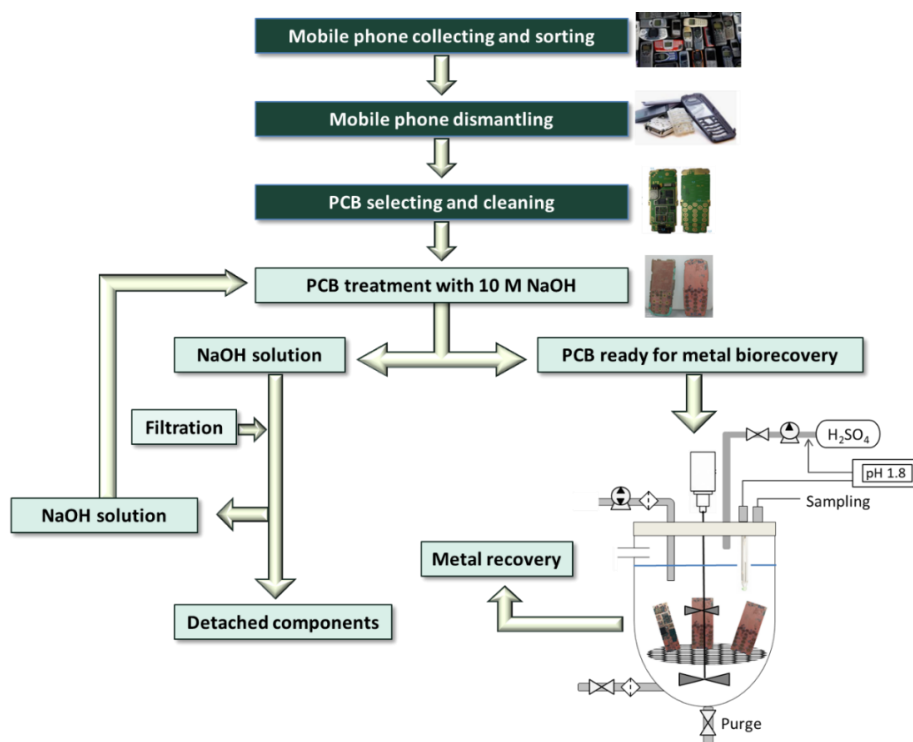


Figure 4.17. Flowchart of the process from obsolete phone collection to metal leaching.

Bearing in mind that the global system proposed in this study involves leaching and biooxidation in separated stages, the plant design draft for metal recovery would comprise three reactors (one LR reactor and two BR reactors), several control and chemical addition equipment and ancillary components.

4.3.5.2. Reactors and components

Among the commonly used bioreactors such as mechanically stirred tank reactors, rotating drum bioreactors, packed bed reactors, pulsed plate bioreactors, bubble column reactors, and airlift bioreactors, the continuous stirred ones (CSTR) were selected for this preliminary design (Ninimol et al., 2020). Thus, two identical CSTR bioreactors were devoted to the oxidant generation in two different media. One of them (biological reactor BR1) was used for biogenerating the leaching fresh medium, and the other one (biological reactor RB2) was used for continuously bioregenerating (recycling) the solution becoming from the PCB leaching system.

The rationale of using two separate bioreactors lies in complying with the objective of improving the sustainability of the process by prolonging the lifespan of the biologically active material and reusing of the biogenerated leaching solution.

Regarding the biological reaction system, the following features can be ascertained (Figure 4.18):

- **Bioreactor:** The bioreactors should be manufactured in borosilicate glass resistant to low pH values (1.5-2.0 range). The reactors and the upper covering could be sterilized. Several inlet and outlet pipes for liquid or air addition/extraction should be required (described below). The pH measurement would be carried out by immersing a pH probe through one port at the covering. Samples would be collected through an additional port.
- **Agitation:** The reactor bottom should be flat for magnetic agitation. Other agitation system (i.e., mechanical agitation) could damage the immobilized biomass due to attrition with the moving components and the reactor walls.
- **Support grille:** Immobilized biomass would be placed onto a grille separated from the agitation magnet. The grid material must be inert to prevent it from rusting or being damaged by the acid medium. As concluded in Chapter 2, the number of pieces of biologically activated material is a function of the nutrient medium volume-to-external surface area ratio (NMV:ESA), being the selected ratio 1:0.6 (mL:cm²).
- **Air compressor:** Air compressor would provide oxygen through an immersion pipe with sparger. No oxygen probe has been considered in this reactor because oxygen can be supplied by a regular air sparging, complying with metabolic uptake rates. Oxygen injection is discarded because it would increase the expenses and could cause

oxidative stress due to the formation of toxic reactive oxygen species (Guezennec et al., 2017).

- Piping: A piping system for the solutions' recirculation would connect the oxidation bioreactor with the regeneration bioreactor and the latter with the leaching reactor or the final waste treatment stage (exit). Another piping system would be devoted to the addition of nutrients, sulfuric acid and air (oxygen). Purges are designed in the two reactors.
- Pumping: Peristaltic hose pumps would be used for solution circulation or draining when necessary. Depending on the function, unidirectional or bidirectional pumps should be installed.
- Side outlets: Additional side outlets are included in the upside of the reactor's wall for air exit and overflowing security.
- Heating: The temperature in the bioreactor would be maintained at 31 °C by pumping hot water into the heating jacket around the reactor.
- Filters: Filters should be used in all the pipes to prevent particles (active material or PCB particles) from entering the leaching tank or the bioregeneration system.

The elements described above are shown in Figure 4.18.

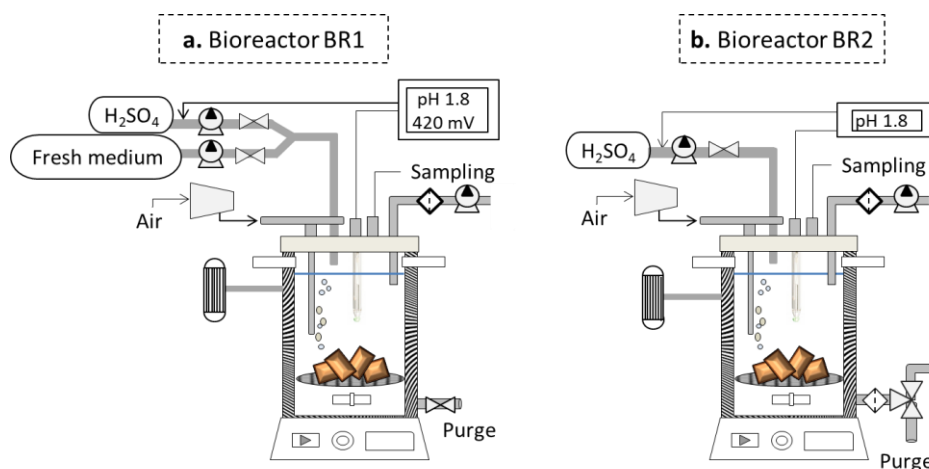


Figure 4.18. Diagram of the biological reactors (BR1 and BR2) for oxidant production (a) and solution regeneration (b).

Regarding the leaching system, the following features can be detailed (Figure 4.19):

- Reactor: The LR reactor should be manufactured in borosilicate glass resistant to low pHs in the 1.5-2.0 range. Round bottom reactor has been selected for better mechanical agitation and cleaning. The reactor volume has been reported to be dependent on the pulp density (Zhang et al., 2020), but this variable is not so relevant

when treating entire PCBs. Thus, the ratio PCB number:volume and the PCB (vertical) arrangement are determinant in this design.

The LR reactor should contain two ports at the top. The first one would be used to immerse a pH control probe. pH control is crucial for avoiding jarosite precipitation and the consequent oxidant loss. Additionally, sample extraction on a regular basis is mandatory for monitoring copper concentration, as this result would be determinant for making a decision on feeding one fraction of the solution to the regeneration reactor or to the final treatment reactor.

- Side outlets: Additional side outlets are included in the upside of the reactor's wall for air exit and overflowing security.
- Agitation: The solution can be agitated by a mechanical (double) stirrer. No attrition problems are expected because biomass is absent and the PCBs are fixed on a grilled plate. Small particles could be detached from the boards.
- Gilled plate: a support for holding the PCBs would be required.
- Pumping: Peristaltic hose pumps would be used for solution addition or draining when necessary. Depending on the function, unidirectional or bidirectional pumps should be installed.
- Piping: A piping system would conduct the leaching solution to the oxidant regeneration treatment (to BR2) or to the final waste treatment stage (exit). Another pipe would add sulfuric acid for pH control.
- Filters: Filters would be used in all the pipes to prevent the PCB small particles from entering the regeneration system or the final waste treatment stage (exit).

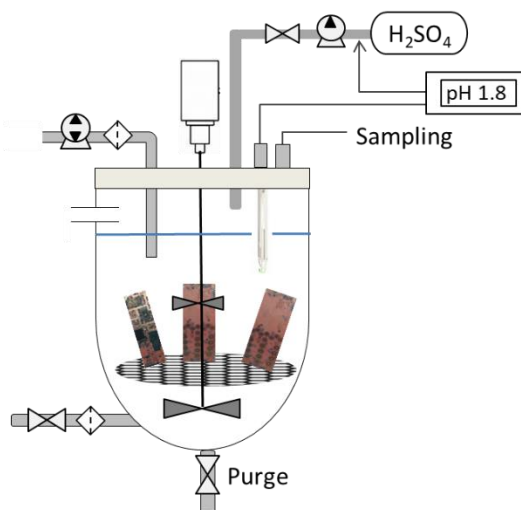


Figure 4.19. Diagram of the CSTR bioreactor for copper leaching (BL reactor).

The assembly of the three reactors (biological system + leaching system) in the global lay-out is shown in Figure 4.20.

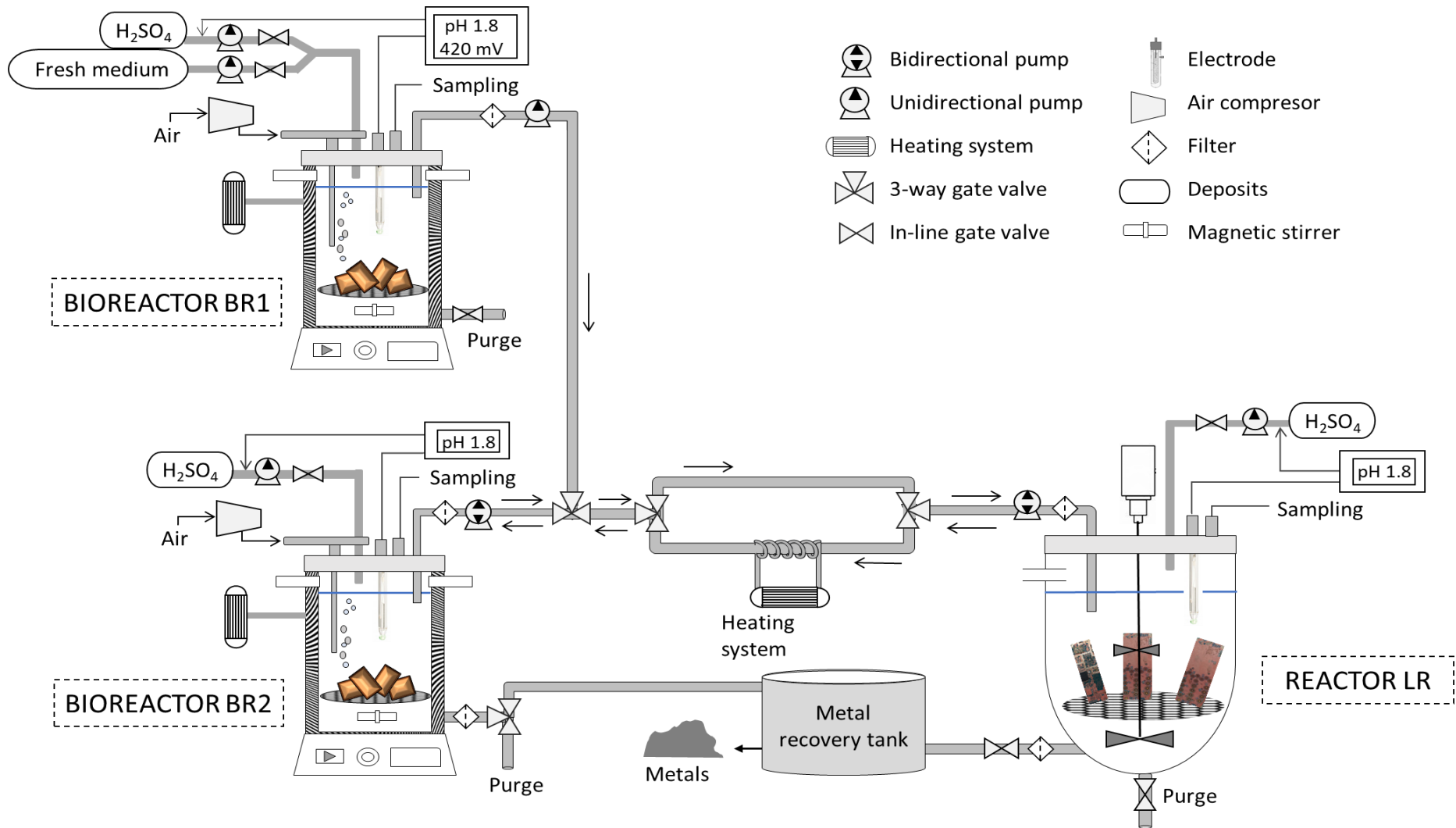


Figure 4.20. Diagram of the global process for PCB bioleaching.

4.4. CONCLUSIONS

Metal bioleaching and recovery from obsolete printed circuit boards (PCB) is a sustainable and necessary process for avoiding depletion of natural sources. In this case, the waste to be treated is very heterogeneous in terms of size, shape and elements, and, consequently, its composition is very variable.

In this chapter, several PCBs from obsolete mobile phones were grinded for homogenization. After acid digestion of the powder sample, the major element was found to be copper with an average content of $435 \pm 54 \text{ mg g}^{-1}$, which was in the wide range published in literature.

In addition to the power sample, the entire PCB without the epoxy covering was also used for bioleaching experiments. The pulverized sample (with a higher surface area) rendered a higher removal efficiency than the entire PCB after 336 h of treatment (78.3% versus 67.9%) being that difference more noticeable during the first 150 hours. Despite these results, pulverization pre-treatment entails an important cost (high energy consumption) and generates particulate matter that can be dangerous for human health. In addition, the use of the entire PCB can facilitate the management and separation of the pieces from the leachate, as well as providing a “cleaner” medium for microbial activity.

In the two-step bioleaching experiment with the entire PCB piece, a total amount of 82 % of copper was dissolved by the end of the assay (300 hours), which was attributed to the relevant contribution of the biomass in regenerating the oxidant. Other metals such as Ni and Zn were simultaneously extracted but the efficiency was considerably lower.

The hydrometallurgical alternative of using Fe^{3+} (not biologically regenerated) or H_2SO_4 as reagents was also tested for comparison purposes. The leaching process with the acid was almost negligible during the first 100 hours and it started to be more significant thenceforth. The copper extraction results obtained with biologically or no-biologically generated Fe^{3+} were similar during the first 200 hours. The biomass regeneration activity was concluded to be more determinat in longer experiments.

Finally, a lab-scale bioleaching system was preliminarily designed for treating entire PCBs in semi-continuous mode. The novelty is that the global bioleaching process is composed of two sections. The first one is devoted to the biological reaction, which comprises two bioreactors that hold the biomass immobilized on a novel support material (bacterial cellulose). The second section contains the leaching reactor. Finally, the metals would be recovered from the bioleached solution in an external tank.

4.5. REFERENCES

- Adhapure, N.N., Waghmare, S.S., Hamde, V.S., Deshmuck, A.M., 2013. Metal solubilization from powdered printed circuit boards by microbial consortium from bauxite and pyrite ores. *Applied Biochemistry and Microbiology*. 49, 256-262.
- Adhapure, N.N., Dhakephalkar, P.K., Dhakephalkar, A.P., Tembhurkar, V.R., Rajgure, A.V., Deshmuck, A. M., 2014. Use of large pieces of printed circuit boards for bioleaching to avoid precipitate contamination problem' and to simplify overall metal recovery. *MethodsX*. 1, 181-186.
- Arshadi, M., Mousavi, S.M., 2015. Multi-objective optimization of heavy metals bioleaching from discarded mobile phone PCBs: Simultaneous Cu and Ni recovery using *Acidithiobacillus ferrooxidans*. *Separation and Purification Technology*. 147, 210-219.
- Arshadi, M., Yaghmaei. S., 2020. Advances in bioleaching of copper and nickel from electronic waste using *Acidithiobacillus ferrooxidans*: evaluating daily pH adjustment. *Chemical Papers*. 74, 2211-2227.
- Benzal, E., Cano, A., Solé, M., Lao Luque, C., Gamisans, X., Dorado, A.D., 2020. Copper recovery from PCBs by *Acidithiobacillus ferrooxidans*: Toxicity of bioleached metals on biological activity. *Waste Biomass Valorization*. 11, 5483-5492
- Birloaga, I., De Michelis, I., Ferella, F., Buzatu, M., Vegliò, F., 2013. Study on the influence of various factors in the hydrometallurgical processing of waste printed circuit boards for copper and gold recovery. *Waste Management*. 33, 935-941.
- Birloaga, I., Coman, V., Kopacek, B., Vegliò, F., 2014. An advanced study on the hydrometallurgical processing of waste computer printed boards to extract their valuable content of metals. *Waste Management*. 34, 2581-2586.
- Birloaga, I., Vegliò, F., 2016. Study of multi-step hydrometallurgical methods to extract the valuable content of gold, silver and copper from waste printed circuit boards. *Journal of Environmental Chemical Engineering*. 4, 20-29.
- Brandl, H., Bosshard, R., Wegmann, M., 2001. Computer-munching microbes: metal leaching from electronic scrap by bacteria and fungi. *Hydrometallurgy*. 59, 319-326.
- Calgaro, C.O., Schlemmer, D.F., da Silva, M.D., Maziero, E.V., Tanabe, E.H., Bertuol, D.A., 2015. Fast copper extraction from printed circuit boards using supercritical carbon dioxide. *Waste Management*. 45, 289-297.
- Chandane, P., Jori, C., Chaudhari, H., Bhapkar, S., Deshmukh, S., Jadhav, U., 2020. Bioleaching of copper from large printed circuit boards for synthesis of organic-inorganic hybrid. *Environmental Science and Pollution Research*. 27, 5797-808.
- Choi, M.S., Cho, K.S., Kim, D.S., Kim, D.J., 2004. Microbial recovery of copper from printed circuit boards of waste computer by *Acidithiobacillus ferrooxidans*. *Journal of Environmental Science and Health*. 39(11- 12), 2973-2982.
- Díaz-Martínez, M.E., Argumedo-Delira, R., Sánchez-Viveros, G., Alarcón, A., Mendoza-López, M.R., 2019. Microbial bioleaching of Ag, Au and Cu from printed circuit boards of mobile phones. *Current Microbiology*. 76, 536-544.
- Díaz-Tena, E., Barona, A., Gallastegui, G., Rodríguez, A., López de Lacalle, L. N., Elías, A., 2017. Biomachining: Metal Etching via Microorganisms. *Critical Reviews in Biotechnology*. 37, 323-332.

- Gautam, P., Sharma, A.K., Sharma S., 2018. Extraction of metals from the discarded printed circuit board by leaching. *International Research Journal of Engineering and Technology*. 5, 243-247.
- Gu, W., Bai, J., Dai, J., Zhang, C., Yuan, W., Wang, J., Wang, P., Xin, Z., 2014. Characterization of extreme Acidophile Bacteria (*Acidithiobacillus ferrooxidans*) bioleaching copper from flexible PCB by ICP-AES. *Journal of Spectroscopy*. 8, 269351.
- Ha, V.H., Lee, J., Jeong, J., Hai, H.T., Jha, M.K., 2010. Thiosulfate leaching of gold from waste mobile phones. *Journal of Hazardous Materials*. 178, 1115-1119.
- Hadi, P., Xu, M., Lin, C.S.K., Hui, C.W., McKay, G., 2015. Waste printed circuit board recycling techniques and product utilization. *Journal of Hazardous Materials*. 11, 234-243.
- Holgersson, S., Steenari, B.-M., Björkman, M., Cullbrand, K., 2018. Analysis of the metal content of small-size Waste Electric and Electronic Equipment (WEEE) printed circuit boards—Part 1: Internet routers, mobile phones and smartphones. *Resources, Conservation and Recycling*. 133, 300-308.
- Hossain, M.S., Yahaya, A.N.A., Yacob, L.S., Rahim M.Z.A., Yusof, N.N.M., Bachmann, R.T., 2018. Selective recovery of copper from waste mobile phone printed circuit boards using sulphuric acid leaching. *Materials Today: Proceedings*. 5, 21698-21702.
- Hubau, A., Minier, M., Chagnes, A., Jouliau, C., Perez, C., Guezennec, A.G., 2018. Continuous production of a biogenic ferric iron lixiviant for the bioleaching of printed circuit boards (PCBs). *Hydrometallurgy*. 180, 180-191.
- Hubau, A., Chagnes, A., Minier, M., Touzé, S., Chapron, S., Guezennec, A.G., 2019. Recycling-oriented methodology to sample and characterize the metal composition of waste Printed Circuit Boards. *Waste Management*. 91, 62-71.
- Ilyas, S., Lee, J., Chi, R., 2013. Bioleaching of metals from electronic scrap and its potential for commercial exploitation. *Hydrometallurgy*. 131, 138-143.
- Ippolito, N.M., Medici, F., Pietrelli, L., Piga, L., 2021. Effect of Acid Leaching Pre-Treatment on Gold Extraction from Printed Circuit Boards of Spent Mobile Phones. *Materials*. 14, 362.
- Isildar, A., van de Vossenberg, J., Rene, E. R., van Hullebusch, E. D., Lens, P. N. L., 2016. Two-step bioleaching of copper and gold from discarded printed circuit boards (PCB). *Waste Management*. 57, 149-157.
- Jadhav, U., Hocheng, H., 2015. Hydrometallurgical recovery of metals from large printed circuit board pieces. *Scientific Reports*. 5, 14574.
- Jadhav, U., Su, C., Hocheng, H., 2016. Leaching of metals from printed circuit board powder by an *Aspergillus niger* culture supernatant and hydrogen peroxide. *RSC Advances*. 6, 43442-43452.
- Joshi, V., Shah, N., Wakte, P., Dhakephalkar, P., Dhakephalkar, A., Khobragade, R., Naphade, B., Shaikh, S., Deshmukh, A., Adhapure, N., 2017. Comparative bioleaching of metals from pulverized and non-pulverized PCBs of cell phone charger: advantages of non-pulverized PCBs. *Environmental Science and Pollution Research*. 24, 28277-28286.
- Kasper, A.C., Berselli, G.B.T., Freitas, B.D., Tenorio, J.A.S., Bernardes, A.M., Veit, H.M., 2011. Printed wiring boards for mobile phones: characterization and recycling of copper. *Waste Management*. 31, 2536-2545.

- Khatri, B. R., Sodha, A. B., Shah, M. B., Tipre, D. R., Dave, S. R., 2018. Chemical and microbial leaching of base metals from obsolete cell-phone printed circuit boards. *Sustainable Environment Research*. 28, 333-339.
- Kim, E.Y., Kim, M.S., Lee, J.C., Pandey, B.D., 2011. Selective recovery of gold from waste mobile phone PCBs by hydrometallurgical process. *Journal of Hazardous Materials*. 198, 206-215.
- Kim, B.S., Lee, J.C., Jeong, J., Yang, D.H., Shin, D., Lee, K.I., 2013. A novel process for extracting precious metals from spent mobile phone PCBs and automobile catalysts. *Materials Transactions*. 54, 1045-1048.
- Le, H.L., Yamasue, E., Okumura, H., Ishihara, K.N., 2013. MEMRECS—a sustainable view for metal recycling from waste printed circuit boards. *Journal of Environmental Protection*. 4, 803-810.
- LME (London Metal Exchange), 2021. LME COPPER. <https://www.lme.com/en-GB/Metals/Non-ferrous/Copper#tabIndex=0> (accessed 14 May 2021).
- Moltó, J., Egea, S., Conesa, J.A., Font, R., 2011 Thermal decomposition of electronic wastes: Mobile phone case and other parts. *Waste Management*. 31, 2546-2552.
- Monneron-Enaud, B., Wiche, O., Schlömann, M., 2020. Biodismantling, a Novel Application of Bioleaching in Recycling of Electronic Wastes. *Recycling*. 5, 22.
- Moyo, T., Chirume, B.H., Petersen, J., 2020. Assessing alternative pre-treatment methods to promote metal recovery in the leaching of printed circuit boards. *Resources, Conservation and Recycling*. 152, 104545.
- Ogunniyi, I.O., Vermaak, M.K.G., Groot, D.R., 2009. Chemical composition and liberation characterization of printed circuit board comminution fines for beneficiation investigations. *Waste Management*. 29, 2140-2146.
- Oliveira, P.C., Cabral, M., Nogueira, C.A., Margarido, F., 2010. Printed Circuit Boards Recycling: Characterization of Granulometric Fractions from Shredding Process. *Materials Science Forum*. 636-637, 1434-1439.
- Patel, S., Patel, R., Gautam, A., Gautam, S., 2017. Influence of oxidizing agent on recovery of metals including gold and silver from printed circuit boards. *International Research Journal of Engineering and Technology*. 4, 830-834.
- Priya, A., Hait, S., 2017. Comparative assessment of metallurgical recovery of metals from electronic waste with special emphasis on bioleaching. *Environmental Science and Pollution Research*. 24, 6989-7008.
- Priya, A., Hait, S., 2018. Extraction of metals from high grade waste printed circuit board by conventional and hybrid bioleaching using *Acidithiobacillus ferrooxidans*. *Hydrometallurgy*. 177, 132-139.
- Rao, M.D., Singh, K.K., Morrison, C.A., Love, J.B., 2020. Challenges and opportunities in the recovery of gold from electronic waste. *RSC Advances*, 10, 4300-4309.
- Rao, M.D., Singh, K.K., Morrison, C.A., Love, J.B., 2021. Recycling copper and gold from e-waste by a two-stage leaching and solvent extraction process. *Separation and Purification Technology*. 263, 118400.

- Senophiyah-Mary, J., Loganath, R., Meenambal, T., 2018. A novel method for the removal of epoxy coating from waste printed circuit board. *Waste Management and Research*. 36, 645-652.
- Sethurajan, M., van Hullebusch, E.D., 2019. Leaching and Selective Recovery of Cu from Printed Circuit Boards. *Metals*. 9, 1034.
- Shah, M.B., Tipre, D.R., Dave, S.R., 2014. Chemical and biological processes for multi-metal extraction from waste printed circuit boards of computers and mobile phones. *Waste Management and Research*. 32, 1134-1141.
- Silvas, F.P.C., Correa, M.M.J., Caldas, M.P.K., de Moraes, V.T., Espinosa, D.C.R., Tenório, J.A.S., 2015. Printed circuit board recycling: physical processing and copper extraction by selective leaching. *Waste Management*. 46, 503-510.
- Silveira, A.V., Fuchs, M.S., Pinheiro, D.K., Tanabe, E.H., Bertuol, D.A., 2015. Recovery of indium from LCD screens of discarded cell phones. *Waste Management*. 45, 334-342.
- Silverman, M. P., Lundgren, D. G., 1959. Studies on the chemoautotrophic iron bacterium *Ferrobacillus ferrooxidans*: I. An improved medium and a harvesting procedure for securing high cell yields. *Journal of Bacteriology*. 77, 642-647.
- Sodha, A.B., Tipre, D.R., Dave, S.R., 2020. Optimisation of biohydrometallurgical batch reactor process for copper extraction and recovery from non-pulverized waste printed circuit boards. *Hydrometallurgy*. 191, 105170.
- Tripathi, A., Kumar, M., Sau, D.C., Agrawal, A., Chakravarty, S., Mankhand, T.R., 2012. Leaching of gold from the waste mobile phone printed circuit boards (PCBs) with ammonium thiosulphate. *International Journal of Metallurgical Engineering*. 1, 17-21.
- Tuncuk, A., Akcil, A., Yazici, E.Y., Devici, H., 2012. Aqueous metal recovery techniques from e-scrap: hydrometallurgy in recycling. *Minerals Engineering*. 25,28-37.
- Ueoka, N., Kouzuma, A., Watanabe, K., 2016. Missing iron-oxidizing acidophiles highly sensitive to organic compounds. *Microbes and Environments*, 31, 244-248.
- Van Yken, J., Cheng, K.Y., Boxall N.J., Nikoloski, A.N., Moheimani, N., Valix, M., Sahajwalla, V., Kaksonen, A.H., 2020. Potential of metals leaching from printed circuit boards with biological and chemical lixiviants. *Hydrometallurgy*. 196, 105433.
- Wu, W., Liu, X., Zhang, X., Zhu, M., Tan, W., 2018. Bioleaching of copper from waste printed circuit boards by bacteria-free cultural supernatant of iron-sulfur-oxidizing bacteria. *Bioresources and Bioprocessing*. 5, 10.
- Xiu, F.R., Qi, Y., Zhang, F.S., 2015. Leaching of Au, Ag, and Pd from waste printed circuit boards of mobile phone by iodide lixiviant after supercritical water pre-treatment. *Waste Management*. 41, 134-141.
- Yamane, L.H., de Moraes, V.T., Espinosa, D.C.R., Tenório, J.A.S., 2011. Recycling of WEEE: characterization of spent printed circuit boards from mobile phones and computers. *Waste Management*. 31, 2553-2558.
- Yang, T., Xu, Z., Wen, J., Yang, L., 2009a. Factors influencing bioleaching copper from waste printed circuit boards by *Acidithiobacillus ferrooxidans*. *Hydrometallurgy*. 97, 29-32.
- Yang, Y., Chen, S., Li, S., Chen, M., Chen, H., Liu, B., 2014. Bioleaching waste printed circuit boards by *Acidithiobacillus ferrooxidans* and its kinetics aspect. *Journal of Biotechnology*. 173, 24-30.

Yang, C., Zhu, N., Shen, W., Zhang, T., Wu, P., 2017. Bioleaching of copper from metal concentrates of waste printed circuit boards by a newly isolated *Acidithiobacillus ferrooxidans* strain Z1. *Journal of Material Cycles and Waste Management*. 19, 247-255.

Yildirim, E., Onwudili, J.A., Williams, P.T., 2015. Chemical recycling of printed circuit board waste by depolymerization in sub-and supercritical solvents. *Waste Biomass Valorization*. 6, 959-965.

Zhu, N., Xiang, Y., Zhang, T., Wu, P., Dang, Z., Li, P., and Wu, J., 2011. Bioleaching of metal concentrates of waste printed circuit boards by mixed culture of acidophilic bacteria. *Journal of Hazardous Materials*. 192, 614-619.

CHAPTER 5.
RECOVERY OF COPPER FROM
SPENT SOLUTIONS

5.1. OBJECTIVE

A sustainable process seeks to reduce the environmental impact by minimizing energy and non-renewable raw materials consumption and waste production. Biotechnology can make a significant contribution to achieving these goals, providing substantial economic and environmental benefits. Among bioprocesses with a potential for future implementation, bioleaching is an attractive alternative to the physical and chemical technologies for recovering metals from WEEE (Jadhav and Hocheng, 2015; Wang et al., 2018). Biomachining is another sustainable application for metal solubilization. The bioleaching and biomachining processes, like many others, generate liquid residues with high metal concentrations. In this particular case, the working solution becomes a residue when cellular metabolism inhibition is high (as a consequence of metal concentration increase) and oxygen availability is too low (Mazuelos et al., 2019). Accordingly, once the recovery of biomass activity is no longer feasible and Fe^{2+} bio-oxidation is considerably reduced, the depleted solution containing high concentrations of metals should be treated before being discharged. Bearing in mind the strategic relevance of copper and the high concentration of that metal in the waste solution, the depleted liquid residue from bioleaching and biomachining processes is a secondary source of copper.

Thus, the objective of this chapter is to assess the technical and economic viability of two simple treatments for the recovery of copper from waste solutions that can be obtained in biomachining and bioleaching processes. The first option involved fractionated chemical precipitation as hydroxides with ulterior calcination. The second alternative was the electrochemical method for copper recovery. The efficient recovery of copper from these waste solutions will not only mitigate the environmental impact of the metal solubilization bioprocesses, but also contribute to improve their economic viability.

Figure 5.1 shows the outline of the experimental section of this chapter.

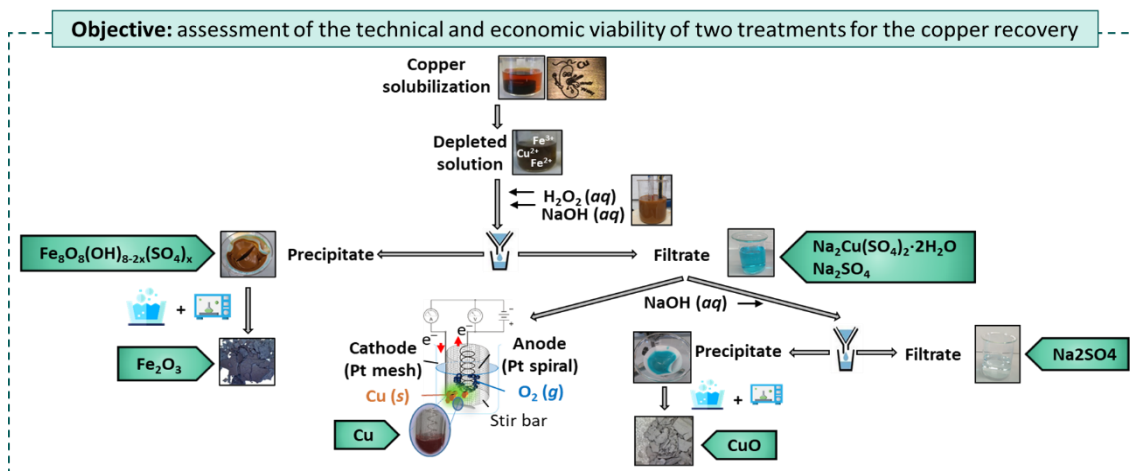


Figure 5.1. Outline of the experimental section of this chapter.

5.2. MATERIALS AND METHODS

5.2.1. Composition of the synthetic liquid residue (SLR)

The liquid residue used in this experimental section was synthesized in the laboratory simulating a real depleted solution obtained in a bioleaching/biomachining process. In a real case, 0.45 μm diameter ultrafiltration would be a mandatory preliminary step for eliminating the microorganisms. The solution is considered depleted when the Fe^{3+} oxidant concentration is too low (attributed to biomass inactivity for regenerating the oxidant) and/or when the copper concentration inhibits microbial activity.

One liter of the SLR was prepared by mixing two solutions with prior pH adjustment to a value of 1.8. The first one contained Fe^{2+} added as $\text{FeSO}_4 \cdot 7\text{H}_2\text{O}$ (44.81 g L^{-1}) and NH_4^+ added as $(\text{NH}_4)_2\text{SO}_4$ (3 g L^{-1}). The second one contained Cu^{2+} added as $\text{CuSO}_4 \cdot 5\text{H}_2\text{O}$ (39.29 g L^{-1}). Once both solutions had been mixed, the final concentrations of the ions of interest were $9.0 \text{ g Fe}^{2+} \text{ L}^{-1}$, $10.0 \text{ g Cu}^{2+} \text{ L}^{-1}$ and $1.0 \text{ g NH}_4^+ \text{ g L}^{-1}$. The copper concentration in the synthetic liquid residue ($10 \text{ g Cu}^{2+} \text{ L}^{-1}$) was selected as representative of the depleted solution. Other minor components of the medium were not considered in this study.

5.2.2. Precipitation procedure

A sequential procedure was designed to precipitate Fe and Cu separately. First, the Fe^{2+} contained in the SLR was oxidized to Fe^{3+} with hydrogen peroxide (H_2O_2) (30 % w:v) until a significant change in the ORP value was measured. This was the starting solution for all the ensuing experiments (SLR_o oxidized solution). To prevent deterioration, the H_2O_2 reagent was stored in a refrigerator at 4 °C.

The precipitation procedure was applied as a two-stage sequential treatment (Figure 5.2) by adding a solution of NaOH 1.0 M to 100 mL of the SLR_o solution (by triplicate). The first stage consisted in increasing the pH from 1.8 to 4.0. The precipitate (P1) was separated by filtration (Filter-Lab No. 1240 filter paper with a 7-9 μm pore diameter), washed and calcined. The filtrate (SLR₁) was used in the second stage. A NaOH 1.0 M solution was added to this filtrate until the pH value was 8.0, resulting in a P2 precipitate and a SLR₂ filtrate. The resulting precipitate (P2) was filtered, washed and calcined, rendering the P2 final precipitate (P2cw). The pH values (4.0 and 8.0) for both precipitation stages were selected on the basis of the solubility constant at 25 °C of the possible solids.

5.2.3. Electrodeposition procedure

Copper was recovered from the SLR_1 solution by electrodeposition (Figure 5.2) at both a constant current intensity of 2.0 A (with variable potential) (IKA ELEKTROLYSE EN 500) and a constant voltage of 10 V (with variable current intensity) (LSCI ACS-160). The temperature was 24 °C and the shaking speed 700 rpm. Both systems were equipped with Pt Winkler electrodes (\varnothing 36x50 mm net cathode and \varnothing 11x70 mm cylinder anode) to avoid contamination caused by other typical electrode materials, such as stainless steel.

The pre-weighted anode and cathode were submerged 35 mm and 25 mm, respectively, in a volume of 100 mL of the Fe-free SLR_1 solution at pH 4.0, and then connected to the voltage. The presence of Fe^{3+}/Fe^{2+} redox couple interferes with copper electrodeposition because the Cu^+ ions generated during the reduction of Cu^{2+} ions can be oxidized by the Fe^{3+} ions in the solution (Milchev and Zapryanova, 2006; Chen et al., 2013). In this study, the prior precipitation of Fe avoided these interferences. At the end of the electrodeposition process, the cathode coated with solid copper (Cu^0) was removed from the solution, dried and weighed. The efficiency of the electrodeposition process was calculated by measuring the copper concentration in the solution before and after deposition. Finally, both Pt Winkler electrodes were cleaned in an ultrasonic bath for five min in diluted nitric acid (HNO_3 50 % v:v), and then washed in 95 % ethanol (v:v).

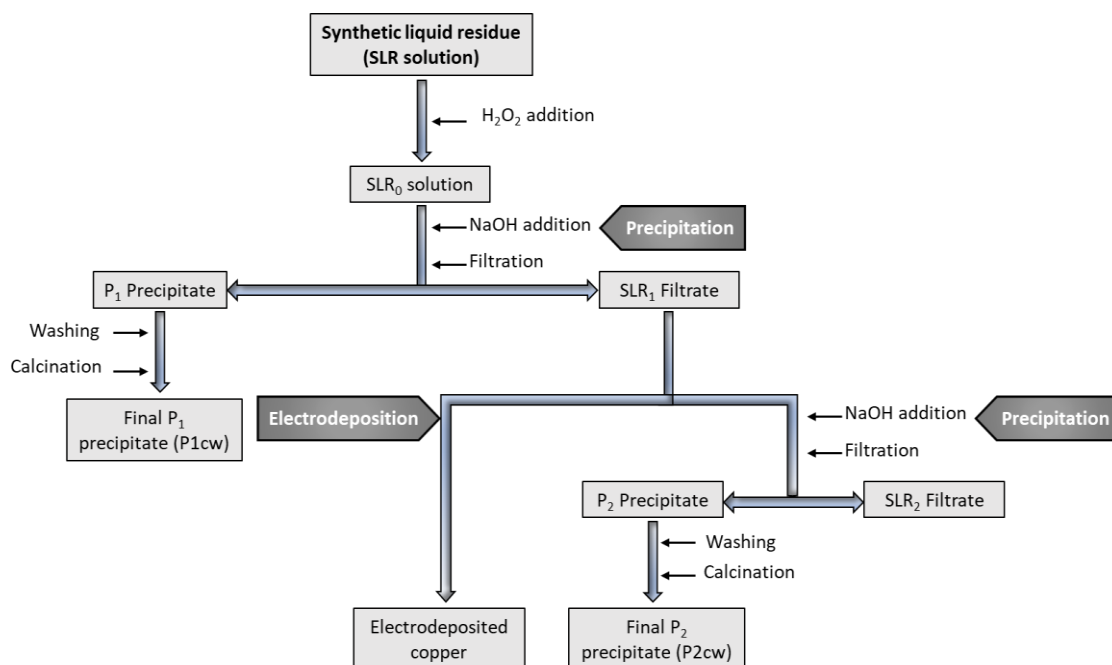


Figure 5.2. Schematic diagram for the recovery process.

5.2.4. Analytical methods

The dry residue of the SLR₁ and SLR₂ filtrates and the residue of the two precipitated solids (P1 and P2) calcined to 800 °C were measured. A thermogravimetric analysis (TG) of both solids was performed using a SETARAM TAG 24 for the 25-800 °C temperature range at a heating rate of 10 °C min⁻¹ in an oxygen atmosphere.

The pH and redox potential were monitored throughout the process by following the procedure described in Sections 2.5 *Determination of iron species in dissolution* and 2.8 *Other methods* (materials and general methods).

The diffraction patterns were registered in a Philips X'Pert-Pro automatic x-ray diffractometer using CuK α radiation in the 2 θ range from 5° to 60° with a step size of 0.02°. The images were obtained by an AXIO Lab A1 Carl Zeiss camera and Leuchtturm magnifying glass.

The Cu content in the solution was measured by atomic absorption spectrometry (AAAnalyst 100, Perkin Elmer) and by inductively coupled plasma optical emission spectrometry (ICP-OES, Optima 2000 DV, Perkin Elmer). The Fe content was measured by the bipyridine method, as described in Section 2.6. *Metal content analysis (ICP and AAS)* (materials and general methods)

5.2.5. Economic Analysis

Only energy and reagent costs have been considered in this section for comparing the two alternatives for copper recovery. The energy cost of the recovery by precipitation or electrodeposition was evaluated as proposed by Collivignarelli et al. (2019) (Equation 5.1):

$$C_{\text{recovery}} (\text{€ kg}^{-1}) = E_{\text{electro}} (\text{kWh kg}^{-1}) \cdot C_{\text{energy}} (\text{€ kWh}^{-1}) \quad (\text{Eq. 5.1})$$

where C_{recovery} is the cost of the copper recovery, E_{electro} is the energy consumed by kg of deposited copper, and C_{energy} is the cost of electricity.

The average cost of one ton raw copper in the London Metal Exchange (V_{Cu}) in May 2021 was around 10,537 US\$ t⁻¹ (LME, 2021), and the average exchange rate of the US dollar to the euro was 1.2069 US\$ €⁻¹. Thus, Equation 5.2 was used as a reference for the cost of 1 kg raw copper.

$$C_{\text{raw}} (\text{€ kg}^{-1}) = \frac{V_{\text{Cu}} (\text{US\$ t}^{-1})}{1000 \cdot \text{Exchange} (\text{US\$ €}^{-1})} \quad (\text{Eq. 5.2})$$

Finally, the maximum energy consumption feasible for Cu recovery (E_{\max}) was calculated by dividing the cost of raw copper (i.e., C_{raw}) into the cost of electricity (C_{energy}) according to Equation 5.3.

$$E_{\max} (\text{kWh kg}^{-1}) = \frac{C_{\text{raw}} (\text{€ kg}^{-1})}{C_{\text{energy}} (\text{€ kWh}^{-1})} \quad (\text{Eq. 5.3})$$

The specific energy consumption (E_{electro}) of the electrodeposition process was calculated according to the equation proposed by Chen et al. (2013) (Equation 5.4).

$$E_{\text{electro}} \left(\frac{\text{kWh}}{\text{kg}} \right) = \frac{A \cdot \Delta V \cdot t}{(C_0 - C) \cdot V} \quad (\text{Eq. 5.4})$$

where A is the operational current (ampere); ΔV is the operational electric potential difference (volt); t is operational time (h); C_0 and C are initial and final copper concentrations (g L^{-1}), respectively; V is operational volume (L).

5.3. RESULTS AND DISCUSSION

Previous studies have shown that the copper removal rate is substantially reduced when the $\text{Fe}^{3+}/\text{Fe}^{2+}$ mass ratio drops below 2:1 (Díaz-Tena et al., 2016). Nevertheless, the initial SLR in this study contained only Fe^{2+} (9 g L^{-1}) in order to simulate the most unfavorable case (absence of Fe^{3+} , and consequently total suspension of the chemical oxidation-reduction process). After preparing the SLR solution, the first step in the experimental process was to complete the oxidation of Fe^{2+} to Fe^{3+} because ferric ion precipitation is more efficient. The addition of H_2O_2 to 100 mL SLR was monitored by the ORP value (Figure 5.3). A total volume of 19 mL H_2O_2 30 % w:v was required until a change in the ORP value from 396.2 mV to 667.4 mV was recorded, indicating complete iron oxidation. Consequently, this simple parameter was concluded to be an effective and quick detector for the preliminary oxidation step.

The pH value increased slightly from 1.8 to 2.4 due to H^+ consumption throughout the process. If technical grade H_2O_2 (30 % w:v, average price for technical grade H_2O_2 7.00 € L^{-1}) is used, and considering the most unfavorable case when all the iron is in its reduced form, the reagent cost of this pre-treatment amounts to 1.33 € L^{-1} (BuyersGuideChem, 2020). Despite this cost, one outstanding feature of using this oxidant is the total absence of secondary products in the treated solution, which contributes to the process's sustainability.

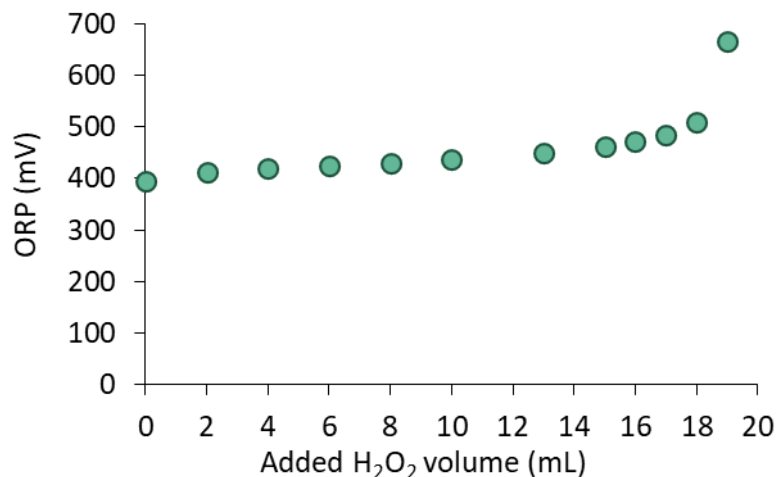


Figure 5.3. ORP evolution during the Fe²⁺ oxidation process with H₂O₂.

5.3.1. Precipitation

The main limitation of any chemical precipitation by neutralization is the lack of selectivity. Nevertheless, when only two or a few metals are present in the solution, it can be effective and convenient for treating liquid residues, such as those obtained from the biomachining of copper pieces. Thus, 100 mL of the SLR₀ was used here for the precipitation procedure. A total volume of 65 mL of NaOH 1 M solution was added slowly until a constant pH value of 4.0 was reached.

A brownish dense solid (P1) precipitated after the addition of the basic reagent, rendering a consumption of 2.88 g NaOH per g of oxidized iron (Figure 5.4a). The ORP value remained almost constant at 667.4 mV until a sudden decrease occurred during the addition of the last 10 mL NaOH, as a consequence of the progressive removal of the oxidized iron from the liquid. The P1 solid was calcined at 800 °C (P1c) (Figure 5.4b) and then washed (P1cw) (Figure 5.4c).

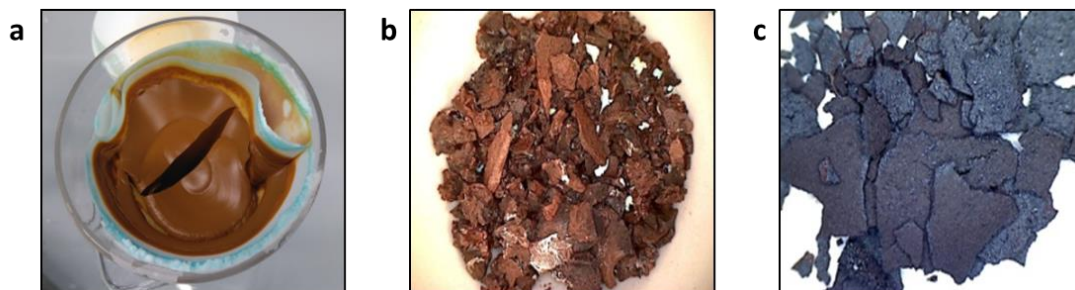


Figure 5.4. Photographs of the three P1 solids: fresh precipitate (a), calcined (b) and calcined and washed (c).

The P1 solid was analyzed by TG (Figure 5.5a) and derivative thermogravimetric (DTG) (Figure 5.5b). The TG and DTG patterns obtained for this solid were very similar to those reported by Jiménez et al. (2019) for schwertmannite, which is a poorly crystalline iron oxyhydrogensulfate mineral with a variable composition, typically represented as $\text{Fe}_8\text{O}_8(\text{OH})_{8-2x}(\text{SO}_4)_x$ (x being in the 1-1.75 range). A total weight loss of 35 % was recorded from 25 to 800 °C, which was attributed to the release of water molecules, hydroxyl groups, and sulfur as SO and SO₂ from the sulfate groups. The partial weight loss at 400 °C was 22 %, consistent with the results obtained by Kim et al. (2002) and Jiménez et al. (2019) for schwertmannite.

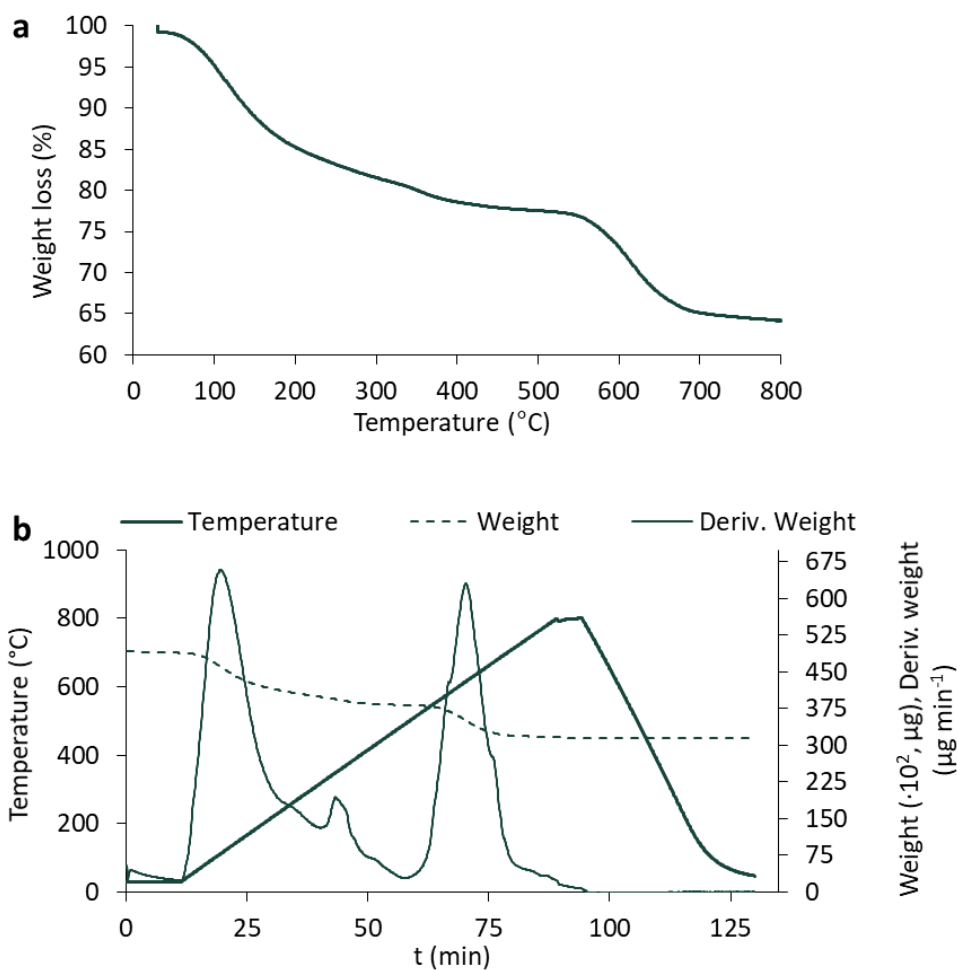


Figure 5.5. Characterization of the P1 precipitated sample: TG (a) and DTG analysis (b).

Previous studies have pointed out that ferric iron can also precipitate as A-jarosités ($(\text{Na}^+, \text{NH}_4^+, \text{H}_3\text{O}^+)-\text{Fe}_3(\text{SO}_4)_2(\text{OH})_6$) depending on the relative concentrations of NH_4^+ and Na^+ (Sandy Jones et al., 2014). At 25 °C, the solubility product ($\log K_{\text{so}}$) of Na-jarosite (natrojarosite) and NH_4 -jarosite (ammoniojarosite) is -8.56 and -9.76, respectively, suggesting that equilibrium conditions favor the formation of NH_4 -jarosite (Gaboreau and Vieillard, 2004). Nevertheless, Sandy Jones et al. (2014) have found that

ammoniojarosite is not the dominant species when the concentration of NH_4^+ is lower than 80 mM. In this study, the NH_4^+ concentration after NaOH addition was 50 mM, and so this jarosite type was concluded not to be abundant. The formation of natrojarosite was also disregarded according to the TG and DTG pattern. Interestingly, Antelo et al. (2013) have found that Cu^{2+} ions can be incorporated into the schwertmannite structure, increasing the stability of this iron oxyhydroxysulfate. The content of Cu^{2+} in the filtrate (SLR_1) showed that only about 3 % of the initial metal was lost in the brownish P1 solid, probably as cuprocopiapite ($\text{CuFe}_4(\text{SO}_4)_6(\text{OH})_2 \cdot 2\text{H}_2\text{O}$) or incorporated into the schwertmannite (Table 5.1). The iron content in the SLR_1 liquid was lower than 0.001 g L^{-1} , rendering a quantitative precipitation of this metal.

Table 5.1. Parameters measured in the SLR_0 , SLR_1 and SLR_2 samples.

	SLR_0	SLR_1	SLR_2
Dried residue (g L^{-1})	78.32 ± 0.98	56.82 ± 0.88	48.71 ± 0.96
pH at 25 °C	1.8 ± 0.1	4.0 ± 0.1	8.0 ± 0.1
Redox potential (mV)	667.4 ± 2.1	531.9 ± 1.5	397.3 ± 1.3
Total Cu ($\text{g L}_{\text{SLR}_0}^{-1}$)	9.9 ± 0.1	9.6 ± 0.1	< 0.04
Total Fe ($\text{g L}_{\text{SLR}_0}^{-1}$)	9.0 ± 0.1	$< 2 \cdot 10^{-3}$	$< 2 \cdot 10^{-3}$

As already stated, the calcination of the precipitate P1 at 800 °C rendered a reddish solid (P1c) that was washed and gently dried. The resulting greyish solid (P1cw) was identified by X-ray analysis as synthetic hematite (Fe_2O_3) (Figure 5.4c). Several other parameters were measured in the SLR_1 filtrate (Table 5.1). The ORP at 25 °C was 531.9 mV (about 20 % lower than in the original SLR_0 sample) due to the removal of Fe^{3+} from the solution. The dried content was 28 % lower in the filtrate than in the original solution attributed to the dilution effect, and the X-ray analysis of the dried residue in the filtrate showed that the main species were monoclinic kröhnkite ($\text{Na}_2\text{Cu}(\text{SO}_4)_2 \cdot 2\text{H}_2\text{O}$) and orthorhombic sodium sulfate (Na_2SO_4), revealing the absence of iron species in the solution.

An additional volume of 20 mL of NaOH 1M was added to the SLR_1 filtrate in order to precipitate the copper at pH 8.0. The blue precipitate in Figure 5.6a (P2) contained three compounds: CuO , $\text{Cu}_3(\text{SO}_4)(\text{OH})_4$ and Na_2SO_4 . After calcination and gentle washing, the resulting grey solid (P2cw) (Figure 5.6b) was weighed (1.0021 g) and identified as synthetic tenorite (CuO). Thus, the amount of Cu recovered in this solid was 80 % of the original metal content in the liquid residue. CuO is a valuable product, as it is a precursor of other copper-containing compounds for diverse applications (e.g., wood preservatives and pigments). Technical grade CuO can be purchased for around 25 € kg^{-1} , although high quality copper oxide can cost 694 € kg^{-1} (Sigma-Aldrich, 2020).

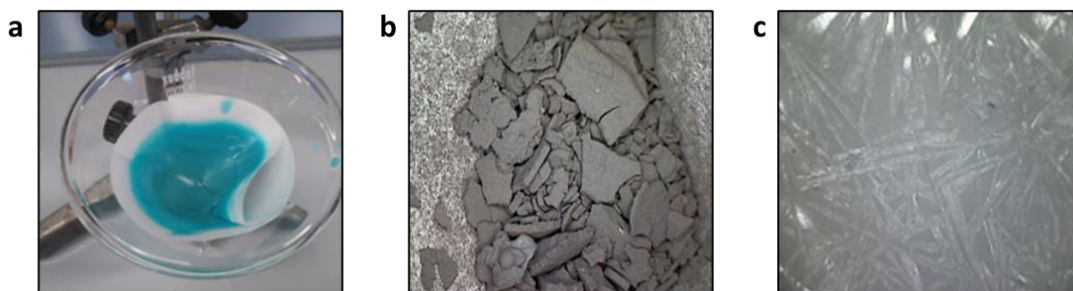


Figure 5.6. Photographs of the three P2 solids: fresh precipitate (a), calcined and washed (b) and dried solid of the SRL2 filtrate (c).

Copper losses during the process can be attributed to the manual recovery of the precipitates and, to a lesser extent, to the formation of soluble Cu-NH₃ complexes when the pH fell within the alkaline range. In the presence of ammonia, Cu²⁺ is stable as the Cu(NH₃)₄²⁺ complex, and it can even work as an oxidizing agent for metallic copper in an ammoniacal alkaline solution (Koyama et al., 2006). Bearing in mind that the *pK_a* for the NH₄⁺/NH₃ system at 25 °C is 9.25, and that the NH₄⁺ concentration in the original acid solution was 59 mM, only a very small amount of Cu could form soluble complexes because the NH₃ available in the solution at pH 8.0 was very scarce (about 3.2 mM).

The residual copper content in the SLR₂ filtrate showed that the metal removal was quantitative (Table 5.1). The dried solid SLR₂ (Figure 5.6c) was identified as Na₂SO₄ (monoclinic system), and the weight obtained was 48.72 g L⁻¹. Despite this considerable weight, sodium sulfate is not particularly toxic for humans (no dose has been established) (TOXNET, 2019).

A total amount of 3.4 g NaOH was required for the two precipitation steps of 100 mL SLR₀, costing 0.27 € L⁻¹ SLR₀ (0.21 € L⁻¹ and 0.06 € L⁻¹ for the Fe and Cu precipitation, respectively). The average price for commercial NaOH in Spain was 8.11 € kg⁻¹ (Panreac, 2021). The overall reagent consumption, including the initial oxidation procedure with H₂O₂ and the alkaline reagent, amounted to a maximum value of 1.60 € L⁻¹ SLR, although this cost is reduced considerably when the Fe³⁺/Fe²⁺ ratio in the depleted solution is high. Additional expenses include the energy supply for pumping and calcination, and personnel. This procedure's main drawback is that it is time-consuming.

5.3.2. Electrodeposition

The SLR₁ solution to be treated by electrolysis was Fe-free, but it contained a high amount of sulfates, as revealed by the dry residue value (56.82 g L⁻¹). Additionally, the possible excess of H₂O₂ in the solution was avoided by halting the addition of oxidant when the ORP value suddenly increased. Several authors have mentioned that the excess of this oxidant in the solution could hinder metal deposition (Balaji, 2006). It is

worth mentioning that the stoichiometric addition of H_2O_2 had a secondary benefit for the process. In the real case in which the biomass should be removed by filtration before treatment, H_2O_2 would promote the elimination of residual bacteria, as also pointed out by other authors (Ma and Lin, 2013; Collivignarelli et al., 2019).

In any electrolysis process, the lower the standard electrode potential of the metal, the weaker oxidation ability of the oxidized state and the stronger reduction ability of its corresponding reduced state (Qiu et al., 2020). Accordingly, the potentials of metal cations present in the media and the composition of electrolyte affect electrodeposition performance.

Considering the main compounds of the SLR_1 solution, the theoretical reactions that could take place during the process are summarized below (Equations 5.5-5.8):

In the cathode:



In the anode:



The main cathodic and anodic reactions are therefore copper deposition (Equation 5.6) and water oxidation (Equation 5.7), respectively, and the minimum voltage required was 0.89 V under standard conditions.

First, a constant current intensity of 2.0 A was applied to 100 mL of the Fe-free SLR_1 solution, corresponding to a current density of 60 A cm^{-2} . Higher current density values have been applied in recent studies with copper concentrations as high as $74,100 \text{ mg L}^{-1}$, although increasing the current density to 1000 A cm^{-2} did not have a positive influence on the copper removal yield (Collivignarelli et al., 2019). Some key factors to optimize electrodeposition process, such as Cu^{2+} and H_2SO_4 concentration, were not a variable in this study since both parameters are predetermined to suit the requirements of the biomachining extraction process (Díaz-Tena et al., 2016).

Efficient stirring prevented the concentration polarization effect. The current density in this study was selected to maximize current efficiency and improve the quality of copper deposition (Giannopoulou et al., 2002). The initial temperature was $25 \text{ }^\circ\text{C}$, and the final one of $41 \text{ }^\circ\text{C}$ was attributed to the Joule heating effect caused by the current flow.

As electrolysis progressed, an asymptotic decrease in the voltage was observed related to the progressive reduction in Cu^{2+} concentration (Figure 5.7a). About 98 % of the copper in the solution was deposited once the voltage had stabilized at 6.7 V (for a reaction time of 20 min), which was close to the theoretical time calculated with Faraday's law (18 min). The high electrodeposition current efficiency was related to the absence of other media components consuming any part of the applied current (Vivas et al., 2019). When the copper was recovered, the pH value remained constant at 1.2, which was attributed to the reaction predicted by Equation 5.7.

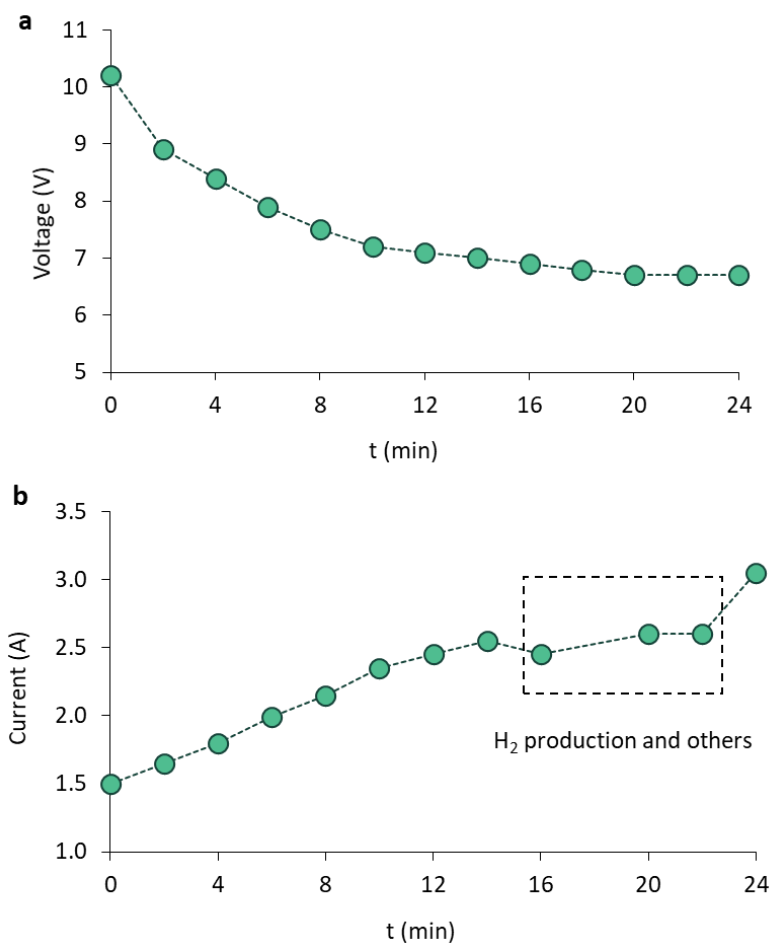


Figure 5.7. Evolution of voltage at constant current intensity (a) and evolution of current intensity at constant voltage (b).

Under the constant voltage mode (at 10.0 V), the current increased from 1.5 A to 2.6 A throughout the experiment (Figure 5.7b). Full copper recovery (> 99 %) was achieved in 14 min. The temperature increased 1.6-fold until 63 °C, causing evaporation losses of 13 %. The solution temperature is an important factor during copper electrodeposition. Ďurišínová (1991) recommended an electrolyte temperature of 45 °C to produce a fine-grained copper powder. Furthermore, the temperature increase favors diffusion speed and the movement of ions, which may lead to the formation of unwanted products. In

this case, the formation of copious amounts of hydrogen gas and the emergence of small white spots on the anode were observed after 20 minutes.

The copper deposition at constant voltage was slightly higher than at constant current intensity, and it was also faster (14 min vs 20 min), which made it recommendable as far as technical feasibility is concerned.

5.3.3. Cost Analysis

The economic viability of the two treatments has been studied. The whole precipitation treatment required H_2O_2 (1.33 € L^{-1}) for iron oxidation and NaOH (0.27 € L^{-1}) for the precipitation of iron and copper (0.21 € L^{-1} and 0.06 € L^{-1} , respectively). The sum of the consumption of both reagents accounted for 1.60 € L^{-1} of the SLR. Thus, a cost of 160 € for recovering 1 kg Cu (as CuO) was calculated. The energy consumption of the calcination oven is not significant.

Regarding the electrorecovery procedure, preliminary iron oxidation and precipitation were again mandatory, with an initial cost of 1.54 € L^{-1} (H_2O_2 1.33 € L^{-1} and NaOH 0.21 € L^{-1} , respectively). The specific energy consumption for the 20 min deposition time at 2 A current intensity was 7.35 and $7.13 \text{ kWh kg}^{-1} \text{ Cu}$ for the 14 min deposition time at 10 V voltage. The cost analysis for the second alternative (constant voltage applied to the Fe-free solution) is shown in Table 5.2. The average electricity cost in the euro area is about 0.16 € kWh^{-1} , although the current price in Spain for non-household consumers is below 0.14 € kWh^{-1} (Eurostat, 2019).

Table 5.2. Cost analysis for copper electrodeposition at 10 V and pH 4.0.

Parameter	Value
E_{electro} (kWh kg^{-1})	7.13
C_{raw} (€ kg^{-1})	8.73
C_{recovery} (€ kg^{-1})	1.00
E_{max} (kWh kg^{-1})	62

The energy cost of copper electrodeposition is 8 times lower than the cost of the raw metal in May 2021 (LME, 2021), whereby electrochemical treatment is both affordable and sustainable. Recovery alternatives for this commodity are very profitable at the present time in the post-pandemic economy, as the price of copper has risen by over 60% in the last 5 years. Due to its indispensable role in modern technologies, copper demand is expected to grow in the next decades, if the world meets the target of having net zero greenhouse gas emissions.

Considering iron oxidation is required for both alternatives, the selection of an extraordinary oxidizing agent such as H_2O_2 (standard reduction potential at 25 °C is 1.77 V) was supported by the fact that its by-products (water and oxygen) do not pose any toxicological risk (Masliy et al., 2009; Gurtubay et al., 2010).

When the particular costs of the two alternatives were compared after iron removal ($0.06 \text{ € kg}^{-1} \text{ CuO}$ and $1.43 \text{ € kg}^{-1} \text{ Cu}$), it was concluded that they are both economically viable, although the precipitation procedure is much more affordable. Nevertheless, the final product obtained by pH modification was CuO (less attractive than Cu^0), and it should be noted that this treatment was time-consuming and the labor costs were higher than direct electrorecovery. In fact, Vivas et al. (2019) underlined the benefits of copper electrodeposition over alkali precipitation for the remediation of artisanal gold smelting wastewaters.

Finally, if the recovery alternative were not applied, the depleted solutions from copper biomachining processes would have to be treated compulsorily before being discharged into the mains sewage system in order to protect the environment and comply with local regulations (local limit on discharge concentration: 7.5 mg Cu L^{-1} and 10 mg Fe L^{-1} for industrial wastewaters) (BBWC, 2020). The compulsory reduction of the concentrations of Cu and Fe to the legal limits requires chemical consumption, compromising the process's economic viability and safety compliance.

5.4. CONCLUSIONS

Bearing in mind the principles of the circular economy, this chapter focused on studying two alternatives for recovering Cu from the depleted solutions that are generated in metal solubilization bioprocesses such as biomachining of copper pieces or bioleaching of PCBs. A liquid residue was synthesized in the laboratory simulating a real depleted solution, and the experimental results revealed that both the precipitation method (CuO recovery) and the electrodeposition method (Cu^0 recovery) rendered promising results (metal recovery higher than 98 %) at a reasonable cost. Both alternatives required the preliminary oxidation and precipitation of iron, which obviously implied the additional consumption of hydrogen peroxide and sodium hydroxide and longer operation time. Nevertheless, this time-consuming step could be automated for reducing labor costs.

Copper (Cu^0) electrodeposition at a constant voltage was finally recommended because it can be performed easily, being the energy cost 8 times lower than the cost of the raw metal in May 2021. Despite the fact that the precipitation method was more affordable (although time-consuming), the final product obtained, CuO , is less attractive than Cu^0 for the stock market.

It should be noted that the remaining solution after both treatments still has a high amount of sulfate that could be removed by precipitation with a Ba^{2+} containing salt. In

summary, the two recovery options for treating the depleted solutions from the engraving of copper pieces contributed to the recycling of this metal and softened the bioprocess's environmental and economic impact, providing the building blocks for a sustainable future.

5.5. REFERENCES

- Antelo, J., Fiol, S., Gondar, D., Pérez, C., López, R., Arce, F., 2013. Cu(II) incorporation to schwertmannite: Effect on stability and reactivity under AMD conditions. *Geochimica et Cosmochimica Acta*. 119, 149-163.
- Balaji, R., 2006. Preparation and characterization of electrodeposits form methane sulphonic acid bath (PhD thesis). Industrial Metal Finishing Division. Central Electrochemical Research Institute. Karaikudi, Tamil Nadu, India.
- BBWC (Bilbao Bizkaia Water Consortium), 2020. Ordenanza reguladora de la prestación de servicio de saneamiento y depuración del consorcio de aguas de Bilbao-Bizkaia. https://www.consorciodeaguas.eus/Web/Normativa/pdf/OSERVICIO_SAN_C.pdf. accessed 10 May 2020
- BuyersGuideChem, 2020. <http://www.buyersguidechem.com/index.php> (accessed May 2020).
- Chen, T.C., Priambodo, R., Huang, R.L., Huang, Y.H., 2013. The effective electrolytic recovery of dilute copper from industrial wastewater. *Journal of Waste Management*. 164780, 1-7.
- Collivignarelli, M.C., Abba, A., Bestetti, M., Crotti, B.M., Carnevale Miino, M., 2019. Electrolytic recovery of nickel and copper from acid pickling solutions used to treat metal surfaces. *Water Air and Soil Pollution*. 230, 1-13.
- Díaz-Tena, E., Gallastegui, G., Hipperdinger, M., Donati, E.R., Ramirez, M., Rodriguez, A., Lopez de Lacalle, L.N., Elías, A., 2016. New advances in copper biomachining by iron-oxidizing bacteria. *Corrosion science*. 112, 385-392.
- Đurišinová, A., 1991. Factors influencing quality of electrolytic copper powder. *Powder Metallurgy*. 34, 139-141.
- Eurostat, 2019. Electricity prices for non-household consumers. https://ec.europa.eu/eurostat/statistics-explained/index.php/Electricity_price_statistics#Electricity_prices_for_non-household_consumers (accessed 02 May 2020).
- Gaboreau, S., Vieillard, P., 2004. Prediction of Gibbs free energies of formation of minerals of the alunite supergroup. *Geochimica et Cosmochimica Acta*. 68, 3307-3316.
- Giannopoulou, I., Panias, D., Paspaliaris, I., 2002. Electrochemical recovery of copper from spent alkaline etching solutions. *Proceedings of TMS Extraction and Processing Division Meeting, Lulea, Sweden*, 631-641.
- Gurtubay, L., Danobeitia, I., Barona, A., Prado, J., Elías, A., 2010. Viability study on two treatments for an industrial effluent containing sulfide and fluoride. *Chemical Engineering Journal*. 162, 91-96.

- Jadhav, U.U., Hocheng, H., 2015. Analysis of metal bioleaching from thermal power plant fly ash by *Aspergillus niger* 34770 culture supernatant and reduction of phytotoxicity during the process. *Biotechnology and Applied Biochemistry*. 175, 870-881.
- Jiménez, A., Hernández, A., Prieto, M., 2019. Crystallization behaviour of iron-hydroxide sulphates by aging under ambient temperature conditions. *Minerals*. 9, 27-39.
- Kim, J., Kim, S., Tazaki, K., 2002. Mineralogical characterization of microbial ferrihydrite and schwertmannite, and non-biogenic Al-sulfate precipitates from acid mine drainage in the Donghae mine area, Korea. *Environmental Geology*. 42, 19-31.
- Koyama, K., Tanaka, M., Lee, J.C., 2006. Copper leaching behavior from waste printed circuit board in ammoniacal alkaline solution. *Materials Transactions*. 47, 1788-1792.
- LME (London Metal Exchange), 2021. LME COPPER. <https://www.lme.com/en-GB/Metals/Non-ferrous/Copper#tabIndex=0> (accessed 14 May 2021).
- Ma, Y., Lin, C., 2013. Microbial oxidation of Fe²⁺ and pyrite exposed to flux of micromolar H₂O₂ in acidic media. *Scientific Reports*. 3, 1979-1989.
- Masliy, V.D., Selyukov, A.V., Skurlatov, Y.I., 2009. Applying hydrogen peroxide for oxidizing underground water iron. *Chemistry for Sustainable Development*. 6, 533-537.
- Mazuelos, A., Garcia-Tinajero, C.J., Romero, R., Iglesias-Gonzalez, N., Carranza, F., 2019. Causes of inhibition of bioleaching by Cu are also thermodynamic. *Journal of Chemical Technology and Biotechnology*. 94, 185-194.
- Milchev, A., Zapryanova, T., 2006. Nucleation and growth of copper under combined charge transfer and diffusion limitations—Part II. *Electrochimica Acta*. 51, 4916-4921.
- PANREAC, 2021. Sodium Hydroxide. <https://itwreagents.com/iberia/es/product/ga-grado-tecnico/potasio+hidr%C3%B3xido+90%25+escamas+grado+t%C3%A9cnico/211514> (accessed 12 May 2020).
- Qiu, R., Lin, M., Ruan, J., Fu, Y., Hu, J., Deng, M., Tang, Y., Qiu, R., 2020. Recovering full metallic resources from waste printed circuit boards: A refined review. *Journal of Cleaner Production*. 244, 118690.
- Sandy Jones, F., Bigham, J.M., Gramp, J.P., Tuovinen, O.H., 2014. Synthesis and properties of ternary (K, NH₄, H₃O)-jarosites precipitated from *Acidithiobacillus ferrooxidans* cultures in simulated bioleaching solutions. *Materials Science and Engineering: C*. 44, 391-399.
- Sigma-Aldrich, 2020. Copper(II) oxide. <https://www.sigmaaldrich.com/catalog/substance/copperiioxide7955131738011?lang=es®ion=ES> (accessed May 2020).
- Silverman, M.P., Lundgren, D.G., 1959. Studies on the chemoautotrophic iron bacterium *Ferrobacillus ferrooxidans*. I. An improved medium and a harvesting procedure for securing high cell yields. *Journal of Bacteriology*. 77, 642-647.
- TOXNET, 2019. Sodium sulfate. URL <https://toxnet.nlm.nih.gov/cgi-bin/sis/search/a?dbs+hsdb:@term+@DOCNO+5042>
- Vivas, E.L., Alfafara, C.G., Migo, V.P., Cho, K., Detras, M.C.M., Trinidad, L.C., Mendoza, M.D., Lee, S., 2019. Comparative evaluation of alkali precipitation and electrodeposition for copper removal in artisanal gold smelting wastewater in the Philippines. *Desalination and Water Treatment*. 150, 396-405.

Wang, L., Li, Q., Li, Y., Sun, X., Li, J., Shen, J., Han, W., Wang, L., 2018. A novel approach for recovery of metals from waste printed circuit boards and simultaneous removal of iron from steel pickling waste liquor by two-step hydrometallurgical method. *Waste Management*. 71, 411-419.

GENERAL CONCLUSIONS AND FUTURE OVERLOOK

GENERAL CONCLUSIONS

This thesis was focused on improving the process of microorganism-assisted mobilization of metals for two applications: the biomachining of copper pieces for engraving microstructures and the bioleaching of copper from printed circuit boards.

Both applications have been studied using the same bacterium (*A. ferrooxidans*). This versatile, resistant and safe microorganism was able to successfully oxidize Fe^{2+} , rendering a bioregenerated oxidant for both applications.

The main general conclusions are summarized below.

- The 9K solution (containing Fe^{2+} or Fe^{3+}) was found to be the most suitable medium for both *A. ferrooxidans* growth and metal oxidation. Copper solubilization was noticeably increased by the presence of microorganisms in comparison to the abiotic system.
- An alternate bioprocess with the regeneration and copper solubilization steps in consecutive stages was proposed. The SMRR peaked during the first hour of treatment and the amount of copper mobilized in five consecutive solubilization steps (471.6 mg cm^{-1}) was 52.4 % higher than the amount obtained in the continuous operation for the same treatment time (15 h) (224.6 mg cm^{-1}). This strategy allowed the reduction of both the treatment time and the amount of depleted solution, which enhances the sustainability of the process by prolonging the solution lifespan.
- The strategy of immobilizing the biomass on a support material was searched by selecting biocellulose (BC), polyvinyl alcohol (PVA), cellulose triacetate (CTA), and chitosan (CH) to be tested for that purpose. Only BC and PVA hydrogels fulfilled the suitability protocol, and, finally the BC was selected for further experiments based on its novelty and its outstanding properties such as its biodegradability, highly porous network structure and chemical stability.
- The best operating conditions for biomass immobilization were established for the BC material. Under these conditions (1:0.6 for the NMV:ESA ratio, 170 rpm for the orbital shaking, and $9 \text{ g Fe}^{2+} \text{ L}^{-1}$), the time required for the oxidant regeneration was reduced by 30 % when compared with the cell suspension. The immobilization time was affected by the presence of increasing concentrations of dissolved copper. Nevertheless, when the active material was consecutively exposed to higher concentrations of the metal, it was finally able to successfully oxidize all the Fe^{2+} in the present of up to $30 \text{ g Cu}^{2+} \text{ L}^{-1}$.
- The biomachining of copper pieces for engraving structures requires the efficient protection the metal surface not to be exposed to the oxidant solution. The combination of one common lacquer (red light bulb lacquer) and a PSA adhesive

was found to be a feasible and efficient alternative for the selective protection of surfaces without impairing bacterial activity.

- The average specific metal removal rate (SMRR_{av}) in the biomachining assays was maximum in the 0-1 h range (20-24 mg h⁻¹ cm⁻²) and, afterwards, it decreased in a logarithmic trend. The equations for predicting the treatment time required for the selected height to be machined were proposed.
- Although similar SMRR_{av} and height values were achieved when suspended or immobilized biomass were used in the biomachining experiments, shorter regeneration times were needed in the presence of the active biocellulose. In addition, other benefit of using immobilized microorganisms would lie in the easily handling (feeding and replacing) of the biomass in large-scale operation.
- The repeatability of the process when reusing the biomachining solution is particularly remarkable for this application, as extends its lifespan and increases the sustainability of the process.
- As far as microorganism-assisted solubilization of metals from PCBs is concerned, the entire pieces without the epoxy cover were selected for the experiments, because grinding pre-treatment entailed an important cost and generated particulate matter in the environment. In addition, the use of the entire PCBs facilitated the management and separation of the pieces from the leachate, as well as providing a “cleaner” medium for microbial activity.
- The alternate (two step) bioleaching experiment with the entire PCBs rendered a total amount of 82 % of copper dissolved by the end of the assay (300 hours), which was attributed to the relevant contribution of the biomass in regenerating the oxidant.
- The bioleaching and biomachining processes generated liquid residues with high metal concentrations. Two alternatives were studied for recovering copper from a synthetic solution: precipitation and electrodeposition. The experimental results revealed that both procedures rendered high metal recovery (98 %) at a reasonable cost and required the preliminary oxidation and precipitation of iron, which obviously implied the additional consumption of reagents and longer operation time.
- Although the precipitation method was more affordable (although time-consuming) than the electrorecovery, the final product obtained (CuO) is less attractive than Cu⁰ for the stock market. Bearing in mind that the world demand of copper (and the LME official prices) has been on the rise during the last three months and is expected to go further up, the metal recovery from these depleted solutions can be an entrepreneurial opportunity integrated in the circular economy.

FUTURE OVERLOOK

The results of this thesis suggested that further research on several additional aspects would benefit the final productive implementation of both applications. Thus, the future overlook could include:

- To search for a consortium of safe microorganisms (instead of one single bacterium type) that could face and mitigate the medium increasing toxicity caused by copper solubilization throughout the process.
- To assess the economical and environmental feasibility of the biomachining in detail, in order to disseminate the suitability of that bioprocess for manufacturing molds for other additional productive applications.
- To investigate how to apply the proposed alternate bioleaching process to other electronic wastes for metal recovery. In addition, the sustainable and affordable bioextraction of other precious metals (Ag, Au, Pt...) could be an attractive opportunity for entrepreneurs.
- To explore the automatization of the mandatory oxidation of iron prior to the copper electrodeposition in waste solutions for operation cost reduction.
- To design and install a pilot-scale plant for the bioleaching of entire PCBs in order to obtain technical information and make a decision about the implementation at higher scale.

APPENDIX 1

LIST OF PUBLISHED ARTICLES

Santaolalla, A., Gutierrez, J., Gallastegui, G., Barona, A., Rojo, N., 2021. Immobilization of *Acidithiobacillus ferrooxidans* in bacterial cellulose for a more sustainable bioleaching process. *Journal of Environmental Chemical Engineering*. 9 (4), 105283.

Santaolalla, A., García J., Rojo, N., Barona, A., Gallastegui, G., 2020. Viability of two alternatives for treating waste solutions from the biomachining process. *Journal of Cleaner Production*. 270, 122549.

Santaolalla, A., Rojo, N., Gutierrez, J., Barona, A., 2020. Immobilization of *Acidithiobacillus Ferrooxidans* on Two Hydrogels. *Chemical engineering transactions*. 79, 7-12.

Santaolalla, A., Alvarez-Braña, Y., Benito-Lopez, F., Basabe-Desmonts, L., Barona, A., Gallastegui, G., Rojo, N. Biomachining: an environmentally friendly technique for the fabrication of PDMS microfluidic devices. *Sent to Lab on a Chip*.

LIST OF CONFERENCES

Rojo, N., Gallastegui, G., Díaz-Tena, E., Santaolalla, A., Elías, A., Barona, A., 2017. Joint assessment of biomachining and e-waste biorecovery. 10th World Congress of Chemical Engineering. 1-5 October; Barcelona, Spain. Type of presentation: poster.

Santaolalla, A., Rojo, N., Crespo, A., Díaz-Tena, E., Gallastegui, G., Barona, A., 2018. Treating waste printed circuit boards from mobile phones: copper leaching in abiotic and biotic media. 23rd International Congress of Chemical and Process Engineering. 25-29 August; Prague, Czech Republic. Poster.

Santaolalla, A., Rojo, N., Gallastegui, G., Barona, A., 2018. A sequential process for biomachining copper pieces including oxidant regeneration. 2nd International Conference on Bioresource Technology for Bioenergy, Bioproducts and Environmental Sustainability. 16-19 September; Sitges, Spain. Type of presentation: poster.

Santaolalla, A., Rojo, N., Elías, A., Gallastegui, G., Benito-Lopez, F., Basabe-Desmonts, L., Barona, A., 2019. Assessment of the biomachining time for the sustainable engraving of microstructures on metal workpieces. 4th Green and Sustainable Chemistry Conference. 5-8 May; Dresde, Germany. Type of presentation: poster.

Santaolalla, A., Rojo, N., Gutierrez, J., Gallastegui, G., Barona, A., 2019. Novel biosupport material for *A. ferrooxidans* immobilization. 5th European Congress of Applied Biotechnology (ECCE12-ECAB5). 15-19 September; Florence, Italy. Type of presentation: oral communication.

Santaolalla, A., Alvarez-Braña, Y., Gallastegui, G., Basabe-Desmonts, L., Rojo, N., Benito-Lopez, F., 2019. PDMS microfluidic devices fabrication by a cyclic biomachining process.

The 23rd International Conference on Miniaturized Systems for Chemistry and Life Sciences (μ TAS 2019). 27-31 October; Basel, Switzerland. Type of presentation: poster.

Gallastegui, G., Santaolalla, A., Rojo, N., Urbina, L., García, J., Barona, A., 2019. Options for Recovering Copper from Biomachining Waste Solutions. 3rd International Congress of Chemical Engineering (ANQUE - ICCE -CIBIQ). 19-21 June; Santander, Spain. Type of presentation: poster.

Santaolalla, A., Rojo, N., Gutierrez, J., Ureña, I., Gutierrez, I., Barona, A., 2019. An Insight into Novel Materials for *A. ferrooxidans* Immobilization. 3rd International Congress of Chemical Engineering (ANQUE - ICCE -CIBIQ). 19-21 June; Santander, Spain. Type of presentation: poster.

APPENDIX 2

LIST OF FIGURES

Figure 1. SEM micrograph: <i>A. thiooxidans</i> (published by Quatrini et al., 2017) (a) and <i>Leptospirillum ferrooxidans</i> (published by Vrdoljak and Spiller, 2005) (b).....	14
Figure 2. SEM micrograph: <i>Pseudomonas aeruginosa</i> (published by Kasuga et al., 2011) (a) and <i>Pseudomonas putida</i> (published by Merum et al., 2017) (b).....	16
Figure 3. SEM micrograph of the mesophilic <i>A. ferrooxidans</i> bacteria (published by Diaz-Tena et al., 2014).	20
Figure 4. Schematic diagram of microbial leaching mechanisms: direct mechanism (contact leaching) (a), indirect mechanism (non-contact leaching) (b) and cooperative leaching (c).....	22
Figure 5. Schematic diagram of thiosulfate (a) and polysulfide (b) mechanisms in bioleaching (adapted from Rohwerder et al., 2003).	25
Figure 6. Some of the geometries biomachined in OFE workpieces published by Díaz-Tena et al. (2016).	35
Figure 7. Main material fractions in WEEE composition (adapted from Widmer et al., 2005)..	38
Figure 8. Total WEEE generation in 2019 per category (adapted from Nithya et al., 2020).	39
Figure 9. Waste hierarchy according to directive 2008/98/CE.	40
Figure 10. Average weight composition of a standard mobile phone PCB.	41
Figure 11. Most probable number (MPN) methodology.	70
Figure 12. Photographs of the tubes before (a) and after (b) being incubated for the most probable number technique.	70
Figure 13. Iron standards for calibration curve.	72
Figure 14. ICP-OES plasma spectrometry (a) and Atomic absorption spectroscopy (b) equipment.....	73
Figure 1.1 . Outline of the experimental section of this chapter.....	79
Figure 1.2. Culture medium before (a) and after (b) the growth period of <i>A. ferrooxidans</i> bacteria for 9. 6 and 1.5K media.	83
Figure 1.3. Evolution of the $[Fe^{3+}]$ (a) and the redox potential (b) during the incubation period in medium containing 1.5, 6 and 9 g $Fe^{2+} L^{-1}$	84
Figure 1.4. Color variation of the culture medium during the oxidation of Fe^{2+} into Fe^{3+} by means of <i>A. ferrooxidans</i> bacteria in 9K medium.....	84
Figure 1.5. Evolution of pH during the incubation period in the medium containing 1.5 g $Fe^{2+} L^{-1}$ (a), 6 g $Fe^{2+} L^{-1}$ (b) and 9 g $Fe^{2+} L^{-1}$ (c). The pH was readjusted to 1.7 after each analysis.....	85
Figure 1.6. Variation of the SMRR during the three-hour experiment for the three initial Fe^{3+} concentrations (9, 6 and 1.5 g $Fe^{3+} L^{-1}$).....	88
Figure 1.7. Evolution of dissolved copper and $[Fe^{3+}]/[Fe^{2+}]$ ratio (a), and SMRR (b) throughout time.	90
Figure 1.8. SMRR as a function of time during six three-hour metal removal stages (a); variation in SMRR (bars), $[Cu^{2+}]$ (grey dots) and $[Fe^{3+}]$ (white dots) during two successive treatment stages (MR1 and MR2) and the oxidant regeneration step (b).	92
Figure 1.9. Copper solubilization in consecutive treatment stages (columns, right axis) and accumulated copper concentration in the solution (white dots, left axis).....	93

Figure 1.10. Resulting solutions after six metal mobilization + regeneration stages (in duplicate).	94
Figure 1.11. Regeneration time as a function of the copper concentration in the medium.....	95
Figure 2. 1. Outline of the experimental section of this chapter.....	102
Figure 2. 2. Molecular structure of bacterial cellulose (BC) (a), polyvinyl alcohol (PVA) (b), cellulose triacetate (CTA) (c) and chitosan (CH) (d).	102
Figure 2. 3. Culture medium and synthesized BC membrane.	104
Figure 2. 4. PVA hydrogel preparation process using Freeze-Thawing technique.	104
Figure 2. 5. Lyophilized PVA (L-PVA) preparation process using Freeze-Drying technique.....	105
Figure 2. 6. Preparation process of modified CTA membrane (M-CTA).	106
Figure 2. 7. Preparation process of CTA spheres (B-CTA).	106
Figure 2. 8. Preparation process of lyophilized chitosan L-CH.....	107
Figure 2. 9. Decision-making protocol.	108
Figure 2. 10. Scheme of bacterial immobilization procedure and subsequent oxidation stages.	111
Figure 2. 11. Selected support materials before (left) and after (right) being submerged in the 9K medium: BC (a) and PVA 10 % w:w (b).	115
Figure 2. 12. Discarded support materials before (left) and after (right) being submerged in the 9K medium: L-PVA (a), CH (b), L-CH (c), M-CTA (d) and B-CTA (e).	115
Figure 2. 13. SEM image at low (right) and high magnification (right) of PVA hydrogels at different weight concentrations: 2.5 % (a), 5 % (b) and 10 % (c).	116
Figure 2. 14. SEM images of BC top surface (a) and b) cross-section image (b).....	117
Figure 2. 15. Evolution of Fe ²⁺ (%) during the incubation period with 2 %, 5 %, 10 % v:v inoculum percentages.	118
Figure 2. 16. Picture and SEM photograph of the pretreated biocellulose (a) and the surface of the biologically active bacterial cellulose (A-BC) obtained after the immobilization protocol (b).	119
Figure 2.17. Average time required for the complete Fe ²⁺ bio-oxidation in two consecutive stages (left axis) and average Fe ³⁺ productivity (right axis) for different NMV:ESA (mL: cm ²) ratios when using A-BC pieces.	122
Figure 2. 18. Fe ²⁺ bio-oxidation time during A-BC preparation and subsequent bio-oxidation stages at different Cu ²⁺ concentrations (a) and evolution of Fe ²⁺ concentration in the reactor with [Cu ²⁺] = 10 g L ⁻¹ (b).....	126
Figure 2. 19. Reactors with A-BC before (a) and after (b) Fe ²⁺ bio-oxidation in the presence of different concentrations of dissolved copper (0-20 g Cu ²⁺ L ⁻¹).	127
Figure 2. 20. Picture and SEM photograph of A-BC after several bio-oxidation stages (a), FTIR analysis of the jarosite (b), and two Erlenmeyers with A-BC pieces and suspended cells respectively (c).	129
Figure 2. 21. BC pieces after use in the iron oxidation process but before washing with oxalic acid (a) and after W1 (b), W2 (c) and W3 (d) washing cycles, respectively.....	131
Figure 2. 22. Fe ²⁺ bio-oxidation time during BAM (BC and 2.5, 5 and 10 % PVA) preparation and subsequent bio-oxidation stages (S1 and S2).	132

Figure 2. 23. Biologically active materials after the immobilization procedure: A-BC (a) and 10 % A-PVA (b).	132
Figure 2. 24. Biologically active materials after successive Fe ²⁺ oxidation stages: A-BC (a), 10 % A-PVA (b), 5 % A-PVA (c) and 2.5 % A-PVA (d).	133
Figure 2. 25. Fe ²⁺ bio-oxidation time at different Cu ²⁺ concentrations (a) and evolution of Fe ³⁺ concentration in the control reactor (b) when using A-BC and A-PVA.	134
Figure 3. 1. Outline of the experimental section of this chapter.....	145
Figure 3. 2. Copper workpiece: dimensions (a) and preparation (b).....	146
Figure 3. 3. Selected geometries for micro-etching: circle (a), microfluidic structure with serpentine channel (b), and rectangular structure (c).....	147
Figure 3. 4. Coating materials for surface protection: bulb lacquer (left) and insulating protective lacquer (right).	147
Figure 3. 5. Glass rod prior to use (a), glass rods with the two coating materials (b) and assay system (c).	148
Figure 3. 6. Stylus profilometer (DektakXT) (a) and workpiece height measurement with profilometer (b).....	152
Figure 3. 7. Evolution of Fe ²⁺ (%) during the <i>A. ferrooxidans</i> incubation period in the presence and the absence of the two studied lacquers.	155
Figure 3. 8. Variation of SMRR and height of the engraved structures with treatment time: 0-1 h (a) and 1-7 h (b).....	157
Figure 3. 9. Resulting solutions after 0.25 to 7 h biomachining treatment.....	158
Figure 3. 10. SMRR _{av} in the samples with the circular geometry and the microfluidic channels.	161
Figure 3. 11. Molds for the fabrication of microfluidic devices obtained after 15 min (a), 30 min (b), 2 h (c) and 6 h (d) of biomachining.	162
Figure 3. 12. Average SMRR for each selected treatment time (a), and variation of mold's height (b) and removed copper (c) with the number of mold-etching stages.	163
Figure 3. 13. Variation of Fe ³⁺ concentration during the successive mold-etching (2 h) and regeneration stages (a), and the regeneration time with stage number (b) and with copper concentration (c).	165
Figure 3. 14. Schematic of the etching + regeneration process for engraving of microfluidic structures.	167
Figure 3. 15. Evolution of SMRR for the experiments with immobilized biomass.	168
Figure 3. 16. Evolution of structure's height (a) and removed copper mass throughout the consecutive mold-etching stages (b), and time needed for Fe ²⁺ oxidation after each regeneration stage (c) for BM-BC _{IN} and BM-BC _{OUT}	169
Figure 3. 17. Photographs of the biomachining solution during the BM- BCIN experiment (where S _x is the number of the mold-etching stage and R _x the corresponding regeneration stage).....	171
Figure 3. 18. Fabrication (a) and performance (b) of a hybrid PDMS/PSA microfluidic device (316.9±5.4 μm height) fabricated using a mold obtained after 36 h of biomachining.....	172
Figure 4. 1. Outline of the experimental section of this chapter.....	182
Figure 4. 2. Dismantling of mobile phones (a) and printed circuit boards (PCBs) (b).	182

Figure 4. 3. RETSCH SM 2000 mill.	183
Figure 4. 4. Detail of the container placement in the digester carousel.	185
Figure 4. 5. Digested samples: blank for 1:40 ratio (a); blank for 1:80 ratio (b); PCB sample (c); final solutions after dilution with nitric acid (d).	185
Figure 4. 6. Pulverized PCB sample according to particle size: > 1.25 mm (a), 1.25-0.75 mm (b), and < 0.75 mm (c) (1:30 augmentation).	186
Figure 4. 7. Particle-size distribution of pulverized PCB.	187
Figure 4. 8. Mobile phone PCB before and after treatment with a 10 M NaOH solution.	187
Figure 4. 9. Copper removal efficiency during the bioleaching experiments for the PCB powder samples and the entire PCB piece without epoxy layer.	191
Figure 4. 10. Copper removal efficiency (a), total iron concentration evolution (b) and pH evolution (c) during the two-step bioleaching experiment.	194
Figure 4. 11. BL solution (a) and PCB pieces (b) before and after bioleaching.	195
Figure 4. 12. Zn, Ni and Pb removal during the two-step bioleaching experiments.	195
Figure 4. 13. Extracted amount of copper, nickel and zinc from PCB in Fe ³⁺ medium.	196
Figure 4. 14. Amounts of Cu, Ni, Zn and Fe extracted from PCBs when employing H ₂ SO ₄ as leaching agent.	197
Figure 4. 15. The leaching solution when using Fe ³⁺ as oxidant (a) and the PCB piece (b) before and after treatment.	198
Figure 4. 16. The leaching solution when using H ₂ SO ₄ (a) and the PCB piece (b) before and after treatment.	198
Figure 4. 17. Flowchart of the process from obsolete phone collection to metal leaching.	201
Figure 4. 18. Diagram of the biological reactors (BR1 and BR2) for oxidant production (a) and solution regeneration (b).	203
Figure 4. 19. Diagram of the CSTR bioreactor for copper leaching (BL reactor).	204
Figure 4. 20. Diagram of the global process for PCB bioleaching.	205
Figure 5. 1. Outline of the experimental section of this chapter.	215
Figure 5. 2. Schematic diagram for the recovery process.	217
Figure 5. 3. ORP evolution during the Fe ²⁺ oxidation process with H ₂ O ₂	220
Figure 5. 4. Photographs of the three P1 solids: fresh precipitate (a), calcined (b) and calcined and washed (c).	220
Figure 5. 5. Characterization of the P1 precipitated sample: TG (a) and DTG analysis (b).	221
Figure 5. 6. Photographs of the three P2 solids: fresh precipitate (a), calcined and washed (b) and dried solid of the SRL2 filtrate (c).	223
Figure 5. 7. Evolution of voltage at constant current intensity (a) and evolution of current intensity at constant voltage (b).	225

LIST OF TABLES

Table 1. Some chemolithotrophic microorganisms used in microorganism-assisted metal mobilization processes reported in literature.....	15
Table 2. Some heterotrophic microorganisms reported in bibliography for microorganism-assisted metal mobilization processes.....	17
Table 3. Some of the microorganism consortiums employed in microorganism-assisted metal mobilization processes.....	19
Table 4. Metal solubilization efficiencies (%) reported in literature employing <i>A. ferrooxidans</i> bacteria.	21
Table 5. Different support materials reported in bibliography for <i>A. ferrooxidans</i> immobilization.....	29
Table 6. Advantages and drawbacks of microorganism-assisted metal mobilization process compared to other metal extraction processes.....	34
Table 7. SMRR ($\text{mg h}^{-1} \text{cm}^{-2}$) values reported in literature for different strains of the <i>A. ferrooxidans</i> bacterium.....	37
Table 8. Economical and environmental assessment comparison of hydrometallurgy and biohydrometallurgy methods for PCB treatment (Sodha et al., 2020).....	42
Table 9. Pulp densities (g L^{-1}) and particle sizes (μm) reported in literature.....	44
Table 10. Composition of culture medium according to final iron concentration.	68
Table 11. Reagents used in the colorimetric method for ferrous and total iron determination.	71
Table 1.1. Experimental conditions for bacterial growth, metal mobilization and abiotic assays.	81
Table 1.2. Total copper amount removed in the biotic (BM1) and abiotic (SN1) experiments after the three-hour immersion of a copper piece.....	87
Table 1.3. Maximum SMRR values obtained in the literature and in this study when using different initial concentrations of Fe^{3+} at $T = 30\text{-}31\text{ }^{\circ}\text{C}$).	89
Table 2.1. Experimental conditions for the iron bio-oxidation experiments using the A-BC pieces at $31\text{ }^{\circ}\text{C}$ and $\text{pH } 1.8$	110
Table 2.2. Copper concentration in the medium during A-BC15 preparation and subsequent bio-oxidation stages with the sample A-BC15.	111
Table 2.3. Selection of suitable materials for <i>A. ferrooxidans</i> immobilization.....	114
Table 2.4. Time required for the bio-oxidation of the Fe^{2+} during the immobilization of <i>A. ferrooxidans</i> on different support materials ($\text{pH} = 1.6\text{-}2.0$ and $T = 30\text{-}31\text{ }^{\circ}\text{C}$).	120
Table 2.5. Influence of shaking speed on bio-oxidation time during both A-BC preparation and A-BC use in two consecutive stages.	125
Table 2.6. Fe^{2+} bio-oxidation time of sample A-BC15 when exposed to higher dissolved copper concentrations.	128
Table 2.7. Optimum operating conditions for A-BC preparation and use.....	129
Table 2.8. Fe^{2+} oxidation time required by A-BC after 15 days of storage (average of two successive bio-oxidation cycles).....	130
Table 3. 1. Immersion times in the mold-etching experiments.....	149
Table 3. 2. Experimental conditions in metal removal experiments when using A-BC and cell suspension (control).....	151

Table 3. 3. SMRR ($\text{mg h}^{-1} \text{cm}^{-2}$), structure's height (H_t , μm), and removed copper (m_{Cu} , mg) variation according to the two treatment time intervals (h) for the circular geometry.	157
Table 3. 4. Height and depths values (μm) reported in bibliography by other authors.....	160
Table 3. 5. Linear equations that correlate mold's height (μm) and removed copper mass (m_{Cu} , g) with the number of mold-etching stage (N).....	164
Table 3. 6. Relationship between the regeneration time (t_{regen} , h) and the concentration of dissolved copper (Cu , g L^{-1}).	166
Table 3. 7. Linear equations that correlate the height of the structure (H_t , μm) and the amount of copper removed (m_{Cu} , g) with the number of mold-etching stages (N).	169
Table 4. 1. Metal concentration (mg g^{-1} PCB) of mobile's PCBs reported in literature and market price according to the London Metal Exchange (LME, € kg^{-1}).	188
Table 4. 2. Average metal content in PCBs in this study (mg metal g^{-1} PCB).....	189
Table 4. 3. Results of the EDXRF analysis of different areas of the PCB powder.....	189
Table 4. 4. Results of the EDXRF analysis of different areas of the entire PCB.	190
Table 4. 5. Metal removal values obtained for Cu, Zn, Ni, and Pb.	192
Table 4. 6. Leaching efficiencies for several metals reported in the literature when treating PCB pieces.	200
Table 5. 1. Parameters measured in the SLR_0 , SLR_1 and SLR_2 samples.	222
Table 5. 2. Cost analysis for copper electrodeposition at 10 V and pH 4.0.	226

